Université de Montréal

From locomotion to Dance and Back
Exploring Rhythmic Sensorimotor Synchronization

Par

Baptiste Chemin, M.D.

Département de Psychologie, Faculté des Arts et Sciences

Thèse présentée en vue de l'obtention du grade de Docteur

en Psychologie, option Sciences Cognitives, Neuropsychologie

Septembre 2021

Université de Montréal

Unité académique : Département de Psychologie, Faculté des Arts et Sciences

Cette thèse intitulée

From Locomotion to Dance and Back

Exploring Rhythmic Sensorimotor Synchronization

Présentée par

Baptiste Chemin

A été évaluée par un jury composé des personnes suivantes

Professeur Pascal Kienlen-Campard
Président-rapporteur

Professeur Isabelle Peretz
Directeur de recherche

Professeur André Mouraux
Codirecteur

Professeur Simone Dalla Bella
Membre du jury

Professeur Sylvie Nozaradan
Membre du jury

Professeur Michael Andres
Membre du jury

Dr. Assistant Professeur Manon Grube
Examinatrice externe

Résumé

Le rythme est un aspect important du mouvement et de la perception de l'environnement. Lorsque l'on danse, la pulsation musicale induit une activité neurale oscillatoire qui permet au système nerveux d'anticiper les évènements musicaux à venir. Le système moteur peut alors s'y synchroniser.

Cette thèse développe de nouvelles techniques d'investigation des rythmes neuraux non strictement périodiques, tels que ceux qui régulent le tempo naturellement variable de la marche ou la perception rythmes musicaux. Elle étudie des réponses neurales reflétant la discordance entre ce que le système nerveux anticipe et ce qu'il perçoit, et qui sont nécessaire pour adapter la synchronisation de mouvements à un environnement variable. Elle montre aussi comment l'activité neurale évoquée par un rythme musical complexe est renforcée par les mouvements qui y sont synchronisés. Enfin, elle s'intéresse à ces rythmes neuraux chez des patients ayant des troubles de la marche ou de la conscience.

Mots-clés : Entrainement Neuronal, Perception Auditive, Mouvement, Perception Musicale, Intégration Sensitivo-Motrice, EEG, SS-EPs, Maladie de Parkinson, Conscience.

Abstract

Rhythms are central in human behaviours spanning from locomotion to music performance. In dance, self-sustaining and dynamically adapting neural oscillations entrain to the regular auditory inputs that is the musical beat. This entrainment leads to anticipation of forthcoming sensory events, which in turn allows synchronization of movements to the perceived environment.

This dissertation develops novel technical approaches to investigate neural rhythms that are not strictly periodic, such as naturally tempo-varying locomotion movements and rhythms of music. It studies neural responses reflecting the discordance between what the nervous system anticipates and the actual timing of events, and that are critical for synchronizing movements to a changing environment. It also shows how the neural activity elicited by a musical rhythm is shaped by how we move. Finally, it investigates such neural rhythms in patient with gait or consciousness disorders.

Keywords : Neural Entrainment, Auditory Perception, Body Movement, Music Perception, Sensorimotor Integration, EEG, SS-EPs, Parkinson Disease, Disorder of Consciousness.

Table des matières

Liste des tableaux

Liste des figures

Liste des sigles et abréviations

ANOVA : analysis of variance

BA44 : Brodmann area 44

CLR : cerebellar locomotor region

CN :caudate nucleus

CPG : central pattern generator

DLP : direct locomotor pathway

DoF : degrees of freedom

EcoG : electrocorticography

EEG : electroencephalography

fMRI : functional magnetic resonance imaging

FS : false sequencing

IBI : interbeat interval

IEI : interevent interval

ILP : Indirect Locomotor Pathway

ISI : interstep interval

ITI : intertap interval

LFP : local field potential

M : mean

MCS : minimally conscious state

Mdn : median

MEG : magnetoencephalography

NMA : negative mean asynchrony

OR : odd ratio

PD : Parkinson's disease

PET : positron emission tomography

PPN : pedonculopontine nucleus

STN :subthalamic nucleus

SMA : supplementary motor area

SMS : sensorimotor synchronization

SS-EP : steady-state evoked-potential

TW : time warping

RMN : resonance magnetic imagery

Glossaire

Oscillation. In physics, an oscillation corresponds to a periodic phenomenon, i.e., a phenomenon that repeats itself over time. It is characterized by three parameters that are its frequency, phase and amplitude. In biological systems, repetitive events are often observed, but the parameters are rarely, or even never, constant over time. Therefore, they are considered as *non-stationary*. In neural systems, repetitive changes in neuronal excitability are usually termed as *neural oscillations*. Importantly, this notion usually implies that neural systems behave as oscillators, and more specifically as *self-sustained oscillators* (Hutcheon and Yarom, 2000). Self-sustaining oscillators can spontaneously generate an activity without the need of an external periodic input, entrain to a periodic input of energy whose period is close enough to the period of the oscillator, and perpetuate the oscillation after the end of the external stimulation.

Rhythm. This is probably one of the most frequently used term in this thesis. A rhythm is a succession of events, in time (London, 2012). It can be physical (e.g., acoustic, visual), biophysical (e.g., motor), or physiological (e.g., neural rhythm). Importantly, this term does not carry inherent assumption regarding the emergent properties of the phenomenon it describes. For example, an acoustic rhythm is not necessarily inducing the perception of a pulse, and a neural rhythm is not necessarily involving a neural oscillation.

Pulse. (Also called the "beat") A subjective feeling of periodicity that structures the perception of musical rhythm and which serves as a framework for synchronized movement to music (Patel & Iversen, 2014)

Beat. The beat is an ambiguous term. In this thesis, it most of the times refers to the acoustic events of an acoustic rhythm. The downbeat is the regular event which is the physical equivalent to the pulse. In many cases, beat is synonym with pulse (e.g., "beat-based" timing). For the sake of clarity, when the meaning of "beat" was not straightforward, an explicit note was added.

Entrainment. A spatiotemporal coordination resulting from rhythmic responsiveness to a perceived rhythmic signal (Phillips-Silver et al., 2010). Entrainment is an important feature of numerous human activities including sport, verbal communication, and art. It is exemplified in music and dance.

Period, Frequency, Tempo, Cadence and Interevent Interval. Several terms used throughout this thesis actually convey the same information, but differed according to the context. Thus, *frequency*, *tempo* and *cadence* correspond to the number of events occurring per time unit, for mathematical, musical and gait related context, respectively. Similarly, *period*, *interbeat interval* and *interstep interval* correspond to the time separating two consecutive events. The relationship between the first and the second category of terms is given by the equation $P = 1/F$, where the period is denoted by P and the frequency is denoted by F.

Autocorrelations and Cross-correlations. The following definitions are adapted from the book *The analysis of time series: an introduction* (Chatfield, 2003). Given K pairs of observations on two variables x and y, say $\{(x_1, y_1), (x_2, y_2), \dots, (x_K, y_K)\}$, the correlation coefficient at sample i is given by

$$r_i = \frac{\sum(x_i - \bar{x})(y_i - \bar{y})}{\sqrt{[\sum(x_i - \bar{x})^2 \sum(y_i - \bar{y})^2]}}$$

This quantity lies in the range $[-1,1]$ and measures the strength of the linear association between the two variables. The correlation is negative if "high" values of x tend to go with "low" values of y. If the two variables are independent, then the true correlation is zero.

The autocorrelation coefficient is given by an analogous formula, applied to a time series data. It measures whether successive observations are correlated. Given K observations $x_1, x_2, \dots, x_K$ on a time series, $K - 1$ pairs of observations can be formed, namely, $(x_1, x_2), (x_2, x_3), \dots, (x_{N-1}, x_N)$, where each pair of observation is separated by one time interval. Regarding the first observation in each pair as one variable, and the second observation in each pair as a second variable,

the autocorrelation coefficient between adjacent observations, x_t and x_{t+1}, at lag one, is given by

$$r_1 = \frac{\sum_{t=1}^{N-1}(x_t - \bar{x}_{(1)})(x_{t+1} - \bar{x}_{(2)})}{\sqrt{\left[\sum_{t=1}^{N-1}(x_t - \bar{x}_{(1)})^2 \sum_{t=1}^{N-1}(x_{t+1} - \bar{x}_{(2)})^2\right]}}$$

where

$$\bar{x}_{(1)} = \sum_{t=1}^{N-1} x_t / (N-1)$$

is the mean of the first observation in each of the $(N-1)$ pairs and so is the mean of the first $N-1$ observations, while

$$\bar{x}_{(2)} = \sum_{t=2}^{N} x_t / (N-1)$$

is the mean of the last N-1 observations. The equation giving r_1 is rather complicated, but can be conveniently approximated and simplified to give the formula

$$r_1 = \frac{\sum_{t=1}^{N-1}(x_t - \bar{x})(x_{t+1} - \bar{x})}{\sum_{t=1}^{N}(x_t - \bar{x})^2}$$

In a similar way, the correlation between observations that are n steps apart is given by

$$r_n = \frac{\sum_{t=1}^{N-n}(x_t - \bar{x})(x_{t+n} - \bar{x})}{\sum_{t=1}^{N}(x_t - \bar{x})^2}$$

This is called the autocorrelation coefficient at lag k.

Acknowledgements

Writing this thesis has been a long journey, along which I was lucky enough to meet several great people that introduced me to a vast field of scientific and human knowledge. I am particularly grateful to my three mentors: André Mouraux and Isabelle Peretz who directed this work, and Sylvie Nozaradan who first guided me almost ten years ago as a research student. André has the gift of unlocking the precise piece of the puzzle needed to solve the problems I have faced, and Isabelle has introduced me to whole different points of view. Together, they sharpened and broadened my scientific mind. Importantly, they also gave me their trust and the freedom to lead the research in my own way, which is a precious gift.

I also want to thank all my colleagues, collaborators and friends who shared this journey with me. I have received particular help from Julien Lambert and Pauline Tranchant and I was pleased to collaborate with Dounia Meulders, Nicolas Lejeune and Gan Huang in two studies. I was also lucky to teach two enthusiastic master students, Anke and Ambre, and to collaborate with them. Furthermore, a consistent team of scientists helped me by discussing and advising me on my research project. Of them, I want to thank all the -patient- members of my academic committees. There is also a long list of people with whom I only briefly interacted, all of whom were important although I cannot mention them all here. I also want to give credit to Heather, Stephanie and Joachim for language correction.

I am extremely grateful to the unconditional support I received from my family and friends. Many things happened during these years, and together we all became a little wiser than before. Finally, my thanks goes to each one of you, the readers, for the attention you are giving to my manuscript. It was a pleasure to build and write it, but your interest is crucially important to the sense of purpose I will keep from it. I hope it will give you a meaningful piece of knowledge, and that it will spark your creativity.

Chapter 1 – Ecology of Rhythmic Movement

Evolutionary Considerations on Locomotion and Control of Rhythmic Movements.

Humans, mammals and birds share similar neural circuitry and patterns of neural activities that drive their automatic locomotion (Dominici et al., 2011). These automatic systems, contained in the spinal cord and the mesencephalon, can produce a large panel of rhythmic limb movements and postural adjustments. In contrast, the cortical and cortico-subcortical loops involved in complex forms of locomotion control, such as the anticipative adjustment of gait to the environment, may largely differ between species (Takakusaki, 2013).

For example, species that have developed arboreal locomotion need to precisely position each grasp in space and time. Then, the apparition of bipedal locomotion freed the forearms and hands from their original locomotion purpose and this allowed the emergence of fine object manipulation (Georgopoulos & Grillner, 1989). Species that have developed articulated rhythmic vocalization, namely humans with the notable exception of a few birds species such as the parrot, display the ability to synchronize movements to acoustic rhythms (Patel, 2006; Schachner, Brady, Pepperberg, & Hauser, 2009). The synchronization of steps to an acoustic rhythm is an example of precise adjustment of gait to the environment. This form of control of rhythmic movement is particularly manifests in dance, when one can produce extremely skilled movements in synchrony with the complex stream of acoustic information contained in music. Similarly to fine manipulation, the synchronization ability appears to be more accurate for the upper limb (Aschersleben & Prinz, 1995).

These elements suggest that the ability to synchronize periodic movements to periodic acoustic rhythms has emerged from a core mechanism of rhythmic motor generation rooted in locomotion, overtaking its automaticity to involve scarce, species-specific and complex cortical processes that are controlled by will (Merker, Madison, & Eckerdal, 2009; Patel, 2014; Patel & Iversen, 2014).

Rhythmic Sensorimotor Synchronization

The ability to perceive a beat in music and align bodily movement synchronized with the beat is called "entrainment"[1] (McNeill, 1995; Phillips-Silver, Aktipis, & Bryant, 2010). It emerges from three functions, all of which could have been favoured by natural selection (Phillips-Silver et al., 2010; Todd, Lee, & O'Boyle, 2002): first, the ability to produce a rhythmic signal, which is critical in locomotion or feeding behaviours; second, the ability to detect rhythmic signals in the environment, which is critical for example in detecting an approaching predator; third, the ability to integrate and temporally adjust sensory information and motor production, which is critical in verbal communication and is much more species-specific than the first two abilities.

An appealing feature in music is that its apparent periodicity comes with predictability: the rhythm is informative about the timing of forthcoming events. Entrainment of rhythmic movement to acoustic rhythms has been extensively studied and described by mathematical models (Jones, 1976; Jones & Boltz, 1989; Large & Jones, 1999). Its core feature is an active, self-sustained, periodic internal oscillation (i.e., the feeling of a "pulse") that synchronizes to an external oscillation (i.e., the music). Because the internal oscillation is self-sustaining (i.e., it continues to oscillate even without external input), it enables the listener to use predictive timing to anticipate the rhythmic upcoming events and accurately synchronize movements to those events rather than react to them (Large, 2000). Yet, sometimes the structure of a music can be surprising, and anticipation cannot be accurate. In such cases, synchrony between the acoustic rhythm and movements can still be maintained, but shifts to a reactive process, called tracking.

---

[1] The term "entrainment", used without adjective, usually refers to the behaviour only and not to its underlying neural mechanisms.

In any case, a process of error correction is necessary to maintain a precise synchronization, and involves at least two distinct mechanisms: period correction (i.e., adaptation to changes in tempo (Repp, 2001b) and phase correction (i.e., adaptation for temporal alignment between motor and acoustic events (Repp, 2002b)). In an influent review, Repp (2005) proposed that these two processes could be mediated by different neural circuits. A first circuit would mediate voluntary control of movements produced in respect to a conscious perception of the errors in synchronization, and a second circuit would mediate automatic adjustments of motor actions, produced in reaction to a subliminal perception of the errors. This proposition was made in analogy to the visual system (Milner & Goodale, 1995), in which anatomically segregated processes subserve either conscious and voluntary adaptation to the visual environment (e.g., precise reaching and grasping of an object) or automatic reaction (e.g., avoidance of a threatening object moving towards the individual) (Fig. 1.A).

However, in both rhythmic sensorimotor synchronization and locomotion, the classification of anticipatory, phase and period correction processes in automatic or voluntary categories remains a matter of discussion (see Hamacher, Herold, Wiegel, Hamacher, & Schega, 2015; Repp & Su, 2013, for reviews). The two functionally and anatomically segregated cortico-cortical pathways projecting from the auditory cortex to the frontal lobe (Fig.1.B) could provide a framework for such a distinction, in analogy with the two streams hypothesis in visual processing (Rauschecker, 2012). The functionally and anatomically segregated neural networks for beat-based and duration-based timing (Teki, Grube, Kumar, & Griffiths, 2011) are yet another framework for automatic and voluntary distinction. However, the dynamics of neural responses (i.e., unvarying vs adaptative responses) is a critical variable to integrate in order to better categorize them.
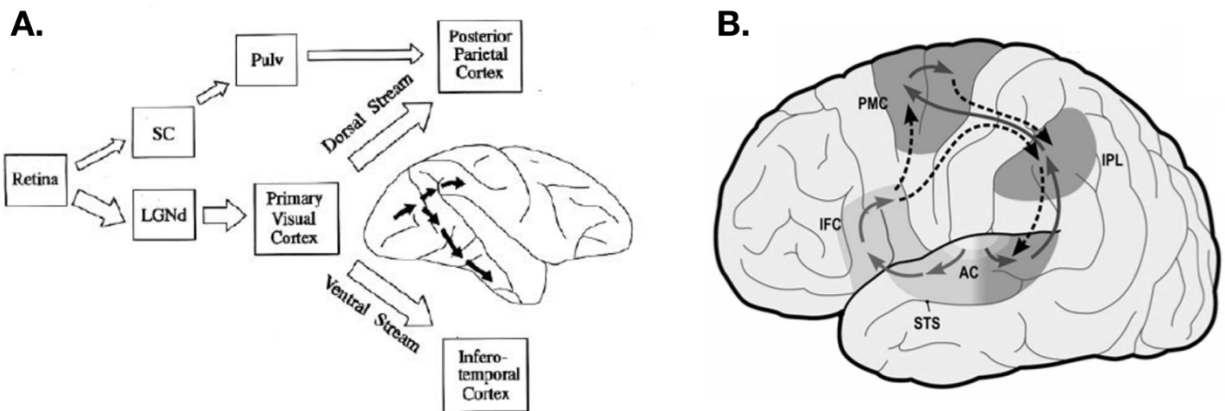
Figure 1. –   Functionally and Anatomically Segregated Cortico-Cortical Routes

A. The two functionally and anatomically segregated cortico-cortical routes projecting from primary visual cortex, as described in the macaque brain. A ventral stream projects to the infero-temporal cortex and subserves conscious monitoring of the visual environment, and a dorsal stream projects to posterior parietal cortex and subserves subliminal monitoring of the visual environment. Reproduced from Milner & Goodale (1995). **B. The two functionally and anatomically segregated cortico-cortical routes projecting from the superior temporal areas to frontal areas.** A ventral stream (in light grey) plays a general role in auditory object recognition, including perception of vocalizations and speech. A dorsal stream (in dark grey) plays a general role in sensorimotor integration and control. Adapted from (Rauschecker, 2012). AC, auditory cortex; IFC, inferior frontal cortex; IPL, inferior parietal lobule; LGNd, lateral geniculate nucleus pars dorsalis; PMC, premotor cortex; Pulv, pulvinar; SC, superior colliculus; STS, superior temporal sulcus.

Historical Considerations on the Neuroscience of Locomotion, Sensorimotor Synchronization, and Entrainment of Neural Oscillations

Exploring the neurological control of locomotion has a long history in science. At the beginning of the twentieth century, researchers asked whether the rhythmic limb movements forming the basic pattern of gait are generated by central neural networks, or by mostly peripheral neural reflex chains. The first evidence of a spinal rhythmic pattern generator was discovered by Graham Brown, who observed rhythmic limb movements in decerebrate cats, both with and without complete de-afferentation of those limbs (Graham Brown, 1911). Half a century later, Shik and colleagues demonstrated that electrical stimulation of specific regions of the brainstem can control walking and running of decerebrate cats (Shik & Orlovsky, 1976; Shik, Severin, & Orlovskii, 1966). Those findings were crucial for the understanding of the descending systems that activate and control the spinal automatisms. Importantly, the role of a parallel system responsible for elaborate adaptation of the gait to the environment was discovered, since Liddell and Phillips (1944) demonstrated that transection of the pyramidal tract in cats preserves locomotion on a flat floor, but provokes an inability to walk on a ladder. Finally, the forebrain mechanisms responsible for the voluntary control of locomotion became the focus of research in the 1990's, with emphasis given to visuomotor integration (Georgopoulos & Grillner, 1989; Grillner, Georgopoulos, & Jordan, 1997; Milner & Goodale, 1995). In humans, functional imaging performed during real locomotion revealed important information about the organization of a direct and an indirect locomotor pathway for "executive" and "planning" functions respectively (la Fougère et al., 2010). The understanding of the neural processes for adapting the gait to complex sensory environment has recently beneficiated from the apport of another field of research that has previously focused on the cognition of a large panel of human rhythmic behaviours, such as the perception of timed information and the production of timed sequences of movements.

The neuroscience of rhythm perception and rhythmic sensorimotor synchronization is still a novel field of research. The early developments were made by scientists whose principal interest lied in timing, i.e., how the brain perceives timed inputs and produces timed outputs (see Wing, 2002

for an early review; see Buzsáki & Llinás, 2017; Nobre & Van Ede, 2017 for recent reviews). Further advances came from speech and music neuropsychology (see Repp & Su, 2013 for review). Importantly, this field of research has shifted the focus to the complex mechanisms in action at diencephalic and telencephalic levels, with a large amount of studies performed in conscious humans. The involvement of traditionally motor-associated neural structures in both perceptual and motor timing has been consistently highlighted by functional imaging techniques (see Halsband, Ito, Tanji, & Freund, 1993; Ivry & Keele, 1989; O'Boyle, Freeman, & Cody, 1996; Penhune, Zatorre, & Evans, 1998 for influential studies, see Grahn, 2012, for review). It was therefore suggested that a core timing system emerges from the interaction between the cerebellum, basal ganglia and supplementary motor area. In addition, behavioural experiments investigating the errors and thresholds in timing (see Treisman, 1963; Wing & Kristofferson, 1973 for pioneer studies) yielded a model of an internal timekeeper, which was based on a pacemaker generating a rhythmic referent time (and error) combined with a counter, a store and a comparator.

Non-motor cortices have also been demonstrated as being necessary components in rhythmic sensorimotor synchronization (e.g., Rao et al., 1997; Rao, Mayer, & Harrington, 2001; but see Peretz, 1990, for precursor study). More recently, a specific contribution of language-related neural networks has been suggested for both rhythmic perception and synchronization (Merchant, Harrington, & Meck, 2013; Patel, 2006, 2014; Patel & Iversen, 2014).

Around 2010, Grube, Teki and collaborators proposed a useful distinction between different subtypes of perceptual and motor timing: a relative, *beat-based* mechanism principally centred on striato-thalamo-cortical circuits and an absolute, *duration-based* mechanism principally centred on the cerebellum (Grube, Cooper, Chinnery, & Griffiths, 2010; Grube, Lee, Griffiths, Barker, & Woodruff, 2010; S Teki, Grube, Kumar, & Griffiths, 2011; Sundeep Teki, Grube, & Griffiths, 2011; see also Kotz & Schwartze, 2011 for similar development, and see Lewis & Miall, 2003, for previous approaches). This distinction did justice to an essential piece of the research on sensorimotor synchronization, that treats the dynamics (i.e., the operating mode, and its evolution as a function of time) rather than the structural (i.e., the part of the brain) substrate of the functions. In this view, rhythmicity can entrain the feeling of a pulse (the "beat"), which is the

substrate for global synchronization between sensory and motor rhythmic processes (see Jones & Boltz, 1989; Large, Herrera, & Velasco, 2015; Large & Jones, 1999 for an overview of the Dynamic Attending Theory). Importantly, the modelled rhythmic dynamics of a beat-based neural activity echoes some of the neural activity that can be sampled using electroencephalography (EEG).

Hans Berger recorded the electrical activity of the human brain for the first time by placing a set of electrodes on the scalp and plotting the changes in voltage over time (Berger, 1929). In his observations of the newly discovered EEG signal, he described different patterns of activity. Some of them were oscillatory, meaning that the signal varied in time, repeatedly, around a central value (Radenoviü et al., 1998). This was the case for the so-called "alpha waves", which are neural oscillations in the frequency range of 8-12 Hz that are principally observed over occipital regions when the eyes are closed. These oscillations were observable in the raw EEG signal, as they reflect the synchronized activity of very large groups of neurons within the visual cortex in interaction with a core subcortical structure, the thalamus (Steriade, Gloor, Llinás, Lopes da Silva, & Mesulam, 1990). Other patterns, so-called "desynchronized" activities, had lower amplitudes, and no apparent oscillatory structure. The discovery of measurable oscillatory phenomena within the electric signals recorded from the human brain re-awakened interests for theories attributing mental functions to rhythmic brain "vibrations" (Hartley, 1749), leading to substantially speculative explanations of human memory, thoughts, or sensations (Grey Walter, 1950).

The first observations of neural oscillations were mostly made in states of low consciousness such as sleep, anaesthesia or epilepsy (see Steriade & Llinás, 1988, for review), suggesting that they should not be related to conscious neural activity. Later in the 1980's, the increasing computational power allowed researchers to measure subtler oscillations that were not directly visible in the raw EEG signal. That was the case, for example, of the 40-Hz event-related potential elicited by a 40-Hz acoustic sine wave (Galambos, Makeig, & Talmachoff, 1981). This oscillatory response, also called the auditory steady-state evoked-potential (Plourde, Stapells, & Picton, 1991), decreased in amplitude with decreased state of arousal. Therefore, it was suggested to reflect a "low-level" process of sensory information. In parallel, some of the intrinsic electrophysiological properties of mammalian neurons appeared to be rhythmic (Llinás, 1988). In

vitro measurements revealed that some neurons are able to generate a sustained rhythmic activity (i.e., to act as "pacemakers"), while some others are able to actively synchronize their activity to a rhythmic input (i.e., to act as "resonators"). Concomitant recordings of neuronal activity, measured invasively using depth electrodes (local field potentials, LFPs), and recordings performed non-invasively using scalp EEG showed that the latter is a spatiotemporally smoothed version of the former, integrated over an area of approximately 10 cm^2 and it is therefore tempting to associate scalp recording of oscillatory-like activity to periodic modulation of neuronal excitability. Therefore, the view in which neural oscillations, as recorded in the EEG, reflect sustained fluctuations in local neural excitability gained considerable momentum (Bishop, 1932; Buzsáki & Draguhn, 2004; Wang, 2010). However, there is little discernible relationship between the firing patterns of individual neurons and the EEG signals (see Buzsáki, Anastassiou, & Koch, 2012 for review). The lack of direct evidences of the exact nature of neural activity recorded non-invasively in conscious humans is probably one factor of an important debate that is still actual, in which the "oscillatory" nature of the signal is challenged by another view in which the so-called "oscillations" could simply consist in repetition of transient neural activity (see, e.g., Capilla, Pazo-Alvarez, Darriba, Campo, & Gross, 2011; Plourde et al., 1991 for studies argueing for the transient hypothesis; see e.g., Zhang, Peng, Zhang, & Hu, 2013, for a study argueing for the oscillatory hypothesis; see Haegens & Zion Golumbic, 2017; Thut, Miniussi, & Gross, 2012; Zoefel, ten Oever, & Sack, 2018, for reviews from both sides). It is now commonly accepted that the entrainment of sustained neural oscillation constitutes a neurophysiological basis for elaborated cognitive processes, such as the anticipation of upcoming rhythmic events (i.e., the anticipation of the upcoming "beat" in music) (Morillon & Schroeder, 2015), or the sensory selection of rhythmically-relevant information (Lakatos, Karmos, Mehta, Ulbert, & Schroeder, 2008).

It is likely that an increased integration of the different fields of research introduced in this brief historical review will further improve the understanding of the various neural mechanisms that control rhythmic movements, rhythm perception and the synchronization thereof. In particular, multimodal imaging has the potential to combine both structural and functional observations to form a unified model. In addition, further collaborations between researchers interested in automatic, spinal, and cognitive, cortico-subcortical control of movements could delineate a more

global view. Few of the existing models provide comprehensive integration of the automatic rhythmic processes taking place at the spinal level and the more cognitively controlled process taking place in cortico-subcortical circuits, but it appears rational to search for a unified system, rather than two different processes distinct in their evolution, their anatomical substrate, and their biological function.

Clinical Perspectives

There are multiple perspectives that arise from a better understanding of the neurological control of rhythmic movements and in particular locomotion movements. For example, Parkinson's disease is a neurodegenerative disorder that can seriously debilitate the gait. The *primum movens* of this disease is a progressive loss of dopaminergic neurons in the substantia nigra, which projects to the basal ganglia (Santens, Boon, Van Roost, & Caemaert, 2003). This group of subcortical nuclei plays a prominent role in motor behaviour, and its dysfunction leads to the cardinal motor manifestations of Parkinson's disease, which include bradykinesia and postural instability (Alexander & Crutcher, 1990; Fig. 2.A). These motor impairments are one of the causes of gait disorder (Wu, Hallett, & Chan, 2015).

Importantly, when normal gait control mechanisms are altered, patients tend to compensate with greater cognitive control (Iansek, Danoudis, & Bradfield, 2013). However, the basal ganglia are also part of a large network connecting various cortical areas responsible for non-motor, cognitive functions (Obeso, Rodriguez-Oroz, Stamelou, Bhatia, & Burn, 2014; Fig. 2.B), and its dysfunction also leads to deficits in the perception and production of rhythm (Merchant, Luciana, Hooper, Majestic, & Tuite, 2008; Parker, Lamichhane, Caetano, & Narayanan, 2013; Pastor, Artieda, Jahanshahi, & Obeso, 1992). These specific deficits are associated with considerable morbidity affecting gait and speech (Hove & Keller, 2015; Kotz, Schwartze, & Schmidt-Kassow, 2009).
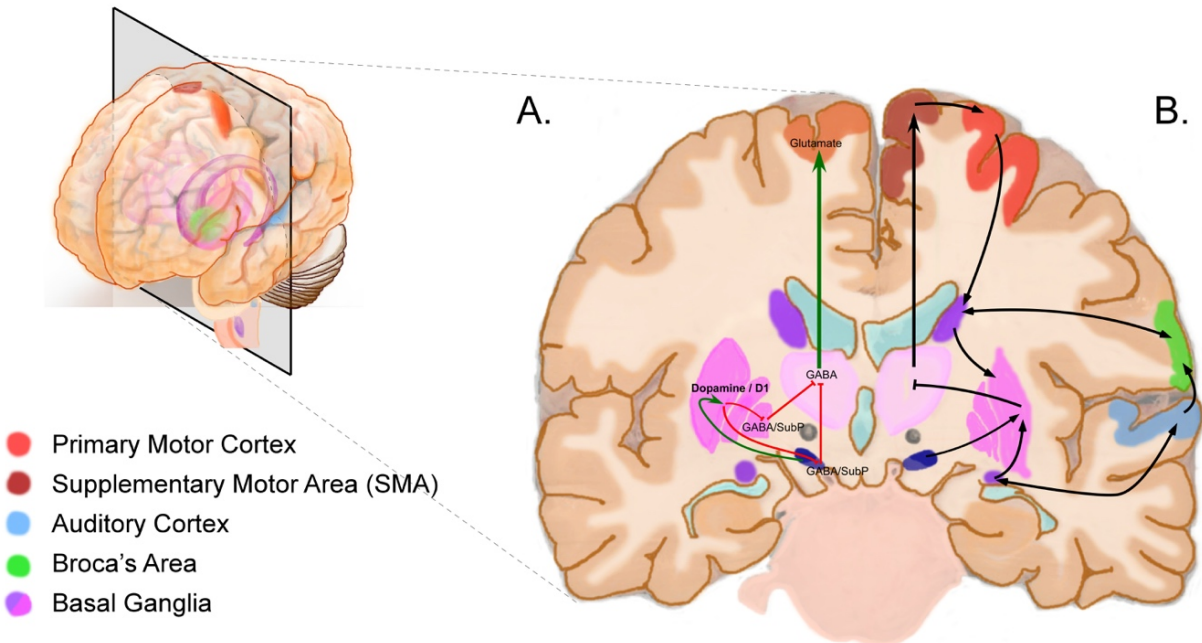
Figure 2. –   Neural Networks Involving the Basal Ganglia

A. Classical model of the "direct pathway" that is disrupted in Parkinson's Disease. The depletion of dopaminergic input in the basal ganglia results in a decreased activation of the motor cortex. Adapted from Alexander & Crutcher (1990). **B. Structural view of the cortico-basal-ganglia-thalamo-cortical network** thought to underlie multimodal integration and sensorimotor interactions in the context of rhythmic inputs. Inspired from Grahn & Rowe (2009); Jarbo & Verstynen (2015); Jeon, Anwander, & Friederici (2014); Kotz, Anwander, Axer, & Knösche (2013); Merchant et al., (2013); Nagy, Eördegh, Paróczy, Márkus, & Benedek (2006).

A comprehensive approach to addressing gait disorder in Parkinson's disease must take into account the interactions between motor and cognitive aspects of locomotion. Furthermore, a better characterization and quantification of the neural mechanisms underlying motor and cognitive functions could markedly improve patient stratification and prognosis accuracy (Insel & Cuthbert, 2015; Marras, 2015; Merchant et al., 2008; Santens et al., 2003). Most importantly, it could provide the basis for the development of new therapies aiming at modulating neural dynamics (Karas, Mikell, Christian, Liker, & Sheth, 2013; Nombela, Hughes, Owen, & Grahn, 2013).

At the end of this thesis, I will present a study aiming to establish a correlation between an EEG marker representing how body movements shape the neural representation of an acoustic rhythm and the benefits that a training program of one month consisting in walking with music can have on the gait of patients with Parkinson's disease. The implications of these results on the understanding of clinical heterogeneity will be discussed.

I will also discuss another example that illustrates the importance of an in-depth understanding of automatic and voluntary control of movement. The distinction between automatic and voluntary movements is a common clinical tool in the evaluation of patients with disorder of consciousness (Seel et al., 2010). This thesis focuses for the very first time on the case of two young women who, despite being in a minimally conscious state (MCS), were able to walk spontaneously. The findings of this thesis demonstrate that they were able to synchronize their gait to music. The interpretations regarding both the clinical significance of this observation for the classification of their state of consciousness and the implications on current models of locomotion control will be discussed.

Chapter 2 – Neural Basis for Rhythmic Entrainment

Functional Neuroanatomy of the Locomotor System

Central Pattern Generators

Central pattern generators are neuronal circuits capable of producing a rhythmic motor pattern without receiving extrinsic phasic timing information. Those circuits rely on both intrinsic electrophysiological membrane properties and synaptic properties of its constituent neurons (Getting, 1989). In its core schematization, a central pattern generator consists of two reciprocally inhibiting neurons. The active neuron shows a progressive decrease in the frequency of firing during its phase of constant depolarization (the so-called "spike-frequency adaptation"). When the active neuron stops firing, the release of inhibition on the other neuron generates a post-inhibitory rebound. Thus, the second neuron becomes active and starts the inhibition phase of the first neuron (see Marder and Bucher, 2001 for review). Such automatic circuits are highly present in limb-related spinal segments and are responsible for the rhythmic movements observed during locomotion because they control the motor neurons innervating limb muscles (Minassian, Hofstoetter, Dzeladini, Guertin, & Ijspeert, 2017).

Of course, the rhythmic locomotor system is highly versatile, and one should be able to initiate or terminate gait movements in appropriate circumstances, as well as to produce a whole range of different outputs with respect to frequency (e.g., the frequency range of human gait rate spans from 0.4 to 3.6 Hz (Nilsson & Thorstensson, 1987), and sometimes even to phase (e.g., during a military march). In fact, different modulators influence the rhythmic limb movements. They can directly modulate the intrinsic membrane properties and synaptic strength of a central pattern generator, provoke a switch between different pattern generators, influence the synapses between the generator and the motor neuron whose activity it controls, or directly command the motor neuron (Marder & Bucher, 2001). The sources of spinal modulation are multiple and comprise propriospinal interneurons and afferents, extrapyramidal and pyramidal descending tracts (Fig. 3).

Mesencephalic Locomotor System

The extrapyramidal tracts (such as the reticulospinal tract) originate from locomotor-related nuclei of the brainstem. Of them, the pedonculopontine nucleus, the nucleus cuneiformis and the subthalamic nucleus, which prolong in the pontine reticular formation (see Hamacher, Herold, Wiegel, Hamacher, & Schega, 2015 for recent review), are part of what corresponds to the so-called "mesencephalic locomotor region" in animals (Grillner et al., 1997). This is the area whose activation using electrical stimulation was reported to elicit locomotion in decerebrate cats by increasing its speed when increasing the strength of the electric current (Shik et al., 1966). In humans, deep brain stimulation delivering 25 Hz electric bursts to the pedonculopontine nucleus is suspected to alleviate freezing of gait in patients with Parkinson's disease (Stefani et al., 2007; see Thevathasan et al., 2018 for review). Furthermore, the locomotor-related brainstem nuclei show oscillatory properties, which are thought to temporally bind neuronal ensembles to produce coherent behaviours, including locomotion (Garcia-Rill, Hyde, Kezunivic, Urbano, & Petersen, 2015; Noga et al., 2017). However, it remains unclear whether the oscillatory components occurring at brainstem level are synchronized with spinal and forebrain locomotor-related neural rhythms. Nevertheless, the mesencephalic locomotor region is functionally different than other brainstem locomotor regions, as it seems to be more specifically related to the regulation of rhythm and pattern of locomotion rather than postural adjustments (see Takakusaki, 2013 for review). Importantly, this area receives inputs from the cerebellum and from forebrain centers, principally the basal ganglia and the supplementary motor area. Therefore, it is an important center in the locomotor networks that integrates information from basal ganglia and cerebellar loops (Aravamuthan, Muthusamy, Stein, Aziz, & Johansen-Berg, 2007).

Direct and Indirect Locomotor Pathways

Goal-directed locomotion involves a large panel of behaviors which are probably not controlled by a single neural network. Nevertheless, distinct networks are not expected to subtend each and every different modes of activity. Actually, locomotor networks are proposed to be organized in two distinct pathways (Hamacher et al., 2015; la Fougère et al., 2010; Takakusaki, 2013), a direct pathway and an indirect pathway. The direct pathway consists in a loop originating from the primary motor cortex that projects to spinal central pattern generators via the pyramidal tract.

The feedback runs from the spinal cord to the cerebellum then to the thalamus, and the motor cortex. The cortical locomotor commands of the indirect pathway would originate in premotor and supplementary motor areas and converge to medium spiny neurons of the basal ganglia. Its outputs would be transmitted to the brainstem nuclei through the release of tonic inhibition maintained by the substantia nigra pars reticulata. Locomotor commands would be transmitted to the spinal centers and further ascending projections would transmit to the basal ganglia and then to the thalamus, which finally projects it back to the cortex (Fig. 3).
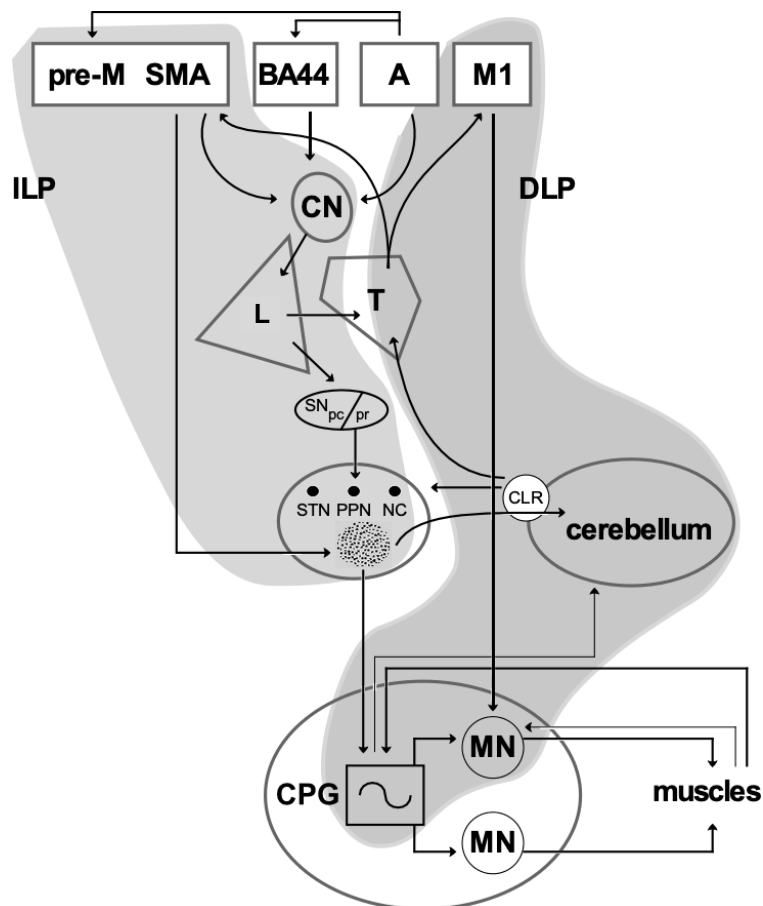
Figure 3. – Neurophysiology of Gait: a Global Model

A, auditory cortex; BA44, Brodmann area 44; CLR, cerebellar locomotor region; CN, Caudate nucleus, CPG, central pattern generator; M1, primary motor cortex; MN, motoneuron; NC, cuneiformis nucleus; L, Lenticular Nucleus, pallidum; PPN, pedonculopontine nucleus; PMC, premotor cortex; $SN_{pc/pr}$, substantia nigra pars compacta/pars reticulata; STN, subthalamic nucleus; DLP, direct locomotor pathway; ILP, indirect locomotor pathway. Note the different modulator afferences converging to the central pattern generators (the direct afference from M1 is not represented), the convergence of multiple locomotor pathways to the mesencephalic locomotor region, and the convergence of multiple cortical areas to the caudate nucleus.

It has been initially proposed that the direct locomotor pathway is involved in continuous, steady-state locomotion (e.g. locomotion on a flat ground), whereas the indirect locomotor pathway is responsible for modulation of locomotion and goal-directed actions (e.g. visuomotor control) (Hamacher et al., 2015; la Fougère et al., 2010). This view, in which the cerebellum is mostly involved in steady-state locomotion, could be coherent with the fact that the cerebellar locomotor region regulates the speed of gait trough rhythmical impulses to the brainstem and the spinal cord (Armstrong, 1988; Jahn et al., 2004). Hence, the speed is *a priori* not a high-level feature of gait, and might be controlled by relatively simple mechanisms (e.g., by modulating the tonus of mesencephalic nuclei). The prominent role of the basal ganglia in coordinating the activity of different cortical regions of the brain (e.g., Kotz et al., 2013) is also coherent with the view in which the indirect locomotor pathway is responsible for gait initiation, planning and sensori-guided walking.

However, there are several observations that are not easily integrated in the dual locomotor pathway model. Of these, the fact that patients with cerebellar damage can make reactive changes in locomotion but cannot learn predictive changes (Morton & Bastian, 2006) is contradictory with the view of a primary locomotor pathway principally responsible for steady-state locomotion. Furthermore, this view appears somehow contradictory with the importance of the pyramidal tract in the control of a variety of motor patterns such as reaching and grasping (Georgopoulos, 1995), as well as in the control of precise motor steps, leg and foot movements (Drew, Jiang, Kably, & Lavoie, 1996). Finally, the neural activity measured by Armstrong and Drew (1984) in the primary motor cortex of cats was periodically modulated and phase-locked to the steps of the animals. Whether this rhythmic activity, observed at the cortical level and presumably in the direct locomotor pathway, has an importance in the control of gait or is a simple redundancy to the spinal rhythmic pattern generators remains an open question.

Functional Neuroanatomy of Perceptual and Motor Timing

Overviews

Synchronizing rhythmic movements to an external rhythm that is perceived in the environment requires specific neural processes. Several neuroimaging experiments have linked perception and reproduction of acoustic rhythms to various cortical and sub-cortical regions of the brain. Those regions included the premotor cortex, the supplementary motor area (SMA), the cerebellum and the basal ganglia. Many of these areas are traditionally associated with the motor system, but were nevertheless critically activated in rhythmic tasks that did not involve any overt nor explicit covert movement (e.g., Middleton & Strick, 2000; see Grahn, 2012, for review). This suggests a common neural substrate for perceptual and motor timing (Teki, Grube, & Griffiths, 2011). Within this network, accurate (e.g., steps that are well aligned with the musical beat), adaptive (e.g., cadence of gait that follows the tempo of music when it changes), and robust (e.g., gait that perpetuates even if there are some perturbations in the music) timing processes emerge from the integration and the interactions of the different neural effectors.

The neural network responsible for rhythmic sensorimotor synchronization integrates information about the underlying periodicity that is perceived in the external rhythm (i.e., the pulse) with information about the errors in timing measurements (Teki, Grube, & Griffiths, 2011). The former information would be processed primarily by cortico-basal-baso-thalamo-cortical loops (Grahn & Rowe, 2009; Teki, Grube, Kumar, et al., 2011), while the latter would be processed primarily by an olivo-cerebellar network comprising the inferior olive, the vermis, and deep cerebellar nuclei (Grube, Cooper, et al., 2010; Grube, Lee, et al., 2010; Teki, Grube, Kumar, et al., 2011).

An important dynamic property emerges from the interconnections of different effectors of the neural network. Hence, some effectors possess oscillatory properties and their interconnection, i.e., their *coupling*, allows them not only to synchronize, but also to adapt and sustain their rhythmic activity, i.e., to *entrain* (Large & Jones, 1999).

Structural Basis

Acoustic rhythms that specifically entrain the perception of a pulse (so called "beat rhythms") elicit activity in the caudate nucleus, the putamen, and the pallidum (the two formers form the striatum), together with greater connectivity between the putamen and the SMA, the premotor cortex and the auditory cortex (Fig. 4), as compared to non-beat rhythms (Grahn & Rowe, 2009). Importantly, both the intensity of the activation and the connectivity are greater for beat rhythms that rely more on an internal generation of the pulse than on external induction (e.g., with physical accents). Furthermore, striatal activity is greater for beat continuation (i.e., feeling a pulse that is already present) than beat finding (i.e., initiating the perception of a pulse) and beat adjustment (i.e., adapt the pulse when the external rhythm changes) (Grahn & Rowe, 2013).
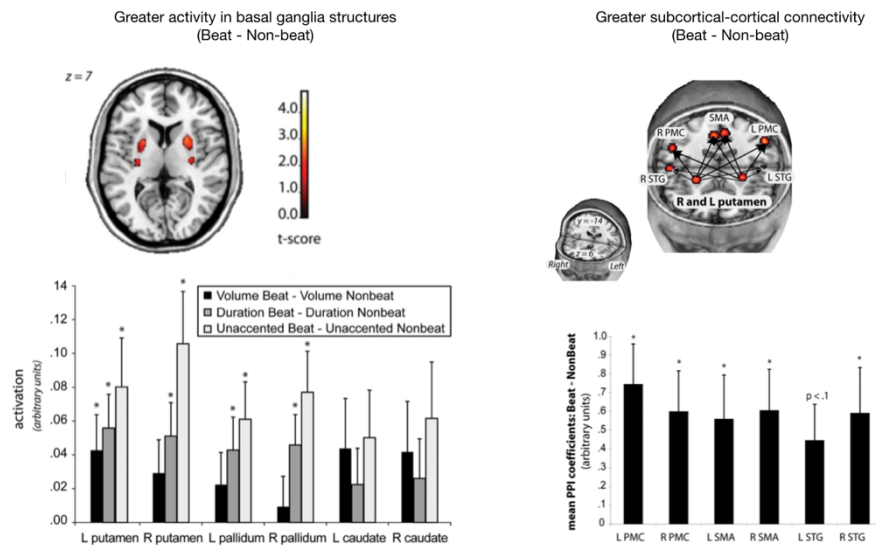
Figure 4. –   Activation of Basal Ganglia when Listening to Acoustic Rhythms

Left Panel. The activation is bilateral, and dependent of the internal generation of a pulse: the condition in which the perception of pulse strongly depends on endogenous activity ("unaccented beat") elicited the most intense activation, whereas conditions in which the beats are accented with modulation of volume amplitude ("volume beat") or with prolongation of the duration of the beat ("duration beat") elicited weaker activations.
Right Panel. Top displays regions showing increased coupling with the anterior putamen in beat vs. non-beat conditions. Mean psychophysiological interaction (PPI, arbitrary units) for each of the target regions are shown in the graph. R, Right; L, Left; PMC, premotor cortex; SMA, supplementary motor area; STG, superior temporal gyri. Adapted from Grahn & Rowe (2009).

The basal ganglia are an ensemble of subcortical structures that are strongly connected to the cerebral cortex, the thalamus, and the brainstem. The caudate nucleus receives afferent projections originating from multiple cortical regions, including the primary and supplementary motor areas (Alexander & Crutcher, 1990) and the dorsolateral prefrontal cortex (DLPFC), which is traditionally associated with attentional processes and working memory (Jarbo & Verstynen, 2015). However, the existence of projections from primary visual and auditory cortices to the caudate nucleus remains unclear (Grahn, Parkinson, & Owen, 2008; Rauschecker, 2012), although caudate neurons are responsive to visual and auditory sensory stimulation (Nagy et al., 2006). Therefore, the pathways from the auditory cortices to the basal ganglia appear to involve either or both ventral and dorsal auditory streams, which are particularly developed in humans and crucial for speech and language (Merchant & Honing, 2013; Patel, 2014; Patel & Iversen, 2014; Rauschecker, 2012; Rilling et al., 2008).

One hypothesized function of the striatum is to collect, funnel, and temporally analyse cortical information. For example, medium spiny neurons are neurons of the dorsal striatum that receive several thousands of inputs from cortical neurons, and may act as coincident detectors of synchronous activity across their broad receptive fields (Matell & Meck, 2004). Importantly, over periodic stimulation, the medium spiny neurons learn to predict the period, and therefore may constitute a specialized mechanism for the processing of a musical pulse (Teki, Grube, & Griffiths, 2011). After processing, the basal ganglia output their signal to the cortex, through projections to the thalamus, and to the mesencephalic locomotor system, through the substantia nigra pars reticulata (see section 2.1.3).

Dynamic Basis

The core dynamic neural correlates of the ability to perceive a pulse in music and to align bodily movements with it consists in the entrainment of endogenous neural oscillations to an external stream of rhythmic information, across multiple brain regions. Low-frequency (e.g., delta waves: < 4 Hz) neural oscillations are commonly regarded as rhythmic shifting of excitability in local neuronal ensembles, meaning that they influence the likelihood of neuronal firing in a periodic fashion (Bishop, 1932; Buzsáki et al., 2012; Buzsáki & Draguhn, 2004; Kayser, Montemurro,

Logothesis, & Panzeri, 2009). (Lakatos et al., 2008). Because of hierarchical cross-frequency coupling of neural oscillations (i.e., the modulation of high frequency neural oscillations by an envelope of lower frequency), the phase of an entrained oscillation can determine momentary power in neural oscillations of higher-frequencies. Such oscillations play a role in a variety of brain operations including stimulus processing, neuronal interactions across areas, and active, attentive processes of sensory information (Fries, Reynolds, Rorie, & Desimone, 2001; Womelsdorf et al., 2007).

Large & Jones (1999) proposed a mathematical model in which an internal oscillation (representing the neuronal ensembles responsible for the feeling of a pulse) is coupled to an external oscillation (representing, for example, the acoustic stream of music). In this model, each period p, indexed by n, of the internal oscillator corresponds to the time separating the last expected event (e.g., a musical beat), denoted by B_n from the next expected event, B_{n+1}. This period is defined by the relation

$$p_n = p_{n-1} + P\eta_p F(\phi_{n-1}) \, ;$$

with

$$F(\phi_{n-1}) = (2\pi)^{-1} \sin 2\pi \, \phi_{n-1} \, ;$$

$$0 < \phi_{n-1} \leq 2;$$

where P corresponds to the last period of the external oscillator and $\eta_p F(\phi)$ describes the coupling strength between the two oscillators. This relation corresponds to a system in which the expected time of the next external event is dependent on the preceding events. This serial dependency is what makes the system of internal oscillators *flexible*, as it adapts to each new event in function of the history of past events.

The coupling of an internal oscillation with an external oscillation results in a modulation of attentional energy (i.e., the likelihood for the internal system to detect an external event), which is shaped as a repeat of attentional pulses (Fig. 5.A). Those attentional pulses correspond to temporal windows within which the internal system "expects" the next event to occur. In the model proposed by Large and Jones (1999), the attentional pulses have a Gaussian distribution,

centered on each expected event, B_n. The width of the distribution is determined, for each event, by the coherence between the time B_{n-1} at which the last event was expected to occur and the time at which it actually occurred. If the coherence is high (the last event respected the last expectation), the attentional pulse for the next expectation will have a narrow dispersion and the peak of attentional energy will be high (Fig. 5.B, black line). In contrast, if the coherence is low (the last event violated the last expectation), the attentional pulse for the next expectation will have a broader dispersion and the peak of attentional energy will be lower (Fig. 5.B, dark grey line). The broader attentional pulse allows the system to entrain to events occurring at times that vary, at the cost of a lower attentional energy. This dynamic adaptation of the attentional pulse is what makes the system *robust* to perturbations, as small deviations between the phase of the internal and the external oscillators will not abrogate the entrainment. However, if the external rhythms vary to the point that no periodicity can be extracted, the internal oscillator will no longer produce attentional pulses (Fig. 5.B, light grey line). Therefore, the model system can respond to an external rhythm using two different modes: a periodic and a sustained mode.
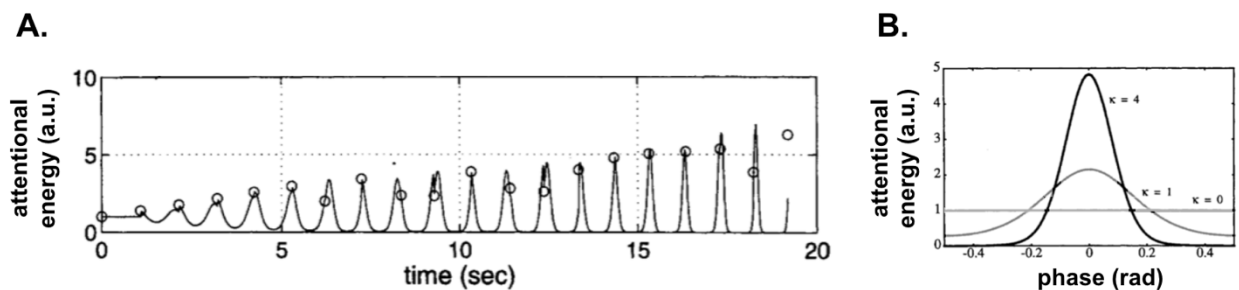
Figure 5. –   Attentional Energy

A. Modulation of the attentional energy as a function of time. The succession of external events (e.g., musical beats, represented by empty circles) entrains an internal oscillation (black line), which correspond to a modulation of attentional energy as a function of time. The coherence between the expectations and the actual beats shapes how the internal oscillation evolves with time. **B. Shape of three different attentional pulses, regarding the coherence between the last expectation and the last event.** Representation of three different attentional pulses, according to previous coherence between expectation and actual beat.

The model is compatible with a periodic modulation of neural excitability, as expected with the entrainment of neural oscillations. Essentially, it is coherent with experimental results showing an entrainment of neural oscillations in the primary visual cortex of macaque monkeys when they attended visual stimuli, as compared to when they attended auditory stimuli, presented in rhythmic streams at an average rate of 1.54 Hz (Lakatos et al., 2008). Interestingly, the entrainment of neural oscillations observed in the cortex of macaque monkeys was associated with increased event-related response amplitude, and decreased reaction times for tasks that were related to the attended modality (i.e., make a manual response to an infrequently presented "oddball" visual stimulus).

In addition, listening to an acoustic rhythm can modulate neural oscillations in motor-related areas, despite the absence of an intention to move (Fujioka, Trainor, Large, & Ross, 2012). Conversely, oscillations in the motor cortex can modulate oscillations in the auditory cortex, which could in turn influence auditory processing (de Lange, Rahnev, Donner, & Lau, 2013; Schroeder, Lakatos, Kajikawa, Partan, & Puce, 2008). These results suggest that the entrainment of neural oscillations to rhythmic streams of sensory information allows their optimal processing, and could be a core mechanism in dynamic attentional selection, in the formation of the pulse percept (Large et al., 2015), and in the synchronization of rhythmic movements to music (Fujioka et al., 2012).

Chapter 3 – Research Techniques to Investigate Entrainment

This section aims to describe the main techniques that are used throughout this work to study entrainment in humans. It also describes the relevant and robust observations that are usually made with those techniques. Furthermore, this section introduces an experimental paradigm that was designed to test the synchronization of gait in patients, and a new electrophysiological method that was designed to study, using EEG, the nearly periodic brain activity related to the production of rhythmic movements.

Sensorimotor Synchronization: Behavioural Measures

Introduction and Preliminary Considerations

The evaluation of sensorimotor synchronization (SMS) has a long history, and emerged from research fields investigating the perception of time (Fraisse, 1984; Stevens, 1886), and the psychology of music (Jaques-Dalcroze, 1920). More recently, the interest on SMS gained a considerable momentum in clinical research. Particularly, the measures of SMS are robust behavioural data that are indicative of the individual's ability to perceive time intervals, to react to the environment, or to anticipate and adapt to changes (Repp, 2005; Repp & Su, 2013). Therefore, those tools can serve to evaluate various neurological functions, including motor (Merchant et al., 2008) and cognitive (Allman & Meck, 2012) functions, in patients. Furthermore, the use of external cues to improve gait in patients, which was first reported in 1942 (Von Wilzenben, 1942), is now gaining considerable evidence-based support (e.g., Ellis et al., 2005; Hausdorff et al., 2007; Thaut et al., 1996, see Lim et al., 2005; Spaulding et al., 2013 for reviews).

SMS is defined as "the coordination of rhythmic movement with an external rhythm" (Repp & Su, 2013). Therefore, one should be cautious when comparing or extrapolating the following concepts to non-rhythmic sensorimotor behaviours (e.g., motor responses elicited by transient, or highly aleatory sensory events). As discussed in section 1, rhythmic behaviours are fundamentally distinct from non-rhythmic behaviours in the way that the firsts can involve *entrainment*, a phenomenon by which the periodic repetition of events creates periodic windows

of anticipation, in which the upcoming events are expected to occur (Jones, 1976; Jones & Boltz, 1989). In contrast, non-rhythmic behaviours rely on different mechanisms of anticipation, in which the expectation rather follows a "hazard function" distribution, i.e. an increasing conditional probability over time that an upcoming event will occur given that it has not already occurred (Coull, 2009).

SMS can be performed with rhythmic stimulation presented in any sensory modality. For a long time, a "superiority" of the auditory modality over other modalities for SMS was observed: SMS was consistently more accurate when participants had to synchronize with acoustic rhythm stimuli than with visual or somatosensory rhythm stimuli (e.g., Jäncke, Loose, Lutz, Specht, & Shah, 2000, see Repp & Su, 2013, for review). However, recent evidence suggests that appropriate stimuli design (e.g., a bouncing ball rather than a visual flash) can at least reduce this superiority (Hove, Fairhurst, Kotz, & Keller, 2013; Y. Huang, Gu, Yang, & Wu, 2017). The rhythmic patterns that are involved in SMS can vary widely. The simplest form of stimulation is an isochronous rhythm (e.g., a metronome), but the pattern can be highly elaborated. For example, multiple hierarchical levels of periodicity (Povel & Essens, 1985) and/or syncopation (Velasco & Large, 2011) can be used in order to differentiate the synchronization to external physical events from the synchronization to internal pulse perception. Perturbations of the phase (Repp, 2001b, 2001a, 2002b) or variations of the period (Keller, 2008; Repp & Keller, 2004) can be added to the rhythm in order to study how participants will react or adapt to changes. Finally, the rhythmic stimulation can be removed (in a "synchronization-continuation task"; Stevens, 1886) or even absent (the participants move therefore at their spontaneous rhythm) in order to evaluate the "internal time keeper" (Drake, Jones, & Baruch, 2000; Semjen, Schulze, & Vorberg, 2000).

SMS can involve movements produced by any part of the body, and those movements can either be discrete (e.g., finger taps on a hard surface, or steps) or continuous (e.g., rocking the upper body). Those parameters do not solely determine the type of data that has to be analysed (e.g., a discrete time series of events vs. a continuous variation of position as a function of time), they also have a direct influence on the performance of SMS. For example, SMS was found to be more precise when participants clapped in their hands than when they bounced to the same acoustic rhythms (Tranchant, Vuvan, & Peretz, 2016).

This work focuses on discrete rhythmic movements synchronized to discrete sensory events (this is the case, for example, for steps that are synchronized to the beats of music). This section presents the main measures and analyses that can be performed, the values that are usually observed, and the usual interpretations that are made from those data. It also presents some important measures and analyses that can be performed on discrete rhythmic movements produced without external sensory cues.

Usual Measures

Interevent Intervals Time Series and their Structure

The Interevent Intervals Time Series

Interevent intervals (IEI) are defined as the time interval between two consecutive events (expressed in seconds). They can either concern the events from a sensory rhythm (in this case, the more specific denomination of interbeat[2] intervals (IBI) can be used), or the events from a motor rhythm (in this case, the more specific denomination of intertap intervals (ITI), interstep intervals, or interstride intervals (ISI) can be used). The interevent intervals time series is the series of IEI, indexed in time order.

Spontaneous Motor Interevent Intervals Distribution, Autocorrelations and Spectral Distribution

When a motor rhythm is produced spontaneously, the motor interevent intervals time series can reveal pertinent information regarding a participant's rhythmic skills.

A measure of the central tendency is the *median IEI* (in seconds, but often converted in Hz). Its value is approximately 500–600 ms (Repp & Su, 2013; Tranchant et al., 2016). It appears to be shorter for musicians than non-musicians, at least during childhood (Drake et al., 2000). This measure is considered to reflect an individual's general subjective tempo, called the "referent period". Taking a dynamic-system approach, this measure is further interpreted as a reflection of

---

[2] In this case, the "beat" refers to the acoustic events that convey the rhythmic information. One should be aware that the "beat" is also defined as the regularity perceived in acoustic rhythms (i.e., the "pulse"). Some authors use interonset interval (IOI) instead of interbeat interval.

the natural frequency of an internal *attentional* oscillator (Drake et al., 2000). However, it could as well reflect the natural frequency of any motor pacemaker oscillator involved in the production of the rhythmic movement, or simply correspond to range of frequency determined by biophysical constraints.

A measure of the spontaneous variance is the *coefficient of variation of IEI* (i.e., the standard deviation, expressed in % of the mean IEI). Its value is approximately 20–25% (Drake et al., 2000), and is proportional to the IEI duration, within a relatively wide range (Michon, 1967). This measure reflects how unstable a spontaneous rhythmic movement can be. Wing and Kristofferson (Wing, 1980; Wing & Kristofferson, 1973a, 1973b) introduced a model in which the motor IEI variance is attributed to two distinct processes: a central timekeeper, and peripheral motor constraints. Because the peripheral variance is small, most of the individual differences in variability are attributed to differences of the internal timekeeper.

The *variations of the IEI over time* have received a notable research interest. Rather than being a simple aleatory noise, each IEI varies in a way that is dependent on the preceding IEIs. The sequential dependencies translate into long-range positive autocorrelations in IEI time series (Hausdorff et al., 1996). That is to say, its function of autocorrelations (i.e., the correlation of the signal with a delayed copy of itself, as a function of delay, or lag[3]) decays slowly as the lag increases. Long-range autocorrelations can be visualized as a particular frequency distribution: the magnitude of the variation is exponentially decaying as a function of frequency, i.e., it follows a 1/f spectral distribution (see Fig. 8, in section 3.1.2.2.3). The 1/f distribution has the particularity to be scale-independent, and is therefore sometimes called "fractal noise."

The presence of autocorrelations in the motor IEI variability is sometimes interpreted as reflecting intrinsic properties of the internal timekeeper (Repp, 2005), but it is more commonly considered as an emerging property of a complex dynamic system, in which different processes are operating at different time scales (Wing, Daffertshofer, & Pressing, 2004).

---

[3] A formal, mathematical, definition of correlation functions is provided in the glossary, at the end of this work. (Chatfield, 1989).

It has been shown that some gait debilitating disorders, such as Parkinson's disease, can be associated with a degradation of the long-range autocorrelations of interstride intervals variability (Hausdorff, 2009). Furthermore, this degradation was strongly correlated with other clinical scores, suggesting that the temporal organization of gait variability is related to the degree of functional impairment in Parkinson's disease, and can be used as quantitative measure of gait stability (Warlop, 2017).

Comparison of Motor and Sensory Interevent Intervals

Non-parametric tests comparing the median IBI and ITI can be used to test sensorimotor synchronization. A mismatch reflects a poor synchronization, but a match does not necessarily imply good synchronization (Repp & Su, 2013).

The variance of ITI can be an indicator of a participant's synchronization skill (Repp, 2005). However, this variable is strongly dependent on the variability of the interonset intervals that form the sensory rhythm. For example, if a participant is perfectly synchronized to an acoustic rhythm, and the later has important fluctuations of tempo, the variance of ITI will necessarily be high. This is not indicative of poor synchronization, but this is not either indicative of good synchronization.

Actually, direct comparisons of motor and sensory IEI distributions are blind to a significant part of the synchronization dynamics. For example, some studies showed that the fractal properties present in acoustic IBI were also observed in the synchronized motor ITI (Rankin, Large, & Fink, 2009; Stephen, Stepp, Dixon, & Turvey, 2008; Warlop, Chemin et al., 2015). However, such findings are not indicative of predictive behaviour, nor passive tracking (Repp & Su, 2013). Likewise, the long-range autocorrelations that are observed in spontaneous ITI time series changed to short range negative autocorrelations when the participants synchronized to a metronome, whereas such a structure was not present in the acoustic rhythm (Torre & Delignières, 2008). Per se, such findings are not particularly informative. Actually, an adequate description of synchronization behaviours necessitates finer characterizations of sensory and motor events time series.

The *coefficient of cross-correlation* between motor and sensory IEIs is a reliable measure. It quantifies the similarities between the sensory and motor event time series, for different lags between the two signals. For example, if an acoustic rhythm has random variations of IBI, and if the participant follows these variations, the fluctuations of ITI will probably echo the variations of IBI, with a lag of +1 (e.g., a short IBI would be followed by a short ITI). A high coefficient of correlation at lag1 would ensue (Michon, 1967). In contrast, if the participant anticipates the variations of IBI, the participant would adjust his movements such that his taps would coincide with the acoustic beats. Then, the fluctuations of ITI would probably match the variations of IBI, with no lag. A high coefficient of correlation at lag 0 would ensue. Therefore, lag1 and lag0 cross-correlations are indices of *tracking* and *anticipation*, respectively. Several authors have proposed to quantify those behaviours with those two values, or their ratio, eventually corrected for the autocorrelations presents in the IBI time series (e.g., Nozaradan, Peretz, & Keller, 2016; Repp, 2002a; Repp & Keller, 2008).

However, this approach reaches a limit a soon as the data do not meet some strict assumptions. First, an equal number of IBI and ITI is required. Second, tracking has to faithfully occur right after each perturbation, and anticipation has to occur precisely at the time of each perturbation. While it may be the case in strictly controlled situations, with well-trained participants, it is obviously not the case when evaluating patients with motor disorder. Therefore, an adapted method is proposed in this work, at section 3.2.2.

Asynchronies and their Variability

Asynchronies

Asynchronies are defined as the difference between the time of a motor event (e.g., a finger tap, or a step) and the time of the corresponding event onset in the acoustic rhythm (e.g., the click of a metronome) (Repp & Su, 2013). They are usually expressed as a measure of relative time (in seconds), with 0 s being the time of the reference acoustic event. However, they can also be expressed as a measure of relative phase (in radians). In this case, 0π corresponds to the angle of the reference acoustic event, and 2π corresponds to the distance between the reference event and the preceding or the next event (Fig. 6).

relative time

relative phase
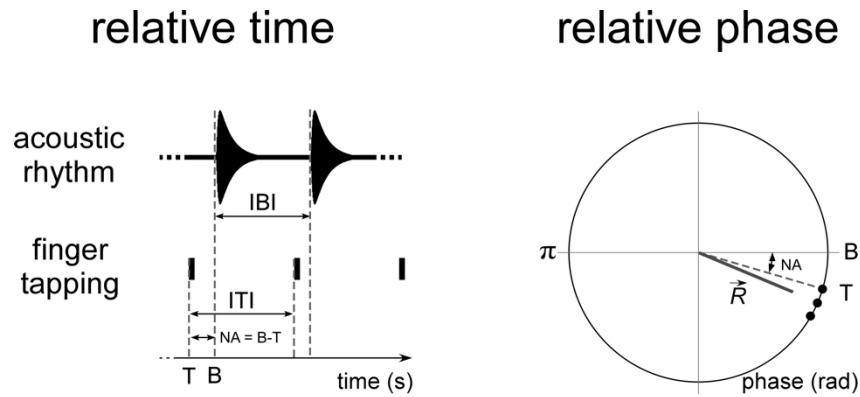
Figure 6. –   Asynchronies and Interevent Intervals

Left panel: the acoustic beats and finger taps are represented on a linear time scale. The interbeat interval (IBI) corresponds to the time between two beats, and the intertap interval (ITI) corresponds to the time between two taps. The (negative) asynchrony (NA) corresponds to the time between and acoustic beat (B) and the corresponding tap (T). **Right panel:** the finger taps are represented on a circular time scale, where the acoustic beats are all aligned at 0π. The asynchrony corresponds to the value of T, in radians. The vector $\vec{R}$ corresponds to the resultant of each phase deviation between the motor event and the acoustic events.

Expressing the asynchronies as relative phases, and the measures related to the asynchronies as circular variables (Fisher, 1993), offers several advantages. They have a significant importance when it comes to the study of SMS in potentially poor synchronizer individuals (e.g., patients with gait disorder), or with acoustic rhythms whose tempo fluctuates in time. First, circular statistics easily deal with great variability in synchronization (e.g., when a participant sometimes walks in phase, and sometimes in antiphase relative to the acoustic rhythm, or when a participant walks at a different tempo than the acoustic rhythm). In contrast, analyses of asynchronies expressed in relative time usually require rejecting motor events that are too distant from the corresponding acoustic events (e.g., Keller, Schultz, van der Steen, & Mills, 2015). Second, circular statistics are insensitive to variations of tempo along a synchronization sequence, as each asynchrony is expressed as a proportion of the time between two acoustic events (e.g., Fujii et al., 2014).

Central Tendency of the Asynchronies

The central tendency of the asynchronies is expressed as the *mean asynchrony* (in seconds), or as the angular deviation of the resultant vector of phase deviation of each motor event relative to the acoustic events (in radians, Fig. 6). It is an index of synchronization precision.

The mean asynchrony is typically negative (and thus, often referred to as the negative mean asynchrony, or NMA). Its value is approximately -50 ms for SMS to an 500 ms IBI isochronous acoustic rhythm and tends to be approximately 30 ms shorter for musicians (Krause, Pollok, & Schnitzler, 2010). It is also dependent on the tempo of the acoustic rhythm, and the tempo of the rhythmic movement (Repp & Keller, 2008; Zendel, Ross, & Fujioka, 2011).

The NMA is commonly interpreted as a sign that participants anticipate rather than react to the rhythmic stimulus (Repp, 2005). In fact, as the shortest reaction time to a transient event is approximately 150 ms, any asynchrony inferior to this value is a demonstration of anticipation (Repp & Su, 2013).

Multiple neurophysiological models of the NMA have been suggested, but none of them fully predict all the experimental data (see Repp, 2005; Repp & Su, 2013, for review). A first category of explanations consider that the negative asynchrony is necessary to achieve perceptual synchrony. In this model, the negative asynchrony reflects the fact that the time to process auditory information is different than the time to process somatosensory information, either because of the differences in nerve transmission times (Fraisse, 1984) or because of different accumulation rates of sensory evidence (Aschersleben, 2002). The perception of synchrony with different timing of sensory processing is represented in Fig. 7.
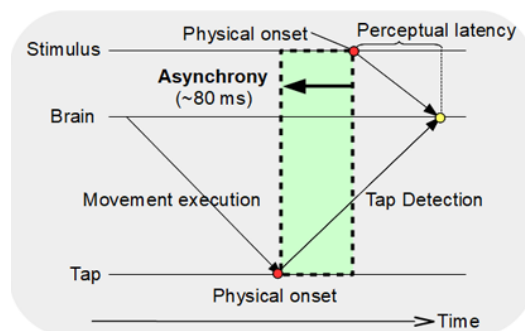
Figure 7. –   Negative Asynchrony as the Result of Different Sensory Processing Time.

(Sugano, Keetels, & Vroomen, 2017)**.**

Another category of explanation postulates that the negative asynchrony is the consequence of a small mismatch between the natural frequencies of auditory and the motor oscillators. In this model, the motor oscillator would be intrinsically faster than the auditory oscillator, and a phase lag would thus result between the two oscillations (Yu, Russell, & Stenard, 2003). Similarly, the NMA could be a consequence of perceptual underestimation of the time between two successive acoustic events, resulting in a shortened period of the oscillator that controls the tapping tempo (Craig, 1973).

Variance of the Asynchronies

The variance of asynchronies is expressed as the standard deviation of asynchrony (expressed in seconds, or expressed as % of the period, in which case it should be referred to as a coefficient of variation), or as the length of the resultant vector of phase deviation of each motor event relative to the acoustic events (Fig. 6). It is an index of synchronization stability, or consistency.

The variance of asynchronies is usually small. Its value is approximately 5–6 %, and does not differ between amateur musicians and non-musicians (Repp & Su, 2013). However, it is smaller in trained musicians, and was reported to be as small as 1.6% in professional drummers (Fujii et al., 2011). It is linearly dependent on the tempo of the acoustic rhythm, and the tempo of the rhythmic movement, within a relatively large range of tempi (Zendel et al., 2011).

A wide variance of asynchronies is significant of poor synchronization (Dalla Bella & Sowiński, 2015; Repp, 2005; Repp & Su, 2013; Tranchant et al., 2016). This variable is actually one of the best indexes of a participant's rhythmic synchronization skill.

The variance of asynchronies appears to be structured in time, in a similar fashion than the spontaneous motor IEI time series (Torre & Delignières, 2008). This structure contrasts with the negative, short-range autocorrelations that are observed in the motor IEI, when participants synchronize their movements to a metronome (Fig. 8).

asynchronies

interevent intervals
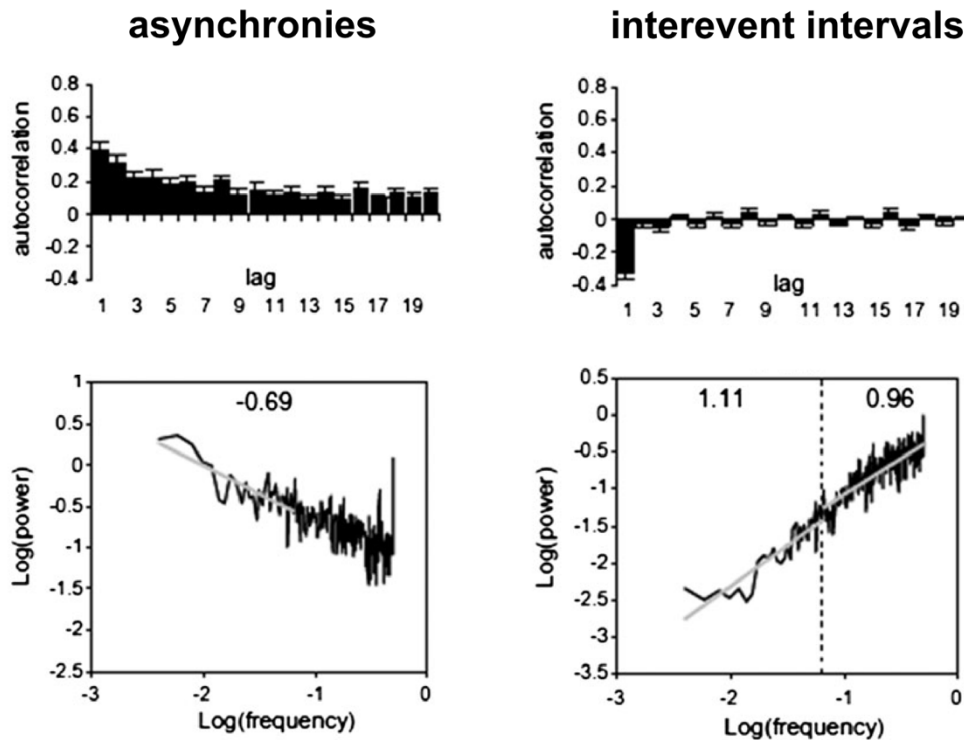
Figure 8. –   Structure of the Variability of Asynchronies

Upper Panel: Autocorrelation functions in the times series of the asynchronies between isochronous acoustic events and synchronized taps, and in the time series of the intertap intervals. **Lower panel:** Loglinear relationship between the magnitude of the signal and its frequency. Long-range positive autocorrelations and 1/f frequency distribution are observed in the asynchronies time series, whereas short-range negative autocorrelations are observed in the intertap intervals time series. Adapted from Torre & Delignières (2008).

The neurophysiological model that accounts for the presence of long-range positive autocorrelations in asynchrony time series proposes that synchronized rhythmic movements are under the control of an internal oscillatory process (the so-called "internal timekeeper"), which generates the fractal noise. In contrast, a local phase correction process that constantly adjusts the motor rhythm to the external rhythm would be responsible for short-range negative autocorrelations.

Error correction and coupling strength

Models of error correction

A constant process of correction is necessary to maintain the synchronization of a motor rhythm to a sensory rhythm. Without this process, the intrinsic variability of any periodic motor activity would accumulate from event to event and progressively lead to desynchronization, even to an isochronous rhythm, which is the simplest expression of a rhythm (Hary & Moore, 1987).

Various models describing rhythmic sensorimotor synchronization error correction have been proposed (Wing & Kristofferson, 1973a), and reviewed by Bruno Repp (2005; 2013). Those models usually involve two parameters, which are measures of sensorimotor coupling strength: a *phase correction* parameter (often denoted α) and a *period correction* parameter (often denoted β).

These different parameters can be experimentally estimated. To do so, researchers introduce perturbations (i.e., phase or period changes) in acoustic rhythms, and measure how these perturbations affect the SMS of participants (see Michon, 1967 for an introduction to the concept; see Repp, 2001b; van der Steen et al., 2015, for further development).

Local perturbations and error correction parameters to transient changes

Unpredictable perturbations. Different local perturbations can be introduced in an isochronous sequence, and the participant's reaction can be evaluated by averaging a number of trials containing the same perturbation (see Repp, 2005, for review). The typical reactions to three types of local perturbations (a phase shift, an event onset shift, and a period shift) are represented in Fig. 9.
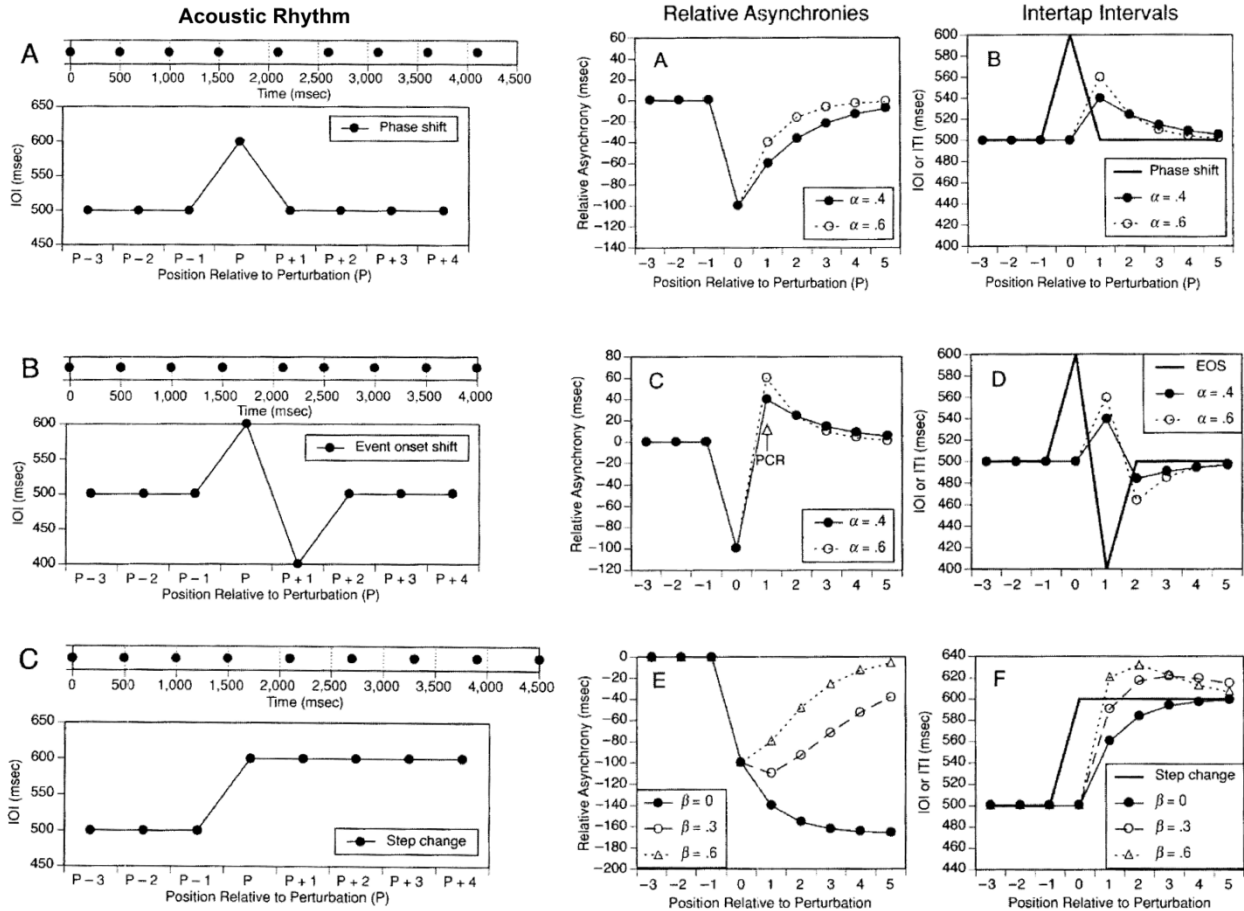
Figure 9. –   Local Perturbation in Rhythm

Local perturbations consisting in phase shift **(A),** event onset shift **(B),** and period shift **(C),** and the average error corrections observed in relative asynchronies and intertap intervals. Adapted from Repp (2005)**.**

A convenient way to estimate the phase correction parameter (α) is to measure the so-called phase correction response (PCR), for different magnitudes of phase perturbation. The PCR corresponds to the shift in asynchrony of tap that follows the perturbation, as compared to the asynchrony at the tap corresponding to the perturbation (Fig. 9; Repp & Su, 2013). The slope of the PCR as a function of perturbation magnitude is an estimate of the phase correction parameter.

Remarkably, it has been shown that the correction following phase shifts that are well below the perceptual detection threshold are as quick as the correction following detectable phase shifts (Repp, 2000, 2001a). Moreover, participants were shown to be unable to prevent the PCR

following an event onset shift, even when they were instructed to ignore the perturbation (Repp, 2002b). In contrast, period correction depended on whether or not a tempo change had been detected, and can be inhibited by will (Hary & Moore, 1985; Repp, 2001b; Repp & Keller, 2004). Those observations suggest that phase correction to local and unpredictable perturbations is rapid and automatic, whereas period correction is at least in part dependent on awareness of a tempo change.

Predictable Perturbations. When (musician) participants have advance knowledge of an upcoming local phase shift, they are able to advance or delay the tap relative to the perturbed acoustic event and therefore reduce the asynchrony occurring at that point (Repp & Moseley, 2012). This suggests that phase correction can be under intentional control, and is therefore not solely an automatic behaviour, as it was suggested from experiment investigating unpredictable local perturbations.

Global perturbations

Series of perturbation can be introduced into an acoustic rhythm, in order to create global perturbations. Importantly, the structure of the perturbed rhythm can implicitly carry the information necessary for participants to anticipate the upcoming perturbation. This information principally emerges from sequential dependencies, i.e., autocorrelations, between the interevent intervals (Rankin, Fink, & Large, 2014; Rankin et al., 2009).

The cross-correlations of the IEIs are a way to explore tracking or anticipative behaviours (see section 3.1.2.1.3). In a series of paper, van der Steen et al. (2013;2015) introduced a system that adapts the timing of acoustic events according to real time measures of a participant's synchronization. The adaptive system can either counteract or worsen the different corrections parameters, and therefore estimate them in individuals. Three important observations were made from the study of coupling strength in SMS with globally perturbed rhythms.

First, Repp, Keller, and Jacoby (2012) compared the phase correction (α) estimates for musically trained participants synchronizing with isochronous rhythms (i.e., no perturbation), adaptively timed acoustic rhythms (i.e., global predictable perturbations), and isochronous rhythms with local phase perturbations (i.e., local unpredictable perturbations). They showed that the α

estimates were much larger for local phase perturbations than for the two other conditions. Actually, positional analysis of the data revealed a strong but not long-lasting α increase (i.e., phase coupling) immediately following a local phase shift. Second, Launay, Dean, and Bailes (2011) showed that global but unpredictable perturbations weakens the phase coupling strength, as compared to a condition with no perturbation. Third, van der Steen et al. (2015), compared the estimates for both phase (α) and period (β) correction, in participants synchronizing to acoustic rhythms with global and predictable perturbations. Importantly, they showed that period coupling was more important and yielded better synchronization than phase correction.

In summary, a strong, transient, and automatic phase coupling is observed after local and unpredictable phase perturbations. A weak phase coupling is observed when the perturbations are global and unpredictable. No information is available about period coupling when the perturbations are global and unpredictable, but it can be assumed that it would not be very strong, and that participants would probably not synchronize accurately to such acoustic rhythms. Finally, a strong period coupling, but weak phase coupling, is observed when the perturbations are global and predictable.

Importantly, those results suggest that the response to local phase perturbation is both quantitatively and qualitatively different from the mechanisms that are at work during SMS with isochronous or continuously perturbed sequences.

Evaluation of Gait Synchronization to Acoustic Rhythms: Proposed Protocol

This experimental protocol and the prototype set-up were developed in the course of my research project, and used in studies 4 and 5. The code necessary to produce the acoustic rhythms and to analyse the data was made available as an open-source Matlab toolbox on the GitHub repository: https://github.com/BaptisteChemin/BCToolbox.

Experimental design

Overview

The synchronization of gait to acoustic rhythms is evaluated in individual sessions. Each session contains five trials, corresponding to five different walking conditions. The first trial consists in walking spontaneously, in silence. The four following trials consist in walking with four different acoustic rhythms. The order of the last four trials is randomized for each session.

Acoustic Rhythms

For the spontaneous walking condition, participants receive a warning signal indicating the beginning of the trial, and a second signal to indicate the end of the trial. The four acoustic rhythms, used in the other conditions, are the following: a rhythm with predictable tempo fluctuations, a rhythm with non-predictable tempo fluctuations, a rhythm with no tempo fluctuation, and an adaptation of the popular music ("Happy", by Pharrell Williams). The four acoustic rhythms have different interests: rhythms with predictable tempo fluctuations have gradual changes of tempo, which participants usually easily follow (Rankin et al., 2014); rhythms with non-predictable tempo fluctuations have aleatory changes of tempo, which are difficult to follow; isochronous rhythms can be considered as the simplest expression of beat; and the music has a high groove, which is a feature of music that naturally entrains movement (Janata, Tomic, & Haberman, 2012). All the acoustic rhythms have a tempo set to 85% of a participant's spontaneous walking cadence, assessed one hour prior to the evaluation session (Benoit et al., 2014).

The acoustic rhythms with predictable tempo fluctuations consists in sequences of K acoustic events. The number of events is fitted to the experimental constraints (i.e., time constraints in clinical evaluations, or statistical power constraints in certain time series data analyses that demand a large sample of events; Torre & Delignières, 2008). The acoustic events (or "beats") are made of a white noise lasting 150 ms (7.5 ms rise time, 142.5 ms fall time), and occur at a mean interbeat interval of the length determined prior to the evaluation session. Predictable fluctuations are introduced by adding a certain amount of jitter to each interbeat interval, as follows. First, a K-points jitter time series is generated from white noise. Second, the time series is filtered using a 1/f FFT-filter. The 1/f FFT-filter presents the advantage to be scale-independent, i.e., the jitter time series always present the same overall spectral characteristics, regardless of the chosen number of events, K. Third, the filtered time series is scaled such that its coefficient of variation is controlled (e.g., at 5% of the mean interbeat interval). The coefficient of variation is chosen in order to limit the amplitude of the tempo fluctuations within a range of anisochrony that is known to preserve the perception of a certain regularity (Madison & Merker, 2002). Finally, jitter time series having a non-normal distribution (assessed using an Anderson-Darling test) are excluded from the experiments. The predictable aspect of the rhythm emerges from the gradual, 1/f, changes in tempo (i.e., the rhythm tends to progressively change from longer to shorter interbeat intervals, allowing the participants to anticipate the duration of the upcoming interval (Rankin et al., 2014, 2009).

The non-predictable tempo fluctuations are generated by shuffling the order of the interbeat intervals of the interbeat interval sequence with predictable fluctuations (Fig. 10). This operation results in removing all the auto-correlations of the 1/f-filtered sequences, thereby removing all gradual changes in tempo and, hence, all information that would allow predicting the length of the upcoming interbeat interval.

The isochronous acoustic rhythms consist in sequences of K similar acoustic events, occurring at a constant interbeat interval whose length is determined prior to the evaluation session.
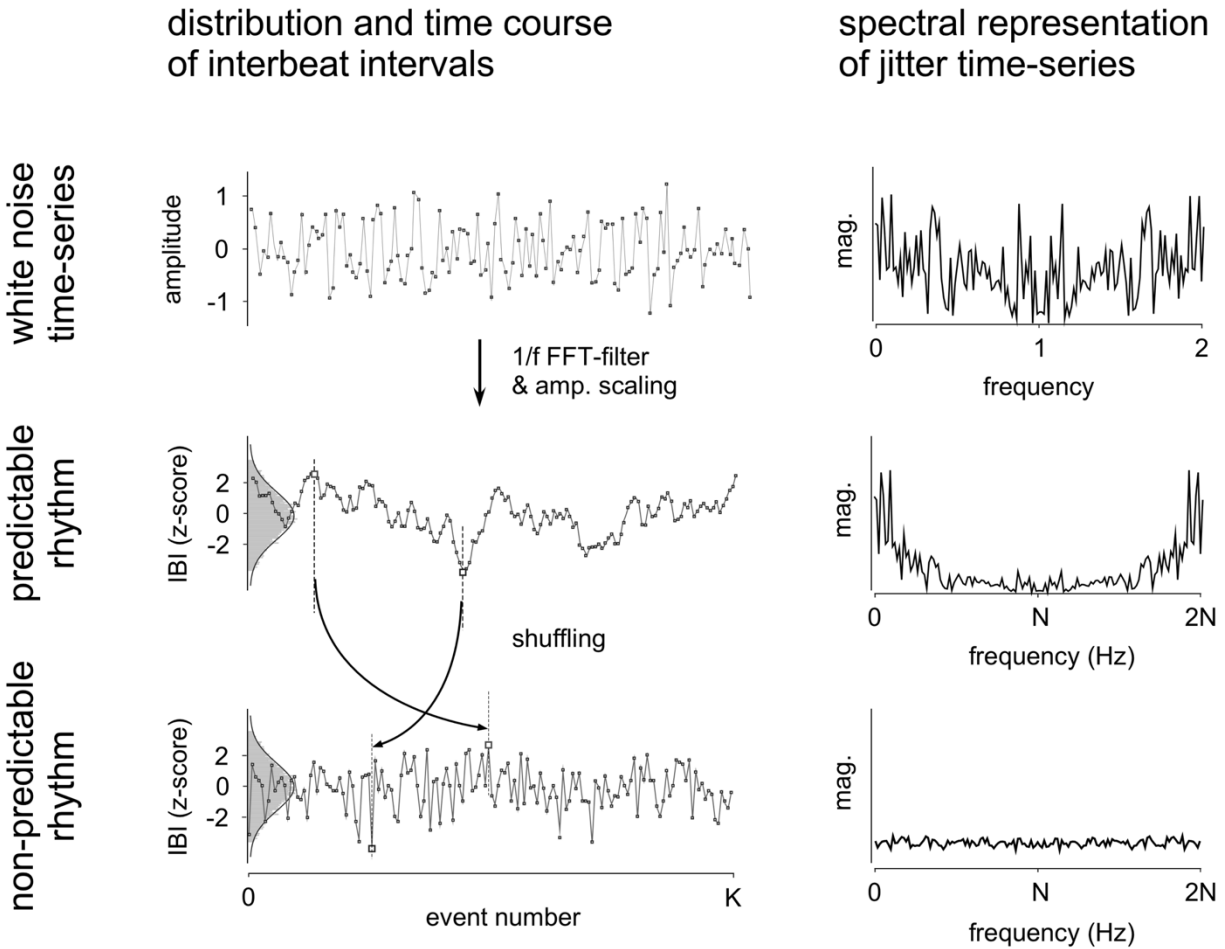
Figure 10. –   Generation of Predictable and Non-Predictable series of Interbeat Intervals

Acoustic rhythms with predictable fluctuations are generated from K-points white noise, filtered using a 1/f FFT-filter. Acoustic rhythms with non-predictable fluctuations are generated by shuffling the order of the interbeat intervals of the interbeat interval sequence with predictable fluctuations. Note that the filtered time series are scaled such that the coefficient of variation is controlled (e.g., at 5% of the mean interbeat interval).

The acoustic events of the music (i.e., the "musical beats") have been manually identified by one investigator (Chemin B.) and assessed by an independent professional musician (Filbrich A.). The tempo of the music is adapted to the target tempo using an algorithm that yields the minimal possible acoustic distortion (ZTX algorithm, Zynaptic, Germany), and an electronic beat is superimposed on every identified event. This electronic beat serves as an additional cue of musical beat and ensures the perfect alignment of acoustic events and triggers latency.

Testing

Participants walk in a neutral sound environment. They wear a pouch at their waist, which contains the stimulating/recording set-up (Fig. 11). The acoustic rhythms are played via a portable MP3-player (Sansa Clip, SanDisk, USA) and headphones (HP H2800, Hewlett Packard, USA), at comfortable, low volume. Limb motions are captured by four two-axis accelerometers, whose signals are recorded together with the acoustic stimulation, at a sampling rate of 250 Hz. The accelerometers are attached on the radiocarpal joint (upper limb) and on the lateral malleolus (lower limbs), bilaterally (Fig. 11).
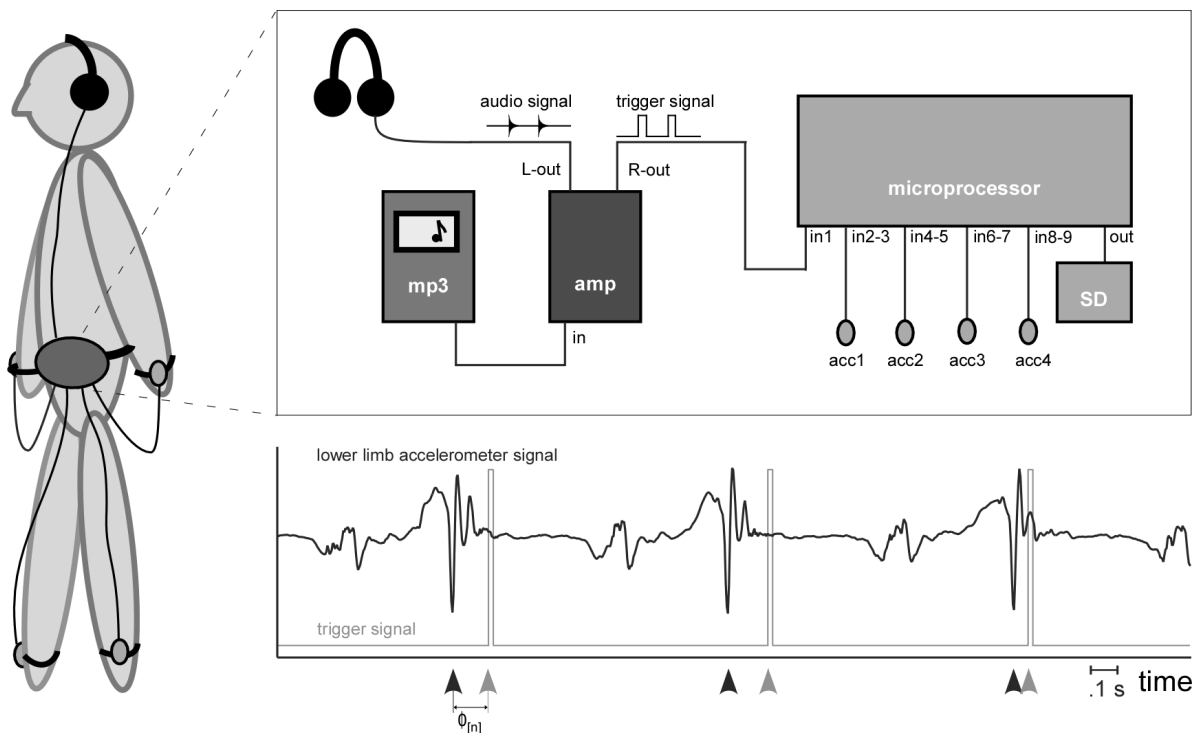
Figure 11. – Evaluation of Gait: Set-Up

Upper panel: Schematic representation of the stimulating/recording set-up. A portable mp3 player read the files (.wav; 44.1 kHz) containing the audio and the trigger signals. The signals are amplified and delivered to the participant and the data acquisition box via separated channels. Four two-axis accelerometers senses limbs motions. A microprocessor (Arduino-UNO) coupled with an SD-card writer records the trigger and the accelerometer signals in real time, at a sampling rate of 250 Hz. **Lower Panel:** Signal generated by the lower limb accelerometer. The peak of maximal negative acceleration accounts for each step latency (black arrows). The state level changes of the trigger signal accounts for each acoustic event (or "beat") latency (grey arrows). The relative phase ϕ_n^{beat} corresponds to the time between a step and an acoustic event, relative to the instantaneous interbeat interval.

Analysis

Pre-Processing

The step latencies (i.e., the latencies at which the heels reach the floor) are identified in the vertical accelerometer signals of both lower limbs as the latencies of the peaks of maximal negative acceleration (Fortune, Morrow, & Kaufman, 2014) (Fig. 11). The acoustic event latencies are identified in the trigger signals as the latencies at which state level transitions from 0 to 1. The first two step latencies following the initiation of the trial are discarded for further analysis, as participants always need a short time to align their movements to the acoustic rhythms (Repp, 2005).

For each of the five trials, indexed by n, each acoustic event (or "beat") latency is denoted by $B_{n;k}$ (in seconds, at beat k). Each interbeat interval is denoted $IBI_{n;k}$, with $IBI_{n;k} := B_{n;k} - B_{n;k-1}$, for $k = 3, ..., K$. Each step latency is denoted by $S_{n;k'}$ (in seconds, at step k' which corresponds to the step that is the closest to the kth acoustic event). Each interstep interval is denoted $ISI_{n;k'}$, with $ISI_{n;k'} := S_{n;k'} - S_{n;k'-1}$ for $k' = 3, ..., K$, and the median ISI is denoted $\widehat{ISI}_n$.

The phase deviation $\phi_{n;k'}^{step}$ (in radians, at step k') of each step relative to the median ISI is computed as

$$\phi_{n;k'}^{step} = 2\pi S_{n;k'} / \widehat{ISI}_n .$$

For each of the four acoustic rhythms, a "virtual" relative phase $\phi_{n;k'}^{virt}$ (in radians) between each step measured in the *spontaneous* gait trial, whose index is n_{spont}, and the closest acoustic event latency extracted from each of the four acoustic rhythms, indexed n_{rhythm}, is computed as

$$\phi_{n_{rhythm};k'}^{virt} = 2\pi \left(B_{n_{rhythm};k} - S_{n_{spont};k'} \right) / \left(B_{n_{rhythm};k} - B_{n_{rhythm};k-1} \right) .$$

Finally, the relative phase, $\phi_{n;k'}^{beat}$ (in radians) between each step measured in each of the four trials involving an acoustic rhythm, indexed by n, and the closest acoustic event latency extracted from the acoustic rhythm of the same trial n, is computed as

$$\phi_{n;k'}^{beat} = 2\pi \left(B_{n;k} - S_{n;k'} \right) / \left(B_{n;k} - B_{n;k-1} \right) \text{ (Fujii et al., 2014b).}$$

Measures

A measure of the consistency of the walking cadence, R_n^{step}, is computed for each trial. This measure, which reflects the variance of the walking cadence[4], is obtained by calculating the resultant vector length of phase deviation of each step relative to the median ISI ($\phi_{n,k'}^{step}$ for $k = 3, ..., K$), using the *circ_r* function of the CircStat matlab toolbox (Berens, 2009). The resultant vector (R_n^{step}) has a value equal to 1 when the walking cadence remains perfectly stable along the entire trial and tends towards 0 when the walking cadence is highly non-stationary.

A measure of the synchronization consistency occurring by chance between the spontaneous gait and each of the four acoustic rhythms, R_n^{virt}, is obtained by calculating the resultant vector length of the phases of each step relative to their corresponding beat ($\phi_{n,k'}^{virt}$ for $k = 3, ..., K$), using the *circ_r* function of the CircStat toolbox. This measure is inversely proportional to the spontaneous step dispersion around the acoustic events, and spans from 0 (i.e., a participant's spontaneous gait is not synchronized by chance to an acoustic rhythm), to 1 (i.e., a participant's spontaneous gait cadence is, by chance, perfectly matching the tempo of an acoustic rhythm (Fujii et al., 2014b; Repp, 2005). This "virtual synchronization" measure serves as a detection of false positive results: if the spontaneous gait happens to be synchronized by chance to one of the acoustic rhythms, the actual measures of synchronization that are developed here after cannot be interpreted properly.

For each of the four trials using a real acoustic rhythm, a measure of consistency of the synchronization between the steps and the acoustic beats, R_n^{beat}, is obtained by calculating the resultant vector length of the phases $\phi_{n,k'}^{beat}$. This measure is inversely proportional to the tap dispersion around the acoustic events, and spans from 0 (i.e., maximal dispersion, i.e., poor synchronization) to 1 (i.e., no dispersion, i.e., perfect synchronization). A measure of the mean accuracy of the synchronization between the taps and the beats[5], θ^{beat}, is obtained by calculating the mean of the phases $\phi_{n,k'}^{beat}$ using the *circ_mean* functions of the CircStat toolbox. This measure of accuracy reflects the mean deviation between the steps and the acoustic events, and spans

---

[4] see section 3.1.2.1.2 & section 3.1.2.1.3
[5] see section 3.1.2.2.2 on negative mean asynchrony.

from 0 (i.e., perfect phase alignment) to $\pm\pi$ radians (negative value: the steps precede the beats; positive value: the steps follow the beats).

Finally, the cross-correlation function is computed between the waveform that corresponds to the time course of the interbeat intervals as a function of time, and the waveform that corresponds to the time course of the interstep intervals as a function of time, for the predictable and the non-predictable trials. Consequently, the abscissa of those waveforms corresponds to the elapsed time along a trial, and the ordinate corresponds to the gait cadence, at any given time of the trial (see, e.g., Fig. 45 in section 5.1.2.4.2). This approach slightly differs from prior approaches in that the cross-correlation function is not computed from the interevent intervals classed on an *ordinal* axis (Michon, 1967). Actually, these prior approaches are valid under the assumption that the ordinal classification of the interbeat intervals is the same as the one from the interstep intervals. This assumption is met only in good synchronization datasets, where one and only one step is associated with each acoustic event.

 In the obtained cross-correlation function, the maximal value $xcorr_{max}$, and its lag lag_{max} are measured within a range spanning from -5 to +5 s. The value $xcorr_{max}$ represents the maximal similarity between the fluctuations of the gait cadence and the fluctuations of the acoustic rhythm tempo. This value spans from -1 (gait fluctuations are the exact opposite of the acoustic fluctuations) to +1 (gait fluctuations match perfectly the acoustic fluctuations). A value of 0 indicates no correlation between the two signals. The value lag_{max} indicates the lag at which the maximal correlation is observed, in seconds (i.e., whether the participant followed or anticipated the acoustic rhythm fluctuations).

Statistical Validation of Individual Measures

Each step time series is tested for circular uniformity using a Rayleigh test (Fisher, 1993). This test indicates if the steps occur periodically on the circle whose circumference is determined by the target period (i.e., the mean interstep interval in the case of R^{step}, and the fluctuating period of the beat in the case of R^{beat}). The interpretation of this result requires some caution: for spontaneous step time series, a significant result indicates that the walking cadence is stable, but

in the synchronized step time series, a significant result is not sufficient to prove that the observed level of synchronization could not arrive by chance.

The probability to observe a particular measure within each given time series is computed with Monte-Carlo statistics (Prichard & James, 1994). This method consists in generating, for each single trial, 10,000 phase randomized surrogate time series. Then, the observed measures (R^{beat} and $xcorr_{max}$ in the case of step time series recorded during acoustic rhythms trials, R^{virt} in the case of step time series recorded in silent trials) are compared to the 10,000 surrogated measures. The one-tailed significance level is set to 95% of the surrogated measures (Fig. 12). This test quantifies the probability to observe the synchronization measures, given the step time series that are actually recorded, at the single observation level. In other words, it tests the probability that the measured degree of synchronization is significant, or if it could just be measured by chance with a similar step time series. Importantly, because the basis of the test is a phase randomization, its result is indicative of phase adaptation, regardless of the direction of the mean relative phase θ^{beat}.

A. Probability Density Function

B. Illustrative Data
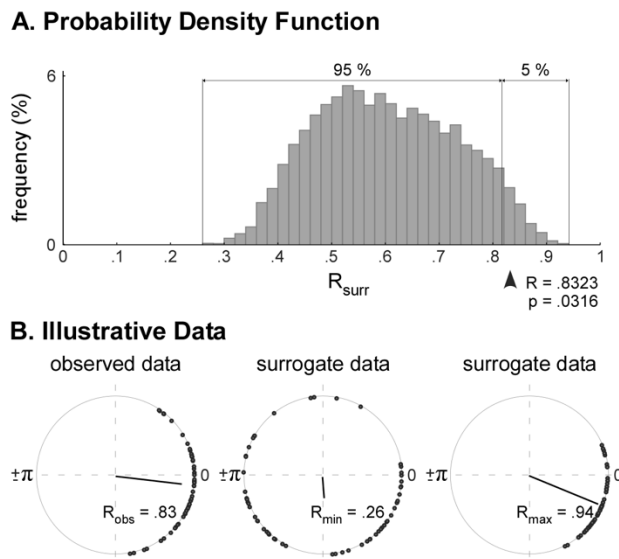
Figure 12. – Statistical Validation of the Measure of Synchronization Consistency, at Individual Level

The measure made in the original time series ("observed data", B. left plot) is higher than 95% of the surrogated data, generated from the observed time series. For comparison, the surrogated data yielding the lowest and the highest measure of synchronization consistency are represented in middle and right plot, respectively (B. R_{min} and R_{max}).

Comparison of Spontaneous and Synchronized Gait

To statistically test the frequency synchronization of the gait to the acoustic rhythm, the distribution of the interstep intervals measured during each of the four acoustically paced trials is compared to the distribution of the ISI measured in the spontaneous trial, using a Wilcoxon rank sum test. This test reflects the adaptation of gait cadence to the acoustic rhythm.

An index comparing the consistency of step synchronization to the auditory rhythm and the consistency of step dispersion around its median interstep interval is computed as R^{beat}/R^{step}. This index is <1 if the participant's gait is more consistent to its own cadence than to the acoustic tempo (e.g., when the participant walks at a different tempo than the stimulation, with a gait tempo nevertheless stable, or when the participant walks at the mean tempo of a fluctuating rhythm, but ignoring the fluctuations), and the index was>1 if the participant gait is more coherent to the acoustic rhythm than to its own cadence (e.g., the participant adapted his gait cadence to the fluctuating stimulation tempo).

Electrophysiological Approaches to Study the Neural Processes Related to the Perception of Sensory Rhythms, the Production of Rhythmic Movements, and the Synchronization Thereof

Introduction

At first glance, electrophysiological approaches appear to be ideal to study neural entrainment. It is in the EEG signal that rhythmic neural activity was observed for the first time (Berger, 1929). This rhythmic activity was noticeably proposed to reflect intrinsic neuronal oscillatory properties, or at least to be a manifestation of those properties integrated at the level of neural ensembles (Buzsáki et al., 2012; Buzsáki & Draguhn, 2004; Buzsáki & Llinás, 2017; Llinás, 2014; Steriade, 2001, 2006; Steriade et al., 1990). In this view, the measured rhythmic activity (the "neural oscillations") reflects fluctuations of excitability within neuronal assemblies, which influence the likelihood of neuronal firing in a periodic fashion (see section 2.2.3; Bishop, 1932; Buzsáki & Draguhn, 2004; Lakatos et al., 2008). The neural oscillations can either arise endogenously, i.e., they reflect the activity of neural pacemakers that generate periodic outputs, or be entrained by exogenous stimuli, i.e., they reflect the activity of neural resonators that actively synchronize to periodic inputs (see Llinás, 1988; Llinás & Yarom, 1981, for the description of in vitro neural oscillators, see also Lakatos et al., 2008; Thut, Schyns, & Gross, 2011 for the concept of neural entrainment).

But is it really so easy? Over the years, many arguments have cast doubt on this assumption. There is robust and undisputed evidence that the periodic presentation of a sensory stimulus induces a periodic response measurable in the EEG signal, and that the production of rhythmic movements coincides with periodic variations of EEG signal amplitude. However, there is a long debate about the underlying physiology of such electroencephalographic measures. Besides the view of neural oscillations, it has been proposed that the rhythmic activity that is measured in the electroencephalogram is nothing more than a regular repetition of transient evoked responses (Plourde et al., 1991; Regan, 1966). In this view, the transient evoked responses are often

considered to be constant in phase and amplitude, across the repetitions. Those responses are also assumed to reflect "low-level"[6] processes of sensory information.

Importantly, the theoretical frameworks of dynamic attending (Drake et al., 2000; Jones, 1976; Jones & Boltz, 1989; Large & Jones, 1999), active sensing (Schroeder, Wilson, Radman, Scharfman, & Lakatos, 2010), and predictive timing (Lakatos et al., 2008; Morillon & Schroeder, 2015) constitute an interesting bridge between, on one hand, the physiological phenomena of neural oscillations and neural entrainment, and on the other hand, many behavioural phenomena including the perception of sensory rhythms, the production of rhythmic movements, and their synchronization to a sensory rhythm. Therefore, determining the presence, or the absence, of oscillatory phenomena is a crux in many studies relying on those frameworks. Furthermore, the distinction between oscillatory or transient phenomena has far-reaching implications in developing approaches to numerous neurological disorders, as new strategies aiming at recovering normal neural dynamics imply to accurately understand and measure those dynamics (Kringelbach, 2011).

Discrimination between the two phenomena is not an easy task: the two phenomena can occur concomitantly, and therefore the presence of an evident transient evoked response does not exclude the presence of an oscillatory activity. One of the major limitations of electrophysiological techniques is the poor signal-to noise ratio, which is often enhanced by averaging multiple segments of signals recorded in similar conditions. This operation can "blur" all the relevant dynamics of the neural activity (Mouraux & Iannetti, 2008). Therefore, particular caution should be used when inferring, from averaged responses, that a neural activity is steady or invariant. However, one thing remains certain: the high sampling rate of electroencephalography and

---

[6] The distinction between "low" and "high" levels is primarily an anatomical criterion, but is often associated with a (fallacious) functional assumption, which is that the cognition is hierarchically organized, and that the most complex processes take place at the cortical level (see, e.g., Schroeder & Foxe, 2005; Sporns, Tononi, & Edelman, 2000, for discussion). In electrophysiology, this distinction roughly corresponds to the difference between early and late components. The early components correspond to the first stages of sensory information processing, that occur at "low" anatomical levels. The late components correspond to the last stages of information processing, that occur at "high" anatomical level. The late components are the components that usually change under different cognitive experimental conditions (but see Nozaradan, Schönwiesner, et al. (2016), for interesting alternative results.

related techniques (MEG, ECoG, …) is a major advantage over other techniques (such as PET, fMRI, …) that often lack the temporal resolution to study the dynamics of neural entrainment.

The Steady-State Evoked-Potentials

In an early study following the publication of Hans Berger's work, Adrian and Matthews (1934) demonstrated that a rhythmic sensory stimulation (e.g., a visual flicker) can induce a measurable rhythmic change in voltage amplitude of the EEG signal, at the frequency of the stimulation (Fig. 13.A).
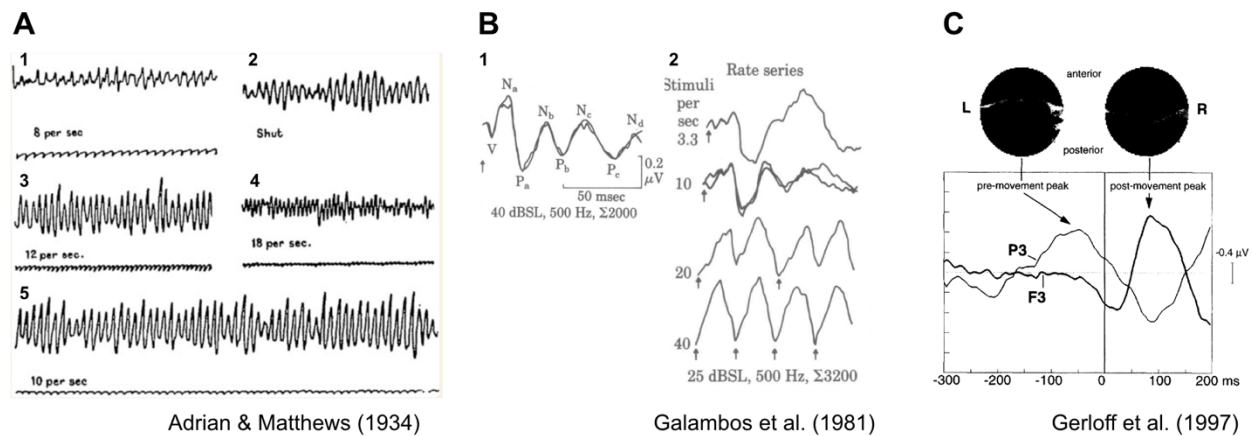
Figure 13. – Examples of Different Rhythms Observed in the EEG Signal

A. EEG signal elicited by visual flicker (signal line shows frequency of flicker). 1. Flicker at 8/s. 2. Eyes closed and field dark. Berger rhythm at 10/s. 3. Flicker at 12/s. 4. Flicker at 18/s. 5. Flicker at 10/s. Reproduced from Adrian & Matthews (1934). **B.** EEG signal elicited by auditory rhythm. 1. Unitary response to a single tone. 2. Auditory response elicited by the repetition of the tone, at increasing frequency. Reproduced from Galambos et al. (1981). **C.** EEG signal recorded during self-paced repetitive (2 Hz) finger-tapping. Reproduced from Gerloff et al. (1997).

It is much later that a periodic signal was recorded in concordance with a periodic movement (Fig. 13.C; Gerloff et al., 1997, 1998). The context in which this activity was first described was largely shaped by previous studies focusing on the preparation of single movements (Kornhuber & Deecke, 1965), and is therefore less anchored in the oscillatory paradigm. Moreover, several obstacles may have slowed research on motor-related rhythmic EEG signals. For example, strong movement-related artefacts are still an important limitation in the study of gait-related EEG

signals (Gwin, Gramann, Makeig, & Ferris, 2010; Kline, Huang, Snyder, & Ferris, 2015). The lack of spatial resolution usually renders difficult the disentangling of movement-related and sensory cueing related EEG activities elicited in sensorimotor synchronization tasks (Nozaradan, 2014). The important non-stationarities present in self-paced rhythmic movements can also blur the related signal (Chemin, Huang, Mulders, & Mouraux, 2018).

A classical representation of a periodic signal is obtained using a Fourier transform. This operation reveals the spectrum of the EEG signal (i.e., magnitude as a function of frequency). This representation has multiple interests. First, all the signal of interest is "concentrated" on a limited, and a priori known, number of frequency bins (i.e., the fundamental frequency, which is defined as $F = \frac{1}{p}$ (in hertz) with p being the period (in seconds) at which the stimulus is repeated, and its harmonics $2F, 3F, ...$). Second, because the background noise is distributed across the spectrum, this representation yields a good signal-to-noise ratio. Those first two elements make it easy to measure the overall magnitude of the signal of interest. Third, this representation is convenient when multiple streams of periodic stimulation are presented concomitantly, at different frequencies, because the responses to each of those streams are segregated on different frequency bins (e.g., Nozaradan, Peretz, & Mouraux, 2012a). Fourth, it is insensitive to variations of phase-alignment, which can be important across individuals, e.g., in the case of musical pulse perception (Nozaradan, Schönwiesner, Keller, Lenc, & Lehmann, 2018).

The electrophysiological method consisting in identifying and measuring the periodic responses to periodic stimulation in the frequency domain is often called the "frequency-tagging" approach (Nozaradan, 2014). Obviously, representing a signal in the time - or in the frequency domain is, most of the time, simply a convenient way to envision it from different points of view (Fig. 14). Some caution is needed, however, when processing the signal in one domain or the other, as some operations do not yield the same result (e.g., averaging multiple segments of a signal in the time domain blurs non-phase-locked activity, while the same operation carried out in the frequency domain preserves it).

time domain
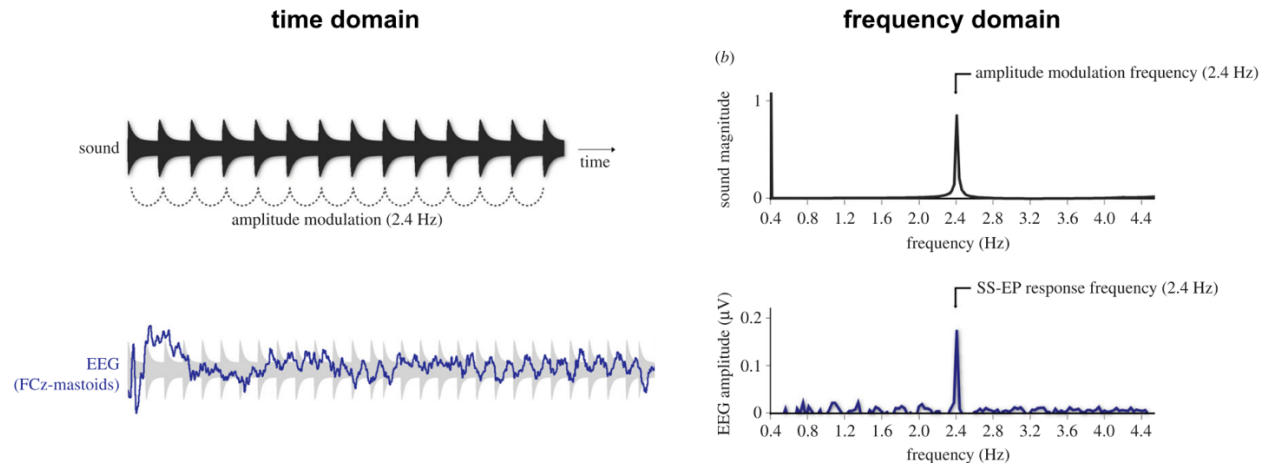
frequency domain

Figure 14. – Acoustic Rhythm and EEG response in Time and Frequency Domains

Representation of an isochronous acoustic rhythm (top) and the EEG signal (bottom) elicited by this rhythm (averaged across trials, in eight participants). Time domain representation (left) and frequency domain representation (right). Adapted from Nozaradan, Peretz, Missal, & Mouraux, 2011.

Transient Events vs Sustained Oscillation

Modeling the Signal from a Transient Response

Some early studies showed that the superposition (in the time domain) of the transient response evoked by a single presentation of the stimulus, at the rate of the stimulus repetition, can predict the shape of the measured rhythmic change in voltage amplitude of the EEG signal (e.g., Hari, Hamalainen, & Joutsiniemi, 1989). This observation led to several conclusions regarding the nature and the origin of the signal. First, the fact that the rhythmic signal can be predicted from the transient response indicates that this response contains both brainstem and cortical contributions. Indeed, the transient response contains components that are generated in both the brainstem and the cortex (wave V and wave Pa, respectively, Fig. 13.B.1) (Plourde et al., 1991). Second, because the rhythmic signal could be constructed from the superposition of identical unitary waveforms, it was assumed to be stable in phase and amplitude over time, and was therefore denominated the "steady-state" evoked potential (Regan, 1966). Finally, because of the apparent invariance of the rhythmic EEG signal elicited by the periodic repetition of a sensory stimulus, the steady-state evoked-potential was interpreted as a measure of "low-level" sensory processes (e.g., Picton, John, Dimitrijevic, & Purcell, 2003).

Nonlinear Input-Output Transformation, as a Marker of Resonance

Any oscillator possesses a natural frequency, i.e., a frequency at which it tends to oscillate in the absence of any driving or damping force. The phenomenon of resonance is a consequence of oscillators natural frequencies. It corresponds to the fact that a resonating oscillator, stimulated by an external rhythmic input, preferentially entrains at specific frequencies (i.e., the frequencies that are close to the natural frequency). Therefore, the response of a neural oscillator should show a natural bias towards certain frequencies, rather than linearly translate each of the stimulus frequency. The pulse perception, i.e., the perception of a periodicity at certain frequencies when listening to music, is hypothesized to emerge from this phenomenon (van Noorden & Moelants, 1999).

In a series of studies, Nozaradan and colleagues showed that such a nonlinear transformation can be measured in the EEG spectrum of participants listening to complex acoustic rhythms (Nozaradan, Mouraux, et al., 2016; Nozaradan et al., 2012a, 2018, also see Henry, Herrmann, & Grahn, 2017; Nozaradan, Keller, Rossion, & Mouraux, 2017, for discussion). Participants were presented with various acoustic rhythms, each of them designed to induce a pulse[7] perception at 1.25 Hz (Povel & Essens, 1985). However, for some rhythms, the acoustic energy was low at the frequency of the pulse (this is characteristic of "syncopated" rhythms). Nevertheless, the measured rhythmic responses revealed a selective enhancement of pulse-related (1.25 Hz) over pulse-unrelated frequencies, even though pulse-related frequencies were not physically marked in some rhythms. Critically, participants showing the strongest neural responses at the pulse frequency also revealed superior predictive behaviours in sensorimotor synchronization tasks, as evaluated by the cross-correlations between the fluctuations of an acoustic rhythm and the fluctuations of the synchronized tapping rhythm (Nozaradan et al., 2018). The later observation further strengthens the hypothesis of a functional relationship between entrainment of neural oscillations to sensory rhythms and temporal anticipation embedded in rhythmic behaviours.

Another mean to disclose the resonance phenomenon is to measure the frequency-tuning response of neural ensembles presumably entraining to sensory rhythms of gradually changing

---

[7] In those studies, the pulse is called the "beat", and the pulse-related frequencies, the "beat-", or the "meter-related frequencies".

frequency. For example, when an acoustic rhythm is presented at two different tempi, a low-pass bias (i.e., a bias towards the resonance frequency range of neural oscillators) can be observed: therefore, the selective enhancement of frequencies would not only be related to the pulse (in which case, higher frequencies would be prominent at the fastest acoustic tempo), it would also be dependent on the natural range of resonance frequencies. Furthermore, this bias can also observed in behavioural data, as participants tend to tap at (subharmonic) frequencies within the .5-5 Hz range, independently of the tempo (Nozaradan et al., 2018).

The interpretation of "nonlinear" selective enhancement of frequencies within the range of neural resonance should be made with caution. In fact, Fig. 15 shows how the spectrum of a transient evoked response acts as a confounding "resonance frequency band", which selectively enhances the magnitude of the frequencies that are close to, for example, 6 Hz (Zhou, Melloni, Poeppel, & Ding, 2016). Critically, this example strictly assumes the hypothesis of a neural response that is only built from the repetition of an invariant transient response, at the rate of the stimulus repetition. At present, no study categorically determined whether the selective entrainment cannot simply be explained by the repetition of transient responses, at event-related times only. The present work introduces a tool that allows one to model a rhythmic EEG signal from a transient response, and such a tool could be useful to answer this question.
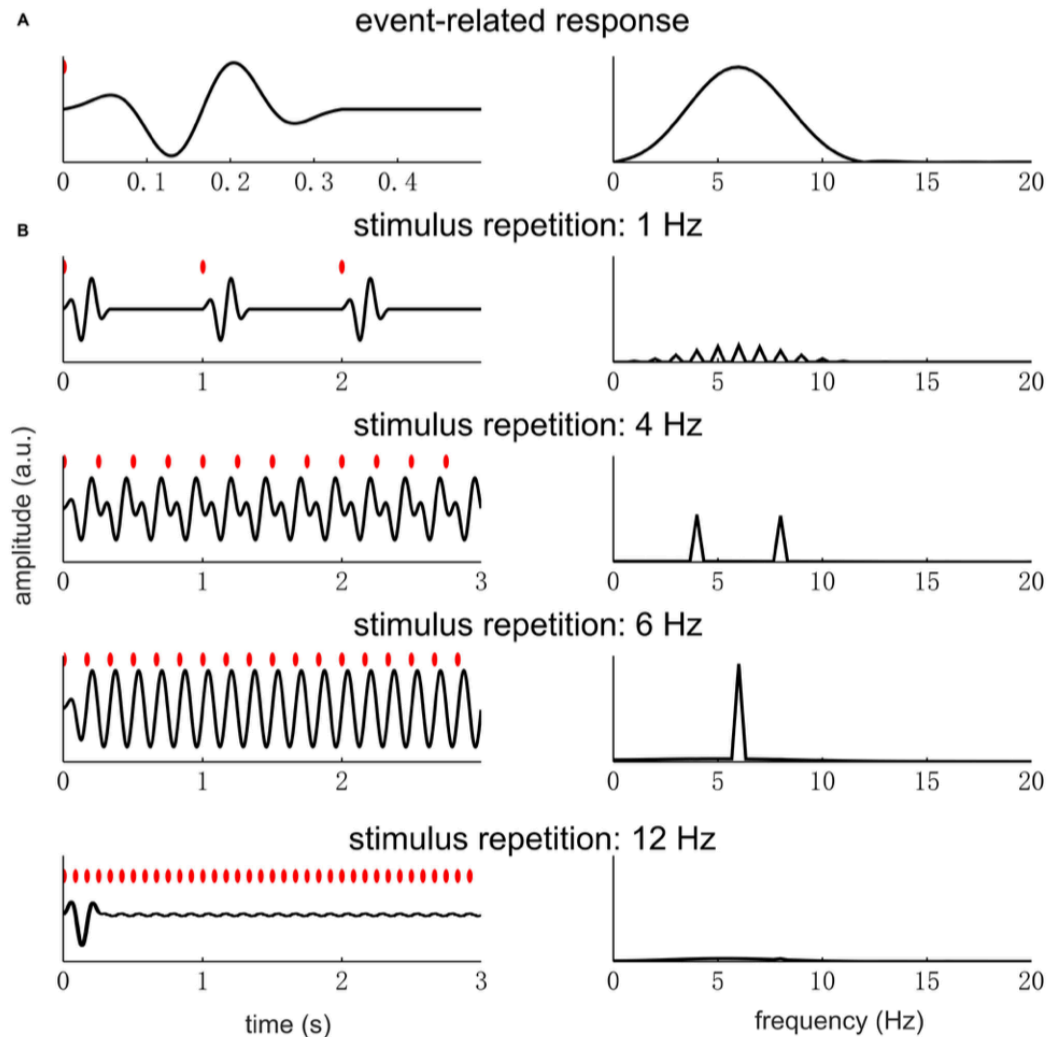
Figure 15. – Transient Responses Repeated at Different Rates, Represented in the

Time and the Frequency Domains

Left panel : Time Domain; Right panel : Frequency Domain. A. Single event-related transient response, whose power concentrates around 4–8 Hz. **B.** Rhythmic responses made from the superposition of the transient response, at different rates. At lower rates, no overlap occurs between the transient responses. In the spectrum, the response power is weak and distributed over a large number of harmonically related frequencies. At "resonance" rate, the response can be clearly identified in a limited number of frequencies, which contains all the power. If the stimulus rate is very high, a clear response only appears at the stimulus onset. Reproduced from Zhou et al. (2016).

Sustained Response, Even in the Absence of a Sensory Pacer

Responses Measured in Phase with the Ongoing Oscillation, in the Absence of its Corresponding Sensory Event.

Some studies emphasize that a response can be recorded in the absence of a sensory event, given that the missing event matches the phase of an entrained oscillation (Lehmann, Jimena Arias, Schönwiesner, Arias, & Schönwiesner, 2016; Näätänen, Paavilainen, Rinne, & Alho, 2007; Tal et al., 2017). In an experimental paradigm that is very close to the one from Nozaradan and colleagues (2012a), participants were presented with different acoustic rhythms, that were either syncopated (i.e., the downbeats were not physically marked, but the perception of a pulse could emerge), or aleatory (i.e., some beats were not physically marked, but they did not correspond to a downbeat, and no perception of pulse could emerge from the rhythmic pattern). A neural response could be measured at the time of the physically missing downbeats, in the syncopated rhythms. In contrast, no response could be identified at the time of aleatory missing events (Fig.16; Tal et al., 2017).
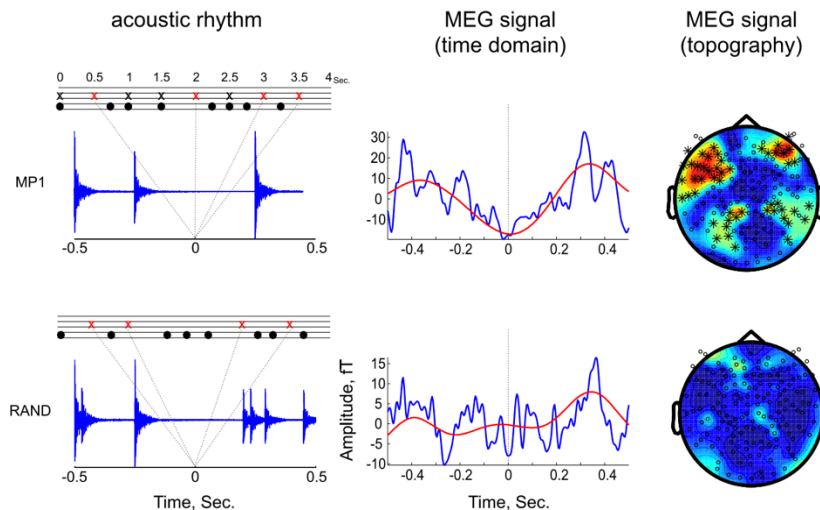
Figure 16. –   The "Missing Pulse" Phenomenon.

Blue lines: acoustic and MEG signals segmented relative to the onset of the events that are missing in the acoustic signal. The upper panel represents a syncopated rhythm, known to elicit the perception of a pulse. The lower panel represents an aleatory rhythm, from which no perception of pulse can emerge. The missing events are represented as red dots in the musical staff. A clear "response" was measured at the time of missing downbeat, in the syncopated rhythm. In contrast, no clear response was elicited by the missing events in the aleatory sequence. Adapted from Tal et al. (2017).

Those results appear more coherent with the entrainment of an endogenous oscillation at the frequency of the expected downbeat (i.e., the pulse), than with a simple repetition of transient responses to the acoustic events only. However, such a result could also be fully explained by constructive interferences occurring between small components of an invariant transient response repeated at the onsets of acoustic events only (Rajendran, Harper, Willmore, Hartmann, & Schnupp, 2013). Similarly, the absence of response observed in the aleatory rhythms could be explained by nonconstructive interferences.

Continuation After the Offset of the Pacer

One characteristic of neural oscillations is that their perpetuation is not solely dependent on driving sensory stimulation. Rather, neural oscillations should also be self-sustaining. Therefore, the measure of a sustained oscillatory activity after the offset of a rhythmic stimulus (e.g., Fig. 17) can be interpreted as evidence of a process that is not only occurring in response to external events, but also occurring in response to the expected occurrence of the sensory rhythm. Such ongoing oscillations have been reported for the auditory modality, in intracortical recordings carried on in macaques (Lakatos et al., 2013), and in the visual modality (e.g., Spaak, de Lange, & Jensen, 2014). Interestingly, a delay between the onset of the rhythmic stimulation and the appearance of the oscillation is also observable (e.g., Fig. 17), and can be interpreted as a necessary time to "build up" the entrainment. In contrast, transient responses elicited to each sensory event are expected to be detectable at the first event.
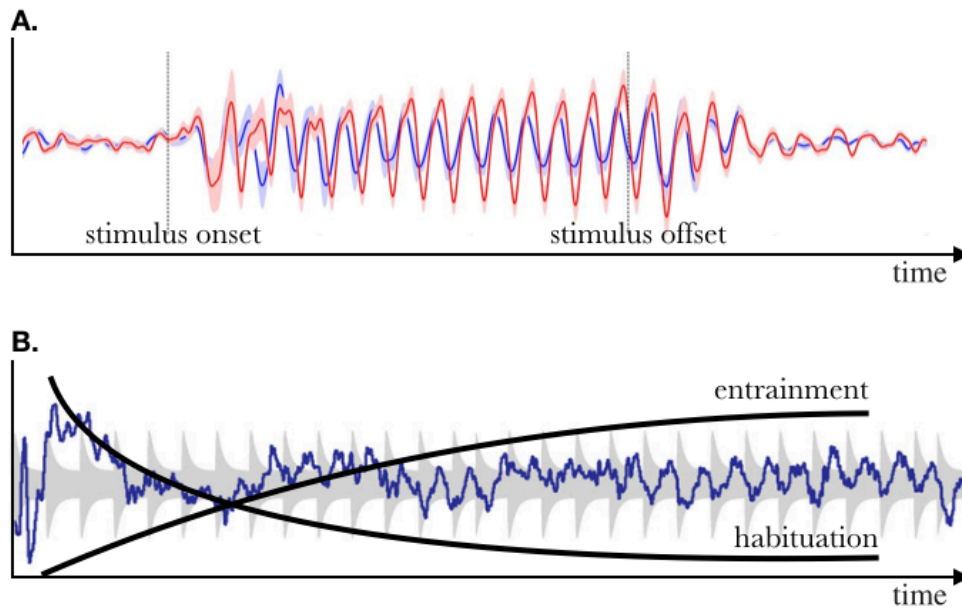
Figure 17. –   Neural Oscillations

A. Neural oscillations measured after the stimulus offset. MEG planar gradient recorded from the occipitoposterior cortex, in response to a rhythmic visual stimulation. Adapted from Spaak et al. (2014). This observation is strongly suggesting that the neural rhythm is not a simple superposition of transient responses to repeated but independent events. In this case, it is rather an entrained oscillation, that is sustained after the offset of the entraining sensory rhythm. **B. Neural oscillations measured in response to an acoustic rhythm.** EEG signal recorded in frontocentral electrodes. Adapted from Nozaradan, Peretz, Missal, & Mouraux, (2011). In this segment, a transient response can be clearly identified at the onset of the sensory rhythm. The neural rhythm does not appear until at least eight repetitions of the sensory event, suggesting that the neural oscillations are progressively built up (i.e., the entrainment occurs after a certain time of stimulation). Furthermore, the transient response observed at the onset of the stimulation seems to attenuate rather than superimpose with the repetition of acoustic events, which could be compatible with a habituation effect.

Anticipatory Responses, Occurring Before the Onset of the Sensory Events.

Any neural activity occurring before the onset of a sensory event could be interpreted as a proof of anticipation (or entrainment), in a similar fashion that the negative mean asynchrony is interpreted in sensorimotor synchronization tasks (see section 3.1.2.2.2). The contingent negative variation (Grey Walter, Cooper, Aldridge, McCallum, & Winter, 1964) is a classic example of electrophysiological component that precedes anticipated sensory or motor event, in a non-rhythmic context. Several studies focused on the neural activity that precedes rhythmic sensory

events (e.g., Arnal, Doelling, & Poeppel, 2015; Pfeuty, Ragot, & Pouthas, 2003; Stefanics et al., 2010).

In one study performed by Fujioka and colleagues (2012), participants listened to either regular or irregular acoustic rhythms, while the neuromagnetic activity was recorded. The induced time-frequency decomposition of auditory responses was analysed and revealed patterns of signal power modulation that was synchronized to the periodicity of the stimuli (Fig. 18.A). This power modulation occurred predominantly in the 20–22 Hz band (i.e., in the beta band). Importantly, the time course of the initial modulation did not change with the stimulus conditions. This suggests that the initial response reflects a deterministic process driven by the stimulus input. In contrast, the rebound following the initial decrease of power reached the maximum value again around the time of the next stimulus, in the regular conditions only. In the irregular condition, the beta rebound was significantly earlier compared with the other conditions (Fig. 18.B). This indicates that a consistent pattern of beta increase preceding stimulus onset was only observed with periodic stimulation, which is coherent with a dynamic modulation of attention. It also suggests that, when the time of the next auditory beat is uncertain, the system prepares for the possibility of an early beat rather than simply expecting the next sound to occur at the mean time of previous events.
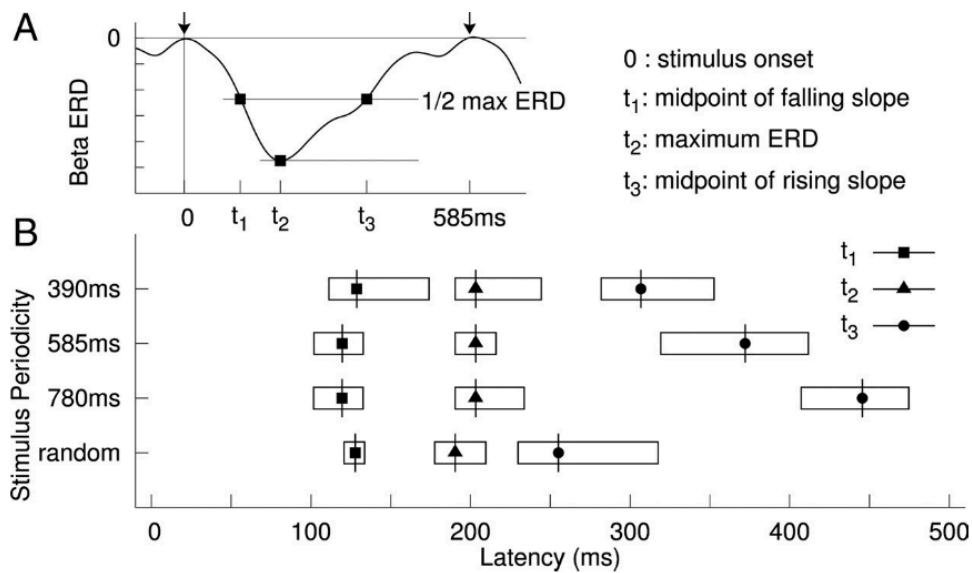
Figure 18. –   Latency of Stimulus-Related Beta Power Modulation

A. Schema indicating the different peak latency and the latencies of the midpoints of falling and rising slopes.

B. Group mean latencies and their 95% confidence limits indicated by the length of the horizontal bars. Four different stimuli are compared: three regular stimuli, with increasing interonset intervals (i.e., 390, 585 and 780 ms) and one stimulus with random interonset intervals (390 to 780 ms). The midpoint of the rising slope is dependent of the interonset interval, for the regular conditions (the time of t3 delays with increasing interonset intervals), but not for the random condition.

Resistance to Perturbations

Rhythmic perception and rhythmic temporal anticipation do not require strict periodicity. Actually, it has been extensively theorized and robustly demonstrated that certain fluctuations of tempo convey information that allows a listener to adaptively synchronize to the changing rhythm (Jones & Boltz, 1989; Keller, 2008; Large & Jones, 1999; Madison & Merker, 2002; Pecenka & Keller, 2011; Rankin et al., 2009).

The neural oscillations that are entrained to predictable fluctuating rhythms are expected to adapt to the variations of interevent intervals, in a different fashion than repeated evoked responses would. For example, in stimulus-aligned oscillatory activities that reflect a predictive process, the onset of the upcoming event should be anticipated by some proactive phase alignment of the ongoing oscillation (see section 3.1.2.2.3 for similar logical, in an isochronous

context). Importantly, the pre-stimulus context in which each event would occur (e.g., a context in which the events are anticipated or not) would also influence the eventual transient response to each sensory event. More specifically, a decreased evoked auditory responses can be expected when the timing of the event is correctly anticipated (Arnal & Giraud, 2012). Conversely, an increase evoked response amplitude can be expected when the timing of the event is not anticipated, in a similar way that an increase of response amplitude is observed in response to any discriminable change in auditory stimulation (Costa-Faidella, Baldeweg, Grimm, & Escera, 2011; Näätänen et al., 2007).

While those hypotheses are specifically investigated in one of the studies of the present work (see study 2, section 4.1), some previous studies already investigated whether quasi-rhythmic visual inputs can lead to frequency-specific brain responses, (Capilla et al., 2011; Cravo, Rohenkohl, Wyart, & Nobre, 2013; Keitel, Thut, & Gross, 2017), yielding ambiguous results. One of the challenges of paradigms that introduce jitter in rhythmic stimulation is that the jittered stimuli can both evoke jittered neural responses and entrain dynamically adapting neural oscillations, with unknown effects on the quantification of mutual information (Zoefel et al., 2018). However, the present work introduces a new method that could potentially address this challenge (Chemin et al., 2018, section 3.4).

Entrainment of Endogenous Rhythms

One characteristic of endogenous oscillations is that they should eventually occur independently from a driving sensory rhythm. Thus, it has been proposed that a straightforward way to distinguish endogenous oscillatory activity from regular evoked responses is to create a paradigm in which participants would perform a rhythmic covert task (e.g., imagine a musical pulse, or imagine a periodic movement), while no external rhythm is presented (Zoefel et al., 2018). Importantly, natural rhythms are known to be non-stationary, i.e., to fluctuate in time (Chen, Ding, & Kelso, 1997; Goodwin, 1997; Repp, 2005). Therefore, if such paradigms are easily implemented in low temporal resolution techniques that are relatively insensitive to non-stationarities (e.g., la Fougère et al., 2010), it is extremely difficult to accurately track an endogenous rhythm in EEG or MEG signals, in the absence of any reliable indication regarding the timing of this rhythm. Studies that do not take into account the non-stationarities of natural

rhythms probably face important limitations, particularly when across-trials averaging is required to increase the signal-to-noise ratio (Chemin et al., 2018; Mouraux & Iannetti, 2008).

In a study published in 2011, Nozaradan and colleagues took advantage of the frequency-tagging approach to measure the endogenous neural activity related to the mental imagery of a metric structure, superimposed to the perception of an isochronous acoustic rhythm. The EEG signal of participants was recorded, while they listened to the acoustic rhythms, in three different conditions: (1) passive listening of the acoustic rhythm; (2) metrical mental imagery of a binary beat (i.e., a downbeat every two events); (3) metrical mental imagery of a ternary beat (i.e., a downbeat every three events). With this paradigm, the endogenous neural activity could be fairly controlled for non-stationarities (i.e., the interevent interval should not vary, because it was controlled by the external rhythm), and the spectral decomposition of the EEG response (see section 3.3.2) allowed disentangling the externally driven and the endogenous neural activities. A response was measured at the frequency of the acoustic rhythm, in three conditions. In the mental imagery conditions, an additional response was measured at the frequencies of the imagined downbeat (i.e., a half or a third of the acoustic rhythm frequency, and harmonics). Those results were interpreted as evidence of neural entrainment, directly recorded in the electroencephalogram.

Interestingly, visual inspection of the topographical distribution of the different responses shows that the response directly elicited by the acoustic rhythm is distributed over frontocentral areas. This topography is coherent with the projection of electric dipoles originating from the left and right auditory cortices. In contrast, the responses measured at the fundamental frequency of the imaginary beat appear to project differently, on a cluster of electrodes located over right centroparietal regions (Fig. 19). This observation is coherent with the hypothesis of an endogenous oscillator that is distinct from neural resonators located in the auditory cortices. However, the results presented in this study are not sufficient to exclude the hypothesis that the performed task did rely on mental strategies purely based on assigning an imagined number to each acoustic event (e.g., counting from one to two in the binary task, and from one to three in the ternary task), and hence not involving the entrainment of pulse perception (see Tranchant & Vuvan, 2015, for the concept of alternative strategies). In this case, the recorded activity would

simply be related to transient language-related neural activity, and not on the entrainment of endogenous neural oscillations.
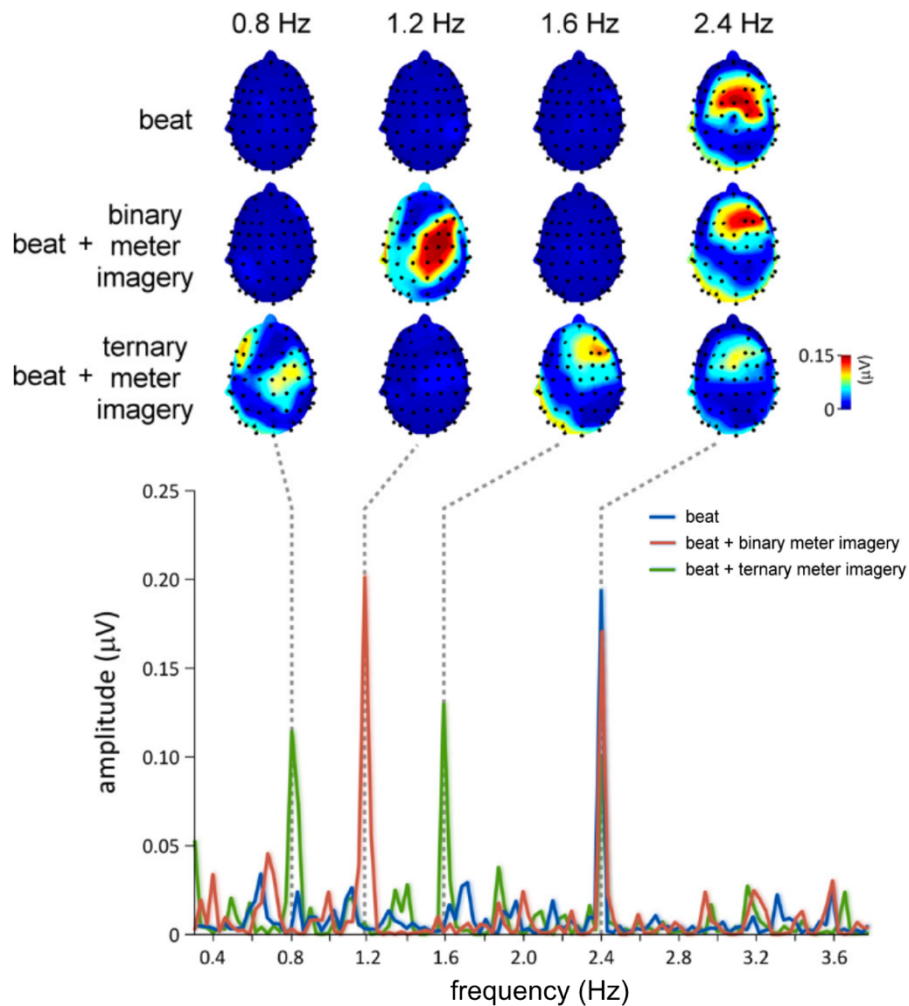
Figure 19. – Acoustic Rhythm- and Mental Imagery- Related Neural Responses, Identified in the Frequency Domain

The results are those of a single representative subject. Top: topographical maps of EEG signal amplitude at 0.8 (1F ternary meter), 1.2 (1F binary meter), 1.6 (2F ternary meter), and 2.4 (1F acoustic rhythm) Hz, obtained in each of the three conditions. Bottom: EEG amplitude spectrum (in microvolts) within a frequency range comprising the frequency of the acoustic rhythm and the frequency of the imagined binary and ternary meters. Note that in all three conditions, the auditory stimulus elicited, at f = 2.4 Hz, a clear beat-related response. Also note the emergence of a meter-related response at 1.2 Hz in the binary meter imagery condition, and at 0.8 and 1.6 Hz in the ternary meter imagery condition.

Discussion

It seems that there is an implicit, but critical, question that lies in labelling the rhythmic electroencephalographic signal as a "neural oscillation", or as "repeated transient response", which can be formulated as follows. Does the measure reflect a deterministic processing of sensory information, or not? Is the input-output transformation constant, or not? If the input-output transformation is constant (i.e., a same repetitive sensory stimulation yields a same measurable response), then the electrophysiological measure would reflect a deterministic processing of the sensory information, which many would consider "low-level". In contrast, if the same sensory input can yield different neural outputs, then the electrophysiological measure would reflect a non-deterministic process of sensory information, which many would call a "higher-level process".

There is compelling evidence against the hypothesis of a purely sensory-driven response. However, this does not exclude the hypothesis of repeated transient events, as it is well established that such responses can be modulated, and also reflect high level processes. Therefore, if a modulation of the input-output transformation is observed upon different experimental conditions, can one conclude that the measured oscillatory EEG signal is a reflect of an anticipative process underlined by the entrainment of neural oscillations?

Unfortunately, there are obvious methodological limits for the characterization of the dynamics of the neural response, at the level of individual events.

Study 1: EEG Time-Warping to study non-strictly-periodic EEG signals related to the production of rhythmic movements (Chemin B., Huang G, Mulders D, Mouraux A.)

This article has been published in the Journal of Neuroscience Method in 2018.

Abstract

Background. Many sensorimotor functions are intrinsically rhythmic, and are underlined by neural processes that are functionally distinct from neural responses related to the processing of transient events. EEG frequency tagging is a technique that is increasingly used in neuroscience to study these processes. It relies on the fact that perceiving and/or producing rhythms generates periodic neural activity that translates into periodic variations of the EEG signal. In the EEG spectrum, those variations appear as peaks localized at the frequency of the rhythm and its harmonics.

New method. Many natural rhythms, such as music or dance, are not strictly periodic and, instead, show fluctuations of their period over time. Here, we introduce a time-warping method to identify non-strictly-periodic EEG activities in the frequency domain.

Results. EEG time-warping can be used to characterize the sensorimotor activity related to the performance of self-paced rhythmic finger movements. Furthermore, the EEG time-warping method can disentangle auditory- and movement-related EEG activity produced when participants perform rhythmic movements synchronized to an acoustic rhythm. This is possible because the movement-related activity has different period fluctuations than the auditory-related activity.

Comparison with existing methods. With the classic frequency-tagging approach, rhythm fluctuations result in a spreading of the peaks to neighbouring frequencies, to the point that they cannot be distinguished from background noise.

Conclusions. The proposed time-warping procedure is as a simple and effective mean to study natural non-strictly-periodic rhythmic neural processes such as rhythmic movement production, acoustic rhythm perception and sensorimotor synchronization.

Introduction

Many sensorimotor functions are intrinsically rhythmic. This is the case for the perception of music, the production of gait movements, or the synchronization of complex motor performance to complex sensory stimulation as observed in dance or music playing.

It has been suggested that the neural processes underlying these rhythmic sensorimotor functions may at least partly differ from the sensorimotor processes underlying the processing and/or production of discrete transient events (Van Ede, Quinn, Woolrich, & Nobre, 2018; Zoefel et al., 2018). For example, neural oscillations, which reflect rhythmic variations of excitability within a neural population (Buzsáki & Draguhn, 2004; Llinás, 1988), can be entrained to the frequency of a rhythmic process. By reinforcing phase and frequency specific information, this phenomenon could play a role in sensory selection (Schroeder & Lakatos, 2009), dynamic attention and temporal anticipation (Large & Jones, 1999), or the coupling of remote neural oscillators for multimodal integration (Lakatos, Chen, O-Connell, Mills, & Schroeder, 2007).

EEG frequency tagging is a technique that is increasingly used to study rhythmic brain functions (Nozaradan, 2014). Classically, an event is repeated at a constant frequency such as to elicit a periodic and synchronized neural response, which can be measured in the spectrum of the recorded EEG signals at the frequency of stimulation and its harmonics. This "frequency-tagged" EEG activity can correspond to the periodic repetition of transient neural activities related to the processing of a periodic sequence of transient events. Furthermore, it may reflect the synchronized activity of neurons having the ability to entrain their activity to the periodic repetition or modulation of that stimulus, i.e. neurons that align the frequency and phase of their activity to the frequency and phase of the stimulus. A well-known example of this approach is the so-called "auditory steady-state evoked-potential", which refers to the periodic EEG signal elicited by a sound whose intensity is modulated periodically over time (Galambos et al., 1981).

A periodic signal is a signal formed by a unitary waveform repeated at a regular interval, called the period. Mathematically, this periodic signal corresponds to the convolution of the unitary waveform with a periodic train of impulses, or Dirac comb (Fig. 20). The number of impulses per second corresponds to the fundamental frequency of the signal. When represented in the

frequency domain, a pure sine wave appears as a single "peak", at the fundamental frequency of the sine wave. When the unitary waveform is more complex, its spectrum consists of a set of peaks at the fundamental frequency and its harmonics. Mathematically, the spectrum of a periodic signal corresponds to the spectrum of the unitary waveform multiplied by the spectrum of the Dirac comb. Therefore, the amplitude of the peaks obtained at the different harmonics is determined by the frequency spectrum of the unitary waveform (Fig. 20; Collura, 1995; Zhou et al., 2016).
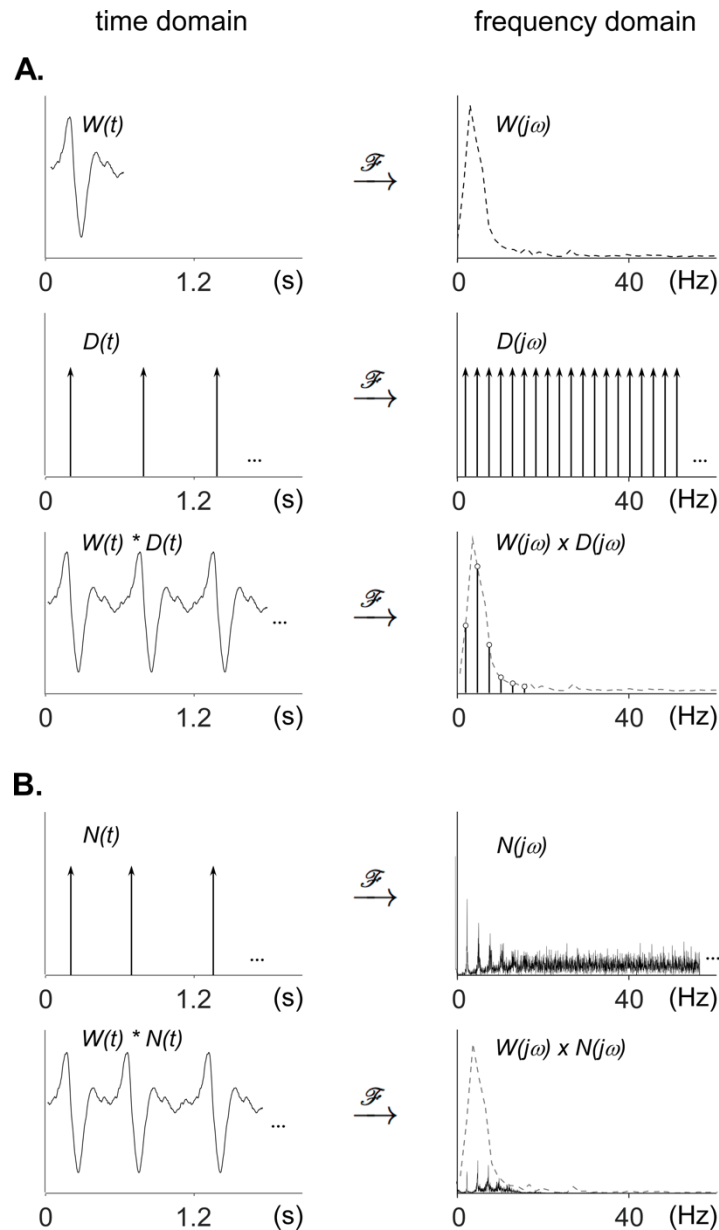
Figure 20. – Time and Frequency Domain Representation of Periodic and Non-Strictly-Periodic Signals.

A. Time domain and frequency domain representations of a unitary waveform $W(t)$, a periodic train of impulses (Dirac comb; $D(t)$), and a periodic signal corresponding to the convolution of $W(t)$ and $D(t)$ in the time domain, and the multiplication of $W(j\omega)$ and $D(j\omega)$ in the frequency domain. *Note that the* Fourier transform of the periodic signal has a spectrum that concentrates on the fundamental frequency and harmonics determined by the periodicity of the Dirac comb, with a relative amplitude distribution that is determined by the shape of the spectrum of the unitary waveform. **B.** Time domain and frequency domain representations of a non-strictly-periodic signal corresponding to the convolution of $W(t)$ with a non-strictly-periodic train of impulses $N(t)$. In contrast to the spectrum of the strictly-periodic Dirac comb $D(j\omega)$, the frequency spectrum of the non-strictly-periodic train of impulses $N(j\omega)$ is not constituted of isolated peaks at the fundamental frequency and harmonics. Instead, the energy of the signal spreads to surrounding frequencies, and the spectrum will become more and more random if the non-periodicity is increased. The spectrum of the non-strictly-periodic signal obtained by multiplying the spectrum $W(j\omega)$ of the unitary waveform with the spectrum $N(j\omega)$ of the non-strictly-periodic train of impulses, contains peaks having a lower amplitude as compared to the strictly-periodic signal.

Taking advantage of the spectral decomposition of periodic signals, the EEG frequency-tagging approach is able to isolate EEG signals elicited by periodic stimulation, even if it does not constitute sharp transients (e.g. EEG activity elicited by progressive sinusoidal modulation of stimulation amplitude) (Nozaradan et al., 2011). The frequency-tagging approach is also able to identify frequency-specific responses despite high inter-individual phase variability (Nozaradan et al., 2018). Importantly, several studies have shown that EEG frequency tagging can be used to tag cortical activity related to high-level perceptual processes such as the processing of musical rhythms (Chemin, Mouraux, & Nozaradan, 2014; Nozaradan, Peretz, et al., 2016; Nozaradan et al., 2011; Nozaradan, Peretz, & Mouraux, 2012b; Nozaradan, Zerouali, Peretz, & Mouraux, 2013; Nozaradan, Schönwiesner, Caron-Desrochers, & Lehmann, 2016; Nozaradan, Schwartze, Obermeier, & Kotz, 2017), linguistic constituents (Buiatti, Peña, & Dehaene-Lambertz, 2009) and face perception (Rossion, 2014; Rossion, Torfs, Jacques, & Liu-Shuang, 2015).

However, an important limitation of the EEG frequency-tagging approach comes from the fact that natural rhythms are not *strictly* periodic, i.e. their periodicity fluctuates over time (Chen et al., 1997; Goodwin, 1997; Repp, 2005). For example, when performing self-paced hand tapping movements, the variations in period duration reach approximately 4% of the average period

(Semjen et al., 2000). Similarly, the subjective experience of a musical pulse is robust to period fluctuations, within a range of anisochrony evaluated to 8.6% of the mean period (Madison & Merker, 2002). The frequency-tagging approach implies to perform a Fourier transform on relatively long sequences of EEG signals, which is only valid under the assumption that the signal of interest is stationary, i.e., that its distribution parameters such as mean and variance do not change over time (Chatfield, 1989). As compared to the sharp peaks observed in the Fourier transform of a signal that is strictly periodic, the peaks observed in the Fourier transform of a fluctuating signal have lower amplitudes because each peak spreads out to neighbouring frequencies (Fig. 20). In the case of EEG where the non-strictly-periodic signal is embedded within large-amplitude background activity, this reduction in peak amplitude and sharpness often renders their identification impossible.

In this paper, we propose a simple time-warping method to "render periodic" EEG signals related to activities that are not strictly periodic and, thereby, make it possible to "concentrate" non-strictly-periodic neural responses in the frequency domain. In other words, we propose to transform the signal in order to meet the assumption of stationarity that is necessary for the frequency-tagging approach.

The proposed time-warping method consists in stretching, i.e. contracting and dilating, the EEG signal such as to "accelerate" or "decelerate" it when the time interval between two events is respectively greater or smaller than the mean period of the non-strictly-periodic events. This time-warping procedure is fundamentally different from another method referred to as EEG "false-sequencing", consisting in reconstructing a periodic signal by concatenating non-warped segments of the EEG signal having a constant length corresponding to the mean period (Quek & Rossion, 2017). The superiority of one approach over the other is actually dependent on the nature of the frequency-tagged EEG signal. If the waveform of the periodic EEG signal is independent of the period fluctuations, EEG false-sequencing should be superior to EEG time-warping, as compressing and dilating the EEG signal would distort the unitary waveform. Conversely, if the waveform of the periodic EEG signal is not invariant but is contracted or dilated as a function of the periodic fluctuations, EEG time warping could be superior to EEG false-

sequencing, because compressing and dilating the EEG signal could actually enhance the unitary waveform similarity across repetitions.

To assess our time-warping method, we applied it to EEG signals recorded while participants performed self-paced and acoustic-paced periodic tapping movements of the hand, as well as simulated EEG data.

Methods

Participants

Nine right-handed healthy volunteers (6 females, 3 males; all right-handed; mean age = 28 years, SD = 4) took part in the experiment after providing written informed consent. All participants were familiar with EEG, but had no prior experience with the experimental setting. They had no history of hearing, neurological, or psychiatric disorder, and none were taking any medication at the time of the experiment. The experiment was approved by the local ethics committee.

Experimental Design

The experiment contained three conditions, corresponding to three different tasks: (1) finger tapping synchronized to an acoustic beat, (2) finger tapping alone, and (3) passive listening to the acoustic beat (Fig. 21). The three conditions were presented in separate blocks, whose order of presentation was randomized across participants.
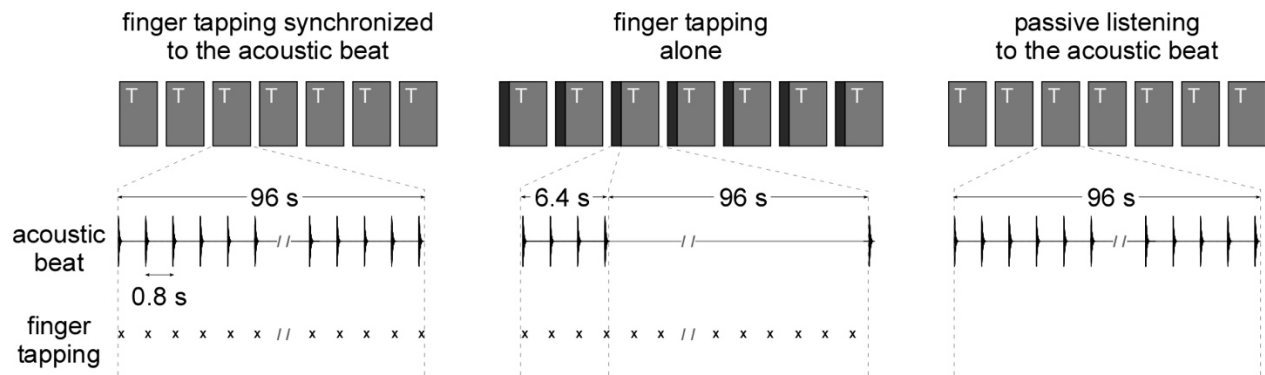
Figure 21. – Experimental design of the EEG experiment.

The experiment was composed of three experimental conditions, presented in separate blocks, whose order was counterbalanced across participants. Each block started with up to five dummy trials of 16 s to allow the participant to become familiar with the task. Then, trials of 96 s (T) were repeated seven times, forming one block. The *finger tapping synchronized to an acoustic beat* task consisted in tapping the index finger in synchrony with an acoustic beat. The acoustic beat consisted in a 96 s sequence of 120 isochronous pure tones presented at an 800 ms inter beat interval. The *finger tapping alone* task consisted in tapping the right index against the table, at a rate as constant as possible. A short 6.4 s pacing acoustic sequence of eight isochronous beats (800 ms inter beat interval) was presented before each trial. The *passive listening to the acoustic beat* task consisted in listening to the 96 s sequence of 120 isochronous pure tones occurring at an 800 ms inter beat interval.

Finger tapping synchronized to an acoustic beat. The task consisted in tapping the right index finger against the table, in synchrony with an acoustic beat. The acoustic beat consisted in a 96 s sequence of 120 isochronous 990 Hz pure tones lasting 150 ms (7.5 ms rise time, 142.5 ms fall time), occurring with a period of 800 ms. The tapping consisted in a flexion of the metacarpophalangeal articulation of the right index, until the fingertip touched the table, followed by finger extension. Participants were instructed to synchronize their tapping to the acoustic rhythm such that the tapping of the index with the table coincided with the acoustic beats. A sequence of 96 s composed one trial, and the trial was repeated seven times to form one block.

Finger tapping alone. The task consisted in tapping the right index against the table, at a rate as constant as possible. A short 6.4 s pacing acoustic sequence of eight isochronous beats occurring with a period of 800 ms was presented before each trial. Participants were instructed to

synchronize their tapping to this acoustic pacer, and to continue the tapping movements after the acoustic pacer stopped, keeping the tapping rhythm as constant as possible. The end of the trial was indicated by presenting a single tone. One trial lasted 96 s and was repeated 7 times to form one block.

Passive listening to the acoustic beat. In this condition, participants were requested to listen passively to the 800 ms periodic acoustic beat. Such as in the other blocks, each trial had a duration of 96 s and was repeated 7 times.

During the whole experiment, participants were seated comfortably in a chair, with their arms resting on a table and the right elbow placed on a cushion at wrist height. The right hand was attached to an orthosis used to record the movements performed in the finger tapping tasks (Fig. 22). The tapping hand was hidden from participants with a sheet of fabrics. Before the beginning of the experiment, participants could familiarize with the orthosis. Furthermore, each block was preceded by up to five dummy trials of 16 s in order to allow the participant to become familiar with the task. Before starting the actual EEG recording, the experimenter witnessed that the task was performed adequately.

In all conditions, the onset of each trial was initiated by the participant pressing a button. A random 1.5 to 3 s delay separated the button press from the onset of the trial. In order to encourage the participants to focus their attention to the task, at the end of each trial, they were asked to "rate" how much they paid attention to the task and how "precise" their tapping was. The instructions and questions were displayed on a computer screen, using MATLAB 2014a (The MathWorks, Natick, MA). The acoustic stimuli were presented binaurally using pneumatic earphone inserts (Etymotic ER1, Etymotic Research, Elk Grove, IL), and played using an externally-triggered zero latency audio stimulus generator (AUDIOFile, Cambridge Research System, Rochester, United Kingdom).

EEG Recording

During the EEG recording, participants were instructed to relax, avoid any unnecessary head or body movement, and keep their eyes fixated on a point marked on a white surface in front of them. To avoid any visual feedback, the tapping hand was hidden from the participant using a

sheet of fabric. The experimenter remained in the recording room with the participant at all times to monitor compliance to the procedure and instructions, as well as to monitor the EEG signals and, eventually, provide feedback to the participant in case of important eye or movement artifacts.

The EEG was recorded using 64 Ag-AgCl electrodes placed on the scalp according to the international 10-10 system (Waveguard64 cap, Cephalon A/S, Norresundby, Denmark). Electrode impedances were kept below 10 kΩ. The signals were amplified, low-pass filtered at 500 Hz, digitized using a sampling rate of 1,000 Hz, and referenced to an average reference (64-channel high-speed amplifier, Advanced Neuro Technologies, Enschede, The Netherlands). A trigger, produced by the audio stimulus generator was sent to the EEG amplifier at the beginning of each trial.

Finger-Movements Recording

Movements of the finger were recorded using a galvanometer (OSST8062, Sintec Optronics Pte Ltd, Singapore) mounted on an orthosis placed around the first two phalanges of participant's right index, and a touch sensor (Makey Makey, MIT Media Lab's Lifelong Kindergarten, USA) placed on the table, in regard to the tapping finger (Fig. 3). The galvanometer generated a continuous signal proportional to the speed of the finger movement (range: ± 0.5 V; positive and negative values corresponding to finger flexion and extension, respectively) and the touch sensor measured the impedance between the finger and the touch pad. The signals generated by the galvanometer and the touch sensor were digitized at a sampling rate of 1,000 Hz using two auxiliary channels of the EEG system. Both signals were normalized such that, for the galvanometer signal, the unit corresponded to the maximal speed of the finger flexion, and for the touch sensor signal, the unit corresponded to the value at contact of the finger with the sensor.
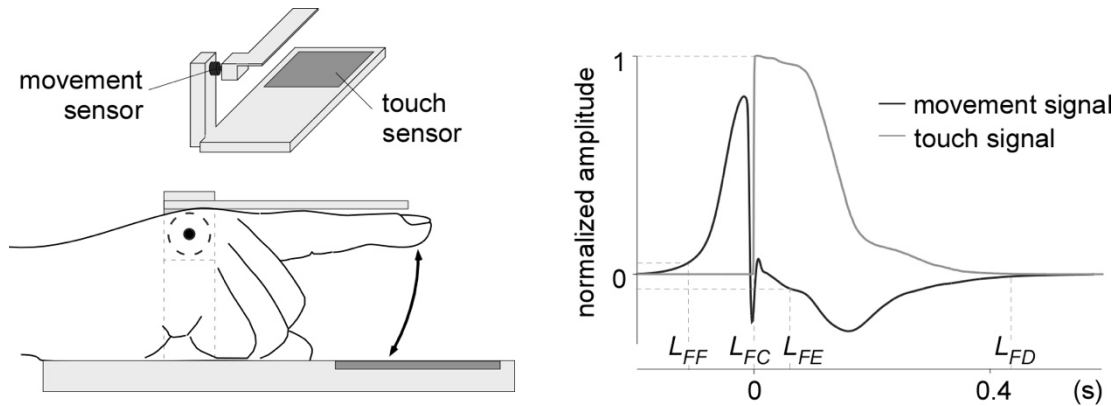
Figure 22. – Finger Movement Recording.

Movements of the finger were recorded using an orthosis placed around the first two phalanges of participant's right index (left panel). A movement sensor was mounted on the orthosis and a touch sensor was embedded in the surface onto which the finger tapped. The right panel shows the normalized amplitude of the two sensor signals, averaged across participants, conditions and taps. The point L_{FF} corresponds to the initiation of the finger flexion. L_{FC} corresponds to the time at which the fingertip touches the table. L_{FE} corresponds to the initiation of finger extension. L_{FD} corresponds to the time at which the finger returns to the default position. Note that the dynamics of finger flexion, measured by the time interval between L_{FF} and L_{FC}, was quite constant across participants and taps, whereas the dynamics of finger extension, measured by the time between L_{FE} and L_{FD}, was more variable. Those results are consistent with the fact that participants were requested to synchronize the tapping of the finger against the touch sensor.

For each movement (indexed by k) of the finger tapping trials, the onset of finger flexion movement (latency of finger flexion: $L_{FF\,k}$) was arbitrarily defined as the moment when the normalized galvanometer signal became >0.05, and the time at which the fingertip came in contact with the table (latency of finger contact: $L_{FC\,k}$) was defined as the moment when the touch signal passed from 0 to 1.

The two measures were used to compute, for each movement k, the duration of each finger flexion ($D_{FF\,k} = L_{FC\,k} - L_{FF\,k}$) and the duration between the finger tap and the preceding finger tap (inter-tap-interval: $ITI_k = L_{FC\,k} - L_{FC\,k-1}$).

EEG Preprocessing

The continuous EEG signals recorded in each condition were segmented in epochs lasting 96 s, extending between 0 to 96 s relative to the onset of each task. A 50 Hz notch filter and a 0.1 Hz high-pass Butterworth zero-phase filter were applied to remove artifacts due to environmental noise as well as slow signal drifts. Artifacts produced by eye blinks or eye movements were removed from the EEG signal using a validated method based on an independent component analysis (Jung et al., 2000), using the *runica* algorithm (Bell & Sejnowski, 1995; Makeig, 2002). Those artifacts were identified visually based on their spatio-temporal distribution (waveform features typical of eye blinks, topographical distribution maximal at frontal electrodes).

Non-Time-Warped EEG Signals

The 96 s preprocessed EEG epochs were further segmented to only keep the 2nd to the 106th event (i.e. from the second beat in the finger tapping synchronized on an acoustic beat task and the passive beat listening task, and the second finger tap in the finger tapping alone task). The EEG signal recorded during the first event was discarded to avoid contamination by the transient evoked potentials related to the onset of the task (e.g. Nozaradan et al., 2011). Especially in the finger tapping alone task, the number of tapping events varied from trial-to-trial. Across all trials, conditions and participants, the minimum number of tapping events was 106. Therefore, to perform the analyses on epochs having the same number of events across trials, conditions and participants, the EEG signals were segmented such as to include up to the 106th event. On average, we thus discarded 10 % of the 120 original events per trial. To ensure that the Fourier transform of these signals would yield discrete spectra with a frequency resolution respecting the alignment of the bins corresponding to the beat frequency and its harmonics, the final length of the epochs was set to a multiple of the beat period. In the tapping synchronized to the beat task and the passive beat listening task, this corresponded to 0.8 s x 105 events = 84 s. In the tapping alone task, the length of the different segments of 105 taps was not consistent across the epochs, because of the fluctuations of the tapping rate. The range of lengths spanned from 68.0 to 88.8 s.

Time-warped EEG signals

The 96 s EEG epochs recorded in the two finger tapping tasks were warped in the time domain to remove the fluctuations of the ITIs. The warping was performed by dilating or compressing each ITI segment of the EEG signals, using a linear interpolation, such as to obtain a constant number of bins for each ITI segment (800 bins corresponding to 0.8 s at a 1,000 Hz sampling rate). This procedure resulted in "accelerating" the EEG signals when the time interval between two touch onsets exceeded the 0.8 s target period, and in "decelerating" the EEG signal when the time interval between two touch onsets was shorter than the 0.8 s target period (Fig. 23, see Supplementary Material for algorithm and technical details). Such as for the original signals, the time-warped EEG signals were then segmented to only keep 105 events starting from the second event following the actual performance of the task. In all the conditions, the length of the epochs corresponded to 0.8 s x 105 events = 84 s.
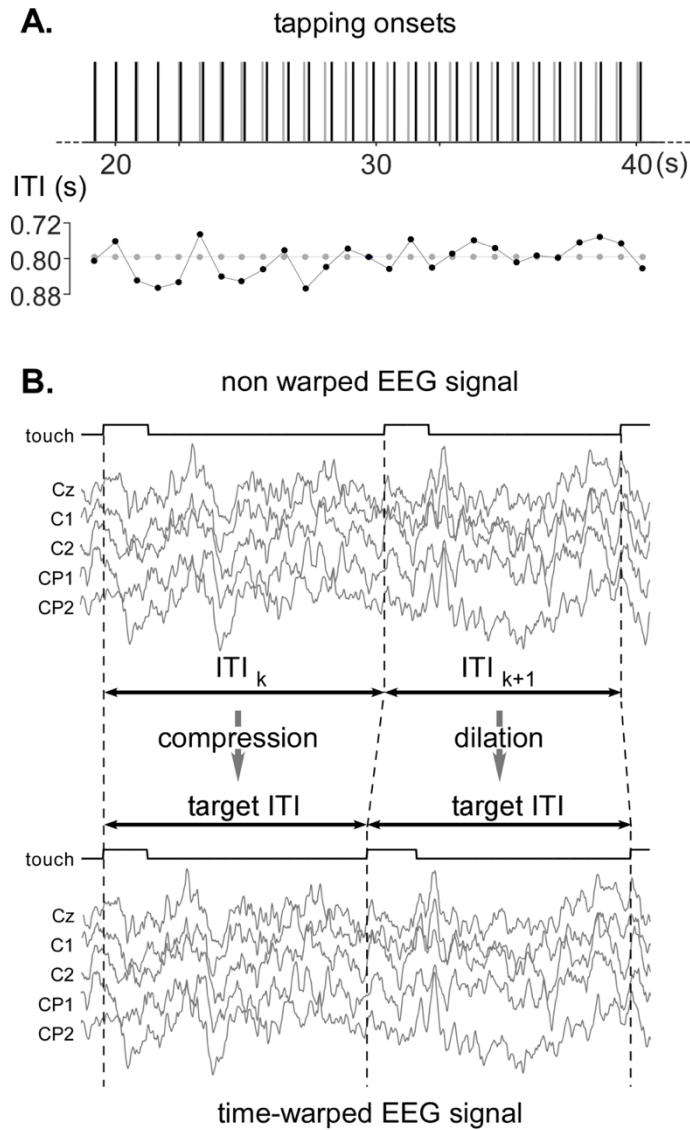
Figure 23. – EEG Time-Warping Procedure

A. As shown in this representative trial of the finger-tapping to the beat task, the inter-tap interval (ITI) fluctuated from tap to tap, with a mean ITI of 800 ms. **B.** The time-warping procedure consists in compressing or dilating the EEG signals recorded within each ITI such as to scale it to a fixed target ITI of 800 ms. The compression and dilation of the EEG segments was computed by linear interpolation of the non-time-warped signals.

Frequency-Domain Analysis

The non-time-warped and time-warped EEG epochs were transformed in the frequency domain using a discrete Fourier transform (Frigo & Johnson, 1998). In the tapping synchronized to the beat and the passive beat listening conditions, the discrete Fourier transform yielded a frequency spectrum of signal amplitude (μV) ranging from 0 to 500 Hz with a frequency resolution of 0.0119 Hz (Bach & Meigen, 1999). In the tapping alone task, the frequency resolution ranged between 0.0113 Hz and 0.0147 Hz, because of the variations in epoch duration. Therefore, these frequency spectra were resampled using the nearest interpolation method such as to obtain a resampled resolution of 0.0119 Hz.

The periodic EEG activity related to beat perception and finger tapping can be expected to generate peaks in the EEG frequency spectra at the fundamental frequency (F=1.25 Hz) and harmonics (2F=2.5 Hz, 2F=3.75 Hz, etc.). To quantify these responses, the contribution of background noise was removed by subtracting, at each bin of the frequency spectra, the average amplitude measured at neighbouring frequency bins (eight frequency bins ranging from −0.14 to −0.05 Hz and from +0.05 to +0.14 Hz relative to each frequency bin). The validity of this subtraction procedure relies on the assumption that, in the absence of a strong periodic signal, the signal amplitude at any given frequency bin should be similar to the signal amplitude of the mean of the surrounding frequency bins (Mouraux et al., 2011; Retter & Rossion, 2016). This subtraction procedure using neighbouring frequency bins is important because background EEG noise is not equally distributed across scalp channels and, most importantly, is greater at lower frequencies as compared to higher frequencies (the power spectrum of background EEG typically follows a 1/f function; Freeman et al., 2003).

The noise-subtracted spectra were then averaged across epochs, for each condition and each individual. Within these averaged spectra and for each condition, we identified the frequencies at which the periodic EEG activity generated a significant increase in amplitude across individuals, by performing a t-test against zero of the amplitudes measured at the fundamental frequency (F=1.25 Hz) and the 23 first harmonics (from 2F=2.5 to 23F=30 Hz), averaged across all scalp channels (Fig. 24). The significance level was set at p < 0.05, corrected for multiple comparisons (Bonferroni). Finally, a summary measure of the amplitude of the periodic EEG response was

computed by summing the noise-subtracted amplitudes at the fundamental frequency and harmonics that were significantly greater than zero (t-test against zero), and hemispheric lateralization was assessed by performing a paired-sample t-test between the average of the signals measured over the left and the right hemisphere.

Time-Domain Analysis

The non-time-warped and time-warped EEG signals of the tapping alone condition were segmented from -0.3 to +0.5 s relative to the latency of each contact of the fingertip with the table (L_{FC}). The obtained segments were averaged across trials and across participants, in order to visualize and compare the shape of the unitary waveform in both the non-time-warped and the time-warped signals.

Additionally, the segments were categorized in two equal groups according to the length of the ITI. For each trial, segments were assigned to the short or long ITI group depending on whether the trial ITI was shorter or longer than the trial median ITI. Categorized segments were then averaged across trials and participants, in order to visualize and compare the shape of the unitary waveforms for long and short ITIs.

Estimation of similarity between non-time-warped and time-warped unitary waveforms, as well as short-ITI and long-ITI related waveforms, was made by computing, for each participant, the correlation coefficient between the two signals.

All EEG processing steps including the time warping procedure were carried out using Letswave 6 (Institute of Neuroscience, University of Louvain; www.letswave.org), an open-source MATLAB (The MathWorks, Natick, MA) toolbox. The EEG time-warping algorithm is available as supplementary material, and can be downloaded on the Github repository:

github.com/BaptisteChemin/EEG-Time-Warping.

Control Experiment: Resting EEG Signals

To examine whether the time-warping procedure could generate an artefactual enhancement of amplitude at the frequencies of interest due to the periodic compression or dilation of successive EEG segments, we conducted a control experiment in which resting EEG was recorded in nine

healthy volunteers. During the experiment, participants were instructed to remain still, with their eyes open, during seven trials of 96 s. The signals were then processed using the same procedures as for the main experiment. Time-warping of the resting EEG signals was performed using the tapping latencies of the nine participants in the finger-tapping alone task.

Control Analysis Using Simulated Data

Time warping is likely to generate a certain quantity of signal distortion. Its ability to recover non-strictly-periodic EEG signals is likely to depend on the period duration, the amount of period fluctuation, and the shape of the unitary waveform. Most importantly, its depends on whether decreases/increases in period duration are associated with compression/dilation of the unitary EEG waveform, as would be expected if the period fluctuations are determined by neural processes reflected in the unitary waveform (Large & Jones, 1999).

To assess the influence of these factors, we generated simulated EEG data using as unitary waveform the group-level average unitary EEG waveform recorded at electrode Cz in the tapping alone condition. First, we generated a strictly-periodic 1.25 Hz signal by concatenating 105 unitary waveforms having a length of 0.684 s. Second, we generated a series of 1,000 non-strictly-periodic signals using the same unitary waveform separated by a fluctuating interval (normal distribution, mean interval = 0.8 s, controlled coefficient of variation (CV)). In this dataset, the shape of the unitary waveform was invariant. When the interval was greater than the length of the unitary waveform, the empty gap was replaced by a segment of ongoing EEG randomly taken from the resting EEG signals recorded in the control experiment. Conversely, when the interval was smaller than the length of the unitary waveform, the overlapping portions of the two consecutive unitary signals were summed. Third, we generated another series of 1,000 non-strictly-periodic signals in which the unitary waveform was contracted or dilated such as to adjust their length to the period duration, as could be expected if period fluctuations are determined by the temporal dynamics of the neural processes underlying the unitary waveform. All signals were band-passed using a 0.1 to 60 Hz Butterworth filter. Various amounts of period CV were tested, ranging between 0-30%, in steps of 0.5 %. After FFT transform, a measure of the amplitude of the periodic signal was obtained by summing the peaks at 1.25 Hz and the 9 following harmonics in the frequency spectrum of each signal. Finally, for both non-strictly-periodic datasets, an amplitude ratio was

computed by dividing the amplitude of the periodic signal measured in the non-strictly-periodic dataset (averaged across the 1000 signals) by the amplitude of the periodic signal measured in the strictly-periodic signal. The Matlab toolbox developed to run these simulations is available on the GitHub repository.

Results

Finger Tapping Latencies

The ITIs between finger taps were normally distributed, with a narrower dispersion in the finger tapping synchronized to the acoustic beat condition (800 ± 46 ms; coefficient of variation: 5.7%) as compared to the finger tapping alone condition (779 ± 65 ms; coefficient of variation: 8.4%). The greater variability in ITI in the tapping alone task was expected, as in that condition, participants could not use the external acoustic pacer to improve their performance (Repp, 2005).

Frequency-Domain Analysis

Periodic EEG Responses Observed in the Non-Time-Warped Signals

The group-level average frequency spectra obtained in the finger tapping synchronized to an acoustic beat, the finger tapping alone and the passive beat listening conditions are shown in Fig. 24.
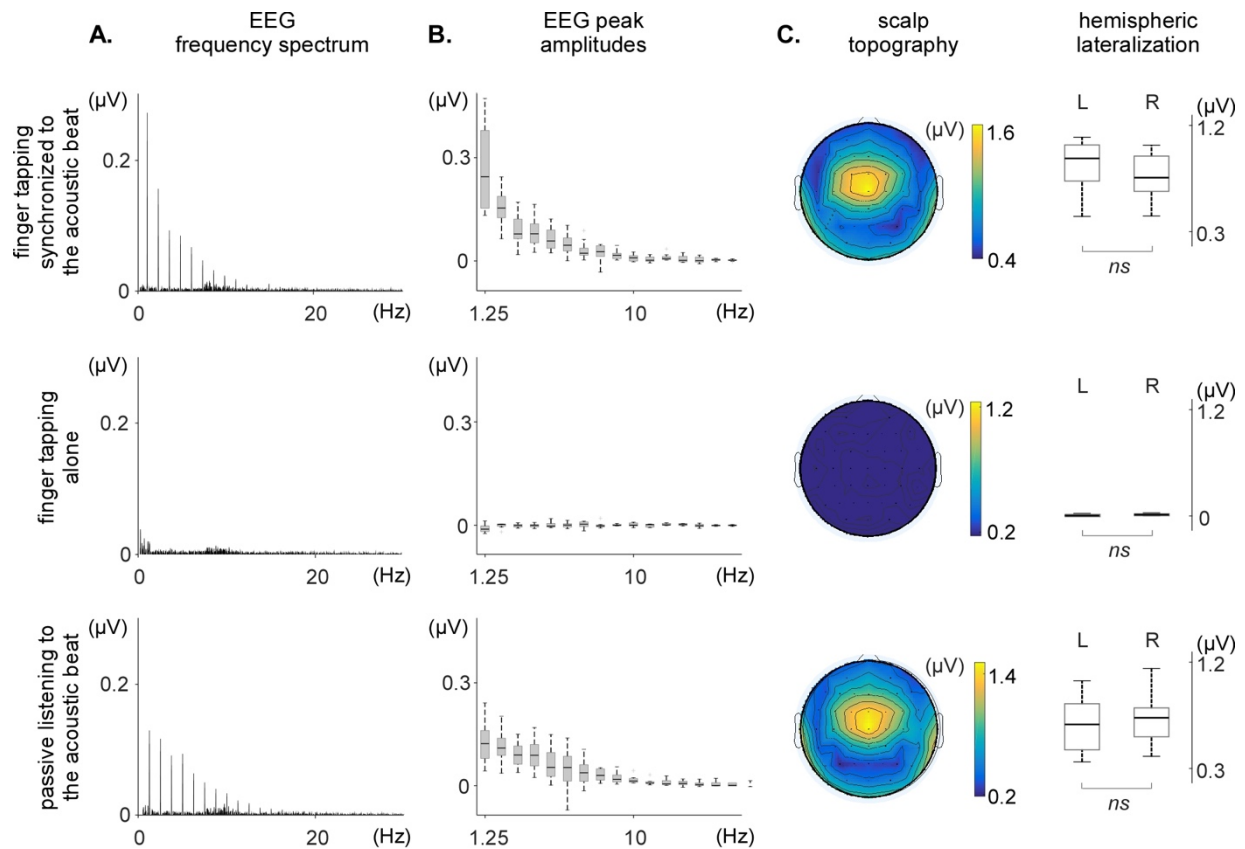
Figure 24. – Frequency-domain analysis of the non-time-warped EEG signals obtained in each of the three conditions (finger tapping synchronized to the acoustic beat, finger tapping alone, and passive listening to the acoustic beat).

A. Frequency spectrum of the EEG signals, averaged across participants and across the 64 EEG channels. Note the clear peaks at beat frequency and harmonics in each of the EEG spectra, except for the EEG signals recorded in the finger tapping alone condition. **B.** Peak amplitude at the fundamental frequency and harmonics, across participants (median, lower/upper quartile and minimum/maximum values). **C.** Scalp topography and hemispheric lateralization of the periodic EEG response (sum of the spectrum amplitude at beat frequency and harmonics significantly greater than zero). The non-time-warped signals obtained in the finger taping synchronized to the acoustic beat and the passive listening conditions show similar scalp topographies, maximal over fronto-central electrodes, and symmetrically distributed over the two hemispheres (L: left; R: right). No significant activity is identified in the finger tapping alone condition.

In the finger tapping synchronized to the acoustic beat condition, clear peaks were observed in the EEG spectra at 1.25 Hz and harmonics. The noise-subtracted amplitudes at the beat frequency (1.25 Hz) and at the harmonic frequencies 2.5, 3.75, 5, 6.25, 7.5, 8.75, 10, 11.25, 12.5, 15, 18.75, 20, 22.5, 28.75 and 30 Hz were significantly greater than zero. The scalp topography of this periodic EEG response was maximal at fronto-central electrodes, and did not show any clear hemispheric lateralization relative to the tapping hand. This absence of lateralization was confirmed by the fact that the average of the signals measured over the left hemisphere (M=0.8461 µV, SD=0.2246 µV) was not significantly different from the average of the signals measured over the right hemisphere (M=0.778 µV, SD=0.197 µV); t(8)=2.30, p=0.0506.

In the finger tapping alone condition, no clear peaks were observed in the EEG frequency spectra, and only the noise-subtracted amplitude at 15 Hz was marginally greater than 0, amongst the 24 tested frequencies (t = 2.53, p = 0.035, uncorrected for multiple comparisons).

In the passive listening to the acoustic beat condition, clear peaks were observed in the EEG spectra, whose amplitudes were significantly greater than zero at 1.25, 2.5, 3.75, 5, 6.25, 7.5, 8.75, 10, 11.25, 12.5, 13.75, 15, 16.25, 17.5, 21.25, 22.5, 25, 26.25, and 27.5 Hz. The scalp topography of the response obtained during passive beat listening resembled closely the scalp topography of the response obtained in the finger tapping synchronized to the acoustic beat condition, being maximal at fronto-central electrodes and symmetrically distributed over the two hemispheres. The average of the signals measured over the left hemisphere (M=0.677 µV, SD=0.245 µV) was not significantly different from the average of the signals measured over the right hemisphere (M=0.703 µV, SD=0.229 µV; t(8)=-0.64, p=0.5424).

Periodic EEG Responses Observed in the Time-Warped Signals

The group-level average frequency spectra of the time-warped EEG signals obtained in the tapping synchronized to the acoustic beat and tapping alone conditions are shown in Fig. 25.
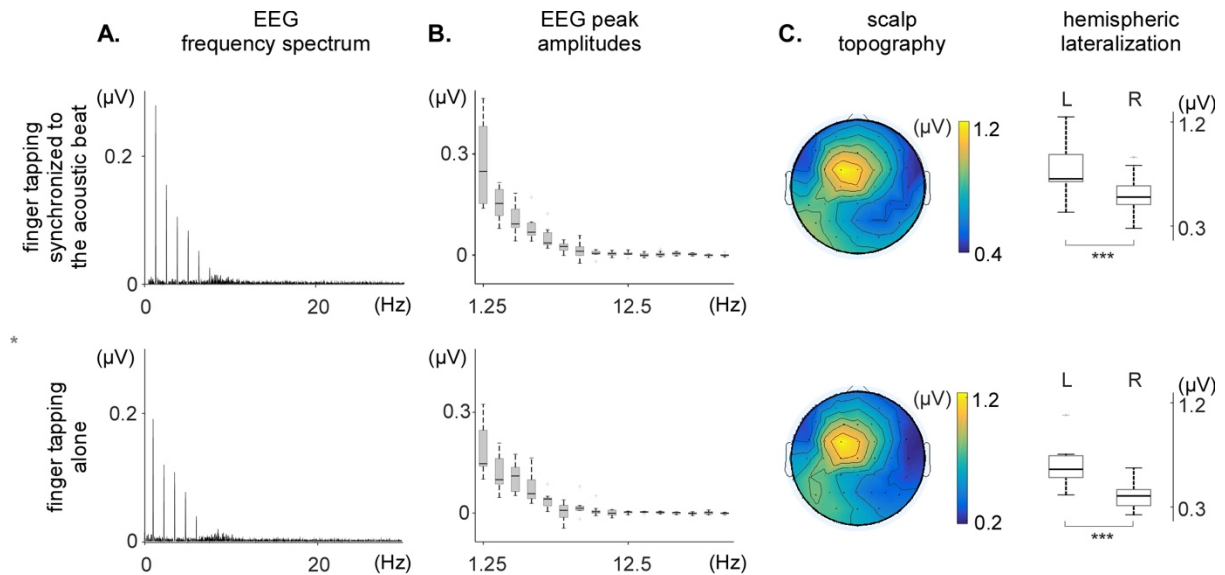
Figure 25. – Frequency-Domain Analysis of the Time-Warped EEG Signals

Obtained in Two of the Three Conditions (Finger Tapping Synchronized to the Acoustic Beat

and Finger Tapping Alone Conditions).

A. Frequency spectrum of the EEG signals, averaged across participants and across the 64 EEG channels. Note the clear peaks in both spectra. **B.** Peak amplitudes at the fundamental frequency and its harmonics, across participants (median, lower/upper quartile and minimum/maximum values). **C.** Scalp topography and hemispheric lateralization of the periodic EEG response (sum of the spectrum amplitudes at beat frequency harmonics significantly greater than zero). The time-warped EEG signals recorded in the finger tapping synchronized to the acoustic beat and finger tapping alone conditions show similar topographies, lateralized onto the (left) hemisphere contra-lateral to the tapping hand (L: left; R: right).

In the tapping synchronized to the beat condition, clear peaks were observed in the EEG spectra at 1.25 Hz and harmonics. The noise-subtracted amplitudes at the beat frequency (1.25 Hz) and at the harmonic frequencies 2.5, 3.75, 5, 6.25, 7.5, 16.25, and 17.5 Hz were significantly greater than zero. The scalp topography of this periodic EEG response was maximal over left central and parietal electrodes, and was thus clearly different from the scalp topography of the response observed in the non-time-warped EEG signals, which was symmetrical and maximal over fronto-central electrodes. This was confirmed by the fact that the average of the signals measured over the left hemisphere (M=0.798 μV, SD=0.261 μV) was significantly greater than the average of the signals measured over the right hemisphere (M=0.569 μV, SD=0.184 μV; t(8)=7.72, p<0.001) .

In the tapping alone condition, clear peaks were observed in the EEG spectra of the time-warped signals at 1.25 Hz and harmonics. This was in striking contrast with the lack of any clear response in the EEG spectra of the non-time-warped signals of the same condition. The noise-subtracted amplitudes at the beat frequency (1.25 Hz) and at the harmonic frequencies 2.5, 3.75, 5, 6.25, 12.5, 13.75, 15, and 28.75 Hz were significantly greater than zero. The scalp topography of this periodic EEG response resembled closely the periodic EEG response obtained in the time-warped signals of the tapping synchronized to the acoustic beat condition, both being maximal over left central and parietal electrodes. The average of the signals measured over the left hemisphere (M=0.638 µV, SD=0.203 µV) was significantly greater than the average of the signals measured over the right hemisphere (M=0.385 µV, SD=0.119 µV); t(8)=7.53, p<0.001.

Time-Domain Analysis

Comparison of Non-Time-Warped and Time-Warped EEG Signals

The unitary waveforms obtained by averaging non-time-warped and time-warped EEG segments across ITIs are shown in Fig. 26A. Visual inspection of those waveforms showed very little differences between the non-time-warped and time-warped signals. The differences were mostly characterized by a smoothing of high-frequency components in the time-warped signals. The correlation coefficient between the two signals confirmed the high similarity between the two waveforms, across participants (R=0.971 +- 0.034).

Comparison of Long and Short ITI Related EEG Signals

The unitary waveforms obtained by averaging EEG segments separately for short and long ITIs are shown in Fig. 26B. The unitary waveforms obtained by averaging short ITI segments tended to differ from the unitary waveforms obtained by averaging long ITI segments (R=0.902 +- 0.062). Specifically, for long ITI segments, the period preceding contact onset was more negative and, most importantly, the negative peak concomitant to the finger contact was broader. Furthermore, the baseline preceding the negative peak was more negative for short ITIs.

A. time-warped vs. non time-warped

B. short vs. long Inter Tap Intervals
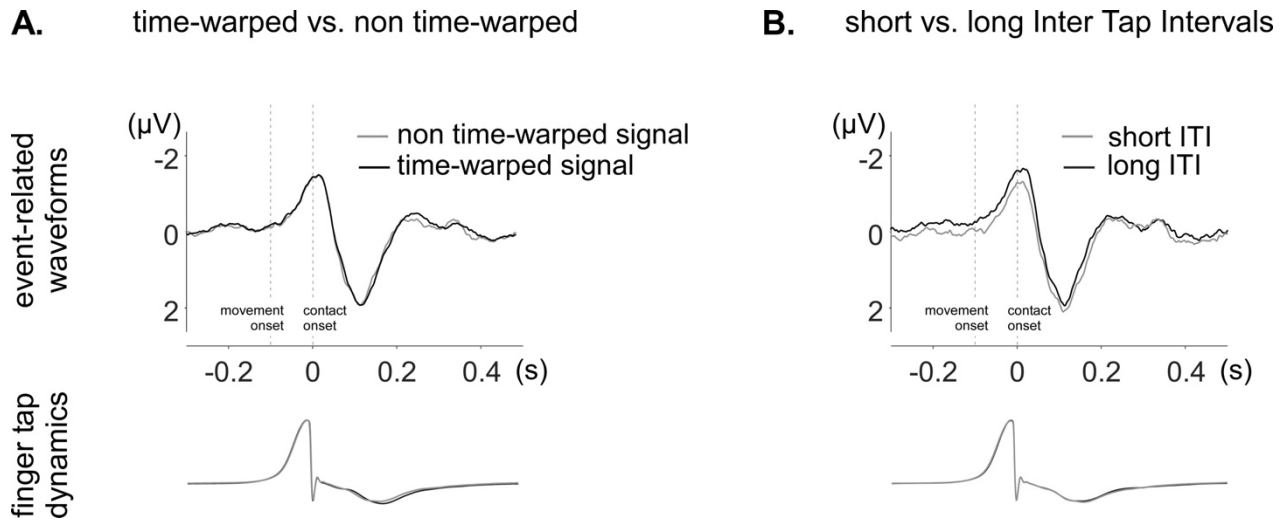
Figure 26. –   Time-Domain Analysis of the Unitary EEG Waveforms Obtained in the

Tapping Alone Condition

The average waveforms (electrode Cz) were obtained by aligning EEG segments to the onsets of the contact of the fingertip with the table. The finger tap dynamics recorded by the movement sensor are shown in the lower part of the figure, also averaged relative to contact onset. **A.** Average waveform of the non-time-warped EEG signal (grey) and the time-warped EEG signal (black). In both non-time-warped and time-warped signals, a clear EEG response is observed, time-locked to the contact onset, and consisting of a negative peak concomitant to the tapping, followed by a positive peak maximal approximately 110 ms after tapping. The non-time-warped and time-warped waveforms are highly similar, except for a slight smoothing of rapid activities in the time-warped signal. **B.** Waveforms obtained by averaging EEG segments separately for short ITIs (grey) and long ITIs (black). The period preceding contact onset was more negative for long ITIs as compared to short ITIs. Furthermore, the negative peak concomitant to the finger contact was broader.

Control Experiment: Time-Warping of Resting EEG Signals

As shown in Fig. 27, the frequency spectra of the time-warped resting EEG signals recorded in the control experiment showed no significant enhancement of amplitude at 1.25 Hz and harmonics, indicating that the time-warping procedure did not introduce any artefactual enhancement of signal amplitude at the frequencies of interest.
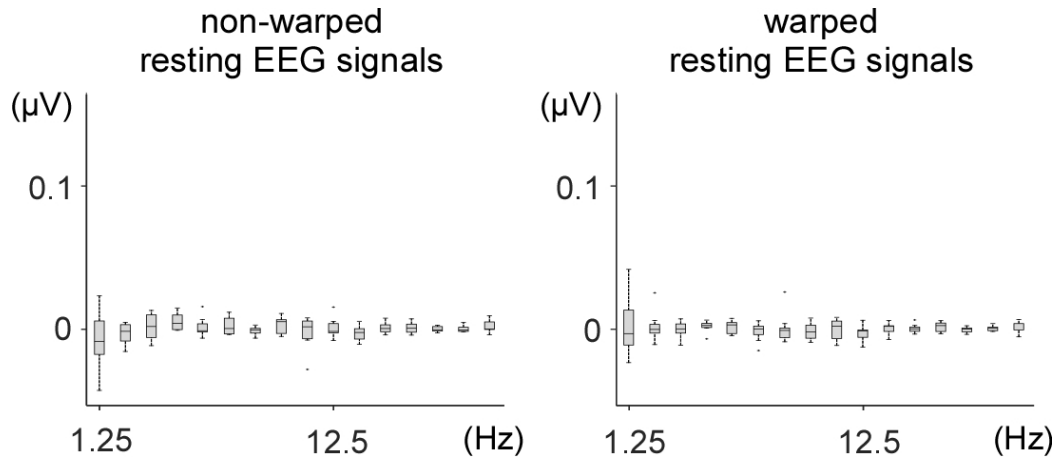
Figure 27. – Frequency-Domain Analysis of Non-Time-Warped and Time-Warped Resting EEG Data

The time-warping procedure was applied to resting EEG data using the tapping latencies of the nine participants in the finger-tapping alone task, with an average 800 ms ITI. The graphs show the peak amplitudes at the fundamental frequency and its harmonics, across participants (median, lower/upper quartile and minimum/maximum values). Time-warping did not introduce any artefactual enhancement of peak amplitude at those frequencies.

Control Analysis Using Simulated Data

In both the invariant unitary waveform dataset and the adaptive unitary waveform dataset, increasing the period fluctuations led to a rapid decrease of the amplitude ratio when no time-warping was applied. When time-warping was applied to the non-strictly-periodic dataset constructed using an invariant unitary waveform, a slow decrease in amplitude ratio was observed, reaching 0.95 at a coefficient of variation of 5.5%. Expectedly, the amplitude ratio remained 1 independently of period fluctuations when the time-warping was applied to the non-strictly-periodic dataset constructed by contracting/dilating the unitary waveforms. The results are displayed in Fig. 28.
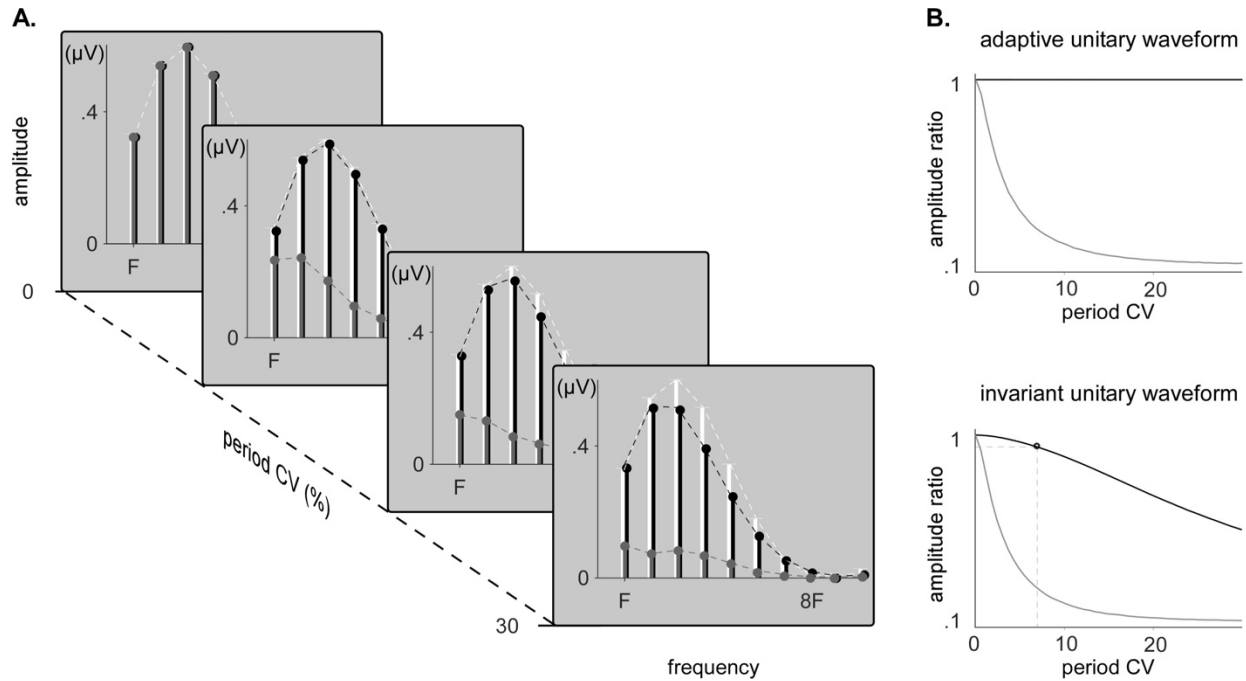
Figure 28. – Amplitude Recovery of Original and Tested Synthetic Signals.

A. Amplitude of the peaks measured in the spectra of strictly-periodic simulated EEG signals (white), non-strictly-periodic simulated EEG signals with a unitary waveform of invariant shape (grey) and time-warped non-strictly-periodic simulated EEG signals with a unitary waveform of invariant shape (black), for increasing coefficients of variation (CV) of the period fluctuation. **B.** Amplitude ratio between both time-warped (black) or non-time-warped (grey) non-strictly periodic signals and the strictly periodic signals, when the unitary waveform dynamically adapts to the period fluctuations or stays invariant and independent to the period fluctuations.

Discussion

Our results show that time-warping EEG signals is a simple and efficient method to concentrate non-strictly-periodic EEG signals in the frequency domain, such as the EEG activity elicited while performing self-paced periodic movements of the hand. Importantly, our results also show that the time-warping procedure does not generate any artefactual periodic response when it is applied to resting EEG signals.

Without time-warping, the EEG signals recorded when participants regularly tapped their right index against a table without any external synchronization cue showed almost no response in the frequency domain. In striking contrast, the same EEG signals showed clear responses in the frequency domain when they were time-warped using the tapping latencies. The scalp topography of these responses was maximal over the hemisphere contralateral to the tapping finger, compatible with activity originating predominantly from primary sensorimotor cortices. Most interestingly, when participants performed the hand tapping synchronized with an acoustic beat, the time-warping procedure was able to disambiguate, in the frequency domain, the periodic EEG signals related to processing the acoustic rhythm from the periodic EEG signals related to the performance of the finger tapping movement. In the non-time-warped EEG signals, the topography of the response was maximal over fronto-central electrodes, resembling closely the topography of the response recorded when participants listened passively to the acoustic beat, compatible with activity originating predominantly from auditory areas bilaterally (Nozaradan et al., 2011). In contrast, in the time-warped EEG signals, the topography of the response was maximal over the hemisphere contralateral to the tapping finger, resembling closely the response obtained in the tapping alone condition. This selective concentration of auditory- and movement-related activities was possible because each signal had a unique pattern of period fluctuations. In the non-time-warped signals, the activity related to processing the acoustic beat could be expected to be more periodic than the activity related to the fluctuating hand tapping movement. Hence, the peaks in the EEG frequency spectrum concentrated activity related to processing the acoustic beat. Conversely, in the time-warped signals, the activity related to processing the beat was rendered less periodic and the activity related to movement

was rendered more periodic, leading to a stronger concentration of movement-related activity in the frequency domain.

Therefore, in the case of multiple response streams having the same average period but distinct period fluctuations, the time-warping method can be used to tease out different response streams by selectively concentrating the periodic activity of a specific response stream. The method does not allow to strictly isolate one stream from the other, but it does allow emphasizing one response stream over the others. An important advantage of time-warping over EEG false-sequencing, which concatenate segments of non-warped EEG signals (Quek & Rossion, 2016), is that false-sequencing cannot split coincident responses that are temporally overlapping. Hence, it cannot disentangle concurrent streams of sensory- and movement-related neural activities (Besle, Bertrand, & Giard, 2009; Perez, Kass, & Merchant, 2013). Provided that the different streams originate from different brain areas and, therefore, project differently on the scalp, additional tools such as current source density analysis or blind source separation methods could be used to further disambiguate different response streams (Cohen & Gulbinaite, 2017; Ding, Ni, Sweeney, & He, 2011).

The time-warping method assumes that the unitary waveform related to not-strictly periodic events dynamically adapts to the fluctuating inter-event-intervals. This seems to be at least partly the case for the periodic EEG signals elicited by self-paced rhythmic tapping movements. Indeed, the waveforms obtained by averaging separately the non-time-warped EEG segments corresponding to short and long inter-tap-intervals showed some dissimilarity: the negative wave occurring at tapping onset was broader for long ITIs as compared to short ITIs, indicating that its temporal dynamics are dependent on the period fluctuations.

The time-warping procedure was applied to nearly-periodic rhythms that fluctuated with an ecological coefficient of variation of 8.4% of the 0.8 s average period. The time-warping procedure could be used in future experiments to gain a better understanding of the mechanisms underlying neural entrainment to periodic stimuli. In the context of rhythm perception, Large & Jones (1999) proposed that the entrainment to a periodic rhythm emerges from the dynamics of neural systems acting as "internal oscillators" which can be entrained to nearly-periodic rhythms, and

are tolerant to period fluctuations up to a certain amount (Madison & Merker, 2002). In this view, the neural processing of rhythms that are strongly non periodic would differ from the neural processing of periodic and nearly-periodic rhythms (Teki, Grube, Kumar, et al., 2011). Because the time-warping procedure can be used to cancel out the effects of period fluctuations on the frequency representation of non-strictly-periodic signals, the approach could be used to compare EEG responses elicited by rhythms fluctuating within or beyond the ecological range for rhythm perception. Furthermore, the contrasted effect of EEG time-warping and EEG false sequencing on the amplitude recovery of the signal of interest, given its dynamics at the single event level, could be further exploited in such experimental paradigms.

Finally, the EEG time-warping approach opens new perspectives in various research areas. For example, it could be used to compare EEG responses in participants displaying varying abilities to produce synchronized movements such as musicians vs. non-musicians, or healthy participants vs. motor-impaired patients. The approach could also be exploited to remove nearly-periodic movement-related artifacts, by concentrating these artifacts in the frequency domain, and filtering them out in the frequency domain (also see Gwin et al., 2010; Kline et al., 2015 for complementary approaches).

However, even after applying time warping, one should be cautious when comparing non-strictly-periodic EEG signals having different amounts of period fluctuations. If period fluctuations are associated with contractions/dilations of the unitary waveform, time warping will recover all the signal power, regardless of the amount of period fluctuations. In contrast, if the unitary waveform is invariant, the recovery will depend on the amount of period fluctuations. If the difference in the amount of periodic fluctuations is relatively small (lower than 5.5% of CV in our simulated EEG dataset), the difference in recovery will be negligible. However, if the difference in the amount of periodic fluctuations is very large, this will significantly affect recovery.

In conclusion, EEG time warping procedure is a simple and effective tool that makes it possible to use EEG frequency-tagging to study non-strictly-periodic neural processes related to rhythmic movement production, acoustic rhythm perception and, more generally, rhythmic sensorimotor synchronization.

Supplementary Material – Time-Warping algorithm

Practical Information

The EEG time-warping algorithm is available as an open-source Matlab function, and includes a plugin to use it directly in the Letswave Matlab toolbox for the analysis of EEG signals (http://nocions.org/letswave).

The files can be downloaded on the Github repository:
(https://github.com/BaptisteChemin/EEG-Time-Warping).

Technical Introduction to the algorithm

The time-warping removes, in an EEG signal, the period fluctuations between non-strictly periodic events. To do so, the time axis of each inter-event-interval (IEI) is scaled so that it fits a target period defined by the user. In the published study, the non-strictly periodic events correspond to the latencies of finger taps. In other experimental designs, the non-strictly periodic events could be the latencies of any behavioural cues that are recorded concomitantly to the EEG, such as speech prosodic stress, or the latencies of non-strictly periodic stimulations.

The recorded event latencies (sample points) pinpoint the fluctuating IEIs. The target event latencies (query points) are determined by the user and define a target IEI. For each inter-event-interval IEI (indexed by k), a vector x_k specifies the time points at which the non-time-warped EEG data y_k are given. The length L_k of this vector varies according to the value of IEI_k (e.g., an IEI of 0.81 s sampled at 1000 Hz is specified by a vector x of 810 bins). A vector xi_k of constant length given by the target IEI (e.g., a target IEI of 0.8 s sampled at $f_s = 1000$ Hz gives a vector xi_k of 800 bins) and spanning the time segment from $x_k[1]$ to $x_k[L_k]$ is then generated. Finally, a vector yi_k whose entries correspond to the elements of xi_k is computed by linear interpolation of the vector y_k. This step is implemented using matlab $interp1$ function in the following way: $yi_k = interp1(x_k, y_k, xi_k)$.

The goal of the time-warping (TW) method is to enhance the periodicity of a quasi-periodic signal, which concerns the spectrum of the whole EEG signal. However, to achieve this, TW has local

effects affecting differently each EEG segment (the so-called "unitary waveform") within an IEI. The local impact of this operation on the signal spectrum can be split up in three parts.

First, the linear interpolation of the whole data can be seen as a reconstruction of the original continuous signal, which will reconstruct each unitary waveform accurately as long as the original sampling rate is much higher than the Nyquist rate. Indeed, the frequency response of the filter associated to a linear interpolation from discrete to continuous time is given by

$$H_l(f) = T_s^2 \cdot \left(sinc(f \cdot T_s)\right)^2 = T_s^2 \cdot \left(\frac{\sin(\pi \cdot f \cdot T_s)}{\pi \cdot f \cdot T_s}\right)^2 ,$$

where T_s is the sampling period $(= 1/f_s)$. Although this spectrum has an infinite support and only vanishes at the multiple of the sampling frequency $(n \cdot f_s$ for all integers $n)$, it is reasonable to use it when the frequencies of interest are small compared to f_s (Fig.29; Oppenheim, 1999).
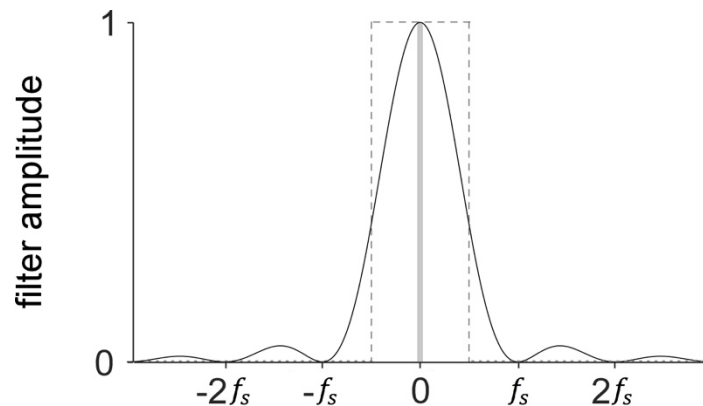
Figure 29. – Frequency Response of the Linear Interpolator.

The filter amplitude allows to quantify the aliasing effects. The grey area represents the frequencies of interest in the case of the EEG time-warping (i.e., frequencies < 30 Hz), in the case of an EEG signal sampled at $f_s = 1000$ Hz. Because those frequencies are small compared to f_s, virtually no aliasing is introduced in the time-warped signal. The dashed lines represent the frequency response of the ideal reconstruction filter.

Second, a time rescaling with a factor of a_k is applied to each IEI (indexed by k) in order to span the target IEI. If the spectrum of the kth linearly interpolated EEG segment $x_k(t)$ is denoted by $X_k(j\omega)$, then the spectrum of the associated distorted unitary waveform $x_k(a_k \cdot t)$ will be

$\frac{1}{|a_k|}X_k\left(\frac{j\omega}{a_k}\right)$. Therefore, to avoid aliasing of the compressed segments (i.e. segments for which $|a_k| > 1$, as opposed to dilated segments), the following condition should be fulfilled: $a_k \cdot f_k^{max} < \frac{f_s}{2}$, where f_k^{max} is the highest frequency of x_k. This step modifies (locally) the spectrum of each unitary waveform, which is desirable if its dynamics depend on the period fluctuations. Third, now that each unitary waveform covers the same time interval, the signal is resampled at frequency f_s. As long as the aforementioned condition is verified for each compression (leading to a downsampling of the unitary waveform), this will not further affect the waveform spectrum.

The alignment of the event latencies on the target event latencies, obtained through the distinct scaling of each IEI, has the most important - and desired – effect on the signal spectrum, by concentrating the spread spectrum on a fixed fundamental frequency and harmonics. The global signal spectrum periodicity will hence be enhanced even if some local distortions occur. Satisfying the above condition on each a_k might hence not be necessary to have an improvement, and the simulation results (see Time-Warping Modeling toolbox) can rather indicate a practical applicability range for the warping. Linear interpolation has been chosen in the method for its flexibility, since the rescaling of each IEI is different, and aliasing introduced by this operation should not affect the results as long as the signal spectrum occupies a small fraction of the whole frequency range (Oppenheim, 1999). In the case of the present study, in which the frequencies of interest are all below 30 Hz, a sampling rate of 1000 Hz allows to guarantee no significant amplitude modulation due to aliasing. However, if one wants to concentrate higher-frequency activities, the time-warping procedure should be used with caution. In order to avoid any significant aliasing of the signal, its sampling frequency should be chosen so that the frequencies of interest are far lower than the Nyquist frequency. Finally, the time scaling of each segment of the EEG signal has a different effect regarding the local dynamics of the event-related waveform. If the event-related waveforms have a steady dynamic across the signal, with a length that is independent of the local period, the scaling will change the shape of the waveforms, and therefore its spectrum. This distortion increases with increasing incongruity between the local and target periods (i.e. with increasing "jitter"). As a result, the amplitude distribution across the spectrum of the periodic signal will be increasingly affected with greater period fluctuation. An

empirical measure of this distortion can be performed with the Time-Warping Modeling toolbox available in Supplementary Material. If the event-related waveforms have a length proportional to the local period, scaling them according to a target period will not affect their spectrum.

Chapter 4 – EEG Experiments Performed in Healthy Participants

Study 2: Tracking Time-Varying Events: Revealing Error Detection and Neural Entrainment in Rhythmic EEG Activity (Chemin, B., Peretz, I., Mouraux, A.)

Introduction

Rhythm perception and rhythmic temporal anticipation do not necessitate strict isochrony. For example, when a pianist plays an expressive sonata, s/he might slow down the piece at critical times (Palmer, 1997), and this enriches the interpretation of the musical piece (Chapin, Jantzen, Scott Kelso, Steinberg, & Large, 2010). When accompanying a violinist, the pianist needs to anticipate any change of tempo and to adapt the accompaniment in real time. This adaptation is typically smooth and rests on sophisticated prediction mechanisms.

Interestingly, fluctuations in tempo may convey information regarding the forthcoming changes (Jones & Boltz, 1989; Keller, 2008; Large & Jones, 1999; Madison & Merker, 2002; Pecenka & Keller, 2011). In music interpretation, each time interval separating consecutive beats (i.e., interbeat interval) can be slightly adapted in regard to the preceding interbeat intervals. This sequential dependency translates in progressive, predictable fluctuations of tempo (Rankin et al., 2009) which are used by musicians to anticipatively adapt their performance (Keller, 2008; Repp, 2002c).

To accurately anticipate the timing of upcoming events, our central nervous system is thought to rely on a phenomenon of entrainment of neural oscillations to the external rhythm (Lakatos et al., 2013; Nobre, Correa, & Coull, 2007; Nobre & Van Ede, 2017; Schroeder & Lakatos, 2009; Thut et al., 2011). Neural oscillations reflect periodic variations in excitability of neural ensembles (Bishop, 1932; Buzsáki et al., 2012; Buzsáki & Draguhn, 2004) and share two fundamental properties of any oscillator: they can self-sustain and they can adapt their dynamics (Glass, 2001;

Pikovsky, Rosenblum, & Kurths, 2003). When a neural oscillator is periodically stimulated by rhythmic sensory input, its oscillation can become synchronized to the periodic stimulation and the forthcoming high-excitability phase of the neural oscillation is likely to correspond to a forthcoming periodic external event (see, e.g., Haegens & Zion Golumbic, 2017; Thut et al., 2011 for review). Thus, the periodic input will receive optimal processing – a phenomenon called attentional selection, selective attention, or sensory selection (Lakatos et al., 2008). Furthermore, the neural oscillator can adapt its dynamics in regards to consistent changes in the driving sensory input (e.g., progressive fluctuations of tempo in music) or resist to inconsistent (but limited) perturbations – a phenomenon called dynamic attending (see, e.g., Large & Jones, 1999 for a mathematical model of dynamic attending). Finally, neural oscillations can synchronize, or at least modulate each other across different parts of the brain and therefore facilitate the synchronization of rhythmic movements to predictable acoustic rhythm – a phenomenon called predictive timing (see, e.g., Arnal & Giraud, 2012).

However, the interbeat intervals do not always carry sequential dependency. When they fluctuate in a random fashion, their sequence does not convey information regarding the forthcoming changes. Participants trying to synchronize to such unpredictable rhythms are more likely to react (i.e., track) to the fluctuations of tempo (Michon, 1967; Rankin et al., 2014; Thaut, Tian, & Azimi-Sadjadi, 1998), or simply to ignore the perturbations if they remain sufficiently small (see, e.g., Madison & Merker, 2002 on the limits of anisochrony in beat perception).

Even though the oscillatory processes allow the neural system to pick out relevant information, dynamically adapt to slight fluctuations in the flow of information, and anticipatively trigger responses to forthcoming events, an additional monitoring process is necessary to maintain the synchronization of the entrained oscillation to the external rhythm (Hary & Moore, 1987; Repp, 2002a; Repp & Moseley, 2012; van der Steen & Keller, 2013), as it will always come with a part of uncertainty. This process of error detection and correction detects any deviation between the anticipated and the actual timing of each event and can either lead to a posteriori correcting the parameters of the entrained oscillation (such as its phase) or lead to ignoring the perturbations (Merker et al., 2009). In the first case, a posteriori correction translates in tracking behaviour (e.g., Michon, 1967). This so-called copying mode (Merker et al., 2009) consists in copying the timing

interval immediately preceding the last perceived interval, and prevails when individuals engage in joint rhythmic activity (Keller, 2008; Repp & Keller, 2008). In the second case, ignoring the perturbations translates in a self-relying behaviour. This so-called central tendency mode (Merker et al., 2009) consists in producing an average tempo corresponding to the perceived regular pulse. This behaviour comes with reduced variability in the motor tempo, at the cost of a reduced consistency of the produced movement with the acoustic rhythm. We hypothesize that this is an effective way to maintain a relative synchronization to a rhythm with unpredictable fluctuations of tempo. In contrast, the copying mode should prevail in synchronization to a rhythm with predictable fluctuations of tempo, and reinforce the synchronization by increasing the consistency of the produced movement with the acoustic rhythm.

At the neural level, the response following acoustic events occurring in rhythmic sequences can be parsed in functionally distinct responses (Fujioka et al., 2012). In the case of an acoustic rhythm having a constant interbeat interval of 568 ms, the average time course of the power modulation of magnetoencephalographic (MEG) signals following each acoustic event showed an initial modulation consisting in a decrease of power, followed by a rebound reaching a maximum value again around the time of the next stimulus (see Fujioka et al. (2012), Fig. 18A). In two other conditions in which the constant interbeat interval of the acoustic rhythm was set to 390 and 780 ms, the timing of the rebound changed so that it always matched the time of the next stimulus. Importantly, in a condition in which the acoustic rhythm had unpredictable (i.e., random) interbeat intervals uniformly fluctuating between 390 and 780 ms, the rebound occurred earlier compared with the average rebound of the other conditions despite the fact that the interbeat intervals were uniformly distributed around the same range of durations than the constant interbeat conditions. Therefore, this response was interpreted as resulting from anticipation of the forthcoming event, which could be predicted in the rhythms having a constant inter-beat interval, and appeared to be biased towards the possibility of an early event when the inter-beat intervals were variable and unpredictable. In striking contrast, the initial modulation of neural signal following the acoustic events did not change with the stimulus condition. Therefore, this response was interpreted as reflecting an exogenous process driven by the stimulus input,

independently of the fact that the acoustic event was embedded in any rhythmic stream of acoustic events.

In this paper, we suggest that the neural response to each acoustic event should partially reflect the oscillatory process of predictive timing, and partially reflects the error detection process. Therefore, the neural response should change according to the context in which each acoustic event occurs. Furthermore, we suggest that the conjunction of those two functionally distinct features should determine the mode of synchronization. To test our hypothesis, we recorded the electroencephalographic (EEG) activity in participants while they listened or synchronized their finger taps to acoustic rhythms with predictable or unpredictable fluctuations of tempo. Importantly, we segregated the functionally distinct neural responses in two categories: responses that are phase-locked to each period between two acoustic events (i.e., responses represented on a relative time scale, in radians); and responses that are time-locked to each acoustic event (i.e., responses represented on an absolute time scale, in seconds). Hence, phase-locked responses should preferentially reflect the dynamically adapting processing of the acoustic rhythm which include the entrainment of neural oscillations (Chemin et al., 2018), as predictive processes aiming at aligning the high-excitability oscillatory phase with the predicted timing of the expected events are highly phase dependent, while time-locked responses should preferentially reflect the transient processing of each acoustic event which include the error detection process. Importantly, there is a polarizing discussion about whether the rhythmic neural activity measured in response to rhythmic sensory stimulation corresponds to the repetition of transient evoked responses or corresponds to actual neural oscillations (Zoefel et al., 2018). Whereas it was already suggested that the two phenomena could coexist, it is not (yet) common to clearly disentangle them in studies investigating the neural correlates of entrainment to musical rhythms.

We predicted that the general organization of the acoustic sequence (e.g., a rhythm that is predictable or not) will influence the phase-locked responses. Most specifically, the neural oscillations could dynamically adapt to the variations of interbeat intervals, in order to align their phase with upcoming events. We predict that this adaptation will be better in predictable

conditions. We also predict that the production of an overt tapping movement could facilitate this dynamic adaptation.

More importantly, we predicted that the context in which each acoustic event occurs (e.g., a context in which the event is anticipated or not) will critically influence the time-locked responses. More specifically, we predicted a decrease of the response amplitude when the timing of the event is correctly anticipated (Arnal & Giraud, 2012). Conversely, an increase of amplitude is expected when the timing of the event is not anticipated, in a similar way that an increase of response amplitude is observed in response to any discriminable change in auditory stimulation (Costa-Faidella et al., 2011; Näätänen et al., 2007). We postulated that the time-locked response should reflect a process of error detection. Therefore, we further expected that the synchronization of an overt movement, which provide the participants with a direct sensory feedback regarding the accuracy of the anticipation, would reinforce the eventual differences in error detection between the predictable and the unpredictable conditions.

Methods

Participants

Thirteen healthy volunteers (9 females; all right-handed; age = 34 ± 16 years) took part in the experiment after providing written informed consent. All participants had no prior experience with the experimental design. They had no history of hearing, neurological, or psychiatric disorder, and none were taking any medication at the time of the experiment. Their musical practice spanned from none to thirty years. The local ethics committee approved the experiment.

Experimental Design

The experiment was divided in two sessions. The first session consisted in listening passively to acoustic rhythms. The second session consisted in tapping the finger in synchrony to the same acoustic rhythms. Both sessions contained two conditions: a condition in which the acoustic rhythms showed predictable tempo fluctuations, and a condition in which the acoustic rhythms showed unpredictable tempo fluctuations of the tempo. The two conditions were presented in separate blocks, whose order was counterbalanced across participants. (Fig. 30).
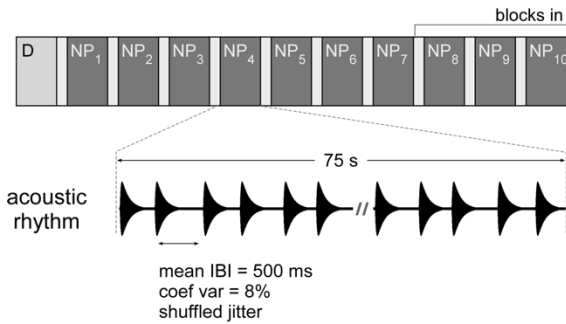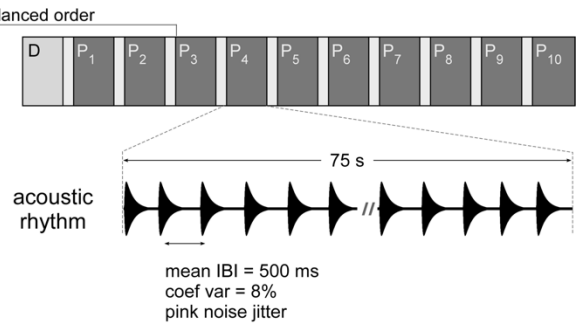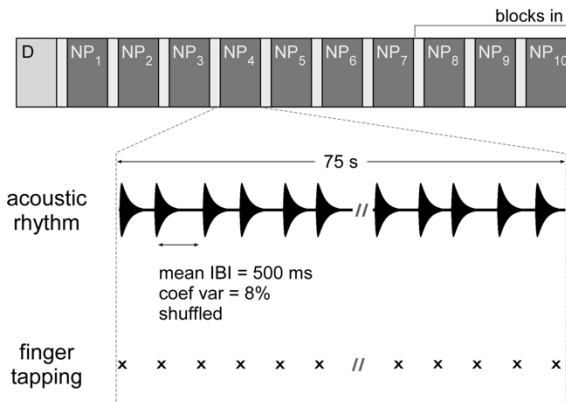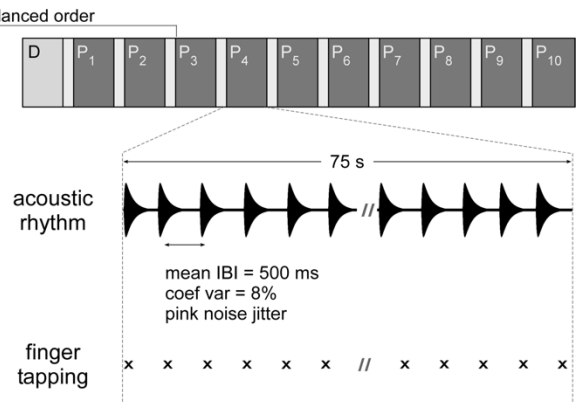
Figure 30. – Experimental Design.

The experiment was composed of two sessions, each containing two conditions presented in separate blocks. In each session, the order of the blocks was counterbalanced across participants. Each block started with one dummy trial (D), consisting in an isochronous acoustic rhythm, to allow the participant to become familiar with the task without fluctuations of tempo. Then, ten trials of 75 s, consisting in either acoustic rhythms with predictable (P) or unpredictable (NP) tempo fluctuations (P), depending on the condition, were presented to the participant. The ten NP sequences corresponded to the shuffling of the interbeat interval (IBI) order of the ten P sequences, and the same set of twenty sequences was used in both experimental sessions. A unique set of twenty sequences was used for each participant. The passive listening to acoustic rhythms task consisted in listening to the 75 s sequence of 150 acoustic events occurring at a mean IBI of 500 ms. The finger tapping synchronized to acoustic rhythms task consisted in tapping the right index finger in synchrony with the acoustic events.

126

Acoustic Rhythms with Predictable Tempo Fluctuations. The acoustic rhythms with predictable tempo fluctuations consisted in 75 s sequences of 150 acoustic events. The acoustic events (or "beats") were made of a white noise lasting 150 ms (7.5 ms rise time, 142.5 ms fall time), and occurred at an average interbeat interval (IBI) of 500 ms. Predictable fluctuations were introduced by adding a jitter of -60 to +60 ms to each interbeat interval, as follows. First, a 150-point jitter time-series was generated from white noise. Second, the time-series was filtered using a 1/f FFT-filter. Third, the filtered time-series were scaled such that its coefficient of variation was equal to 8% (Fig.2). Finally, jitter time-series having a non-normal distribution (assessed using an Anderson-Darling test), or a maximal absolute value exceeding 60 ms (12% of the 500 ms mean IBI), were excluded from the experiment. For each participant, ten different predictable sequences were generated, to form one block of ten trials. Different sequences were generated for each trial to prevent any effect of reminiscence of the fluctuations from trial to trial. Therefore, the predictable aspect of the predictable acoustic rhythms emerged from the gradual, 1/f, changes in tempo, i.e., the rhythm tended to progressively change from longer to shorter or shorter to longer interbeat intervals, allowing the participants to anticipate the duration of the upcoming interval (Rankin).

Acoustic Rhythms with Unpredictable Tempo Fluctuations. For each participant, ten acoustic rhythms with unpredictable tempo fluctuations were generated by shuffling the order of the interbeat intervals of each of the ten interbeat interval sequences with predictable fluctuations (Fig. 31). This operation resulted in removing all auto-correlations of the 1/f-filtered sequences, thereby removing all gradual changes in tempo and, hence, all information that would predict the length of the upcoming interbeat interval.

distribution and time course
of inter-beat-intervals

spectral representation
of jitter time-series

white noise time-series

amplitude

1

0

-1

1/f FFT-filter
& amp. scaling

mag.

0   frequency (Hz)   1

predictable rhythm

.56

IBI (s)

.5

.44

shuffling

*

mag.

0   frequency (Hz)   1

non-predictable rhythm

.56

IBI (s)

.5

.44

*

mag.

0   frequency (Hz)   1

0   150
event number

* spectrum averaged across
all the trials used in the present study
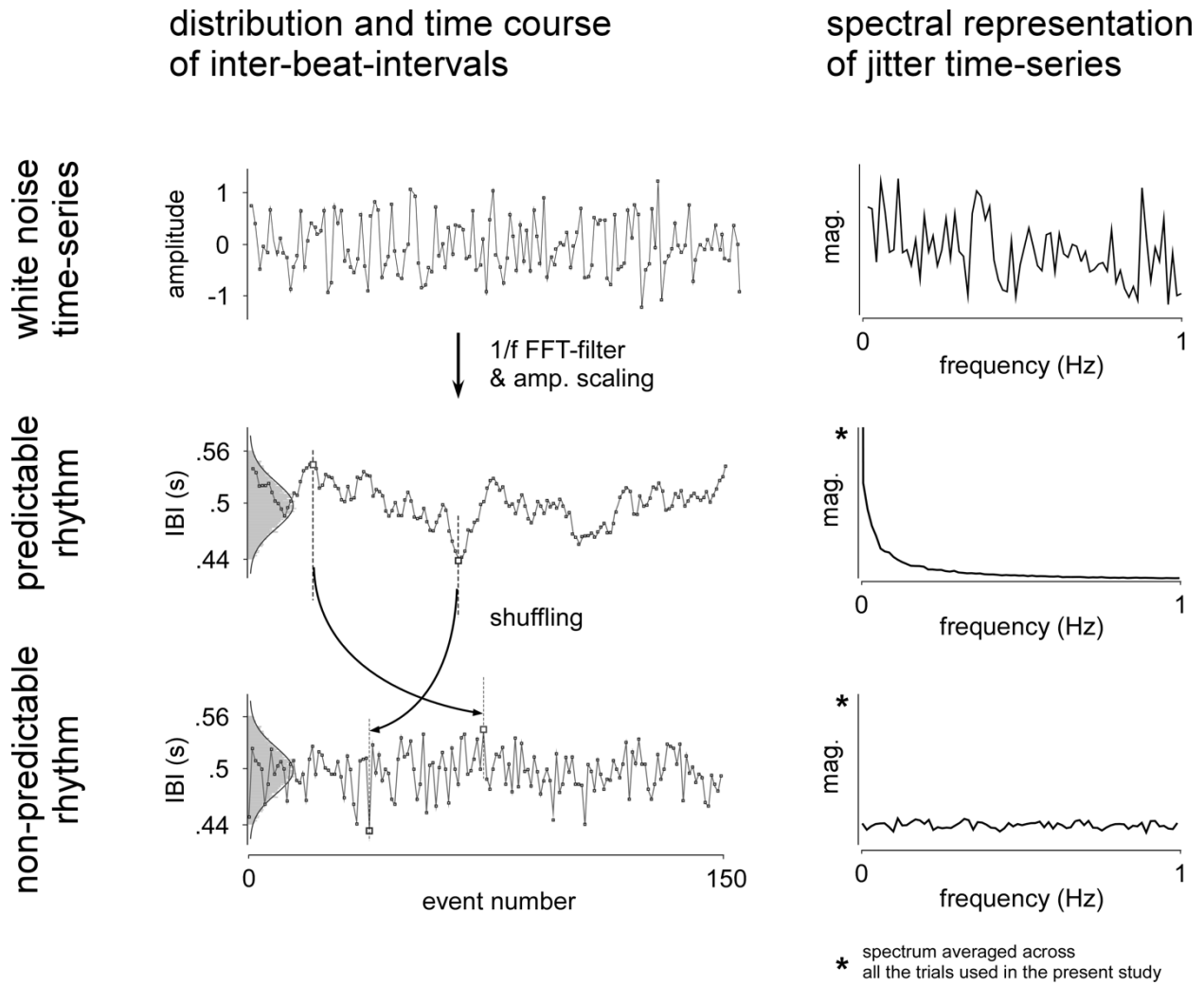
Figure 31. –   Generation of Predictable and Unpredictable Fluctuations of Tempo

Left column: amplitude of tempo variations as a function of event order; Right column: spectrum of the tempo variations. First, a 150-points jitter was generated from white noise (fist line). Second, the 150-points jitter was filtered with a 1/f FFT-filter, scaled to fit the jitter distribution criteria, and added to the interbeat intervals of the acoustic rhythm. These operations yielded a gradually changing tempo (second line). Third, the order of the interbeat intervals of the predictable rhythm was shuffled, in order to create an unpredictable rhythm having the same jitter distribution as the predictable rhythm.

During the whole experiment, participants were seated comfortably in a chair, with their right elbow placed on a table at wrist height. The tapping hand was hidden from participants with a sheet of fabric mounted on a vertical frame. Participants were instructed to relax, avoid any unnecessary head or body movement, and keep their eyes fixated on a point in front of them.

The experimenter remained in the recording room with the participant at all times to monitor compliance to the procedure and instructions, as well as to monitor the EEG signals and, eventually, provide feedback to the participant in case of important eye or movement artifacts.

Participants were requested either to listen passively to the acoustic rhythm (session one), or to perform a hand tapping task synchronized to the acoustic events, such as to synchronize their tapping so that the tapping of the index with the table coincided with the acoustic events (session two). In each session, each of the two blocks was preceded by a dummy trial, consisting in performing the given task with an isochronous acoustic rhythm having a constant inter-beat interval of 500 ms. The dummy trial allowed the participants to familiarize with the task.

At the end of each trial, participants were asked to provide a discrete rating, from 0 to 9, to one of the following questions: (1) "How easy was it to perform the task?" (4 trials/10), (2) "How stable was the rhythm?" (4 trials/10), (3) "Rate your attention level." (1 trial/10), (4) "Rate your comfort level." (1 trial/10). The instructions and questions were displayed on a computer screen, using MATLAB 2017b (The MathWorks, Natick, MA). The onset of each trial was initiated by the participant pressing a button. A random 1.5 to 3 s delay separated the button press from the onset of the trial. The acoustic rhythms were presented binaurally using pneumatic earphone inserts (Etymotic ER1, Etymotic Research, Elk Grove, IL), and played using an externally-triggered zero latency audio stimulus generator (AUDIOFile, Cambridge Research System, Rochester, United Kingdom).

Data Acquisition

EEG Recording

The EEG was recorded using 64 Ag-AgCl electrodes placed on the scalp according to the international 10-10 system (Waveguard64 cap, Cephalon A/S, Norresundby, Denmark). Electrode impedances were kept below 10 kΩ. The signals were amplified using an average reference, low-pass filtered at 500 Hz, and digitized at a sampling rate of 1,000 Hz, using an ASA64 EEG amplifier and digitizer (Advanced Neuro Technologies, Enschede, The Netherlands). A trigger produced by the audio stimulus generator was sent to the EEG amplifier at the beginning of each trial.

Finger-Movements Recording

Movements of the finger were recorded using a touch sensor (Makey Makey, MIT Media Lab's Lifelong Kindergarten, USA) placed on the table, in regard to the tapping finger. The touch sensor measured the impedance between the finger and the touch pad. The signals generated by the touch sensor were digitized at a sampling rate of 1,000 Hz, using an auxiliary channel of the EEG amplifier. The signals were normalized such that the unit corresponded to the value at contact of the finger with the sensor, and zero corresponded to no finger contact.

For all the following analyses, the signals corresponding to the first two events of each trial were discarded (see subsequent sections for details). This was done because a short time to align movements to rhythmic acoustic stimulation is always needed in auditory-motor synchronization tasks (Repp, 2005).

Quantification of Auditory-Motor Synchronization

The synchronization of the finger taps with the acoustic beat was assessed for each trial of the *finger tapping synchronized to acoustic rhythms* session. The tap latencies (i.e. the latencies at which the finger tapped on the table) were identified in the touch sensor signals, as the latencies at which state level transitioned from 0 to 1.

For each trial, each acoustic event (or "beat") latency was denoted B_k (in seconds, at beat k). Each interbeat interval was denoted IBI_k, with $IBI_k := B_k - B_{k-1}$ for $k = 3, \dots, 150$ (the first two acoustic events were therefore discarded). Each tap latency was denoted by $T_{k'}$ (in seconds, at tap k', which corresponded to the tap that was the closest to the kth acoustic event). Each inter-tap-interval was denoted by $ITI_{k'}$, with $ITI_{k'} := T_{k'} - T_{k'-1}$ for $k' = 3, \dots, 150$. The median ITI was denoted by $\widehat{ITI}$.

The phase deviation $\phi_{k'}^{tap}$ (in radians, at tap k') of each tap relative to the median ITI was computed as $\phi_{k'}^{tap} = 2\pi T_{k'} / \widehat{ITI}$. The relative phase, $\phi_{k'}^{beat}$ (in radians) between each tap and the closest acoustic event latency was computed as $\phi_{k'}^{beat} = 2\pi(B_k - T_{k'})/(B_k - B_{k-1})$ (Fujii et al., 2014a).

A measure of the consistency of the tapping tempo, R^{tap}, was computed for each trial. This measure, which is a circular analysis that reflects the coefficient of variation of the asynchrony between acoustic and motor events, was computed by calculating the resultant vector length of phase deviation of each tap relative to the median ITI ($\phi_{k'}^{tap}$ for $k' = 3, \ldots, 150$) using the *circ_r* function of the CircStat matlab toolbox (Berens, 2009). The resultant vector length (R^{tap}) reflects the consistency of the tapping tempo along each trial. Its value is equal to 1 when the tapping tempo remains perfectly stable along the entire trial and tends towards 0 when the tapping tempo changes maximally along the trial.

A measure of consistency of the synchronization between the taps and the acoustic beats, R^{beat}, was computed by calculating the resultant vector length of the phases $\phi_{k'}^{beat}$. This measure was inversely proportional to the tap dispersion around the acoustic events, and spanned from 0 (i.e., maximal dispersion, i.e. poor synchronization) to 1 (i.e., no dispersion, i.e. perfect synchronization). A measure of the mean accuracy of the synchronization between the taps and the acoustic beats was computed by calculating the mean of the phases $\phi_{k'}^{beat}$ using the *circ_mean* functions of the CircStat toolbox. This measure reflected the mean deviation between the taps and the acoustic events and spanned from 0 (perfect phase alignment) to $\pm\pi$ radians (negative lag: tapping preceded the beat; positive lag: tapping followed the beat).

Finally, a cross-correlation was computed between the time course of the interbeat intervals as a function of time, and the time course the intertap intervals as a function of time. Those waveforms were generated by connecting the dots having the event (i.e., a tap or a beat) latency, generally denoted E_{k^*} as abscissa and interevent interval $E_{k^*} - E_{k^*-1}$ as ordinate. This approach slightly differed from prior approaches in that the cross-correlation function was not computed from the interevent intervals classed on an *ordinal* axis (e.g., Michon, 1967; Repp & Keller, 2008). These prior approaches are valid under the assumption that the ordinal classification of the tap latencies is the same as that of the acoustic event latencies. This assumption would be met only in the best synchronization datasets, where one and only one tap is associated to each acoustic event. In the obtained cross-correlation function, the maximal value $xcorr_{max}$, and its lag lag_{max} were measured within a range spanning from –5 to +5 s. The value $xcorr$ represents the similarity

131

between tempo fluctuations of the tapping and tempo fluctuations of the acoustic rhythm, spanning from -1 (tapping fluctuations are the exact opposite of the acoustic fluctuations) to +1 (tapping fluctuations matches perfectly the acoustic fluctuations). A $xcorr$ of 0 indicates no correlation between the two signals. The value of lag_{max} indicates the lag at which the maximum positive correlation was observed, in seconds (i.e., whether the participant followed or anticipated the acoustic rhythm fluctuations).

EEG Data Processing

EEG Preprocessing

A 50 Hz notch filter and a 0.1-100 Hz band-pass FFT-filter were applied to remove artifacts due to environmental noise as well as slow signal drifts. The continuous EEG signals recorded in each condition were then segmented in epochs lasting 76 s, extending between -0.5 to 75.5 s relative to the onset of each trial. Occasionally, the signals from noisy electrodes identified by visual inspection, were replaced by interpolation of the signals of 4 to 8 neighbouring electrodes. No more than 3 channels were interpolated per participant. Artifacts produced by eye blinks or eye movements were removed from the EEG signal using a validated method based on an independent component analysis (Jung et al., 2000), using the *runica* algorithm (Bell & Sejnowski, 1995; Makeig, 2002), and a number of independent components corresponding to the number of non-interpolated channels -1. The artifacts were identified visually based on their spatio-temporal distribution. Finally, the signal of each electrode was referenced to an average off all the 64 EEG channels.

In order to emphasize the responses that are *phase-locked* to each period between two events of interest (i.e., acoustic events in *passive listening* conditions; and either acoustic or motor events in *finger tapping* conditions), the filtered EEG signals were processed using a dynamic time-warping method (Chemin et al., 2018). This process contracted or dilated the EEG signal when the time interval between two events was respectively greater or smaller than the 500 ms mean interbeat interval, using a linear interpolation so that each interbeat interval matched a constant number of 500 samples (i.e., the number corresponding to the mean 500 ms interbeat interval

sampled at 1000 Hz). As a result, each EEG epoch was "rendered periodic" on a relative time scale (in radians, with 2π corresponding to each interbeat interval).

For the later time-domain analysis (e.g., analysis consisting in averaging segmented EEG signals aligned to each acoustic event, and measuring the EEG responses in the time-domain), this process allowed to minimize the blurring of phase dependent cortical activity usually provoked by time-domain averaging procedures (Casarotto, Bianchi, Cerutti, & Chiarenza, 2005; Dinov et al., 2016; H. C. Huang & Jansen, 1985; Mouraux & Iannetti, 2008). For the later frequency-domain analysis (e.g., analysis consisting in computing the Fourier transform of each EEG epoch, and measuring the EEG responses at specific frequencies), this process allowed to minimize the spectral blurring related to the non-stationarity of non-strictly-periodic neural responses, entrained by non-strictly periodic acoustic rhythm (Chemin et al., 2018).

Additionally, in order to emphasize the responses that are *time-locked* to each event of interest and minimize the spectral blurring in later frequency-domain analysis, the filtered EEG signals were also processed using a so-called "false-sequencing" method (Quek & Rossion, 2017). This process reconstructed a periodic signal by concatenating segments of the EEG signal having a constant length of 500 ms, going from -200 ms to +300 ms relative to the onset of each event of interest. The limits of those segments were determined according to the averaged response observed in the time-domain.

Anticipation and Dynamic Entrainment of Neural Oscillations

Time-locked and phase-locked EEG signals obtained from each trial of the four conditions (*passive listening vs. finger tapping to predictable vs. unpredictable tempo fluctuations*) were compared using a procedure based on their spectral decomposition. This approach allows to easily concentrate *all* the periodic signals in a single measure (the sum of the magnitude at fundamental frequency and a limited number of harmonics) (see, e.g., Bach & Meigen, 1999; Collura, 1996; Haykin & Van Veen, 1999; Zhou et al., 2016), and was carried out with following procedure.

First, the 76 s EEG epochs recorded in the four experimental conditions were transformed in the spatial domain by computing the current source density (Delorme & Makeig, 2004). This procedure was used to disentangle the EEG signal originating from auditory and motor areas of

the brain. This was important because a strong effect of the movement synchronization task was expected on the anticipation processes (Nozaradan, Schönwiesner, et al., 2016; Nozaradan et al., 2013; Schroeder et al., 2010), and therefore any confounding effect of direct movement-related EEG activity superimposition to auditory-processing related EEG activity had to be avoided. The disentangling of the two signals was further maximized by additional methods that will be described throughout the overall procedure.

Second, the EEG epochs were "rendered periodic" using the false-sequencing and the time-warping methods described in section 3.4. Interestingly, both methods allowed to maximize acoustic-related activity as compared to movement-related activity, because the movement-related activity had different period fluctuations than the auditory-related activity, and therefore spreads over neighbouring frequencies rather than concentrating at the frequencies of interest (Chemin et al., 2018).

Third, the "rendered periodic" EEG epochs were cropped to discard the first two acoustic events and keep an integer number of 148 event cycles. Then, the signals were transformed in the frequency domain using a discrete Fourier transform (Frigo & Johnson, 1998). This yielded a spectrum of signal amplitude (µV) ranging from 0 to 500 Hz with a frequency resolution of 0.0119 Hz (Bach & Meigen, 1999). The background noise was removed by subtracting, at each frequency bin of the EEG spectra, the average amplitude measured at neighbouring bins (eight frequency bins ranging from −0.14 to −0.05 Hz and from +0.05 to +0.14 Hz relative to each frequency bin). The validity of this subtraction procedure relies on the assumption that, in the absence of a strong periodic signal, the signal amplitude at any given frequency bin should be similar to the signal amplitude of the mean of the surrounding frequency bins (Mouraux et al., 2011; Retter & Rossion, 2016). This subtraction procedure using neighbouring frequency bins is important because background EEG noise is not equally distributed across scalp channels and, most importantly, is greater at lower frequencies as compared to higher frequencies. The noise-subtracted spectra were then averaged across epochs, for each condition and each individual.

Fourth, topographical maps related to the motor signals were obtained by averaging the normalized topographical maps obtained for each participant, for both tapping conditions, in

signals rendered periodic for the tapping events with both time-warping and false sequencing methods, and summed for the fundamental frequency (1F = 2 Hz) and nine first harmonics (2F = 4Hz; …; 10F = 20 Hz). Topographical maps related to the auditory signals were obtained by averaging the normalized topographical maps obtained for each participant, for each four conditions, in signal rendered periodic for the acoustic events with both time-warping and false sequencing methods, and summed for the fundamental frequency (F = 2Hz) and nine first harmonics (2F = 4Hz; …; 10F = 20 Hz). A pool of electrodes of interest yielding maximal auditory signal and minimal motor signal interference was selected as the nine electrodes of maximal amplitude after subtraction of the topographical map related to the motor signals from the topographical map related to the auditory signal (electrodes F5, F7, FC5, F4, F6, F8, FC6, FT8, and T8).

Finally, the signals were averaged across the nine electrodes, and summed across the ten frequencies of interest.

Expectations and Reaction to Violation of Expectations

The EEG signals of each trial of the four conditions (*passive listening vs. finger tapping to predictable vs. unpredictable tempo fluctuations*) were segmented from -0.6 to +0.6 s for non time-warped EEG signals and from -2.4π to +2.4π rad for time-warped EEG signals, relative to the latency of each acoustic event. The segments corresponding to the first two acoustic events of each trial were discarded.

The EEG segments were categorized in three equal groups according to the length of the interbeat interval measured between the previous beat and current beat. The categories corresponded to short, medium or long interbeat intervals, and were constructed for each trial and each condition, so that each category contained 47 events per trial. With this categorization, differences across categories were determined by the time at which each event occurred after the previous event, as compared to the entire set of interbeat intervals within one trial. Hence, within each category, the EEG response was predominantly determined by the respect or the violation of the time at which the current beat was expected to occur, according to the expectation created by the mean interbeat interval of the sequence. For example, an event occurring after a short interbeat

interval would be perceived as occurring *too early* as compared to the other events, and an event occurring after a long interbeat interval would be perceived as occurring *too late*.

Importantly, the reaction to each event is not expected to be steadily determined by the average interbeat interval of the trial. Actually, the expectations would rather dynamically adapt to the local context in which the event occurs (Large & Jones, 1999). For example, in the case of an acoustic rhythm with predictable tempo fluctuations, the gradual increase or decrease of interbeat intervals would modulate the expectations along time, so that an event occurring after a short interbeat interval would *not* be perceived as occurring too early as compared to the other events. Therefore, the segments were further categorized, in both *predictable* and *unpredictable* conditions, according to a measure of deviation from dynamically adapting model expectations.

The model expectations were constructed using a phase-shifting 75 Hz low-pass Butterworth filter. This operation produced a signal mimicking the original time course of the acoustic rhythm but ignoring the sharp changes of interbeat interval, with a lag of approximately two interbeat intervals (Fig. 32). The deviation from expectations were computed by subtracting, to each interbeat interval, the value of the corresponding expectation. Then, the events were classified according to the amount of deviation from expectation, in groups of deviations spanning from - 135 to 135 ms, with a step of 30 ms (Fig. 32). This allowed measuring the reaction to unexpected interbeat intervals, with an effect of violation that was controlled between the different conditions.
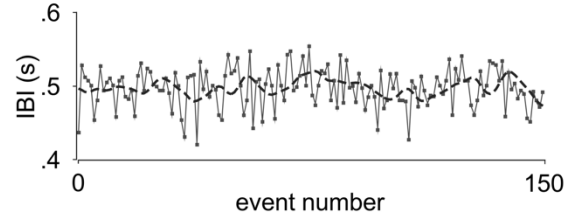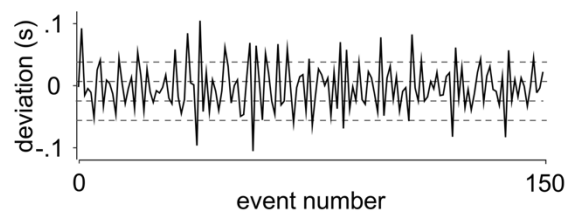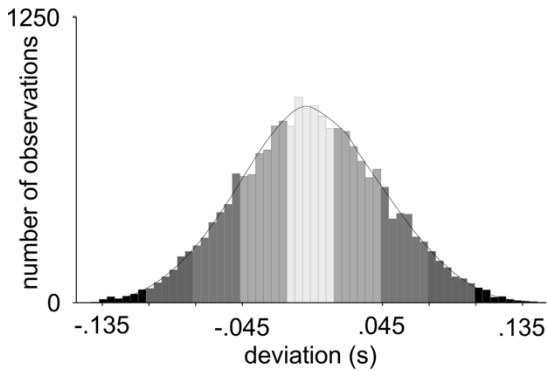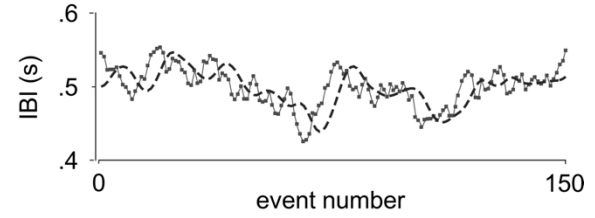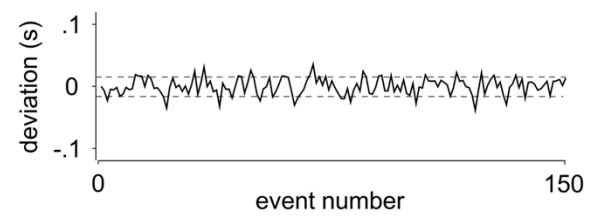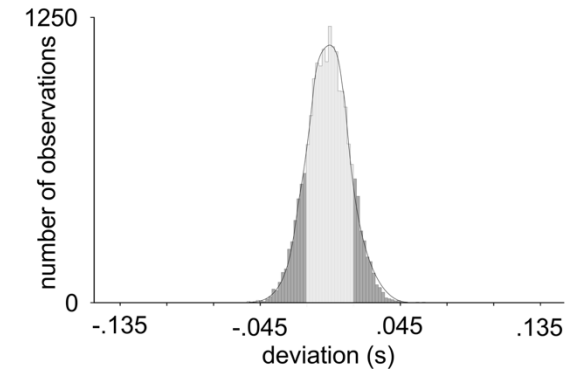
Figure 32. – Classification of the Events According to a Model of Local Expectations.

First line: time series of the interbeat intervals (IBI, grey line and dots) and model expectation (grey dashed line) constructed using a phase-shifting 75 Hz low-pass Butterworth filter, applied to the original IBI time series. This operation produced a signal mimicking the original time course of the acoustic rhythm but ignoring the sharp changes of interbeat interval, with a lag of approximately two interbeat intervals. **Second line:** time series of the difference between the model expectations and the actual beats. **Third line:** distribution and classification of the events, according to the amount of deviation from the model expectations.

Then, both absolute and relative time scaled EEG segments were averaged across trials, within condition, category and participants. Finally, in order to visualize the general shape of the periodic EEG response between the different conditions, the different categories, and the different time scales, the segments were further averaged across participants.

137

Statistical Analysis

Auditory-Motor Synchronization

In order to test whether predictable acoustic rhythms led to the so-called *copying mode* of synchronization and unpredictable acoustic rhythms led to the so-called *central tendency mode* of synchronization, a 2 (condition: *predictable tempo fluctuations* vs. *unpredictable tempo fluctuations*) × 2 (measure of consistency: R^{beat} *vs.* R^{tap}) repeated measures analysis of variance (ANOVA) was conducted on measures of synchronization, averaged across trials for each participant and each condition. Additionally, paired samples *t*-tests were used to perform pairwise comparisons between both fluctuation types, for the five different measures of synchronization (R^{beat}; θ^{beat}; R^{tap}; $xcorr_{max}$; and lag_{max}). The significance level was set at *p* < .05.

Ratings

An ordinal regression was performed to evaluate which predictor variable (condition: *predictable tempo fluctuations* vs. *unpredictable tempo fluctuations*; session: *passive listening* vs. *finger tapping*; and question type: *ease of the task* vs. *stability of the tempo*) influenced the rating of the participants. Wilcoxon signed-rank tests were used to perform post-hoc pairwise comparison in predictor variables that were selected by the ordinal regression. The significance level was set at *p* < .05.

EEG measures

Anticipation and Dynamic Entrainment of Neural Oscillations. In order to compare the overall time- and phase-locked EEG signals entrained to the acoustic rhythms, a 2 (condition: *predictable tempo fluctuations* vs. *unpredictable tempo fluctuations*) × 2 (session: *passive listening vs. finger tapping*) x 2 (method: *time-warping* vs. *false-sequencing*) repeated measures analysis of variance (ANOVA) was conducted on EEG response magnitude, averaged across trials for each participant and each condition, averaged across the nine electrodes of interest, and summed from F to 10F. Paired samples *t*-tests were used to perform post hoc pairwise comparisons between the EEG response magnitudes, for the levels of interest. The two-tailed significance level was set at *p* < .05. A Bonferroni correction was used for multiple comparisons.

Expectations and Reaction to Violation of Expectations. In order to compare the waveforms obtained in different conditions, a cluster-based paired-sample t-tests (1000 permutations) was performed on EEG responses obtained after averaging all the segments, across trials and within participants (Groppe, Urbach, & Kutas, 2011; Maris & Oostenveld, 2007; van den Broeke, Lambert, Huang, & Mouraux, 2016). The test was performed at each electrode. First, the average responses to acoustic events issued from rhythms with predictable vs. unpredictable tempo fluctuations were compared by performing the test on the averaged segments, regardless of the length of the interbeat interval, in both passive listening and tapping sessions. Second, the response determined by the respect or the violation of the time at which the current beat was expected to occur according to the expectation created by the mean interbeat interval of the sequence was evaluated by comparing the segments averaged within a category of interbeat interval (i.e., short or long interbeat interval) to the segments averaged within the medium interbeat intervals, for both predictable and unpredictable conditions and in both passive listening and tapping sessions. Third, the different reactions to violation of dynamically adapted expectations, built according to the local context in which each event occurs, were quantitatively compared using a 2 (condition: *predictable tempo fluctuations* vs. *unpredictable tempo fluctuations*) x 3 (discordance to the model expectation: *-.045 ms to -.015 ms* vs*. -.015 to +.015 ms* vs. *+.015 to +.045 ms* of discordance) x 2 (session: *passive listening* vs. *tapping*) point-by-point repeated measure ANOVA (see, e.g., van den Broeke et al., 2016), conducted on the segments averaged across trials and within discordance category and participant. The significance level was set at $p<.05$. Importantly, this analysis was made possible because the measure concerned the reaction to the amount of discordance between the timing of each event relative to the modeled expectation and was therefore controlled between the conditions.

Then, the amplitude of the component of interest identified by the later ANOVA was extracted for each condition (*predictable tempo fluctuations* vs. *unpredictable tempo fluctuations*), each range of discordance (*-.045 ms to -.015 ms* vs*. -.015 to +.015 ms* vs. *+.015 to +.045 ms*) and each session (*passive listening* vs. *tapping*), for each participant at the main electrode of interest. Post-hoc analysis were performed using those amplitudes.

The tests were computed on non time-warped averaged EEG segments only, as time-locked activities are the main components of interest in reaction to violation of expectation.

All EEG analysis procedures were carried out using Letswave 6 (Institute of Neuroscience, University of Louvain; www.letswave.org), an open-source MATLAB (The MathWorks, Natick, MA) toolbox and the time-warping algorithm that can be downloaded on the Github repository: github.com/BaptisteChemin/EEG-Time-Warping. The auditorimotor synchronization analysis were performed using the CircStat toolbox (Berens, 2009) and additional scripts that can be downloaded on the Github repository:

github.com/BaptisteChemin/AuditoriMotor-Synchronization. Statistical analyses were carried out using SPSS and Letswave 6.

Results

Auditory-Motor Synchronization

The ANOVA revealed a significant interaction between condition and measure of consistency, $F(1,12) = 68.977$, η2 = .064, $p < .001$, which indicates that the measures of consistency of the tapping synchronization to the acoustic rhythm (R^{beat}) and the measures of consistency of the tapping tempo (R^{tap}) were not similarly affected by the type of fluctuations present in the acoustic rhythm. Post hoc pairwise comparisons showed that the consistency of synchronization R^{beat} was significantly higher, $t(12) = 3.213$, $p = .007$ for the acoustic rhythms with predictable fluctuations ($M = .876$) than for the acoustic rhythms with unpredictable fluctuations ($M = .835$). Conversely, the consistency of the tapping tempo across the trial R^{tap} was significantly lower, $t(12) = -7.630$, $p < .001$, for the acoustic rhythms with predictable fluctuations ($M = .177$) as compared to the acoustic rhythms with unpredictable fluctuations ($M = .277$).

The maximal similarity between the fluctuations of the tapping and of the acoustic interevents intervals was significantly higher, $t(12) = 7.876$, $p < .001$, for the acoustic rhythms with predictable fluctuations ($M = .802$) than for the acoustic rhythms with unpredictable fluctuations ($M = .688$).

The lag at which the maximal similarity was measured was significantly shorter, $t(12)$ = -5.895, p < .001, for the acoustic rhythms with predictable fluctuations (M = .364 s) as compared to the acoustic rhythms with unpredictable fluctuations (M = .481 s). Finally, the asynchrony between the motor and the acoustic events did not significantly differ with the two types of rhythm fluctuations (M = -.422 π, i.e., a mean negative asynchrony corresponding to 20% of the interbeat intervals, $t(12)$ = -.131, p = .898). The results are presented in Fig. 33.
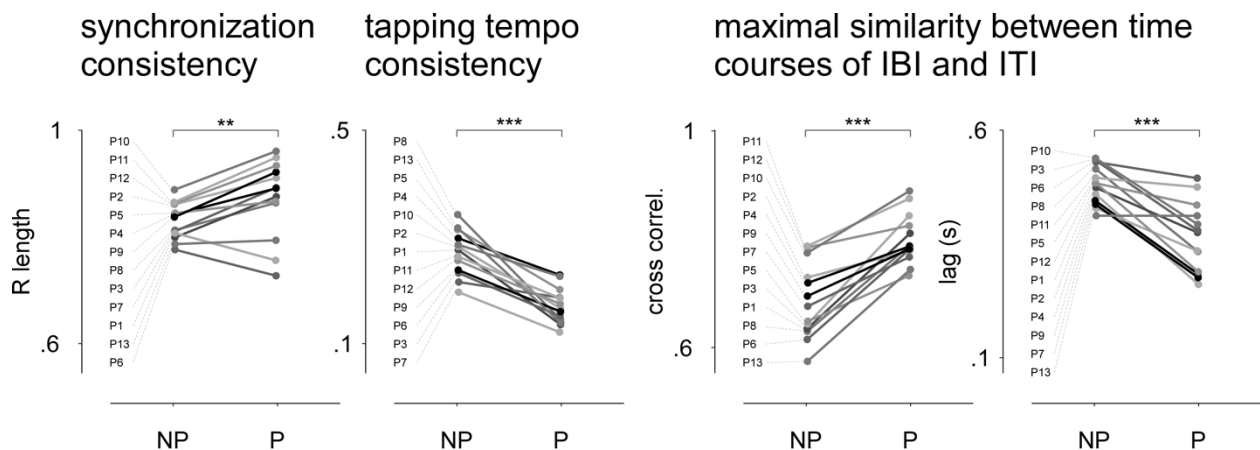
Figure 33. – Main Results in Tapping Synchronization

The synchronization consistency was higher for the predictable condition, together with a higher maximal coefficient of cross-correlation and a shorter positive lag, as compared to the unpredictable condition. The mean asynchronies between the acoustic events and the taps were negative in both conditions (not represented). These results indicate that the participants could easily synchronize to the predictable rhythms, and that they showed both signs of entrainment and tracking. The individual representation reveals some heterogeneity in the individual results. The consistency of the tapping tempo was higher in the unpredictable rhythm, together with a lower maximal coefficient of correlation. These results indicate that the participants tended to *ignore* the unpredictable fluctuations of tempo rather than *tracking* them. NP, non-predictable; P, predictable; IBI, interbeat intervals; ITI, intertap intervals.

Those results confirmed the hypothesis that participants would use different modes of synchronization under different conditions of acoustic rhythm fluctuations. When the fluctuations of tempo were progressive and temporally organized, participants tended to *copy* the fluctuations, at a short lag of .364 s. In contrast, when the fluctuations of tempo were random,

participant tended to ignore them and rather kept a tapping rate matched to a *central tendency* of the estimated average acoustic tempo.

Ratings

The ordinal regression produced a model in which the inclusion of at least one predictor variable improved the fitting of the observed data over the model that does not control for any predictor variable[8], -2 log likelihood = 291.060, χ^2 = 40.601, *DoF* = 3, *p* <.001. Parameter estimates revealed that the predictable fluctuations of tempo yielded a significantly higher overall rating (i.e., participants rated those trials as more stable, and rated the tasks as easier to perform) over unpredictable fluctuations of tempo, *OR* = $e^{0.482}$, Wald χ^2 = 7.774, *DoF* = 1, *p* = 0.005. The questions relative to the ease to perform the task also yielded significantly higher ratings than questions relative to the stability of the tempo, *OR* = $e^{1.004}$, Wald χ^2 = 31.989, *DoF* = 1, *p* < .001. No significant difference could be observed between the ratings performed during the listening and the tapping parts of the experiment, *OR* = $e^{0.142}$, Wald χ^2 = .684, *DoF* = 1, *p* = .408. The results are further reported in Fig. 34. Importantly, the test of proportional odds assumption revealed that the slope coefficients in the model were not the same across response categories, -2 log likelihood = 231.034, χ^2 = 60.027, *p* <.001. This suggests that the ratings were not equally affected by the different predictor variables across the different levels.

Post-hoc analysis showed that, in the listening session, participant did not rate differently the listening task, for the two pattern of tempo fluctuations (*Mdn* = 7), rank = 256, *Z* = .4897, *p* = .6243. Similarly, no significant difference in the rating of tempo stability was observed between the predictable and the unpredictable fluctuating rhythms (*Mdn* = 5), rank = 554, *Z* = 1.6178, *p* = .1057. In the tapping part of the experiment, participants significantly rated the synchronization task as easier for predictable tempo fluctuations (*Mdn* = 7) as compared to unpredictable tempo fluctuations (*Mdn* = 6), rank = 611.5, *Z* = 3.953, *p* < .001. Similarly, they evaluated the rhythm with

---

[8] χ^2 :   Chi-Square
  DoF :   Degrees of Freedom
  OR :   Odd Ratio
  Mdn : Median

predictable fluctuations of tempo (*Mdn* = 6) as more stable than the rhythm with unpredictable

fluctuations of tempo (*Mdn* = 5), rank = 661, *Z* = 2.3001, *p* = .0214.
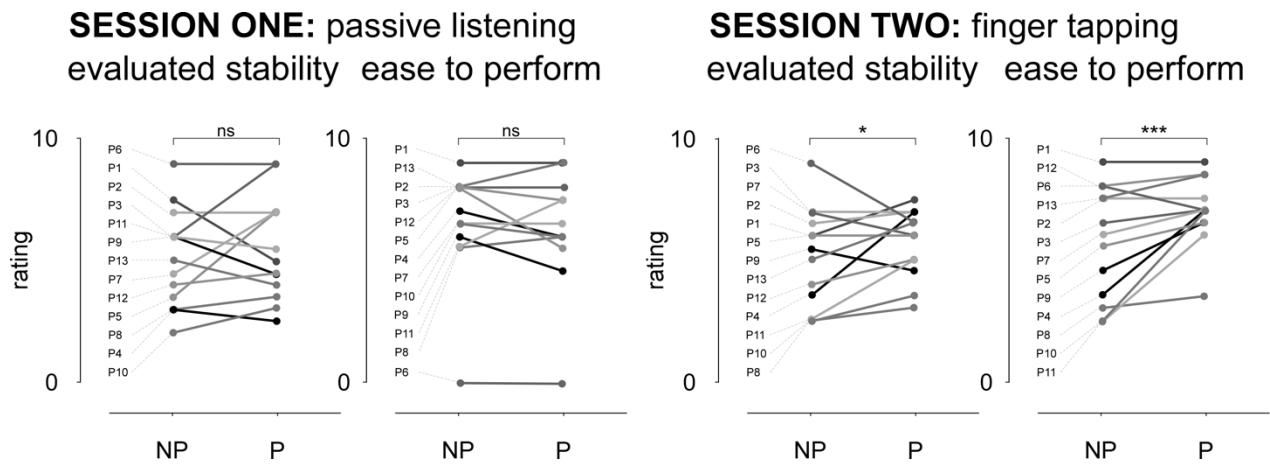
Figure 34. –   Ratings Performed After Each Trial.

Only a few participants (e.g., P3, P7, P5) could clearly feel a difference between the predictable and the unpredictable tempo, when passively listening to it. At the group level, the participants could not explicitly discriminate between the two types of tempo fluctuations. Tapping to the same acoustic rhythms enhanced the discriminating capabilities, and significantly higher ratings were obtained for the predictable condition.

These results suggest that the subjective discrimination between the different patterns of tempo fluctuation is not straightforward. However, the performance of an overt synchronization task, which provide a real-time feedback to the participants, enhanced the discrimination.

EEG

Anticipation and Dynamic Entrainment of Neural Oscillations

The repeated measures ANOVA revealed a significant main effect of session, $F(1, 12) = 28.010$, η2 = 16.05, $p < .001$; a significant main effect of method, $F(1, 12) = 8.716$, η2 = .497, $p < .012$; and a significant interaction between method and session, $F(1,12) = 6.419$, η2 = .189, $p = .026$, which indicates that the difference of magnitude recovered with the time-warping method and the false-sequencing method differed when participants passively listened or tapped to the acoustic rhythm. No significant main effect of condition, $F(1, 12) = 2.945$, η2 = .690, $p = .112$, and no other significant interaction could be observed.

143

The magnitudes of the periodic EEG activity elicited during the passive listening part of the experiment (M = 2.040 µV; sd = 0.304 µV) were significantly lower than the activity elicited during the finger tapping part of the experiment (M = 2.826 µV; sd = .391 µV). Similar enhancement of magnitude of EEG activity elicited by acoustic rhythm during or after rhythmic auditorimotor synchronization task were already observed in previous experiments (Chemin et al., 2018, 2014; Nozaradan et al., 2013), and are usually interpreted as a facilitating effect of overt movement production on the neural processing of acoustic rhythms.

In the passive listening session, the magnitudes of the periodic EEG activity concentrated in the EEG spectrum using the time-warping method (M = 2.066 µV; sd = 0.311 µV) were not significantly different than the activity concentrated using the false-sequencing approach (M = 2.013 µV; sd = 0.297 µV), t(25) = 1.735, p = .095. In contrast, in the tapping session, the magnitudes of the periodic EEG activity concentrated in the EEG spectrum using the time-warping method (M = 2.937 µV; sd = .410 µV) were significantly greater than the magnitudes of the activity concentrated using the false-sequencing approach (M = 2.714 µV; sd = .375 µV), t(25) = 3.714, p = .001.
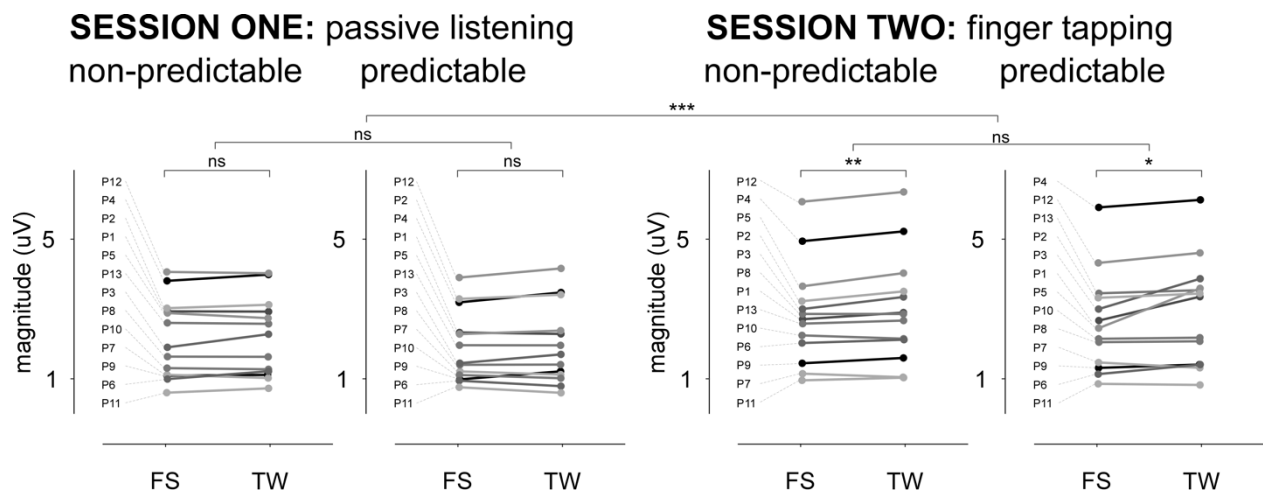
Figure 35. – Magnitudes of the Periodic EEG Activity Concentrated in the EEG Spectrum
Using the False-Sequencing Approach (FS) and the Time-Warping Method (TW).

The false-sequencing approach allows to optimally concentrate repetitive EEG signal that is time-locked to the acoustic beat, while the time-warping method allows to optimally concentrate repetitive EEG that is phase-locked to the acoustic beat. In session two (finger tapping synchronized to acoustic rhythms), the magnitude of the overall phase-locked activity was significantly greater than the overall magnitude of the time-locked activity. These results suggest the involvement of a dynamically adaptive mechanism, with a neural response that adapts to the length of each interbeat interval. Interestingly, while the difference of magnitude between FS and TW signals appears to be relatively constant across participants for non-predictable acoustic rhythms (third graph), there is a great inter-individual variability of this difference for predictable acoustic rhythms (fourth graph). This observation suggests that some participants were able to *entrain* the dynamically adaptive neural mechanism with greater success than others.

Expectations and Reaction to Violation of Expectations

Session One: Passive Listening to Acoustic Rhythms. The averaged EEG responses are shown in Fig. 36. The overall aspect of the waveforms, as observed on the FCz electrode, corresponded to a relatively sinusoidal signal. A slow negative slope started approximately 200 ms before the acoustic event, to reach a peak of maximal negativity approximately 33 ms before the acoustic event. Then, a sharp transition of signal polarity occurred from 33 ms before to 64 ms after the acoustic event, and a plateau of maximal positivity lasted from approximately 64 to 200 ms post

145

event. The following positive slope lasted approximately 100 ms, to finish approximately 300 ms after the acoustic event.

A significant cluster differentiating the average response to acoustic events issued from rhythms with predictable vs. unpredictable tempo fluctuations and extending from approximately +200 to +240 ms relative to the acoustic event, was identified at the following nine neighbouring electrodes: FC1, FCz, FC2, C1, Cz, C2, CP1, CPz, CP2.
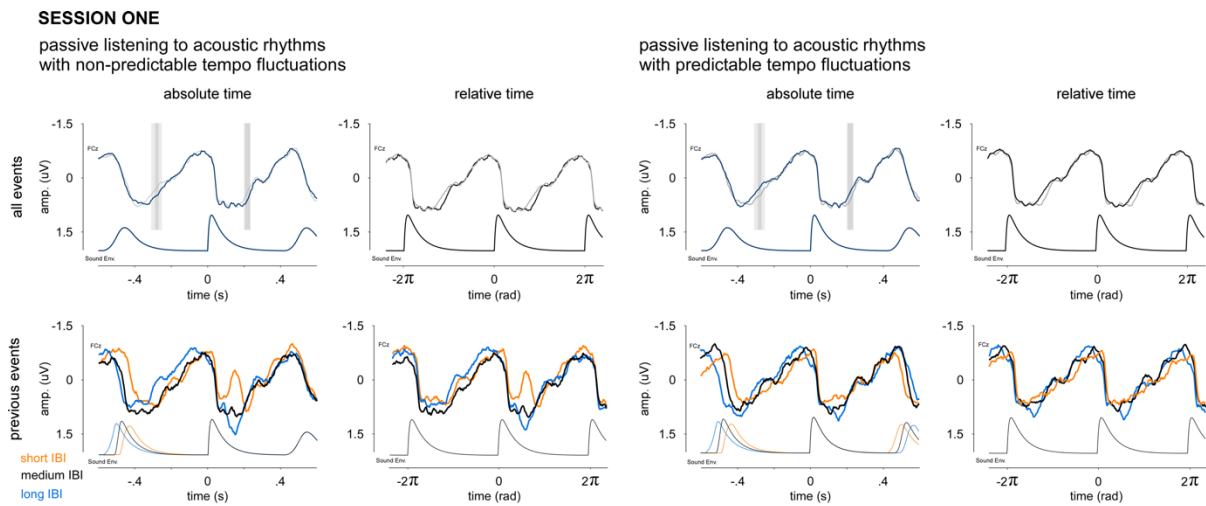
Figure 36. –   EEG Responses to the Acoustic Events of Session One, Shown in
Absolute Time Scale (seconds) and in Relative Time Scale (radians).

First line: EEG response, recorded at FCz and averaged across all the events. The significant differences observed between the response recorded in non-predictable and predictable tempo fluctuations are highlighted by light grey ($p < .05$) and dark grey ($p < .01$) rectangles. **Second line:** EEG response, recorded at FCz and averaged across the events categorized in three groups, according to the length of the interbeat interval preceding the event (short IBI, in orange; medium IBI, in black; long IBI, in blue). An additional component, with a peak of amplitude occurring 149 ms after the onset of the acoustic event, is observed. This component is negative for short IBI, and positive for long IBI.

When the events were categorized according to the length of the preceding IBI, an additional component could be clearly distinguished in the responses measured in the unpredictable condition. This additional component corresponded to a negative peak for short IBI and a positive

peak for long IBI, occurring 149 ms after the acoustic event. In the responses measured in the predictable condition, a visible tendency for such additional component could be observed, but in relatively shorter proportion.

Session Two: Finger Tapping Synchronized to Acoustic Rhythms. The averaged EEG responses are shown in Fig 37. The overall aspect of the waveforms, as observed on the FCz electrode, corresponded to a relatively sinusoidal signal. A slow negative slope started approximately 200 ms before the acoustic event, to reach a peak of maximal negativity approximately 30 ms before the acoustic event. Then, a sharp transition of signal polarity occurred from 30 ms before to 50 ms after the acoustic event, and a relative plateau of maximal positivity lasted from approximately 50 to 200 ms post event. The following positive slope lasted approximately 100 ms, to finish approximately 300 ms after the acoustic event.

Two significant clusters differentiating the average response to acoustic events issued from rhythms with predictable vs. unpredictable tempo fluctuations and extending from approximately -600 to -150 ms and from +60 to +100 ms relative to the acoustic event were identified.
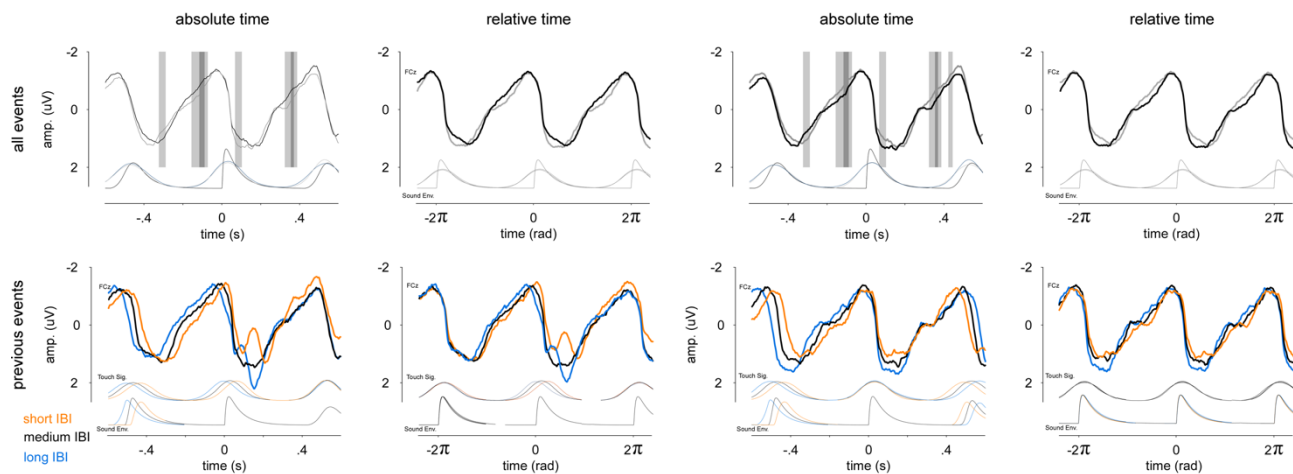
Figure 37. –   EEG Responses to the Acoustic Events of Session Two, Shown in

Absolute Time Scale (seconds) and in Relative Time Scale (radians).

EEG response, recorded at FCz and averaged across all the events. The significant differences observed between the response recorded in non-predictable and predictable tempo fluctuations are highlighted by light grey ($p <$ .05) and dark grey ($p <$ .01) rectangles. **Second line:** EEG response, recorded at FCz and averaged across the events categorized in three groups, according to the length of the interbeat interval preceding the event (short IBI, in orange; medium IBI, in black; long IBI, in blue). An additional component, with a peak of amplitude occurring 149 ms after the onset of the acoustic event, is observed. This component is negative for short IBI, and positive for long IBI.

When the events were categorized according to the length of the preceding IBI, an additional component could be clearly distinguished in the responses measured in the unpredictable condition. This additional component corresponded to a negative peak for short IBI and a positive peak for long IBI, occurring 149 ms after the acoustic event. In the responses measured in the predictable condition, a visible tendency for such additional component could be observed, but in relatively shorter proportion.

Modulation of the Amplitude of the Additional Component Elicited by Violation of Expectation. The point-by-point repeated measure ANOVA revealed a significant main effect of discordance at nine neighbouring electrodes (Fz, F1, F2, F3, F4, FCz, FC1, FC3, Cz, C2), approximately 123 to 188 ms after the acoustic event, $.05 > p > .0001$, $F = 10.5$ on FCz, at .149 ms. A significant main effect

of session was observed on a broader fronto-central cluster of electrodes, $.05 > p > .001$, $13.1 < F < 21.1$ on FCz, throughout the whole time period except from two intervals spanning from -250 to -212 ms and from 20 to 50 ms relative to the acoustic events. No significant main effect of condition was observed, and no significant interaction was observed.

Spearman's coefficient of correlation was computed to analyse the relationship between the amplitude of the 149 ms component and the amount of discordance between the expectation (based on the model described in section 4.1.2.5.3) and the actual occurrence of acoustic events. The amplitude of the 149 ms component was correlated to the quantity of discordance $r_s = .306$, p<.0001, with higher amplitude for the component elicited by events occurring later than expected. A paired-sample t-test was conducted to compare the amplitude of the same component in the passive listening and in the finger tapping session. The component had a significantly higher amplitude in the tapping condition ($M = 1.296$ μV, $SD = 1.012$), as compared to the listening condition ($M = .8001$ μV, $SD = .7215$), $t(77) = -5.229$, $p < .0001$.

Those results suggested that the additional component was dependent off the quantity of mismatch between the expectation built from the local context of tempo fluctuations and the time at which the acoustic event actually occurred, regardless to the predictable or unpredictable aspect of the overall acoustic rhythm. The results are shown in Fig 38.

SESSION ONE

passive listening to acoustic rhythms with non-predictable tempo fluctuations

passive listening to acoustic rhythms with predictable tempo fluctuations

SESSION TWO

finger tapping synchronized to acoustic rhythms with non-predictable tempo fluctuations

finger tapping synchronized to acoustic rhythms with predictable tempo fluctuations

Figure 38. – EEG Responses to the Acoustic Events and the 146 ms Component.

A. EEG responses to the acoustic events of session one and two, recorded at FCz, averaged within categories of discordance to the model expectation, shown in absolute time scale (seconds). The black lines represent the "baseline" response, for events occurring within -15 to +15 ms relative to the expectation. The grey lines represent the responses averaged within each category of violation of expectation. Dashed lines represent the parts of the responses that does not significantly differ from the baseline response, and plain lines represent the parts of the responses that significantly differed from the baseline. **B.** Amplitude of the 146 ms component as a function of the discordance between the model expectation and the actual timing of the acoustic event.

Discussion

When people play music, they show the ability to synchronize movement to a large panel of external rhythms. When a pianist plays a sonata together with a violinist, s/he will adapt the accompaniment in real time. If the violinist is an experienced musician, s/he will lead expressive fluctuations of tempo that convey information regarding the interpretation of the piece, and the pianist will easily understand and anticipate those fluctuations. If the violinist is a novice musician, s/he will probably produce random fluctuations of rhythms and the accompanying pianist will have to find a way to minimize the asynchrony.

In this study, thirteen participants both listened and synchronized their finger taps to acoustic rhythms with predictable and unpredictable fluctuations of tempo. We recorded their tapping and their electroencephalogram in order to determine how they would synchronize to those

rhythms, and how their neural activity would translate the mechanisms of temporal anticipation and error detection.

Participants were able to precisely synchronize their tapping to the acoustic rhythms with predictable fluctuations of tempo. They showed a high tapping consistency in regard to the acoustic targets and a high coefficient of cross-correlation, at a mean lag of .364 s. These results are expected under the *copying mode* of error correction. In contrast, participants were not able to precisely synchronize their tapping to the acoustic rhythms with unpredictable fluctuations of tempo. Actually, they showed a higher consistency of their own tempo as compared to the predictable condition, and showed a lower coefficient of cross-correlation. These results are expected under the *central tendency* mode of error correction. Interestingly, a mean negative asynchrony corresponding to 20% of the interbeat intervals was measured in both conditions, suggesting that the overall directionality (i.e., the phase relationship between the acoustic target and the motor output) was comparable in both conditions, despite the difference in synchronization mode.

We segregated the neural responses to the acoustic events in two categories: responses that are phase-locked to each period between two acoustic events and responses that are time-locked to each acoustic event. Then, using a method based on spectral decomposition of those EEG signals, we compared the overall quantity of each type of response within each condition. We could reveal a significant interaction between the overall quantity of phase- vs. time-locked neural activity and the fact that participants were actively synchronizing their tapping to the acoustic rhythms or passively listening to them. We observed that the overall quantity of phase-locking activity was significantly higher when participants tapped in synchrony with the acoustic rhythms, which probably reveals the facilitating effect of overt movement performance on acoustic rhythm processing. Critically, we used several signal processing artifices in order to get rid of any motor contamination of the measured auditory neural responses, so that this effect can be clearly attributed to a change in the dynamics of the auditory neural response. Interestingly, these results integrate with the perceptual ratings made by the participants, who better discriminated between predictable and unpredictable fluctuations of temp when they were synchronizing their finger taping to the acoustic rhythms.

In contrast with our predictions, no clear difference in overall magnitude of phase- vs. time-locked neural activity could be observed between the predictable and the unpredictable conditions. However, the high interindividual heterogeneity, due to the fact that proper anticipation of fluctuating rhythm is not an easy task could have resulted in a a type II error. The interindividual heterogeneity was well illustrated in the synchronization consistency results (not all participants were able to better synchronize their finger tap to the predictable rhythm), as well as in the difference in magnitude of phase- vs. time- locked periodic neural responses (three participants had evident higher phase-locked activity than time-locked activity, when synchronizing their tapping to the predictable rhythm). We expect that increasing the sample size would reveal a specific increase in phase-locked neural activity as compared to time-locked activity, when participant produce an overt movement to acoustic rhythms with predictable pattern of tempo fluctuation. Furthermore, we expect that increasing the sample size would reveal a correlation between behavioural tapping data and EEG measures.

Most importantly, we suggested that the neural response to each acoustic event partially reflects the error detection process and therefore changes according to the context in which each acoustic event occurs. Our results clearly identified a distinctive component in the EEG response elicited by the acoustic events, once characterized according to the context in which they were processed (e.g., events occurring after a short or a long interbeat interval, which correspond to events occurring "too early" or "too late" as compared to what could be expected from the mean interbeat interval). This component reached a maximal potential at approximately 142 ms post-stimulus onset, and corresponded to a negative deflection for short interbeat intervals and a positive deflection for long interbeat intervals. Importantly, the amplitude of this component linearly correlates with the amount of violation of expectation. Therefore, this component of the EEG response could reflect the error detection process.

Study 3: Body movement Selectively Shapes the Neural Representation of Musical Rhythms (Chemin B., Mouraux A., Nozaradan S.)

Abstract

It is increasingly recognized that motor routines dynamically shape the processing of sensory inflow (e.g., when hand movements are used to feel a texture or identify an object). In the present research, we captured the shaping of auditory perception by movement in humans by taking advantage of a specific context: music. Participants listened to a repeated rhythmical sequence before and after moving their bodies to this rhythm in a specific meter. We found that the brain responses to the rhythm (as recorded with electroencephalography) after body movement were significantly enhanced at frequencies related to the meter to which the participants had moved. These results provide evidence that body movement can selectively shape the subsequent internal representation of auditory rhythms.

Introduction

To gather data from the environment, people most often explore it through movement, and these exploratory movements are thought to shape the processing of sensory inflow (Schroeder et al., 2010). Because exploratory movements are often rhythmic in nature, it has been suggested that the shaping of perception by movement involves some kind of neural entrainment. This is easily conceivable for vision, somatosensation, or olfaction—in which eye, head, finger, or sniffing movements are directly involved in sensory exploration. How movement might shape perception in the auditory system is less straightforward (Schroeder et al., 2010).

To provide evidence of rhythmic motor shaping of audition, we took advantage of a specific context: music. Getting entrained to music is a universal human behaviour that strikingly illustrates how auditory perception can be linked to action patterns (Leman, 2007; Phillips-Silver et al., 2010). Notably, while musical rhythms make people move, movement can, in turn, shape the perception of musical rhythms. Although this idea has long been considered an axiom in music theory and education (Jaques-Dalcroze, 1920), behavioural evidence has been provided only

recently: Phillips-Silver and Trainor (2005, 2007, 2008) have shown that movements performed concurrently with rhythmic sound patterns can, at least momentarily, modulate the perception of musical meter (i.e., the perception of nested temporal periodicities, as in a waltz, which has three beats per meter). However, the manner in which the brain builds a neural representation of musical rhythms and how movements might shape this neural representation remain largely unknown.

To explore this phenomenon, we used an approach based on the electroencephalographic (EEG) recording of steady-state evoked potentials[9] (SSEPs) to identify the neural entrainment to musical rhythm (Nozaradan et al., 2011, 2012a). This approach allows one to objectively capture the neural activities elicited by musical rhythms in the form of multiple SSEPs observed in the EEG spectrum at frequencies corresponding to the rhythm envelope (Nozaradan et al., 2012a). These SSEPs have been shown to be selectively enhanced at meter-related frequencies, even when those frequencies were not prominent in the spectrum of the sound envelope (Nozaradan et al., 2012a); this finding indicates that these neural activities do not merely reflect the physical structure of the sound envelope but, instead, reflect an internal representation of the perceived meter (Large, 2008).

In the current research, we used SSEPs to capture the changes in the neural dynamics of perceived metric structure occurring both after and before body movements thought to induce implicit auditory-motor modulation. EEGs were recorded while participants listened to an ambiguous rhythm, before and after a body-movement session designed to disambiguate the perception of this rhythm by favouring a specific meter (e.g., two beats per measure vs. three beats per measure; Phillips-Silver & Trainor, 2005, 2007, 2008). When comparing the EEGs recorded after and before body movement, we predicted that we would find enhanced SSEPs at frequencies corresponding to the metric interpretation induced implicitly during the movement session, even though participants did not move or focus attention on the metric structure during the EEG

---

[9] In this study, the terminology "Steady-State Evoked-Potential" was used to designate the periodic neural activities identified in the EEG spectrum, and will therefore be used in this thesis chapter. However, this terminology was avoided in later works, as it is connoted with the notion of steadiness, which is not an accurate reflect of the dynamics of periodic neural activities.

recording. Such a finding would provide direct evidence that rhythmic body movements selectively shape the neural representation of musical rhythms.

Method

Experiment 1

Participants. Fourteen healthy volunteers (8 females, 6 males; all right-handed; mean age = 23 years, *SD* = 4) took part in Experiment 1 after providing written informed consent. Only nonmusicians (but with some experience in Western music as amateur listeners or dancers) were asked to participate, as nonmusicians would not be expected to be aware of the theoretic structure of the polyrhythm and of the meter induced by the body movements. None had prior experience with the rhythm task used in the present experiment. They had no history of hearing, neurological, or psychiatric disorder, and none were taking any medication at the time of the experiment. The experiment was approved by the local ethics committee.

Auditory stimulus. The stimulus consisted of a rhythmic pattern lasting 1.2 s, looped continuously for 33 s. The rhythmic patterns consisted of alternating intervals of sound (a 990-Hz pure tone of 200-ms duration with a 10-ms rise and 10-ms fall) and silence, as illustrated in Figure 1a. The auditory stimuli were created using Audacity software (Version 1.2.6; http://audacity.sourceforge .net/) and presented binaurally through earphones (BeyerDynamic DT 990 PRO, Heilbronn, Germany) at a comfortable hearing level, using E-Prime software (Version 2.0; Schneider, Eschman, & Zuccolotto, 2001). Pure tones were used to ensure that the frequency content of the sounds used as unitary events did not interfere with the frequencies of interest. Moreover, rhythmic presentation of pure tones has been shown to elicit SSEPs with significant signal-to-noise ratios (Nozaradan et al., 2012a). The rhythmic pattern used in the experiment was metrically ambiguous, as it could induce the perception of a ternary meter as well as of a binary meter (i.e., a subdivision of the rhythmic pattern by three or by two, or *hemiola* in music; ; Phillips-Silver & Trainor, 2005, 2007, 2008).

Experimental conditions. The rhythmic pattern was presented in three successive sessions (Fig. 39b). In each session, the 33-s auditory stimulus was repeated 11 times (each repeat constituted

155

1 trial). The onset of each pat- tern was preceded by a 3-s period between the time the participant pressed a button to begin the trial and the appearance of the stimulus. The experimenter remained in the recording room with the participant at all times to monitor compliance to the procedure and instructions.
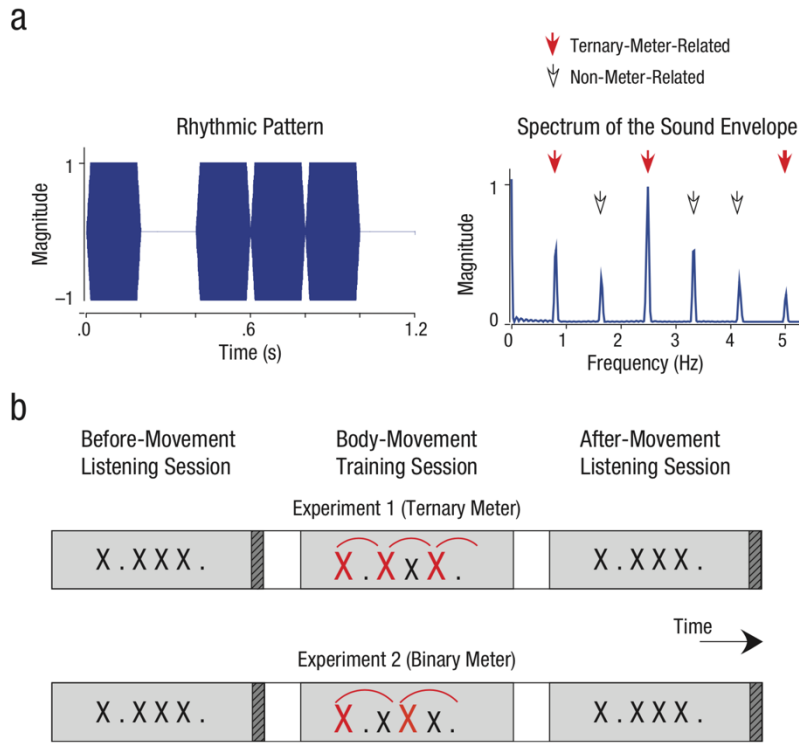
Figure 39. – Experimental Paradigm

Participants listened to a rhythmic pattern consisting of a succession of sounds (pure 990-Hz tone with a 10-ms rise and 10-ms fall) and silences (a), each lasting 200 ms. This rhythmic pat- tern was metrically ambiguous, as it could induce the perception of a ternary meter as well as the perception of a binary meter. The spectrum of the sound envelope shows that the rhythmic pattern contained a series of six equidistant peaks, which can be classified as related or unrelated to a ternary-metric interpretation of the rhythm. Each experiment had three sessions (b). In the before-movement session (10 trials), participants listened to the rhythmic pattern (cross: 200-ms tone, dot: 200-ms silence) looped across 33 s. They were instructed to detect very short accelerations of tempo in two of the trials interspersed within the session. During the 11th trial (dark gray bar), participants were asked to tap with their right hand along with the rhythm. In the movement-training session, participants were trained to move according to a ternary-metric interpretation (Experiment 1) or a binary-metric interpretation (Experiment 2), represented by the crosses and curves. The after-movement listening session was identical to the before-movement listening session.

The first session (the before-movement session) was structured as follows. During the first 10 trials, participants were asked to listen carefully to the stimulus in order to detect very short accelerations of tempo (creating by decreasing the duration of two successive events by 10 ms, i.e., each event was 190 ms). These accelerations were inserted six times at random positions in two of the trials within the session. The participants were instructed to report the change in tempo at the end of each trial. This task ensured that participants focused on the temporal aspects of the presented sound. The two trials containing the tempo changes were excluded from further analyses.

During the 11th trial of the first session, participants were asked to perform a tapping task. The tapping was performed using the right hand: Participants made small up and down movements of the hand starting from the wrist joint, while keeping the forearm and elbow fixed on an armrest. When tapping, the fingers of the tapping hand came briefly in contact with the armrest (Nozaradan et al., 2012a, 2013). The tapping movements were recorded using an accelerometer placed on the tapping hand. Participants were instructed to tap freely to the rhythm, in the way that seemed the most natural for them. This allowed us to obtain a relative indication of their perception of beat and meter as induced by the rhythmic pattern, without suggesting explicitly to the participants that some beat and meter periodicities could be perceived from the pat- tern. Moreover, participants were asked to start tapping as soon as they heard the first sound of the trial and to maintain their movement as consistently as possible throughout the tapping trial.

During the second session (the body-movement-training session), participants were asked to move their body (clap the hands, bob the head, tap the foot, sway the torso) isochronally according to a ternary-metric interpretation of the rhythmic pattern (i.e., a subdivision of the rhythmic pattern by three, as represented in Fig. 39). This training was performed continuously while participants listened to the rhythmic pattern during 11 trials. To entrain participants to these movements, the experimenter demonstrated a similar movement. This training session purposely involved multiple parts of the body as well as multisensory cues for meter induction (visual, auditory, and vestibular) because (a) we aimed to optimize the effect of the movement as measured in the third session, and (b) this training resembled the complexity and natural variability of movements performed on rhythms in ecological musical contexts.

The third session of the experiment (the after-movement session) was identical to the before-movement session. Comparison of performance during the tapping trial of the before- and after-movement sessions provided an indication of the possible changes in perception of beat and meter.

Finally, at the end of the experiment, participants were asked to describe their general feeling about the rhythm and to report whether they noticed any change in the meter of the rhythm subsequent to movement training, either while listening to the rhythm or while tapping to it. To ensure that the movement-training sessions were guided accurately, we enlisted the participation of an expert professional musician with 20 years of violin- and piano-playing experience and a high level of music education.

EEG recording. In the before-movement and after- movement sessions, participants were comfortably seated in a chair with their head resting on a support. They were instructed to relax, avoid any unnecessary head or body movement, and keep their eyes fixated on a point displayed on a computer screen in front of them. The EEG was recorded using 64 Ag-AgCl electrodes placed on the scalp according to the international 10-10 system (Waveguard64 cap, Cephalon A/S, Norresundby, Denmark). Vertical and horizontal eye movements were monitored using four additional electrodes, one placed on the outer canthus of each eye and one above and one below the left orbit. Electrode impedances were kept below 10 kΩ. The signals were amplified, low-pass filtered at 500 Hz, digitized using a sampling rate of 1,000 Hz, and referenced to an average reference (64-channel high-speed amplifier, Advanced Neuro Technologies, Enschede, The Netherlands).

Hand-movement recording. Movements of the hand were measured using a three-axis accelerometer (MMA7341L, Pololu Robotics & Electronics, Las Vegas, NV) attached to the hand dorsum. The signals generated by the accelerometer were digitized using three additional bipolar channels of the EEG system.

Sound-pattern analysis. To determine the frequencies at which SSEPs were expected to be elicited in the recorded EEG signals, we extracted the temporal envelope of the 33-s sound pattern using a Hilbert function, which yielded a time-varying estimate of the instantaneous amplitude of the

sound envelope, as implemented in the MIRToolbox (Lartillot & Toiviainen, 2007). The obtained waveforms were then transformed in the frequency domain using a discrete Fourier transform (Frigo & Johnson, 1998), which yielded a frequency spectrum of envelope magnitude (Bach & Meigen, 1999). We determined that the frequencies of interest were greater than or equal to 5 Hz, that is, the frequency corresponding to the 200-ms period of the unitary event of the pattern. As shown in Figure 39a, the envelope spectrum of the pattern consisted of six distinct frequencies ranging from 0.84 Hz (corresponding to the pattern duration) to 5 Hz (corresponding to the unitary-event duration) with an interval of 0.84 Hz. According to a ternary-metric interpretation of the rhythmic pattern (as induced by the body-movement-training session) and to music theory concerning polyrhythms (London, 2004), these frequencies could be classified in three ternary-meter-related frequencies (0.84 Hz, 2.5 Hz, and 5 Hz, corresponding to the frequency of the measure, the ternary beat, and the unitary event, respectively) and three non-meter-related frequencies (1.6 Hz, 3.3 Hz, and 4.2 Hz).

We then computed z scores using the magnitude of the peaks obtained at each of the six frequencies in the spectrum of the pattern envelope, as follows: $z = (x - \mu)/\sigma$, where μ and σ correspond to the mean and standard deviation, respectively, of the magnitudes of the six peaks (Nozaradan et al., 2012a). This procedure allowed us to assess which frequencies stood out relative to the entire set of frequencies.

EEG analysis. The continuous EEG signals recorded before and after the movement session were filtered using a 0.1-Hz high-pass Butterworth zero-phase filter to remove slow drifts in the recorded signals. Epochs lasting 32 s were obtained by segmenting the recordings from +1 to +33 s relative to the onset of the auditory stimulus. The EEG recorded during the 1st s of each epoch was removed to discard the transient auditory evoked potentials related to the onset of the stimulus (Nozaradan et al., 2011, 2012a, 2012b, 2013). These EEG processing steps were carried out using Analyzer software (Version 1.05; Brain Products, Gilching, Germany). Artifacts produced by eye blinks or eye movements were removed from the EEG signal using a validated method based on an independent component analysis (Jung et al., 2000) that utilized the runica algorithm (Bell & Sejnowski, 1995; Makeig, 2002).

For each participant and condition, EEG epochs were averaged across trials. The time-domain-averaging procedure was used to enhance the signal-to-noise ratio of EEG activities time locked to the patterns. The obtained average waveforms were then transformed in the frequency domain using a discrete Fourier transform (Frigo & Johnson, 1998), which yielded a frequency spectrum of signal amplitude (µV) ranging from 0 to 500 Hz with a frequency resolution of 0.031 Hz (Bach & Meigen, 1999). This procedure allowed us to assess the appearance of frequency components in the EEG elicited by the frequency components of the sound patterns and induced beat and meter percept (Nozaradan et al., 2012). The deliberate choice of computing Fourier transforms of long-lasting epochs was justified by the fact that it improves the frequency resolution of the obtained EEG spectra. This concentrates the magnitude of the SSEPs in a narrow frequency band and, thereby, enhances their signal-to-noise ratio. Furthermore, this is required to disentangle nearby SSEPs in the EEG frequency spectrum (Regan, 1989).

These EEG-processing steps were carried out using Letswave 5 (Institute of Neuroscience, University of Louvain; www.nocions.webnode.com/letswave), MATLAB (The MathWorks, Natick, MA), and EEGLAB (Swartz Center for Computational Neuroscience, University of California San Diego). Within the obtained frequency spectra, signal amplitude may be expected to correspond to the sum of (a) stimulus-induced SSEPs and (b) unrelated residual background noise due to, for example, spontaneous EEG activity, muscle activity, or eye movements. Therefore, to obtain valid estimates of SSEP magnitude, we removed the contribution of this noise by subtracting, at each bin of the frequency spectra, the average amplitude measured at neighbouring frequency bins (two frequency bins ranging from −0.15 to −0.09 Hz and from +0.09 to +0.15 Hz relative to each frequency bin).

The validity of this subtraction procedure relies on the assumption that in the absence of an SSEP, the signal amplitude at a given frequency bin should be similar to the signal amplitude of the mean of the surrounding frequency bins (Mouraux et al., 2011; Nozaradan et al., 2011, 2012a, 2012b, 2013). This subtraction procedure is important (a) to assess the scalp topographies of the elicited SSEPs, as the magnitude of the background noise is not equally distributed across scalp channels, and (b) to compare the amplitude of SSEPs elicited at distinct frequencies, as the background-noise magnitude may be unequally distributed across the frequency spectrum. The

magnitude of the SSEPs was then estimated by taking the maximum noise-subtracted amplitude measured in a range of three frequency bins centered over the expected SSEP frequency, based on the spectrum of the sound envelope. This range of frequencies allowed us to account for possible spectral leakage because the discrete Fourier trans- form did not estimate signal amplitude at the exact frequency of any of the expected SSEPs (Nozaradan et al., 2011, 2012a, 2012b).

Topographical distribution of SSEPs. For each SSEP frequency, topographical maps were computed by spherical interpolation using the EEG frequency spectra obtained in the before- and after-movement sessions. These topographical maps were averaged across meter- related frequencies and non-meter-related frequencies.

Statistical analyses. To exclude any electrode-selection bias, we selected a pool of electrodes of interest as follows. Normalized topographical maps obtained for each participant, condition, and frequency were averaged to select the five electrodes exhibiting the maximum SSEP amplitudes (electrodes Fz, F1, F2, F3, and F4, i.e., predominantly located over fronto-central areas). Notably, because the pool of electrodes was determined on the basis of the scalp distribution of the spectrum averaged across the two conditions, this procedure did not bias our results toward finding a difference between the two conditions.

A 2 (meter: ternary-meter-related vs. non-meter- related) × 2 (session: before training vs. after training) repeated measures analysis of variance (ANOVA) was conducted on mean SSEP magnitude. Paired samples *t* tests were used to perform post hoc pairwise comparisons of the magnitude of the SSEPs measured before and after movement training. The significance level was set at *p* < .05.

In addition, as for the sound-pattern analysis, the amplitudes of the SSEPs obtained at the expected frequencies were expressed as *z* scores, using the mean and standard deviation of the magnitudes obtained across the different peaks, to assess how each of the different SSEPs stood out relative to the entire set of SSEPs and relative to the *z* scores obtained from the sound-pattern envelope (Nozaradan et al., 2012a). To assess specifically whether SSEPs elicited at ternary-meter-related frequencies (0.84 Hz, 2.5 Hz, and 5 Hz) were selectively enhanced, we compared

the average of the *z* scores representing SSEP amplitude at ternary-meter-related frequencies with the average of the *z* scores representing these same frequencies in the sound-pattern envelope, using a one-sample *t* test (Nozaradan et al., 2012a). A similar procedure was used to compare the magnitude of SSEPs and the magnitude of the sound envelope at non-meter-related frequencies. The significance level was set at *p* < .05.

Hand-movement analysis. The hand-movement analysis was based on previous work showing that the frequency spectrum of the vertical-axis acceleration signal can be used reliably to assess the dynamics of repeated hand tapping, appearing as clear peaks at the hand-tapping frequency and its harmonics (Nozaradan et al., 2013). In the current study, this approach was preferred to an approach based on an estimation of inter-tap-latencies because participants were instructed to tap freely to the rhythm in the way that seemed the most natural for them.

The vertical-acceleration signals recorded for each participant and tapping session were segmented from +0 to +33 s according to the sound onset. The discrete Fourier transforms (Frigo & Johnson, 1998) were then computed. The same 2 × 2 ANOVA that was used to com- pare mean SSEP magnitude was used to compare these magnitudes. Paired-samples *t* tests were used to perform post hoc pairwise comparisons of the magnitudes measured in the two sessions. The significance level was set at *p* < .05.

Experiment 2

Fourteen participants (10 females, 4 males; all right- handed; mean age = 25 years, *SD* = 7) took part in Experiment 2. None of these participants took part in Experiment 1 (to avoid possible persistent effect of the movement trained in Experiment 1, which could have interfered in Experiment 2). Experiment 2 was identical to Experiment 1, except that during the body-movement- training session, participants were trained to move to a binary-metric interpretation of the rhythm instead of a ternary-metric interpretation (Fig. 39b).

Notably, although the rhythm used in these two experiments can be considered ambiguous because it can be interpreted according to a ternary or a binary meter, the structure of the rhythm itself is likely to favor a ternary interpretation, as suggested by the distribution of the acoustic energy in the envelope of the rhythm. For this reason, the binary-meter body-movement training

performed in Experiment 2 was not expected to necessarily shape the auditory processing in the form of a selective enhancement of SSEPs at corresponding binary-meter frequencies. Rather, it was expected to prevent shaping the auditory processing toward a ternary-metric interpretation. The aim of Experiment 2 was thus to examine whether the enhancement of ternary-meter-related SSEPs observed in Experiment 1 was due to the body movements being performed according to a ternary meter or simply to continuously listening to this rhythm throughout three sessions, independently of the metric of the body movement. To achieve this aim, we applied the same statistical analysis as in Experiment 1, comparing ternary-meter-related and nonrelated SSEPs before and after the binary-movement session.

However, we also tested whether the binary-movement session affected the SSEPs at binary-meter-related frequencies. According to a binary-metric interpretation of the rhythmic pattern, the SSEPs could be classified in three meter-related frequencies (0.84 Hz, 1.6 Hz, and 5 Hz, corresponding to the frequency of the measure, the binary beat, and the unitary event, respectively) and three non-meter-related frequencies (2.5 Hz, 3.3 Hz, and 4.2 Hz). A 2 (meter: binary-meter-related vs. non-meter-related) × 2 (session: before training vs. after training) repeated measures ANOVA was conducted on mean SSEP magnitude. Paired samples t tests were used to perform post hoc pairwise comparisons of the magnitude of the SSEPs measured between the two sessions. The significance level was set at $p < .05$. The same statistical analyses were used to compare the magnitude of the peaks appearing in the spectrum of the vertical axis of the accelerometer.

Results

Sound-Pattern Analysis

The envelope spectrum of the rhythm was unequally distributed along the frequencies of interest. Indeed, the magnitude of the peaks appearing at ternary-meter- related frequencies stood out relatively to the other frequencies. Although the rhythm we used is theoretically ambiguous (both a binary and a ternary meter can be induced from it), the predominance of ternary-meter- related frequencies suggests that this rhythm is physically biased toward favouring a ternary-meter interpretation.

Self-Reports of Rhythm Perception

At the end of Experiments 1 and 2, participants reported that they did not notice a difference in beat and meter before versus after the movement session. None of the participants reported that the body-movement-training session induced a specific metric interpretation of the rhythm (this was asked by the experimenter while clapping the ternary or binary rhythm at the moment of the self-report) or changed their tapping performance.

However, about half of the participants in both Experiments 1 and 2 reported a qualitative change in their perception of the sound, which they described as "more pleasant" or "more rhythmic," after the movement- training session. Moreover, in Experiment 2, most participants reported that they felt uncomfortable performing the movement according to the binary meter.

Detection Task

During the before- and after-movement sessions, participants correctly detected all targets in both experiments. In Experiment 1, the median number of false alarms was 7 (interquartile range: 3.5–9.5). In Experiment 2, the median number of false alarms was 8 (interquartile range: 4.0–9.5). The number of correct detections did not differ significantly before and after the movement session in Experiment 1, $t(13) = 2.83$, $p = .21$, and Experiment 2, $t(13) = 3.26$, $p = .34$. Similarly, the number of false alarms was not significantly different before and after the movement session in Experiment 1, $t(13) = 2.83$, $p = .21$, and Experiment 2, $t(13) = 3.26$, $p = .34$.

Steady-State Evoked Potentials

In both experiments, each of the six frequencies constituting the envelope spectrum of the rhythmic pattern elicited an SSEP before and after the movement-training session (Figs. 40 and 41). The scalp topography of the elicited SSEPs was, on average, maximal over fronto-central regions and symmetrically distributed over the two hemi- spheres (Fig. 41). Moreover, as shown in Figure 3, the scalp topography of meter-related and non-meter-related frequencies recorded before and after the movement- training session did not differ substantially.

Experiment 1. The repeated measures ANOVA used to examine SSEP magnitude in Experiment 1 revealed a significant main effect of meter, $F(2, 27) = 36.39$, $\eta^2 = .73$, $p < .0001$; a significant main

effect of session, $F(2, 27) = 7.73$, $\eta^2 = .37$, $p = .01$; and a significant interaction between meter and session, $F(2, 27) = 10.43$, $\eta^2 = .44$, $p = .007$, which indicates that meter-related and non-meter-related SSEPs were not similarly affected by the movement-training session. Post hoc pairwise comparisons showed that the amplitudes of meter-related SSEPs were significantly enhanced compared with the amplitudes of non-meter- related SSEPs, both before, $t(13) = 3.7$, $p = .002$, and after, $t(13) = 6.53$, $p < .0001$, the movement-training session (Figs. 2a and 2b). Most important, the amplitude of meter- related SSEPs was significantly greater after than before the movement-training session, $t(13) = 3.63$, $p = .003$, whereas there was no significant difference in the amplitude of the non-meter-related SSEPs recorded after and before movement, $t(13) = 0.26$, $p = .79$.

In the before-movement session, the standardized estimates of the SSEP amplitudes obtained at meter-related and non-meter-related frequencies were not significantly enhanced compared with the standardized estimates of the sound envelope at the corresponding frequencies, $t(13) = 0.31$, $p = .76$, and $t(13) = 0.31$, $p = .76$, respectively. This suggests that there was no clear selective enhancement of neural entrainment related to the meter. In contrast, in the after-movement session, the standardized estimates of SSEP amplitudes were significantly enhanced at meter-related frequencies, $t(13) = 3.47$, $p = .004$, and reduced at non-meter-related frequencies, $t(13) = 3.47$, $p = .004$, which suggests that the movement-training session resulted in the emergence of a selective enhancement of neural entrainment at frequencies related to the meter, as in Nozaradan et al. (2012a).

Experiment 2. Contrasting with the results of Experiment 1, results of the repeated measures ANOVA used to compare the magnitude of ternary-meter-related and non-meter-related SSEPs before and after the movement- training session revealed a significant main effect of meter, $F(2, 27) = 16.78$, $\eta^2 = .56$, $p = .001$, but no significant effect of session, $F(2, 27) = 0.65$, $\eta^2 = .04$, $p = .43$, and no significant interaction between meter and session, $F(2, 27) = 0.01$, $\eta^2 = .001$, $p = .89$. These findings indicate that the movement-training session did not significantly affect meter-related and non-meter-related SSEPs in Experiment 2, either by inducing an enhancement or a

diminishment of the ternary-meter-related SSEPs (Figs. 40c and 40d). There was no significant diminishment of these SSEPs after the binary movement.

In the before-movement session, the standardized estimates of the SSEP amplitudes obtained at meter-related, $t(13) = 0.11$, $p = .91$, and non-meter-related, $t(13) = 0.11$, $p = .91$, frequencies were not significantly enhanced compared with those of the sound envelope at the corresponding frequencies. This suggests that, as in Experiment 1, there was no selective enhancement of neural entrainment at frequencies related to the ternary meter before movement training. In the after-movement session, the standardized estimates of ternary meter-related SSEPs were also not significantly enhanced compared with the standardized estimates of the sound envelope at corresponding frequencies, $t(13) = 0.21$, $p = .83$. There was also no enhancement of non-meter-related SSEPs, $t(13) = 0.21$, $p = .83$. This suggests that in Experiment 2, the movement-training session did not result in the emergence of a selective enhancement of neural entrainment at frequencies related to the ternary meter.

The repeated measures ANOVA used to compare SSEP magnitude revealed a significant main effect of meter, $F(2, 27) = 11.73$, $\eta^2 = .47$, $p = .005$, but no significant effect of session, $F(2, 27) = .65$, $\eta^2 = .04$, $p = .43$, and no significant interaction between meter and session, $F(2, 27) = 1.47$, $\eta^2 = .10$, $p = .24$. Taken together, the results of Experiment 2 indicate that the selective enhancement of the ternary-meter-related SSEPs observed in Experiment 1 after body movement was likely due to the metric of the body movement, as such an enhancement was not observed after participants moved according to a different metric interpretation.
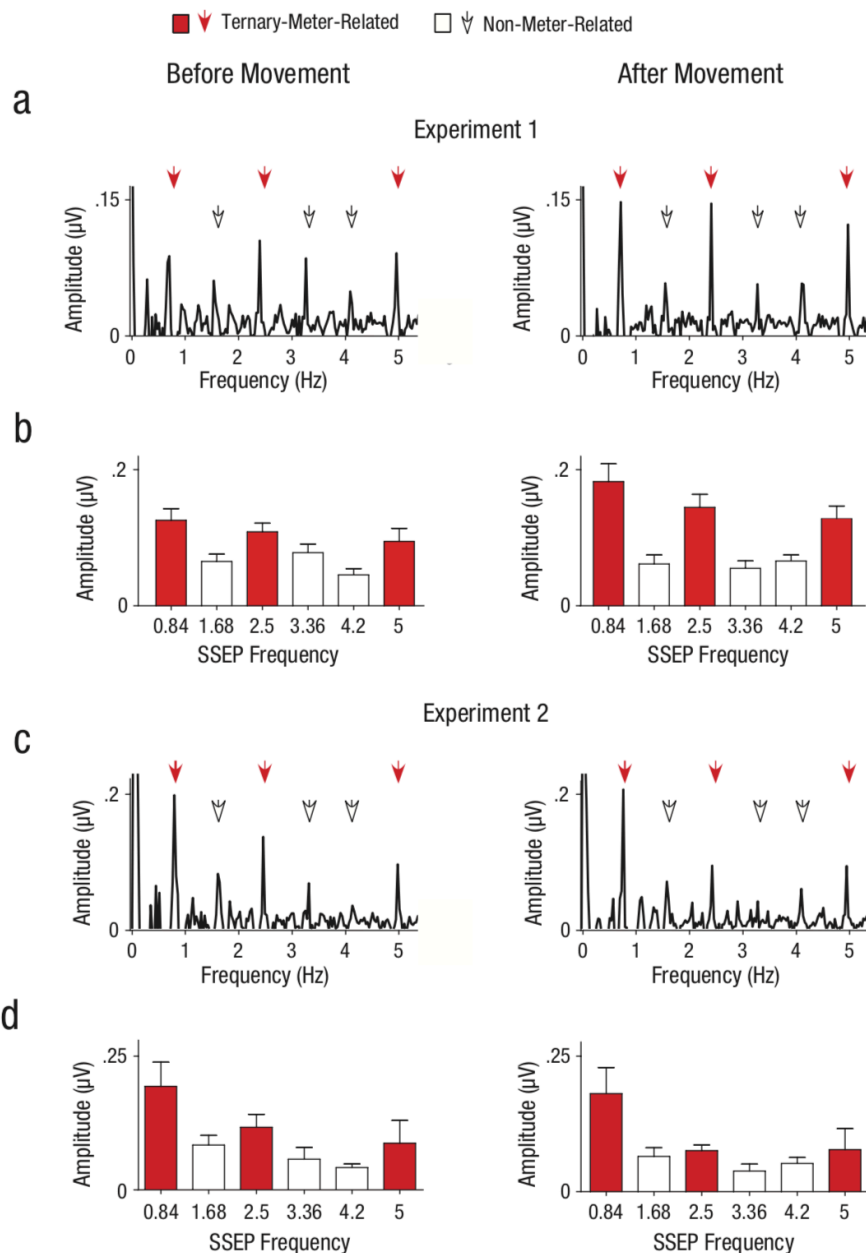
Figure 40. – Ternary-meter-related and non-meter-related steady-state evoked potentials (SSEPs) obtained before (left column) and after (right column) the ternary-movement-training session (Experiment 1) and binary-movement-training session (Experiment 2).

For both experiments, the waveforms (a, c) show electroencephalographic spectra averaged across participants and across electrodes Fz, F1, F2, F3, and F4. Ternary-meter-related frequencies and non-meter-related frequencies are indicated. The bar graphs (b, d) show mean amplitude of the SSEPs at each meter-related or non-meter-related frequency of interest. Error bars indicate standard errors of the mean.

167
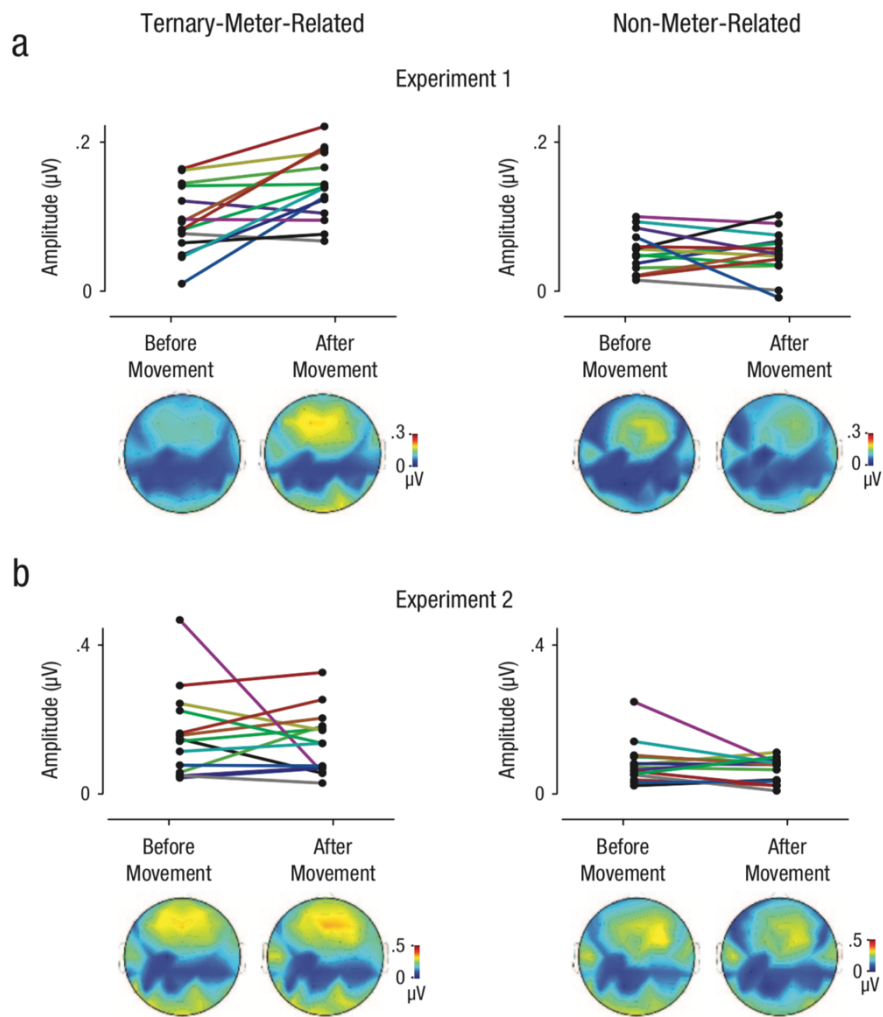
Figure 41. –   Group-level average amplitude and scalp topography of ternary-meter-related
(left column) and non-meter- related (right column) steady-state evoked potentials obtained
before and after the movement-training session for each participant
(colours across left and right plots correspond to the same participants).

Hand-tapping movement

Experiment 1. The analysis on hand tapping in Experiment 1 was performed on 13 participants, as the data of 1 participant were unavailable because of a technical problem during the experiment. As shown in Figure 4a, there was a difference in the tapping performed before and after the movement session. The repeated measures ANOVA conducted on vertical-acceleration signals revealed a significant main effect of meter, $F(2, 25) = 20.57$, $\eta^2 = .63$, $p = .001$; no effect of session, $F(2, 25) = 2.59$, $\eta^2 = .17$, $p = .13$; and a significant interaction between meter and session, $F(2, 25) = 9.67$, $\eta^2 = .44$, $p = .009$. Post hoc pairwise comparisons showed that the magnitudes at meter-related frequencies were significantly greater than the magnitudes at non-meter-related frequencies after the movement-training session, $t(12) = 3.93$, $p = .001$, but not before the movement-training session, $t(12) = 1.21$, $p = .24$ (Fig. 4). Moreover, the magnitude at meter-related frequencies was significantly greater after than before the movement-training session, $t(12) = 3.08$, $p = .008$, whereas there was no significant difference in the magnitudes at the non-meter-related frequencies recorded before and after movement, $t(12) = 0.88$, $p = .39$. Taken together, these results indicate that participants tended to tap according to a ternary-metric interpretation of the rhythmic pattern (increased magnitude at meter- related frequencies) after the body-movement session compared with before and, hence, that the movement- training session exerted an effect on rhythm production.

Experiment 2. The hand-tapping analysis for Experiment 2 was performed on 13 participants, as the data of 1 participant were unavailable because of a technical problem during the experiment. In contrast with the results of Experiment 1, findings from the repeated measures ANOVA conducted on vertical-acceleration signals in Experiment 2 revealed a significant main effect of meter, $F(2, 25) = 37.87$, $\eta^2 = .77$, $p < .0001$, but no significant effect of session, $F(2, 25) = 3.92$, $\eta^2 = .26$, $p = .7$, and no interaction between meter and session, $F(2, 25) = 2.29$, $\eta^2 = .17$, $p = .15$ (Fig. 4b). These results indicate that in Experiment 2, participants did not consistently tap according to a ternary-metric interpretation of the rhythmic pattern after the body-movement session.
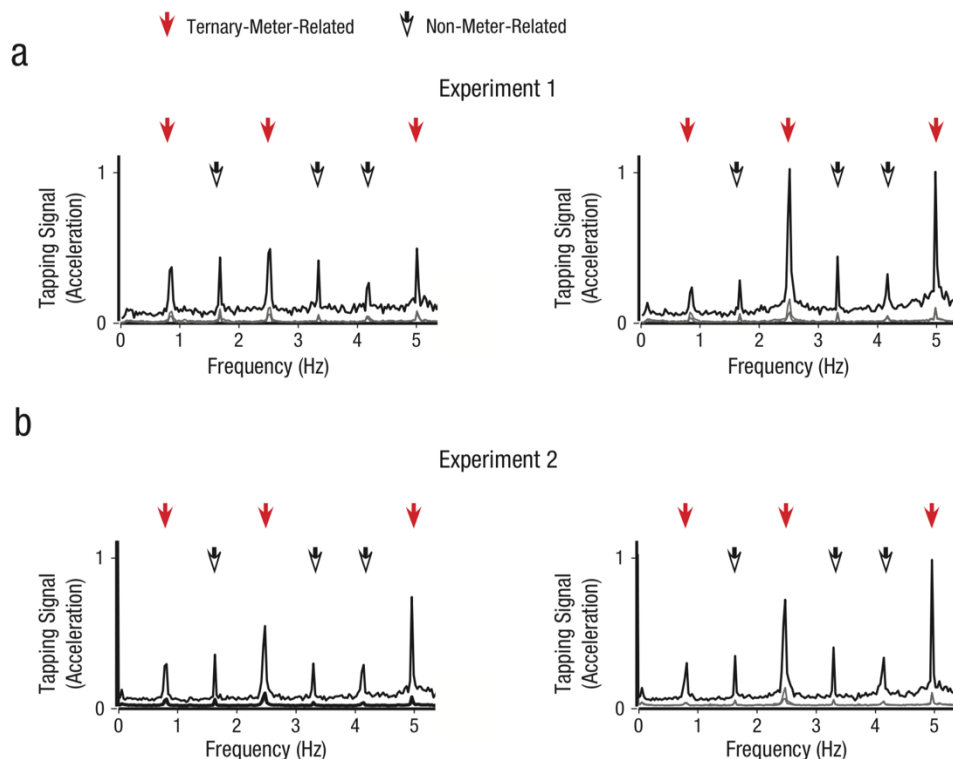
Figure 42. – Mean spectra of hand-tapping movement performed before (left column) and after (right column) the movement-training sessions

(a) Experiment 1 and (b) Experiment 2. Results for the vertical axis are in bold; results for the anteroposterior axis and transverse axis (combined) are shown beneath the results for the vertical axis. The arrows indicate ternary-meter-related frequencies and non-meter-related frequencies.

The repeated measures ANOVA on binary-meter- related and non-meter-related frequencies revealed no significant main effect of meter, $F(2, 25) = 2.35$, $\eta^2 = .17$, $p = .15$, no significant main effect of session, $F(2, 25) = 3.92$, $\eta^2 = .26$, $p = .7$, and no significant interaction between meter and session, $F(2, 25) = 0.29$, $\eta^2 = .026$, $p = .6$.

Discussion

The present study explored the interactions between perception and movement by taking advantage of the strong sensorimotor coupling inherent to musical-rhythm perception and production. One of the most intriguing phenomena related to musical rhythm and meter is that

it powerfully compels one to move (Janata et al., 2012). In turn, body movements shape rhythm perception (Phillips-Silver & Trainor, 2007, 2008).

Here, we showed that the SSEPs elicited by listening to an ambiguous auditory rhythm that can be perceived either as a binary or a ternary meter are significantly enhanced at the frequencies corresponding to a ternary- metric interpretation after body-movement training using this metric interpretation. In contrast, these SSEPs were not enhanced after body-movement training using a binary-metric interpretation. Taken together, these results constitute direct evidence that the neural entrainment to musical rhythms is not only determined by acoustic features of the rhythmic sounds but is also, at least in the context of an ambiguous rhythm—shaped by the previous experience of body movement (Phillips-Silver & Trainor, 2007, 2008).

Both in Experiment 1 and in Experiment 2, the magnitude of ternary-meter-related SSEPs was significantly greater than the magnitude of unrelated SSEPs before the movement-training session, which indicates an a priori bias toward a ternary-metric structure. However, when SSEP magnitudes were compared with the magnitudes of the corresponding frequencies in the spectrum of the sound envelope, ternary-meter-related SSEPs were not greater in the before-movement session, which suggests that the a priori bias toward ternary-meter-related frequencies resulted from the fact that such frequencies were prominent in the sound envelope itself. Building on recent results on neural-entrainment mechanisms to musical rhythms (Nozaradan et al., 2012a), we suggest that the lack of enhancement before movement may be related to the metric ambiguity of the rhythm, which did not elicit a stable perception of meter. This result is also consistent with tapping performance before the movement-training session, which did not show any significant relative enhancement at meter-related frequencies. The selective enhancement of the ternary-meter-related SSEPs compared with the sound envelope appeared only in the after-movement session of Experiment 1, not in Experiment 2. Taken together, these results indicate that there was no significant difference in the a priori metric interpretation across the two groups, but that the difference appeared specifically after the ternary-movement session.

In contrast, selective enhancement of the ternary- meter-related SSEPs compared with the sound envelope appeared only after ternary-body-movement training. This reshaping of the EEG spectrum can be interpreted as evidence of a metric disambiguation of the rhythm, involving neural mechanisms selecting meter-relevant frequencies identified by the body movements. Again, this selective entrainment to meter-related frequencies was reflected in the behavioural measures, which showed improved consistency of tapping at ternary-meter-related frequencies (Fig. 42).

It could be hypothesized that the selective enhancement of the SSEPs subsequent to ternary body movement would occur similarly after moving the body according to any distinct metric interpretation. In other words, the selective neural entrainment could emerge subsequent to non- specific repeated body movement performed to any rhythm, or could even arise from the repeated listening of this rhythm across three sessions, independently of the body-movement temporal pattern. However, the results of the second experiment demonstrate that this was not the case. Indeed, no significant enhancement of the magnitude of ternary-meter-related SSEPs was observed after participants moved their bodies according to a binary-metric interpretation. Furthermore, there was also no enhancement of tapping at ternary-meter-related frequencies.

Of interest, there was an asymmetry between the effect of the ternary- and binary-movement experiments. Although the rhythm used in the present study can be considered ambiguous because it can be interpreted according to a ternary or a binary meter, the stronger priming effect of moving one's body to a ternary meter than to a binary meter could result from the distribution of the acoustic energy in the envelope of the rhythm, favouring the ternary-metric interpretation. Also, this asymmetry could result from other features of the rhythm, such as the tempo chosen for the rhythm presentation (London, 2004), or from perceptual and cultural biases toward the grouping of acoustic events by two (corresponding to the ternary meter in the present study) in Western subjects (Brochard, Abecasis, Potter, Ragot, & Drake, 2003). Hence, the shaping of the neural entrainment to the rhythm by previous movement could be limited to specific interpretations of the stimulus. Namely, the selective enhancement appeared at congruent frequencies between the sound structure and the movement.

The asymmetry between the two metrical interpretations could appear discrepant with previous findings (Phillips-Silver & Trainor, 2005, 2007, 2008). This could be explained by the different methods used to capture the effect. In previous experiments performed with adults (Phillips-Silver & Trainor, 2007, 2008), the metrical interpretation was evaluated on the basis of an explicit behavioural outcome asked to the participants (a forced choice between two differently accented versions of the rhythmic pattern, either binary or ternary). In these studies, as in the current experiments, participants were never instructed to recall or match the movement experience. However, in the current experiments, there was no explicit outcome requested from the participants regarding the metrical interpretation, either during the listening or the tapping trials, in contrast with previous studies. Also, as EEG samples only a fraction of the elicited electrocortical activity, one should be cautious when interpreting a lack of effect of binary movement on SSEP magnitudes. Future studies using, for example, intracerebral recordings of auditory- and motor-cortex activity could help clarify this question. Finally, the relative discomfort reported by participants when performing the binary-movement training could have contributed to the difference between the effects of binary- and ternary- movement priming and could also explain the differences reported in previous studies using this rhythm (Phillips-Silver & Trainor, 2008).

The movement training performed in the present experiments purposely involved multiple parts of the body (the head, the torso, the hands and feet) as well as multisensory cues for meter induction. Having participants move multiple parts of their bodies allowed us to optimize the effect of movement on auditory perception as measured with EEG after the training and also to mimic the complexity and natural variability of movements performed to rhythms in ecological musical contexts (Burger, Saarikallio, Luck, Thompson, & Toiviainen, 2012; Wallin, Merker, & Brown, 2000). Whether the observed shaping of the EEG activities resulted from a change in the transformation of the sound by the auditory system or whether a distinct interconnected auditory-motor network contributed to our observations remain to be investigated.

In addition, it remains an open question what components of body movement were most responsible for the reshaping of the neural entrainment to the rhythm and whether such a reshaping could be obtained using inputs other than body movement, such as auditory accents.

For example, this reshaping could be the result of vestibular input. Indeed, previous behavioural studies have observed that metric encoding of a rhythm can be biased by passive motion of the head, which suggests that vestibular input may play a key role in rhythm perception (Phillips-Silver & Trainor, 2008; Todd & Cody, 2000). The enhancement of meter-related frequencies could also reflect a cross-modal process of dynamic attending.

According to the dynamic-attending model of rhythm perception (Jones & Boltz, 1989; Large & Jones, 1999), the perception of meter would result from a dynamic process in which the perceived meter leads to a periodic modulation of attention as a function of time (Brochard et al., 2003; Fujioka, Zendel, & Ross, 2010; Grube & Griffiths, 2009; Iversen, Repp, & Patel, 2009; Schaefer, Vlek, & Desain, 2010; Snyder & Large, 2005). This view is in agreement with models of perceptual selection describing attention as a neural process by which the brain enhances the representation of task relevant inputs (Lakatos, Karmos, Mehta, Ulbert, & Schroeder, 2008). Such a perceptual selection through dynamic attending is usually embedded in active motor routines, such as the one performed in the present study (Patel & Iversen, 2014; Schroeder et al., 2010). Similar mechanisms of perceptual enhancement through rhythmic priming could be envisioned within (Desain & Honing, 2003) and across distinct types of stimuli, as such rhythmic priming has been observed to shape subsequent speech processing (Cason & Schön, 2012).

Taken together, our results show that the recording of SSEPs to capture the shaping of rhythm perception by movement constitutes a promising approach to investigating the fundamental mechanisms underlying movement-perception integration in adults and even in infants, as it does not require any explicit behavioural outcome.

Chapter 5 – Clinical Perspectives

Study 4: Towards EEG Markers for Finer Characterization of Neural Dynamics in Parkinson's Patients (Chemin, B., Warlop, T., Benoit, CE., Peretz, I., Mouraux, A.)

Introduction

Gait disorder is one of the cardinal features of Parkinson's disease (PD). The progressive depletion of dopaminergic input to the basal ganglia - a group of subcortical nuclei playing a prominent role in motor behaviour - leads to the cardinal motor manifestations of the disease which include bradykinesia and postural instability (Alexander & Crutcher, 1990). In turn, these motor impairments are one of the causes of gait disorder (Wu et al., 2015).

When automatic gait control mechanisms are altered, patients tend to compensate with more cognitive control (Iansek et al., 2013). However, the basal ganglia are also part of a large network connecting various cortical areas responsible for non-motor, cognitive functions (Obeso et al., 2014). Their dysfunction is associated with deficits in the perception and production of *beat-based* rhythms, i.e., rhythms that induce a subjective perception of periodicity, called the beat (Grahn & Brett, 2009; Merchant et al., 2008; Parker et al., 2013; Pastor et al., 1992). These specific deficits are associated with considerable morbidity affecting gait and speech (Hove & Keller, 2015; Kotz et al., 2009).

The use of external cues to improve gait in PD has long been reported (Von Wilzenben, 1942), and has gained considerable attention over the last decade (see, e.g., Lim et al., 2005; Nombela, Hughes, Owen, & Grahn, 2013; Spaulding et al., 2013 for reviews). In particular, music has been consistently reported to improve gait kinematics in PD patient (Benoit et al., 2014; Thaut et al., 1996), and could further improve non-motor symptoms (Dalla Bella, Benoit, Farrugia, Schwartze, & Kotz, 2015). However, a wide heterogeneity is also reported both in experimental timing tasks

(Merchant et al., 2008) and in the clinical benefits of rhythmic auditory cueing (Hove & Keller, 2015).

In this study, we investigated whether we could correlate electrophysiological (EEG) markers to the benefits that a training program of one month consisting in walking with music can have on the gait of patients with PD. The study comprised two experiments: an EEG experiments designed to measure, in each participant, how body movements shape the neural representation of a complex acoustic rhythm (see Chemin et al., 2014 for original experiment), followed by a training of gait experiment designed to measure, in each participant, how a training program of one month consisting in walking with music would improve a series of clinical and experimental parameters (see Benoit et al., 2014 for original experiment).

We hypothesized that the training program should benefit preferentially the patients having relatively preserved *beat-based* rhythmic abilities. In those patients, the gait disorder should have a motor aetiology, and preserved beat-based timing cognitive functions would therefore be useful to facilitate the gait. Conversely, patients having impaired rhythmic abilities could markedly worsen their gait with rhythmic auditory cueing because of the additional cognitive burden. Therefore, we predicted that a positive correlation should be observed between the EEG marker of body movement shaping of neural representation of rhythm and the clinical improvement of patients.

Method

Participants

Twenty participants (10 females) with idiopathic Parkinson's disease (IPD), aged 39-79 years (*Mdn* = 66,5) participated in the study (see Table 1). All subjects were recruited through patient's associations, by physiotherapists, or by word of mouth. Patients were recruited according to the following inclusion criteria: maximal age of 85 years; and ability to walk without external help during minimum 10 minutes. Exclusion criteria included tremor dominant subtype of Parkinson's disease, presence of deep brain stimulation, history of neurological or psychiatric disorders other

than Parkinson's disease, and hearing loss. IPD diagnosis was assessed by independent neurologists.

Patients showed moderate symptoms of IPD, with a mode *Hoehn & Yahr* stage of 2 (range 1-2, on a maximum of 5) and an average score of the *Movement Disorder Society - Unified Parkinson's Disease Rating Scale* (MDS-UPDRS) of 53.375 (range 12-91, on a maximum of 265). Patients medication was variable, as reported in Table 1. Patients were asked to not discontinue their medication during the whole study, and were systematically tested in a period spanning from 30 to 150 minute after medication intake, in order to ensure that they were in an ON-state (Warlop, 2017).

The study was approved by local ethics committee and was in agreement with the latest version of the Declaration of Helsinki. All participant provided written informed consent before taking part in the experiments.

ID	Age/sex/handedness	Height (cm)	Most affected side	Hoehn & Yahr	MDS-UPDRS Total score Pre (/265)	Musical training	Time since diagnosis	PD related Medication
01	69/F/R	158	L	2	63	no formal training	6	A,S
02	62/M/R	170	R	2	88	no formal training	19	A,S
03	68/F/R	161	-	2	19	no formal training	5	A,S
04	79/F/R	158	L	2	65	no formal training	26	A,S
05	75/M/R	172	L	-	-	no formal training	3	S
06	68/F/R	154	R	2	37	basic formal training	7	S
07	64/M/R	177	L	2	32	basic formal training	2	A,S
08	-/ M/-	-	-	2	-	-	-	S
09	-/M/-	-	L	2	64	-	-	S
10	61/M/R	184	L	2	40	no formal training	9	A,S
11	-/F/-	-	L	2	58	-	-	A,S
12	69/M/R	184	R	2	49	no formal training	2	S
13	39/F/-	-	-	2	-	-	-	-
14	68/M/L	173	-	2	59	no formal training	6	S
15	46/F/-	-	L	2	12	-	-	A,S
16	44/F/R	167	R	1	48	no formal training	8	A,S
17	74/M/-	-	L	2	70	-	-	S
18	57/F/R	151	-	2	91	no formal training	2	S
19	65/M/R	172	L	2	59	no formal training	1	S
20	-/F/-	-	-	-	-	-	-	-
	M=63/-/m=R	M=167,77	m=L	m=2	M=53	m=no formal training	m=6	

Table 1. –   Demography of the patient cohort.

Age in years; F = female; M = male, R = right, L = left; Height in centimetres; Time since diagnosis in years;

A = dopamine agonists; S = dopamine substituent; M = mean; m = mode

Experiment 1: Quantifying the Influence of Body Movements on the Neural Representation of an Acoustic Rhythm in Parkinson Patients

Experimental Design

In this experiment, the EEG was recorded while participants listened to an ambiguous acoustic rhythm (i.e., a rhythm that can be interpreted in different ways), before and after a ten to twenty minutes motor training session designed to disambiguate the perception of the acoustic rhythm (Chemin et al., 2014; Phillips-Silver & Trainor, 2005, 2007).

Acoustic Stimuli. The stimulus consisted of a rhythmic pattern lasting 2 s, looped 25 times for a total duration of 50 s. The acoustic rhythm was metrically ambiguous, as it contained a regular beat at the period, half the period and a third of the period of the pattern (i.e., 2 s; 1 s; and .666 s; see Fig. 39 in section 4.2.3). The acoustic stimuli were presented binaurally using a closed dynamic headphone (DT 770 M, Beyerdynamic, Germany), and played using an externally-triggered zero latency audio stimulus generator (AUDIOFile, Cambridge Research System, Rochester, United Kingdom) in order to ensure the correct alignment of the acoustic stimuli with the EEG recordings.

Experimental Conditions. The acoustic rhythm was presented in three successive sessions. In each session, the 50 s stimulus was repeated 10 times (each repeat is further named a trial).

During the first – before training – and the third –after training – sessions, participants were asked to listen carefully to the stimulus and to detect eventual changes in the rhythm pattern (created by replacing certain sounds of the pattern by a silence). These changes were inserted four times in two random trials of each session. Participants had to report whether they had, or not, detected a change after each of the trials. The task prompted participants to focus on the temporal aspects of the stimulation. The two trials containing the pattern changes were excluded from further analysis. At the end of the first and the third sessions, participants were asked to perform a tapping task with the right index, in order to measure a behavioural indication of their perception of the rhythm. Participants were instructed to tap freely to the rhythm. The contact of the finger with the table was recorded using a touch sensor (Makey Makey, MIT Media Lab's Lifelong Kindergarten, USA).

During the second – motor training – session, participants were trained to move in synchrony at a third of the pattern period, while listening to the acoustic stimulation. The performed body movement consisted in clapping hands and rocking the upper body (the movement was verbally described as "clapping the hands like one would do when attending a concert" and "moving the torso like one would do when rocking a baby"). The experimenter performed the movement together with the participants, until the participants were able to continue it correctly by themselves. During the whole motor training session, feedback was provided to the participants to ensure they performed the synchronization task as accurately as possible. After each of the trials, participants were asked to judge the ease or the difficulty of the task on a 0 (difficult) to 9 (easy) scale.

EEG Recording. During the before- and after- training sessions, participants were comfortably seated on a chair and were instructed to relax, avoid head and body movements, keep their eyes opened and fixate on a point displayed on the wall in front of them. The EEG was recorded using 64 Ag-AgCl electrodes placed on the scalp according to the international 10-10 system (Waveguard64 cap, Cephalon A/S, Norresundby, Denmark). Electrode impedances were kept below 10 kΩ. The signals were amplified, low-pass filtered at 500 Hz, digitized using a sampling rate of 1,000 Hz, and referenced to an average reference (64-channel high-speed amplifier, Advanced Neuro Technologies, Enschede, The Netherlands).

Analysis

EEG Signal Processing. The EEG signals were filtered and processed in order to assess the magnitude of the EEG frequency components[10] elicited by the acoustic rhythmic stimulation (Chemin et al., 2014). Six EEG frequency components (F = .5 Hz; …; 6F = 3Hz), corresponding to the six frequency components observed in the spectrum of the sound envelope, were quantified for each participant and each session, across the eight trials. A pool of 3 electrodes of interest (electrodes of maximal magnitude: FC1, FCz, FC2) was selected on the normalized topographical

---

[10] Note that the "Steady-State Evoked-Potentials" terminology used in the original "Body Movements Selectively Shapes the Neural Representation of Musical Rhythms" published study (Chemin et al., 2014, section 4.2) was no longer used in this study, for the reasons discussed in section 3.3. The terminology "EEG frequency components" was preferred instead.

maps obtained across participants, session and frequency, and the magnitudes of each of the EEG frequency component were averaged across those electrodes of interest.

Statistical Analysis. A 2 (meter: movement-meter-related vs. non-movement-related) × 2 (session: before training vs. after training) repeated measures analysis of variance (ANOVA) was conducted on the magnitude of the mean EEG frequency components. Paired samples *t*-tests were used to perform post hoc pairwise comparisons of the magnitude of the EEG frequency components measured before and after movement training. The significance level was set at $p < .05$.

In addition, the magnitude of the EEG components obtained at the expected frequencies were expressed as *z*-scores, using the mean and standard deviation of the magnitudes obtained across the different peaks, to assess how each of the different components stood out relative to the entire set of components and relative to the *z*-scores obtained from the sound-pattern envelope (Nozaradan et al., 2012a). To assess specifically whether the components elicited at ternary-meter-related frequencies (0.5 Hz, 1.5 Hz, and 3 Hz) were selectively enhanced, we compared the average of the *z*-scores representing the magnitudes at ternary-meter-related frequencies with the average of the *z*-scores representing these same frequencies in the sound-pattern envelope, using a one-sample *t*-test (Nozaradan et al., 2012a). A similar procedure was used to compare the magnitude of the EEG and of the sound envelope frequency components, at non-meter-related frequencies. The significance level was set at $p < .05$.

Results

Unfortunately, the EEG data of 5 patients out of 20 were corrupted due to a technical incident with the analog-to-digital conversion system. This incident resulted in an inconsistent sampling rate, which rendered impossible any valid interpretation of the signals. Because the task performed during the experiment was a learning task, we were unable to repeat the test a second time for the concerned participants.

Motor Training Session. All participants achieved the motor training session in 15 to 20 min. All participants succeeded to perform, by themselves, a stable and well-synchronized movement on at least half of the training time. Overall, they judged the ease of the task at 8/9.

Neural Representation of the Acoustic Rhythm. Each of the six frequencies constituting the envelope spectrum of the rhythmic pattern elicited an EEG response before and after the motor-training session. The scalp topography of the elicited responses was, on average, maximal over fronto-central regions and symmetrically distributed over the two hemispheres (Fig. 44).

The repeated measure ANOVA used to examine the mean magnitude of the beat-related and beat-unrelated frequency components, before and after the training session, revealed a significant mean effect of meter, $F(1,14) = 13.682$, $\eta^2 = .021$, $p = .002$; but no significant effect of session, $F(1,14) = 1.001$, $\eta^2 = .001$, $p = .334$; and no significant interaction between meter and session, $F(1,14) = .521$, $\eta^2 = .000$, $p = .482$. The magnitudes of the meter-related frequencies were generally greater ($M = .125$ µV) than the magnitudes of the meter-unrelated frequencies ($M = .088$ µV). This effect was expected, and was already observed in a prior study investigating healthy participants (Chemin et al., 2014). It can be explained by the fact that the acoustic energy present in the auditory stimuli is not equally distributed across the six frequency components, but instead favour F and 3F over the other components. However, the absence of significant effect of session and significant interaction between meter and session constituted an important difference between the previous experiment investigating young healthy volunteers and this experiment investigating Parkinson patients. A comparison with a group of age- and sex-matched healthy volunteers is required to confirm this differential effect between Parkinson and non-Parkinson participants.
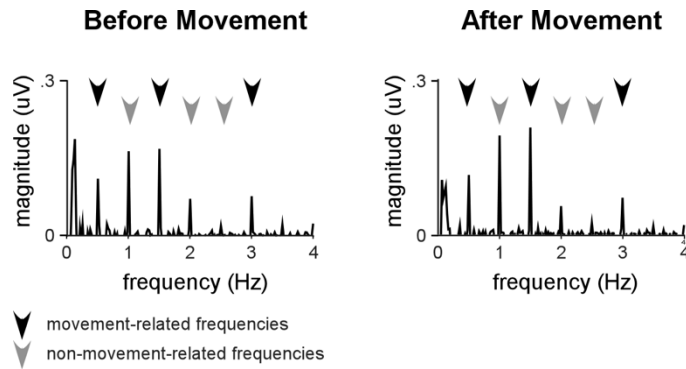
Figure 43. – EEG Spectra

Across participant averaged EEG spectra, *before* and *after* approximately 20 minutes of a motor training session consisting in moving (i.e., clapping the hands and rocking the upper body) to a specific frequency of the acoustic rhythm (movement-related frequencies; black arrows). No significant enhancement of the different frequency components could be observed.
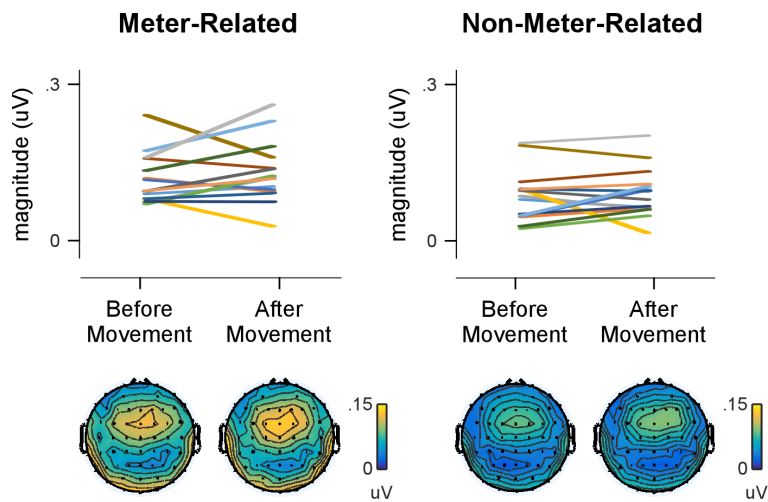
Figure 44. – Amplitude of Responses

Group-level average scalp topography and individual amplitudes of movement, meter-related (left column) and non-meter- related (right column) frequency components obtained before and after the movement-training session (colours across left and right plots correspond to the same participants).

In the before-movement session, the standardized estimates of the EEG responses obtained at meter-related and non-meter-related frequencies were not significantly different compared with the standardized estimates of the sound envelope at the corresponding frequencies, $t(14) = -1.875$, $p = .082$ and , $t(14) = .867$, $p = .401$, respectively. This suggested that there was no clear selective enhancement of neural entrainment to any specific frequency. This absence of significant difference was also coherent with the view in which the significant main effect of meter reported by the ANOVA was attributable to the distribution of acoustic energy across the different frequencies of interest.

In the after-movement session, the standardized estimates of the EEG responses obtained at meter-related were significantly lower ($M = .2148$, $sd = .195$) compared with the standardized estimates of the sound envelope at the corresponding frequencies, $t(14) = -2.593$, $p = .021$. Contrastingly, the standardized estimates of the EEG responses obtained at non-meter-related frequencies were not significantly different from the standardized estimates of the sound envelope at the corresponding frequencies, $t(14) = -1.671$, $p = .117$.

Experiment 2: evaluating The clinical and behavioural benefits of walking with music in Parkinson patients

Experimental Design

In this experiment, the same patients that participated in the electrophysiological experiment were evaluated before and after a training program of one month consisting in walking with music.

Patient Evaluations. All the evaluations were performed at the same time of the day. Before each evaluation, a physician enquired whether the participants had taken their medication within the required time and assessed that the patients were effectively in an ON-state.

A validated clinical rating scale, the Movement Disorder Society – Unified Parkinson's Disease Rating Scale (MDS-UPDRS), was administrated to the patients. The MDS-UPDRS has a total score of 265 (including the Hoehn & Yahr scale) and rates 65 items. There are 5 responses possibilities for each item: 0 = normal, 1 = slight, 2 = mild, 3 = moderate and 4 = severe (Goetz et al., 2008).

The scale is sub-divided into four sub-parts: Part I concerns "non-motor experiences of daily living" (scored on 52); Part II concerns "motor experiences of daily living" (scored on 52); Part III concerns "motor examination" (scored on 137 including Hoehn & Yahr stage); and Part IV concerns "motor complications" (scored on 24). A lower score implies less disability.

An experimental evaluation of gait was performed in order to measure the stride length, the walking speed, the walking cadence, the arm swing amplitude, and (when applicable) the synchronization between performed steps and rhythmic acoustic stimulation. An extensive description of this procedure is provided in section 3.2. The parameters were measured in five different conditions. The first condition consisted in walking spontaneously, and the four following conditions, presented in an aleatory order, consisted in walking with four different acoustic rhythms.

The four acoustic rhythms were the following: a popular music ("Happy", by Pharrell Williams) in which the beat was reinforced with a superimposed electronic drum, a synthetic acoustic rhythm with predictable tempo fluctuations, another with unpredictable tempo fluctuations, and a last synthetic acoustic rhythm with no tempo fluctuation (i.e., isochronous). The acoustic rhythms contained 600 acoustic events. The mean interbeat interval (IBI) was set to correspond to +/- 10 % of a patient's spontaneous cadence (Benoit et al., 2014). The direction of this adjustment was chosen in order to attract the cadence of one participant toward a "target" cadence of 100 steps per minute.

Participants had to walk around an indoor ground of 12 x 6 meters, in a neutral sound environment. An experimenter remained in a corner of the room, in order to monitor the patients and count the number of tours that the patients achieved.

All the evaluation procedures were completed within the week preceding and following the training program.

Training of gait. Patients underwent two training sessions of 30 minutes per week, during four weeks. During each training session, patients were asked to walk while listening to the music used in the evaluation procedure, looped continuously. The music was delivered by an MP3-player and

headphones. Patients were instructed to "walk with the music", and no explicit instructions to synchronize the footsteps to the beat of music were provided.

Analysis

Five patients out of twenty dropped out of the training program: one patient had a knee injury; another started suffering from neurological claudication after the third training session; one patient had a stroke; one patient was hospitalized for severe worsening of his disease, and had major changes in his medication; and another patient simply decided to withdraw from the study.

MDS-UPDRS

Wilcoxon signed-rank tests were used to compare, for each of the four parts and for the total score of the MDS-UPDRS, the median scores obtained before and after the training program. The significance level was set at $p \leq .05$. The sum scores for each parts were evaluated individually, as recommended by the Movement Disorder Society (Goetz et al., 2008).

Gait parameters

The detailed analyses are described in section 3.2.2. An illustration of the measures obtained in one participant is provided in Fig. 45.

The step latencies were identified in the accelerometer signals as the periodic peak of maximal negative acceleration. The quality of the signal was asymmetrical in 9 patients out of 16, with the signal obtained from one lower limb considerably noisier than the signal obtained from the other lower limb. Because this yielded an important uncertainty about the latencies of certain steps (uncertainty estimated at approximately 120 ms), the analyses were limited to the latencies obtained from the limb providing the best signal for all participants.

For each participant, and each of the five walking conditions evaluated both before and after the training program, the mean stride length was computed by dividing the walked distance by the number of steps, and the mean walking speed was computed by dividing the walked distance by the trial time.

An inverse measure of variability of the walking cadence, R^{step}, reflected the consistency of the walking cadence along the trial. It spanned from 0 (i.e., the walking cadence maximally changed along the trial) to 1 (i.e., the cadence remained perfectly stable along the trial).

A measure of synchronization consistency, R^{beat}, reflected the concentration of the steps around a specific point of the circle whose circumference corresponded to the interbeat interval. This measure spanned from 0 (i.e., maximal dispersion, or poor synchronization) to 1 (i.e., minimal dispersion, or perfect synchronization).

A measure of synchronization accuracy, θ^{beat}, reflected the mean deviation between the steps and the acoustic events, and spanned from 0 (phase alignment) to $\pm\pi$ radians (anti-phase alignment).

The cross-correlation function was computed between the time courses of the interevents intervals constructed from the step latencies and the acoustic event latencies, for both predictable and unpredictable conditions. In each of the cross-correlation function, the maximal value $xcorr_n$, and its lag lag_n were measured within a range spanning from -5 to +5 s. The value $xcorr_n$ represented the maximal similarity between the fluctuations of the walking cadence and the tempo fluctuations of the acoustic rhythm. The value lag_n indicated the lag at which the maximal correlation was observed, in seconds (i.e., the participant followed or anticipated the rhythm fluctuations with a lag_n s delay).
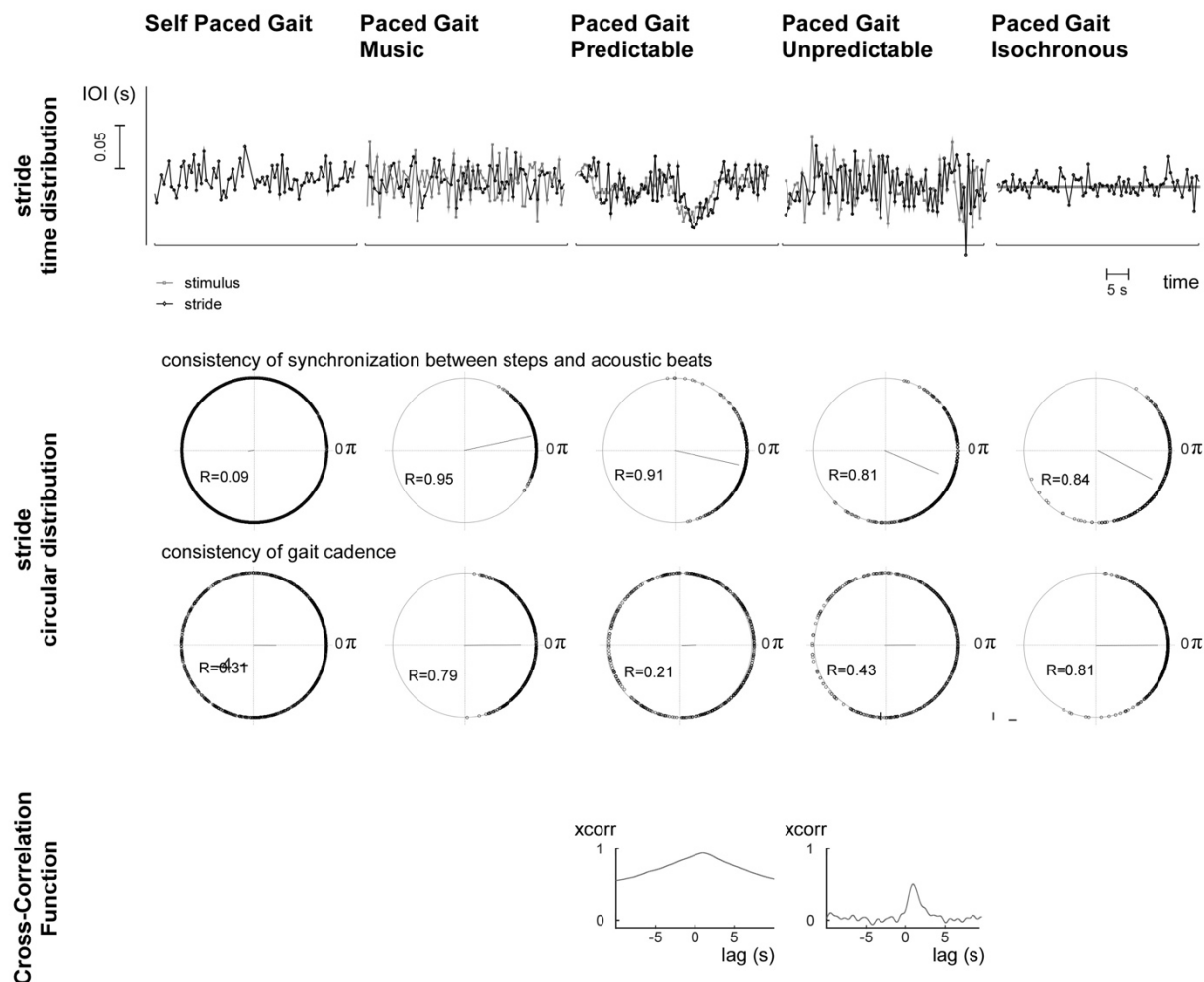
Figure 45. – Illustration of the synchronization analysis performed on the five gait evaluation conditions.

A. Time-period representation of gait (black diamonds) and acoustic (grey squares) time series **B.** Step dispersion around acoustic beats, for the 5 stimulation types, and step dispersion around the median interstep interval (C) Cross correlation functions between the time courses of the interevent intervals, constructed from the step latencies and the acoustic beats latencies.

A 2 (session: before vs. after training) × 5 (walking condition: spontaneous vs. music vs. predictable fluctuations vs. unpredictable fluctuations vs. non-fluctuating rhythm) repeated measures analysis of variance (ANOVA) was conducted on individual mean stride length (m), mean gait speed (m/s), and walking cadence consistency R^{step}. A 2 (session: before vs. after training) × 4 (walking condition: music vs. predictable fluctuations vs. unpredictable fluctuations

189

vs. non-fluctuating rhythm) repeated measures analysis of variance (ANOVA) was conducted on synchronization consistency R^{beat} and synchronization accuracy θ^{beat}. A 2 (session: before vs. after training) × 2 (walking condition: predictable fluctuations vs. unpredictable fluctuations) repeated measures analysis of variance (ANOVA) was conducted on the maximal coefficient of cross correlation between the tempo fluctuations in the acoustic rhythms and the tempo fluctuations in the walking cadence. Greenhouse-Geisser corrections of degrees of freedom and contrast analyses were used when necessary (Field, 2013; Howell, 2002). Significance level was set at $p \leq .05$. When a significant main effect or a significant interaction was observed, paired samples t-tests were used to perform post hoc pairwise comparisons of the individual values measured before and after the training program and for each stimulation.

Results

MDS-UPDRS

The score obtained in the Part I of the MDS-UPDRs was significantly lower after the training program (*Mdn* = 9) than before the training program (*Mdn* = 12), *Z* = -2.88, *p* = .004. The total score of the MDS-UPDRS was also significantly lower after the training program (*Mdn* = 45) than before the training program (*Mdn* = 58), *Z* = -2.0459, *p* = .0408. No significant difference could be observed for the Part II (*Mdn* = 10.5), the Part III (*Mdn* = 24.5), and the Part IV (*Mdn* = 2).

Gait Parameters

Detailed descriptive statistics and ANOVA results for stride length, walking speed, walking cadence consistency, synchronization consistency and synchronization accuracy are reported in Tables 2 and 3.

Session	Condition	M	SD	N
Stride Length (cm)				
Before Training	Spontaneous	63	12	15
	Music	68	16	15
	Predictable	65	12	15
	Unpredictable	66	12	15
	Isochronous	65	12	15
After Training	Spontaneous	63	12	15
	Music	74	14	15
	Predictable	71	13	15
	Unpredictable	66	12	15
	Isochronous	70	11	15
Gait Speed (m/s)				
Before Training	Spontaneous	1.201	0.066	15
	Music	1.263	0.330	15
	Predictable	1.172	0.299	15
	Unpredictable	1.220	0.071	15
	Isochronous	1.192	0.309	15
After Training	Spontaneous	1.201	0.066	15
	Music	1.380	0.318	15
	Predictable	1.271	0.312	15
	Unpredictable	1.220	0.071	15
	Isochronous	1.279	0.252	15
Walking Cadence Consistency (unit interval)				
Before Training	Spontaneous	0.406	0.086	15
	Music	0.762	0.234	15
	Predictable	0.436	0.137	15
	Unpredictable	0.597	0.115	15
	Isochronous	0.783	0.240	15
After Training	Spontaneous	0.489	0.131	15
	Music	0.753	0.234	15
	Predictable	0.434	0.147	15
	Unpredictable	0.577	0.116	15
	Isochronous	0.755	0.222	15
Synchronization Consistency (unit interval)				
Before Training	Music	0.489	0.423	15
	Predictable	0.459	0.308	15
	Unpredictable	0.554	0.296	15
	Isochronous	0.673	0.342	15
After Training	Music	0.488	0.449	15
	Predictable	0.458	0.306	15
	Unpredictable	0.494	0.289	15
	Isochronous	0.627	0.350	15
Synchronization Accuracy (radians)				
Before Training	Music	0.105	1.543	15
	Predictable	-0.179	0.717	15
	Unpredictable	-0.125	0.918	15
	Isochronous	-0.447	1.144	15
After Training	Music	-0.245	1.731	15
	Predictable	-0.205	0.725	15
	Unpredictable	-0.297	0.998	15
	Isochronous	-0.197	1.113	15
Maximal Cross Correlation Coefficient (unit interval)				
Before Training	Predictable	0.460	0.497	15
	Unpredictable	0.150	0.361	15
After Training	Predictable	0.421	0.436	15
	Unpredictable	0.117	0.367	15

Note. *M* = mean, *SD* = standard deviation, *N* = number of observations

Table 2. –   Descriptive Statistics Summary

Source	df	MS	F	p	ES
Stride Length					
Session	1	14	6.170	0.026*	0.041
Condition	2.059	28.827	3.745	0.035*	0.049
Interaction	4	56	2.974	0.027*	0.007
Gait Speed					
Session	1	14	8.475	0.011*	0.103
Condition	2.112	29.567	2.597	0.089	0.127
Interaction	4	56	2.909	0.029*	0.019
Walking Cadence Consistency					
Session	1	14	0.032	0.860	0.001
Condition	1.992	27.886	19.414	< 0.001***	1.568
Interaction	2.324	32.538	0.026	0.421	0.921
Synchronization Consistency					
Session	1	14	2.093	0.170	0.170
Condition	1.767	24.742	3.054	0.071	0.337
Interaction	2.362	33.069	0.232	0.829	0.008
Synchronization Accuracy					
Session	1	14	0.584	0.457	0.611
Condition	2.156	30.182	1.395	0.264	1.069
Interaction	2.121	29.693	0.263	0.783	0.479
Maximal Cross Correlation					
Session	1	14	1.239	0.284	0.095
Condition	1	14	33.689	< 0.001***	1.520
Interaction	1	14	0.039	0.846	0.003

Note. MS = mean squares, ES = effect size ($\eta 2$ or partial $\eta 2$), * = level of significance.

Table 3. –   ANOVA Summary

Post hoc analyses revealed a significant elongation of stride length observed after the training program in predictable fluctuations condition, $t(14) = -2.554$, $p = .023$; music condition, $t(14) = -2.700$, $p = .017$; and non-fluctuating rhythm condition, $t(14) = -3.289$, $p = .005$. No significant difference of stride length could be observed across the different conditions, except in the after-training session where the stride length was significantly longer for the music condition, as compared to the spontaneous condition, $t(14) = 3.004$, $p = .009$, and the unpredictable fluctuations condition,), $t(14) = 2.425$, $p = .029$.

There was a significant fastening in the walking speed observed after the training program in predictable fluctuations condition, $t(14) = -2.674$, $p = .018$; music condition, $t(14) = -3.105$, $p = .008$; and non-fluctuating rhythm condition, $t(14) = -2.742$, $p = .016$; but no significant difference for spontaneous and unpredictable fluctuations conditions, $t(14) = -.732$, $p = .476$ and $t(14) = .014$, $p = .989$, respectively.

The consistency of walking cadence was the highest for music and no fluctuation conditions. The consistency of walking cadence was the lowest for spontaneous and predictable fluctuations conditions, and intermediate for the unpredictable condition.
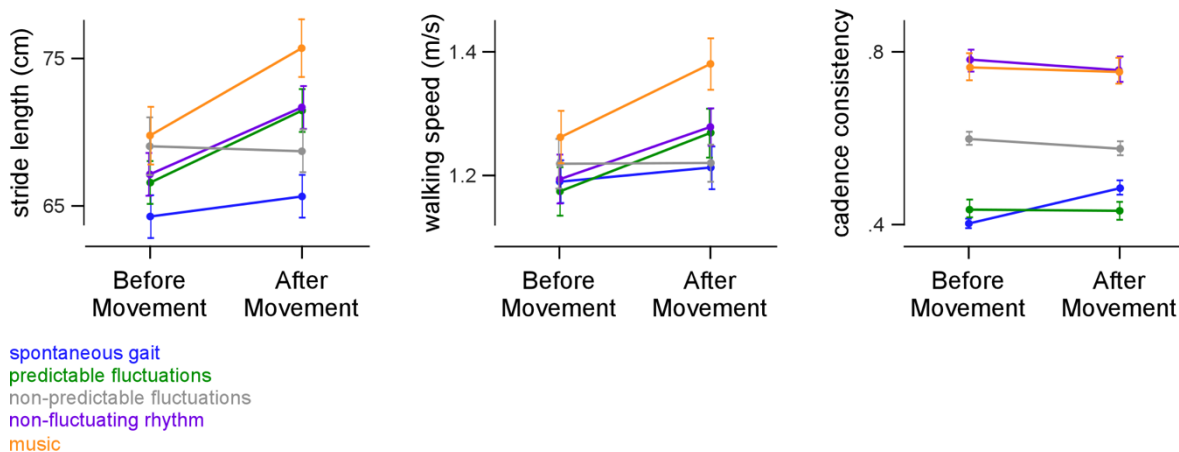
Figure 46. –   Evolution of Stride Length, Walking Speed and Cadence Consistency

Mean and standard error for all participants, before and after one month of training, in each condition.

The absence of significant effect for synchronization consistency at the group level could be due to the inter-individual heterogeneity (see Fig. 47). At the individual level, some patients showed

a substantial increase in synchronization consistency, while some others showed a substantial decrease. Therefore, there is a possibility that not all participants respond to the treatment, or at least that not all participants respond in the same way.

The similarity between the time course of the interbeat interval and the time course of the interstep interval was greater in the predictable condition than in the unpredictable condition, at a mean lag of 1.6 ± 2.3 s.
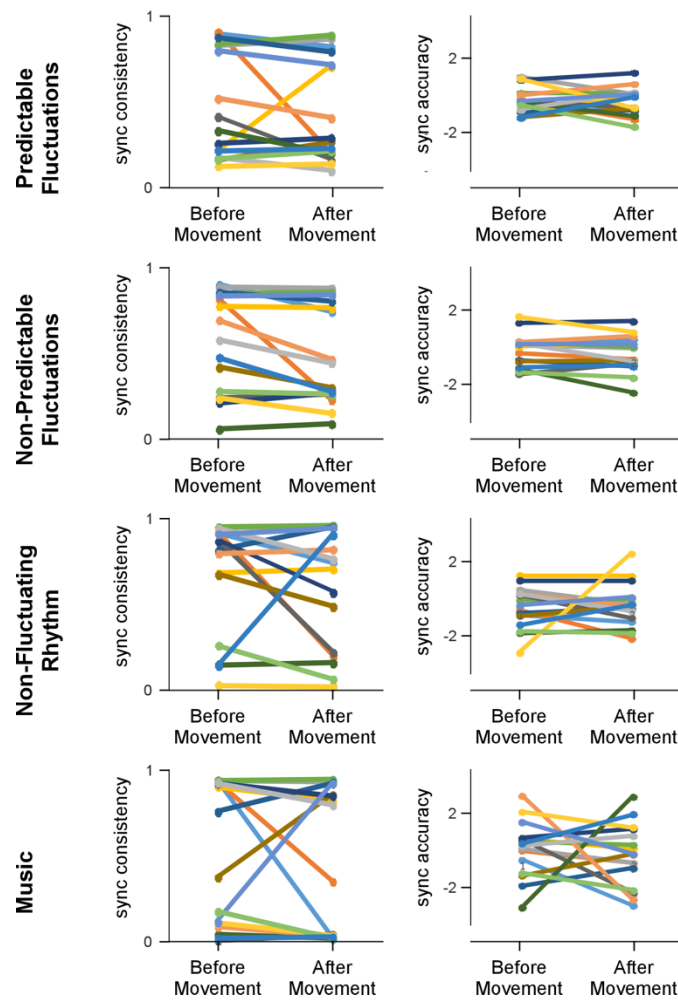
Figure 47. –   Evolution of Synchronisation Consistency and Synchronisation Accuracy.

Individual values, before and after one month of training, for each condition.

Interaction between EEG markers and benefits of the training of gait

Due to the technical issues faced with the analog-to-digital conversion system during the EEG experiment, and to the drop outs that occurred during the training of gait experiment, only twelve patients could be included in the analyses aiming at establishing a correlation between the EEG markers of bodily-movement enhanced *beat-based* internal representation of an ambiguous acoustic rhythm and the clinical benefits of walking with music. This small size of patient cohort resulted in an insufficient statistical power. Particularly, the estimation of correlation on small datasets is very sensitive to deviant data, which can either provoke type I (e.g., a deviant data can provoke a "false positive" finding) or a type II errors (e.g., a deviant data can provoke a "false negative" result). Importantly, the absence of effect at the group level does not question the clinical relevance of the experiment as it focuses on the concept of *precise medicine*, i.e., clinical intervention being tailored to the individual patient. Therefore, an increased sample size could potentially allow to identify a subgroup of patient that respond to the treatment and identify the predictors of their response. The following paragraphs describe briefly the performed analysis, and the main tendencies that resulted.

An individual summary measure of selective enhancement of neural *beat-based* entrainment to movement-related frequencies, obtained in the EEG experiment, was provided by the following operation: for each participant, the measure of enhancement of non-meter-related frequencies (i.e., the difference between the average measure of magnitude at non-movement-related frequencies, after and before the training session) was subtracted to the measure of enhancement of meter-related frequencies (i.e., the difference between the average measure of magnitude at movement-related frequencies, after and before the training session). This operation allowed to account for the specific effect on movement-related vs. non-movement-related frequencies. Hence, a non-specific enhancement of the EEG response would actually lower the individual summary measure. For example, one participant showed an average change of the movement-related frequencies of +.05 μV, and a change of the non-movement-related frequencies of + .03 μV. Her summary measure was therefore +.02 μV. Another patient showed an average change of the movement-related frequencies of +.05 μV, and a change of the non-movement-related frequencies of -.03 μV. Her summary measure was therefore +.08 μV.

The individual benefit of the training of gait program was computed as the difference between the value obtained after vs. before the training program. The benefits were evaluated for the measures of mean stride length and synchronization consistency, in order to limit the total number of correlation analyses. Furthermore, the correlations were only computed for the music condition, as the individual improvement attributable to the training of gait program would be most likely to occur in the music condition that uses the same auditory stimulation.

The distribution of the variables was visually evaluated using Q-Q plots. In the case of too large deviation from a normal distribution, the data were normalized using a logarithmic transformation, after applying a translation of the values to avoid any negative value. This was the case for synchronization consistency, but not for the individual mean stride length. Therefore, a Pearson's correlation coefficient was computed to assess the relationship between the summary measure of selective enhancement of neural entrainment due to motor training and the improvement of stride length and a Pearson's correlation coefficient was computed to assess the relationship between the summary EEG measure of selective enhancement of neural entrainment due to motor training and the log-transformed improvement in synchronization consistency, in the music condition. Whereas no significant correlation could be observed with the mean stride length (r = .537, n = 12, p = .072), a significant correlation could be observed with the synchronization consistency (r = .799, n = 11, p = .003). The results are summarized in Fig. 48.
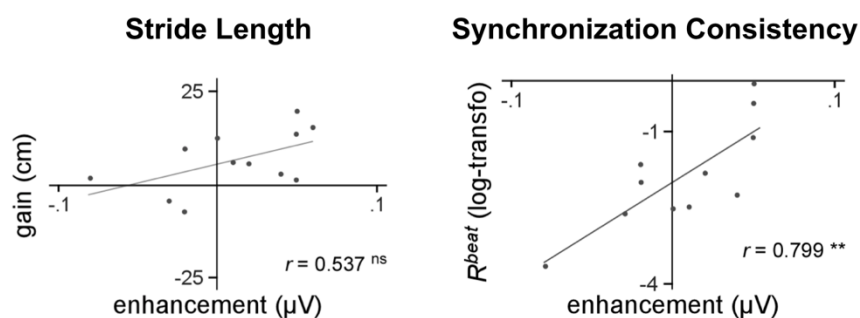
Figure 48. – Correlation between the summary measure of selective enhancement of neural entrainment due to motor training, and the elongation of mean stride length and the log-transformed improvement in synchronization consistency (music condition).

No significant correlation could be observed with the mean stride length. A significant positive correlation ($r = .799$, $p = .003$) was observed with the synchronization consistency. The correlation was particularly driven by four participants. Three of them showed a positive enhancement of neural entrainment (EEG study) and improved their synchrony to the musical beat (training program). One of them showed a diminution of neural entrainment and a lower synchrony to the musical beat after the training program.

Discussion

A comprehensive approach to addressing gait disorder in Parkinson's disease needs to take into account the interactions between motor and cognitive aspects of locomotion. When motor deficits such as akinesia hinder the gait, patients tend to compensate with increased cognitive control (Iansek et al., 2013). However, Parkinson's disease can also cause various non-motor deficits, including deficits in planning and executive functions. Of these, alterations of beat-based timing, i.e., the timing function necessary to perceive a periodic beat in music or to control a periodic movement, could lead to gait disorders (Hove & Keller, 2015). In this study, we investigated whether preserved beat-based timing abilities is a predictive factor of success for beat-based rehabilitation strategies such as cuing the gait with music. Hence, patients with preserved beat-based timing abilities could reinforce this cognitive function during the training program and therefore facilitate their gait. In contrary, patients with impaired rhythmic abilities could endure an additional cognitive burden with rhythmic auditory cueing and therefore worsen their gait.

Our preliminary results are in line with this hypothesis. First, the EEG marker representing how body movements shaped the neural representation of a complex acoustic rhythm revealed some heterogeneity across patients. While a few patients showed a selective enhancement of the movement-related EEG frequency components, most patients showed no evidence of selective change at these frequencies and one patient even showed a selective reduction of movement-related EEG frequency components. No significant difference could be observed at the group level, but this absence of group-level effect corresponds precisely to our expectations. A control group of healthy matched participant should be tested in order to provide a valid comparison. Second, after a training program of one month consisting in walking with music (two times 30 minutes per week), an improvement in synchronization of the steps to the beats of the music could only be observed in some patients. Most interestingly, we observed a positive correlation between the EEG marker hypothesized to be sensitive to *beat-based* timing abilities and the post-training improvement in gait synchronization to music. These results (to be interpreted with caution due to the lack of statistical power) conjectures that the training program was more benefic to patients that had the cognitive resources that allows manipulating beat information.

An alternative hypothesis that has gained considerable momentum postulates that the success of rehabilitation depends on the compensation of beat-based timing deficits by non-beat-based timing processes (Dalla Bella et al., 2015; del Olmo, Arias, Furio, Pozo, & Cudeiro, 2006; Jahanshahi, Jones, Dirnberger, & Frith, 2006). In this case, a cerebello-thalamo-cortical pathway known to be involved in *non-beat based* timing (Grube, Lee, et al., 2010; Teki, Grube, Kumar, et al., 2011) and in error correction of timing processes (Teki, Grube, & Griffiths, 2011) could compensate for the deficits in beat-based timing of the basal ganglia (Dalla Bella et al., 2015; del Olmo et al., 2006; Jahanshahi et al., 2006). However, while non-beat-based timing compensatory mechanisms could play a certain role in the rehabilitation process, we believe that such mechanisms are cognitively demanding, and that an effective rehabilitation could not solely rely on them. Importantly, our hypothesis suggest that a remaining neurologic resource can be identified and targeted during rehabilitation, which is a powerful approach in demented patients.

Importantly, non-beat based compensatory mechanisms could compromise the interpretation of the EEG experiment performed in this study. Hence, patients could develop a non-beat-based

strategy to synchronize accurately their body movements to the complex acoustic rhythm (see e.g., Tranchant & Vuvan, 2015 for details about this confunding factor in behavioral experiments) and the shaping of their neural representation of the acoustic rhythm could be a non-beat-based memory of this strategy. However, under the alternative hypothesis, a stronger correlation should be observed between EEG markers of error detection and error correction (presented in section 3.4), as compared to the EEG marker used in this study. Therefore, we performed an additional experiment, on the same participants and before the training program, in order to measure the error detection and error correction processes elicited when synchronizing finger taps to acoustic rhythms with predictable and unpredictable fluctuations of tempo (see Chemin et al., in prep for original experiment). The analyses of the data obtained in this experiment are still in progress. Furthermore, unlike other behavioural approaches, the EEG approach does not rely on behavioural or motor outputs. Hence, it offers the crucial advantage of not being affected by confounding factors such as tremor, motivational issues, or neurodegenerescence of primary motor cortex pyramidal neurons.

Interestingly, we did not observe a consistent correlation between the first EEG marker and improvement in stride length. While this simple gait parameter is clinically relevant and could appear as a good target outcome of a rehabilitation program, it is probably mediated by different neural mechanisms than beat-based synchronization. We suspect that a confounding factor could have played a significant role in the elongation of stride length. Some participants tended to walk faster when they were hearing the music, without being properly entrained to the beat (i.e., without any sign of synchronization of their step to the musical beat). This could be due to a motivation factor, independent of timing abilities. In line with this hypothesis, the MDS-UPDRS revealed a significant clinical improvement for *non-motor* experiences of daily living only, while it did not suggest any significant improvement in motor components. These results suggest that patients benefit from the training program through improvement of cognitive abilities that extend beyond timing abilities and also imply emotional and motivational factors.

Author Contributions. BC, TW, CEB, IP and AM designed the experiment. Testing and data collection was performed by BC with the support of two students in kinesiotherapy. BC analysed the data. BC and AM interpreted the results. BC wrote the manuscript.

Study 5: Get up, Get UP: emerging consciousness in a thriller walk (Chemin, B., Lejeune, N., Laureys, S., Peretz, I., Mouraux, A.)

The manuscript of this study is in preparation, to be submitted for publication. This chapter presents selected parts of the manuscript.

Abstract

The locomotor system largely relies on automatic processes, which are regulated by adaptive movement control. The neural circuitry underlying these automatic processes are similar in human, other mammals and birds. It can produce a large panel of rhythmic limb movements, postural adjustments, and even goal-oriented behaviours. For example, decorticated cats can forage for food (and even remember its localization), provided that their diencephalon remains present. However, the cortical and cortico-subcortical loops involved in the most complex forms of locomotion control, such as the anticipative adjustment of gait to the environment, may largely differ between species. Of these, the ability to synchronize steps to an acoustic rhythm appears to be (almost) specific to human. Nevertheless, little is known about the specific neural circuitry responsible for the cognitive regulation of gait, as animal models are reaching their applicability limit and neuroimagery techniques are still limited for studying the human brain in motion. Here, we investigate the case of two patients in a minimally conscious state that showed the unique ability to walk and adjust their gait to rhythmic acoustic pacers. It is a very rare condition: the minimally conscious state following anoxic coma is never associated with recovery of gait ability but the two patients presented a rare aetiology, severe hypoglycemic coma. Importantly, we state the specificity of their functional and structural deficits with regards to their rhythmic synchronization abilities. Finally, we discuss the implications of these findings in the current understanding of the neural basis of consciousness.

Introduction

The act of walking is so seemingly related to consciousness that we developed a special concept to describe a wobbly unconscious walking individual: we usually call it a zombie. This study reports for the very first time the case of two young women who, despite being in a minimally conscious state (MCS), were able to walk spontaneously. And the reality sometimes meets the fiction: although the two cases that we report did not have the choreographic abilities of Michael Jackson in his music video "Thriller", they were nevertheless able to synchronize their gait to music.

But why do we associate gait to volitional control, when it is actually mostly dependent on automatic processes? Studies on decorticated cats showed that those animals were still able to walk (Bjursten, Norrsell, & Norrsell, 1976), and the most critical nervous centers responsible for locomotion are purely automatic and located in the spinal cord (Grillner, 1975, 1985; Grillner et al., 1997; Minassian et al., 2017; Takakusaki, 2013). Obviously, automatic processes are regulated by voluntary and adaptive movement control and, in most cases, this control requires cerebral mechanisms that include movement initiation as well as movement-environment coordination such as the visuomotor adjustments that are necessary to spatially orient the gait (Drew et al., 1996; Grillner et al., 1997; Milner & Goodale, 1995; Takakusaki, 2013). The state of relatively high disturbance in functional connectivity across brain regions (e.g., Laureys & Schiff, 2012) of patients with disorders of consciousness (DOC) might affect those later components of gait control, and this is probably why countless number of patients in MCS do not walk, despite having intact spinal and mesencephalic structures (at least in DOC of nonlesional aetiologies). In contrast with cats, human locomotion appears to *require* supramesencephalic functions, as functional decortication suppress their gait while it does not in cats.

The clinical distinction between automatic and voluntary motor acts is not always straightforward, and should probably be made in regard to the context in which it occurs rather than according to which type of movement is involved in the action (Grillner, 1985). For example, a part of an automatic movement sequence (e.g., a step cycle), can either be generated in a reflex loop (e.g., to avoid falling) or be initiated by will. Similarly, the distinction between volitional, automatic and reflex movements is not unequivocal even at the anatomical level. Cortical activity is probably a necessity to consider that there is voluntary control, but the opposite is definitely

not true. For example, long loop reflexes can involve a cortical relay, and this is not sufficient to assert any conscious or voluntary act (Macefield, 2009).

In this paper, we will illustrate the great variability in gait synchronization to acoustic rhythms in healthy and homogenous group of participants matched for their age, gender, music and dance education. Because of this heterogeneity, it is important to not consider a given observation as "normal" or "abnormal" (i.e. as statistically different or not from a group of reference), but rather as a marker of the ability of an individual to perform or not an action (i.e., as a valid observation, by itself). Hence, these data represent a sample of *what are the possible measures* in individual with no neurological disability. Importantly, we consider that if an action can be robustly performed by an individual, it is meaningful of the correct execution of a certain neural process. However, the opposite is hardly conclusive: if an individual does not perform a certain action, one should be cautious about concluding that the neural system is therefore deficient.

We will demonstrate that the two MCS patients showed the ability to adapt and even synchronize their gait to music. Then, we will discuss the underlying neural processes of this particular ability. The spatiotemporal coordination of rhythmic movement to the complex stream of rhythmic information contained in music relies on complex and versatile interactions between multiple supramesencephalic neural centers (e.g., Grahn, 2012; Patel, 2014; Patel & Iversen, 2014; Repp & Su, 2013), and might be one of the highest level of volitional gait control. Hence, it appears difficult to solely incriminate automatic behaviours in the ability to synchronize the gait to a musical rhythm. Finally, we will discuss the implications of clinical distinction between automatic and voluntary control of movement, which is a common tool in the evaluation of patients with DOC (Seel et al., 2010).

Methods

Participants

Six participants were tested for their ability to synchronize their gait to music. They matched the two young women in MCS (i.e., the patients) for their age, gender, music and dance education (8

years of formal dance education for the first patient; 10 years of formal music education for the second patient).

The two patients (23 and 22 years old) had a similar history of severe hypoglycemia (20 mg/dL for an estimated period of time of > 8 hours) following insulin overdose, that caused an initial episode of coma which later evolved to a MCS. Both patients were assed at the GIGA - Coma Science Group center. Their extensive medical record is available as supplementary material. They both started to walk while being hospitalized in rehabilitation unit care. This ability was reported by care givers who observed this spontaneous behaviour without explicitly trying to elicit it. While the first patient evolved to a state of emergence (EMCS) 140 days after the initial accident, the second one remained in MCS to date, four years post-onset. Importantly, the second patient developed epilepsy, which was diagnosed three years after the initial accident. Her seizure originated from the supplementary motor area and reflex seizures could be triggered by sharp sounds.

Experimental Design

Overview

The synchronization of gait was evaluated in individual sessions. An extensive description of the procedure used to evaluate the synchronization of the gait to different acoustic rhythm is provided in section 3.2. Each evaluation tested the gait under five different conditions. The first condition consisted in walking spontaneously and the four following conditions, presented in an aleatory order, consisted in walking with four different acoustic rhythms. At the end of each session, the spontaneous gait was tested again in order to evaluate the reproducibility of this measure.

Four evaluations per healthy participant were conducted along one afternoon. Six evaluations of patient 1 were conducted during her hospitalization, two to six months after the initial accident. Of these, only the first evaluation was conducted while the patient was in minimally conscious state, as she quickly emerged from it. Four evaluations of patient 2 were conducted during a re-hospitalization, four years after the initial accident. Of these, all evaluations were conducted while the patient was in minimally conscious state.

Acoustic Rhythms

The four acoustic rhythms were the following: an acoustic rhythm with predictable fluctuations of tempo, an acoustic rhythm with unpredictable fluctuations of tempo, an acoustic rhythm with no fluctuation of tempo, and a popular music. All the acoustic rhythms were 60 events long, and the spontaneous gait was evaluated over a 60 s period of time. All the acoustic rhythms had a tempo set to 85 % of a participant's spontaneous walking cadence, assessed one hour prior to the evaluation session (Benoit et al., 2014).

Testing

Participants walked around a ground of 23x12 meters, in a neutral sound environment.

For each session involving a patient, two physicians (BC and NL) independently evaluated the cooperative state of the participant using the Agitated Behaviour Scale (ABS) (Bogner, Corrigan, Stange, & Rabold, 1999). This scale was developed to assess the extent of agitation during the recovery from an acquired brain injury and allows serial assessment to describe the course of agitation by clinicians. The scores to ABS ranges from 14 to 56, the lowest score meaning no agitation while a score above 17 is significant for an agitated behaviour. The two physicians remained present during the whole time of each evaluation session. One physician (NL) stayed close behind the participants. The main reason was the potential need for physical assistance because of the patient's high risk of falling, but also because the patients were not able to avoid obstacles and, during some sessions, to remain in the task. The low volume of the acoustic rhythms delivered throughout headphones to the participant only made it impossible to the experimenters to hear it. For additional cautions, the experimenter who stayed close to the patients wore a headphone delivering a masking noise. Therefore, the experimenters avoided to influence the synchronization of the participant's gait. No instruction was given to the participants as the comprehension of such instructions by patients in MCS could not be evaluated.

At the end of the experiment, the healthy participants completed a questionnaire about their experience with the task (such as "How did you feel about the testing?" and "What did you do with the music and the beats?").

Analysis[11]

A measure of the consistency of the walking cadence, R^{step}, reflected the variance of the walking cadence. Its value would equal to 1 when the walking cadence remains perfectly stable along the entire trial, and would tend towards 0 when the walking cadence is highly non-stationary.

A measure of the synchronization consistency occurring by chance between the spontaneous gait and each of the four acoustic rhythms, R_n^{virt}, served as a detection of false positive results: if the spontaneous gait happened to be synchronized by chance to one of the acoustic rhythms, the actual measures of synchronization could not be interpreted properly.

For each of the four trials using a real acoustic rhythm, a measure of consistency of the synchronization between the steps and the acoustic beats, R_n^{beat}, was computed. Its value spans from 0 (i.e., maximal dispersion, i.e., poor synchronization) to 1 (i.e., no dispersion, i.e., perfect synchronization). A measure of the mean accuracy of the synchronization between the taps and the beats, θ^{beat}, reflected the mean deviation between the steps and the acoustic events. Its value spans from 0 (i.e., perfect phase alignment) to $\pm\pi$ radians (negative value: the steps precede the beats; positive value: the steps follow the beats).

Finally, the cross-correlation function was computed between the waveform that corresponded to the time course of the interbeat intervals as a function of time, and the waveform that corresponded to the time course of the interstep intervals as a function of time, for the predictable and the unpredictable conditions.

In the obtained cross-correlation function, the maximal value $xcorr_{max}$, and its lag lag_{max} were measured within a range spanning from -5 to +5 s. The value $xcorr_{max}$ represented the maximal similarity between the fluctuations of the gait cadence and the fluctuations of the acoustic rhythm tempo. This value could span from -1 (gait fluctuations are the exact opposite of the acoustic fluctuations) to +1 (gait fluctuations match perfectly the acoustic fluctuations). A value of 0 indicates no correlation between the two signals. The value lag_{max} indicates the lag at which the

---

[11] see section 3.2.3. for details

maximal correlation is observed, in seconds (i.e., whether the participant followed or anticipated the acoustic rhythm fluctuations).

Importantly, we provided extensive statistical validation of the measures, at the single observation level. The validation procedure is described in section 3.2.2.3. This validation was important because it was hardly conceivable to use traditional frequential statistics in this situation (e.g., comparing our observations with a control group), for the reasons evoked in the introduction section.

Results

Healthy Participants

The results of the healthy participants are partially detailed in Tables 5 and 6. Importantly, those results reveal a great heterogeneity: while some participants synchronized their gait to the acoustic rhythms, some other either ignored the acoustic rhythms, or tried to synchronize but with relatively little success.

	target median period	observed median period	R self	Rayleigh	Wilcoxon	zval	ranksum	R beat	p R beat	Rself / Rbeat	R spont	p R spont (Rayleigh)	xcorrmax	p xcorr	lagmax
Control P1 #4															
Spontaneous	0,712	0,552	0,874	0,000											
Music	0,714	0,712	0,960	0,000	0,000	-10,779	3004,500	0,949	0,030	0,989	0,030	0,354	0,146	0,821	1,984
AC	0,716	0,720	0,164	0,206	0,000	-9,919	3005,000	0,898	0,000	5,485	0,041	0,315	0,835	0,086	0,540
NC	0,720	0,702	0,175	0,165	0,000	-9,899	3009,500	0,708	0,003	4,051	0,020	0,668	0,632	0,253	1,256
I	0,712	0,708	0,674	0,000	0,000	-10,025	3003,000	0,895	0,033	1,328	0,036	0,298			
Spontaneous bis	0,712	0,556	0,926	0,000	0,594	-0,533	5894,000								
Spontaneous	0,712	0,556	0,926	0,000											
Music	0,712	0,712	0,921	0,000	0,000	-10,782	3160,000	0,918	0,026	0,997	0,024	0,493	0,255	0,015	0,728
AC	0,716	0,706	0,156	0,206	0,000	-10,263	3160,000	0,835	0,000	5,348	0,021	0,552	0,868	0,165	1,220
NC	0,716	0,712	0,907	0,000	0,000	-10,264	3160,000	0,923	0,046	1,017	0,032	0,729	0,723	0,205	1,068
I	0,712	0,712	0,937	0,000	0,000	-10,308	3160,000	0,936	0,636	0,999	0,023	0,291	NaN	NaN	NaN
Spontaneous bis	0,712	0,552	0,874	0,000	0,594	0,533	6352,000	NaN	NaN	NaN	NaN	NaN			
Spontaneous	0,577	0,552	0,874	0,000											
Music	0,584	0,584	0,835	0,000	0,000	-9,209	3447,500	0,975	0,079	1,168	0,067	0,817	0,225	0,445	2,324
AC	0,580	0,568	0,294	0,003	0,006	-2,745	4804,000	0,872	0,000	2,964	0,316	0,212	0,895	0,149	0,940
NC	0,580	0,578	0,648	0,000	0,000	-4,184	4457,000	0,840	0,010	1,296	0,288	0,263	0,594	0,200	1,076
I	0,577	0,576	0,859	0,000	0,000	-6,820	3841,000	0,910	0,017	1,060	0,185	0,380			
Spontaneous bis															

Table 4. –   Illustrative Results of a Participant Matched to Patient 1

208

	target median period	observed median period	R self	Rayleigh	Wilcoxon	zval	ranksum	R beat	p R beat	Rself / Rbeat	R spont	p R spont (Rayleigh)	xcorrmax	p xcorr	lagmax
Control P2 #1															
Spontaneous	0,484	0,500	0,906	0,000											
Music	0,488	0,496	0,620	0,000	0,099	1,651	6754,000	0,258	0,344	0,416	0,179	0,298	0,157	0,655	2,548
AC	0,480	0,524	0,961	0,000	0,000	-8,022	3628,500	0,184	0,850	0,192	0,305	0,082	0,015	0,982	-4,996
NC	0,480	0,516	0,877	0,000	0,000	-7,061	3892,000	0,047	0,931	0,053	0,320	0,306	0,368	0,041	-4,400
I	0,484	0,524	0,850	0,000	0,000	-7,831	3708,000	0,139	0,013	0,163	0,260	0,088			
Spontaneous bis	0,484	0,508	0,900	0,000	0,000	-3,525	5269,000								
Spontaneous	0,584	0,508	0,900	0,000											
Music	0,580	0,512	0,874	0,000	0,004	-2,878	5453,500	0,021	0,349	0,025	0,020	0,326	0,231	0,308	1,404
AC	0,588	0,512	0,875	0,000	0,072	-1,802	5590,000	0,111	0,069	0,127	0,090	0,243	0,328	0,031	4,044
NC	0,584	0,524	0,983	0,000	0,000	-6,815	4196,000	0,062	0,359	0,063	0,071	0,073	0,223	0,493	2,840
I	0,584	0,512	0,881	0,000	0,047	-1,986	5573,500	0,016	0,508	0,018	0,039	0,144			
Spontaneous bis	0,584	0,512	0,407	0,000	0,020	-2,326	5545,500								
Spontaneous	0,484	0,516	0,307	0,000											
Music	0,488	0,512	0,649	0,000	0,058	1,896	6825,500	0,192	0,347	0,295	0,120	0,387	0,120	0,932	-0,016
AC	0,480	0,508	0,593	0,000	0,006	2,773	6276,500	0,191	0,475	0,322	0,202	0,283	0,531	0,030	0,920
NC	0,480	0,498	0,296	0,003	0,000	5,538	7052,000	0,263	0,519	0,888	0,042	0,931	0,175	0,808	5,004
I	0,484	0,504	0,475	0,000	0,001	3,399	6476,000	0,035	0,921	0,074	0,090	0,616			
Spontaneous bis	0,484	0,500	0,906	0,000	0,000	5,860	7963,500								
Spontaneous	0,584	0,512	0,407	0,000											
Music	0,584	0,576	0,318	0,000	0,000	-10,298	3139,500	0,791	0,550	2,492	0,043	0,546	0,219	0,125	1,132
AC	0,588	0,576	0,036	0,916	0,000	-8,935	3337,500	0,671	0,002	18,499	0,062	0,602	0,709	0,000	1,336
NC	0,584	0,552	0,544	0,000	0,000	-9,167	3321,000	0,167	0,300	0,308	0,055	0,557	0,277	0,243	-3,120
I	0,584	0,576	0,062	0,771	0,000	-9,527	3191,500	0,150	0,571	2,405	0,029	0,739			
Spontaneous bis	0,584	0,516	0,307	0,000	0,277	-1,088	5737,500								

Table 5. – Illustrative Results of a Participant Matched to Patient 2

Patient 1

On the day of the first testing (D79), CRS-R evaluation met the criteria for minimally conscious state (Total score 17: A3-V4-M5-O3-C1-Ar1). The Agitated Behavior Scale, evaluated independently by the two physicians, scored 18. During the trials, the patient was not able to avoid obstacles (e.g. she was walking to the fence without avoiding it) and so, the physicians needed to push slightly on her right shoulder to make her turn. She was walking round the ground anti-clockwise as it seemed to be the easiest way for her. The results of this first gait evaluation session are reported in figure 49.
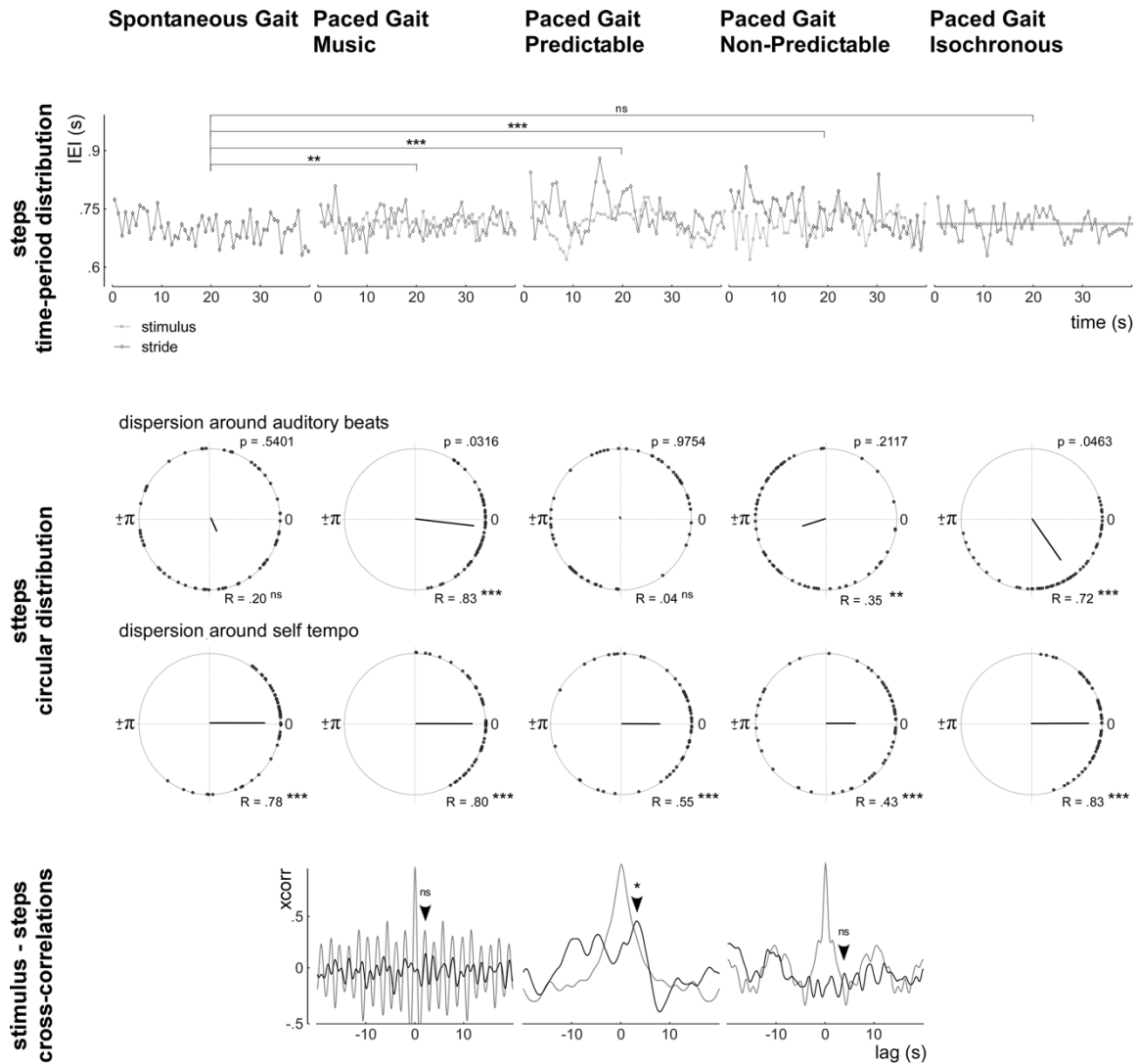
Figure 49. – Results of the Gait Evaluation Performed in Patient 1, while she was in MCS.

A: Time-period representation of gait (black diamonds) and acoustic (grey squares) time series. The results of the Wilcoxon rank sum tests for comparison of the inter-step-interval (ISI) distribution of each paced trial with the ISI distribution of the spontaneous trial are indicated above the time-series. B: Circular representation of step distribution around the acoustic events and around the median ISI. The Monte-Carlo statistic p-value is indicated above the circular diagram of dispersion around acoustic events, and the Rayleigh test significance is indicated after each R value. Note that the diagram representing the dispersion around the acoustic events for the spontaneous trial correspond to the superimposition of a virtual metronome having the median stimulation tempo. C: Cross-correlation functions of the gait and acoustic time-series (black line) and auto-correlation functions of the acoustic time-series (grey). The maximal cross-correlation, measured within a -5 to +5 s lag range, are indicated by the black arrows. The significance of those values was computed using Monte-Carlo statistics.

During the first session, the spontaneous gait of patient 1 showed a relatively stable tempo, which was assessed by the non-homogenous circular distribution around the median ISI ($R^{step}_{n_{spont}}$ = 0.78; $p < 0.001$).

When patient 1 walked with music, her gait cadence adjusted to the tempo of the music. This was assessed by the Wilcoxon rank sum test, which revealed a significant longer ISI for the paced gait, *Mdn* = 715 ms, as compared to the spontaneous gait, *Mdn* = 696 ms, *Z* = -2.6319, p = 0.0085; the median ISI of the acoustic rhythms being 712 ms. The synchronization of her gait to the musical beat showed the best consistency across conditions ($R^{beat}_{n_{music}}$ = 0.832; $p < 0.0316$). The index comparing the consistency of step synchronization to the auditory beat and the self-consistency of step dispersion was 1.0395, which indicated that the patient was slightly better aligned to the musical beat than to her self-tempo. Importantly, the superimposition of the "virtual" musical beat to the spontaneous gait yielded a low measure of virtual synchronization ($R^{virt}_{n_{music}}$ = 0.191; p = 0.6561), indicating that the synchronization measured described above are no type I error.

The gait observed when patient 1 walked with a predictably fluctuating acoustic rhythm was stable ($R^{step}_{n_{predict}}$ = 0.551, $p < 0.001$), but this value was considerably lower than the one of the gait observed when the patient walked spontaneously (*Δ* = -0.179). The paced gait ISI, *Mdn* = 725 ms, was significantly different from the spontaneous gait ISI, *Mdn* = 696 ms, *Z* = -4.175, *p* < .001. However, the measure of synchronization consistency of the patient gait to this acoustic rhythm was the lowest across condition ($R^{beat}_{n_{predict}}$ = 0.040; p = 0.9754). Those results suggest that the patient did not synchronize her steps to the predictable fluctuating rhythm, despite being "disturbed" by it. In fact, the cross-correlation revealed a significant maximal cross-correlation between the fluctuations of the acoustic and the gait rhythm ($xcorr_{n_{predicrt}}$ = 0.4481, p = 0.0429), indicating that the patient tended to "track" the fluctuations of the acoustic rhythm, with a lag of 3.14 seconds.

When patient 1 walked with the unpredictably fluctuating acoustic rhythm, her gait became even less stable ($R^{step}_{n_{unpred}}$ = 0.428, $p < 0.001$) as compared to the other trials. The measure of synchronization consistency of the patient gait to the acoustic beat was low and not significant

($R^{beat}_{n_{unpred}}$= 0.350, p = 0.2117). The cross-correlation revealed no significant positive cross-correlation between the fluctuations of the acoustic and the gait rhythm ($\text{xcorr}_{n_{unpred}}$ = - 0.0324, p = 0.9988). Those results indicated that the patient was unable to synchronize her gait to the stimulation, was unable to "track" the fluctuations of tempo, but that her gait was not unaffected by the stimulation. Those results suggest that the patient tended to compensate for previous disturbances, with little success.

When patient 1 walked with isochronous acoustic rhythm, her gait cadence was stable ($R^{step}_{n_{isoch}}$ = 0.831, $p < 0.001$) and tended towards the tempo of the stimulation, without differing significantly from the spontaneous tempo (*Mdn* paced = 702 ms, *Mdn* spontaneous = 696 ms, Z = -1.8845, p = 0.0595). The synchronization of her gait to the acoustic beat showed a good consistency, which was significant of synchronization ($R^{beat}_{n_{isoch}}$ = 0.722; $p < 0.0463$), and the superimposition of the isochronous beat to the spontaneous gait yielded a low measure of "hazard" spontaneous synchronization ($R^{virt}_{n_{isoch}}$= 0.199; p = 0.628), indicating that the observed synchronization consistency could not be attributed to type I error.

From D88 and until the last testing day (D194), the patient had emerged from MCS, as per the criteria of the CRS-R. After emerging, the patient started to show various signs of frontal syndrome, with repetitions tendencies, opposition, and agitation. Importantly, she started showing signs of perception of her environment, and was easily distracted by it.

She has been tested five times over the next 82 days. For concision, the results of the following evaluations are not reported here. Only the last evaluation could be performed in conditions relatively similar to the first evaluation, with an ABS evaluated at 18 by both physicians. A correct synchronization was never observed again. Sometimes, the patient would change her gait cadence, when being exposed to the acoustic rhythms, but this change would not lead to correct synchronization. Actually, the patient tended to accelerate her gait cadence, instead of slowing down.

Patient 2

On the day of first testing (D1420), CRS-R evaluation met the criteria for minimally conscious state. The Agitated Behaviour Scale, evaluated independently by the two physicians, scored 16. During the trials, the patient was not able to avoid obstacles (e.g. she was walking to the fence without avoiding it), and she needed a light sensory trigger to initiate the gait. Therefore, one physician remained by her side during all the testing sessions, and triggered the patient gait before every trial by touching her hand.

The results of this first gait evaluation session are reported in Fig. 50.
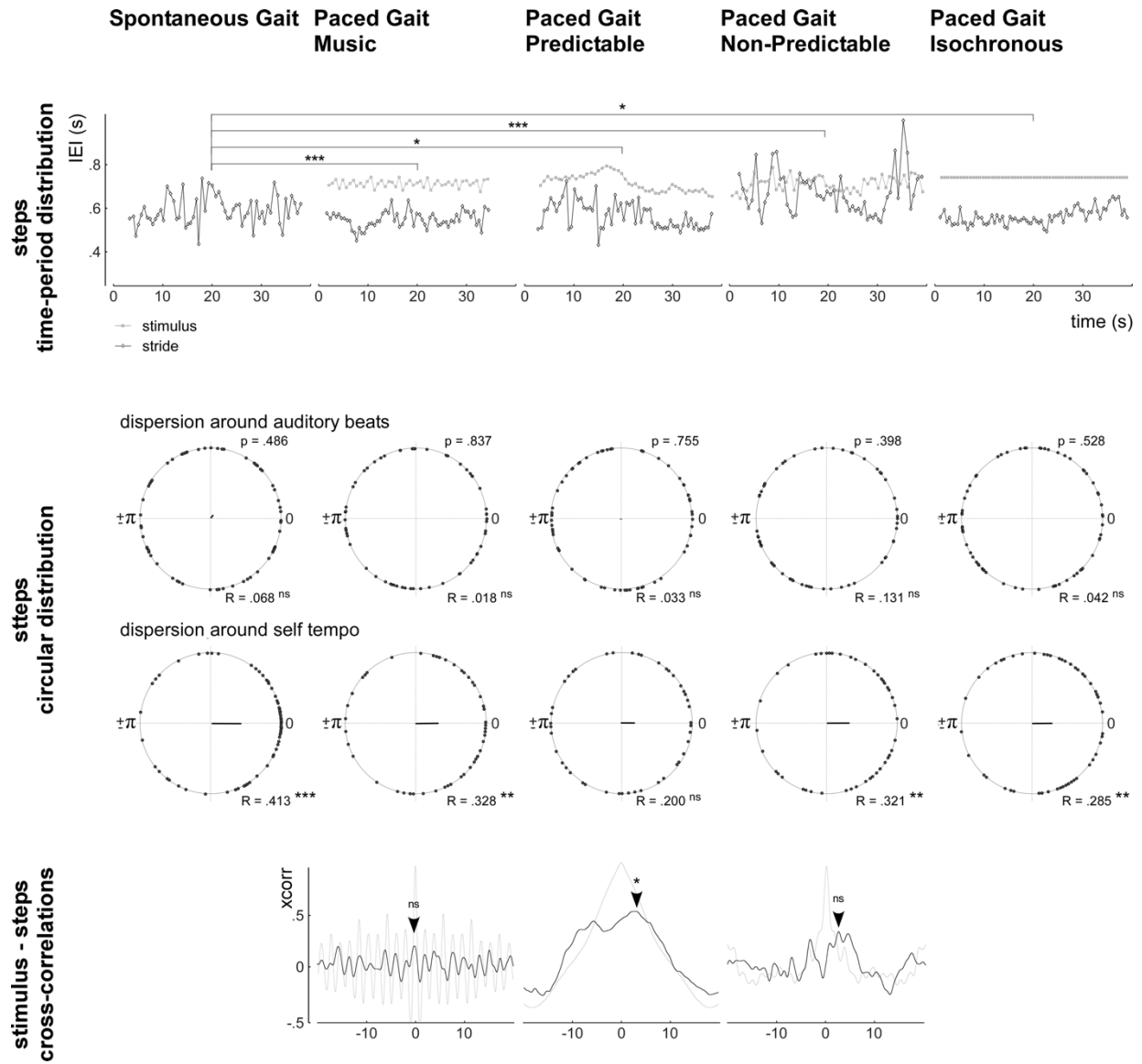
Figure 50. –   Results of the Gait Evaluation Performed in Patient 2 while she was in MCS.

The spontaneous gait of patient 2 showed a slightly unstable tempo, which was assessed by the relatively broad circular distribution of spontaneous steps around the median ISI ($R_{n_{spont}}^{step}$ = 0.413; p < 0.001).

When patient 2 walked with music, her gait tempo changed as compared to her spontaneous tempo. This was assessed by the Wilcoxon rank sum test, which revealed a significant shorter ISI for the paced gait, *Mdn* = 544 ms, as compared to the spontaneous gait, *Mdn* = 576 ms, *Z* = 4.239, *p* < 0.001; the median IEI of the acoustic rhythm being 714 ms. This tempo change was not going in the good direction to perform a correct frequency tuning, as the participant speeded up her gait instead of slowing it down. However, it appeared to be specifically driven by the presence of the acoustic rhythm, as the change abruptly occurred in a range of 3 s after the onset of the music. Furthermore, no significant gait tempo change could be observed between the first spontaneous trial *Mdn* = 576 ms, and a second spontaneous trial performed a few minutes after the test, *Mdn* = 576 ms, *Z* = -1.069, *p* = 0.285. The paced gait, despite not being synchronized and having a different cadence that the spontaneous gait, was relatively stable around its own cadence ($R_{n_{music}}^{step}$ = 0.328; *p* = 0.002). No significant synchronization of her gait to the musical rhythm was observed ($R_{n_{music}}^{beat}$ = 0.018; *p* = 0.837).

The gait observed when patient 2 walked with predictable fluctuating acoustic rhythm was markedly unstable ($R_{n_{predict}}^{step}$ = 0.200, *p* = 0.076), with a value considerably lower than the one of the gait observed when the patient walked spontaneously (*Δ* = -0.128). The paced gait ISI, *Mdn* = 552 ms, was significantly different from the spontaneous gait ISI, *Mdn* = 576 ms, *Z* = -2.093, *p* = 0.036, but this tempo change was not going in the good direction to perform a correct frequency tuning, as the participant speeded up her gait instead of slowing it down. The measure of synchronization consistency of the patient gait to the acoustic rhythm was low and non-significant ($R_{n_{predict}}^{beat}$ = 0.033; *p* = 0.755). However, the cross-correlation revealed a significant maximal cross-correlation between the fluctuations of the acoustic and the gait rhythms ($xcorr_{n_{predicrt}}$ = 0.521; *p* < 0.001), indicating that the patient tended to "track" the fluctuations of the stimulation, with a lag of 3.004 seconds.

When patient 2 walked with the non-predictable fluctuating acoustic rhythm, her gait remained slightly unstable ($R^{step}_{n_{unpred}}$ = 0.321; *p* = 0.002). The gait cadence was affected by the acoustic rhythm, with a ISI (*Mdn* = 648 ms) significantly longer than the spontaneous ISI (*Mdn* = 576 ms), *Z* = -4.565, *p* < 0.001. The measure of synchronization consistency of the patient gait to the acoustic rhythm was low and not significant ($R^{beat}_{n_{unpred}}$ = 0.131; *p* = 0.392). The cross-correlation revealed no significant cross-correlation between the fluctuations of the acoustic beat and of the gait tempo ($\text{xcorr}_{n_{unpred}}$ = 0.323; *p* = 0.194). Those results indicated that the patient was unable to synchronize her gait to the stimulation, was unable to "track" the fluctuations of tempo, but that her gait was not unaffected by the stimulation.

When patient 2 walked with isochronous periodic acoustic beat, her gait cadence remained was slightly unstable ($R^{step}_{n_{isoch}}$ = 0.285; *p* = 0.004) and differed significantly from the spontaneous tempo (*Mdn* paced = 568 ms, *Mdn* spontaneous = 576 ms, *Z* = 2.197, *p* = 0.028). However, no synchronization of her gait to the acoustic rhythm was observed ($R^{beat}_{n_{isoch}}$ = 0.042; *p* = 0.528).

Four sessions were initially planned during the first day of evaluation. During the second session, the patient had an epileptic seizure, most probably triggered by the acoustic stimulation. Therefore, only a second complete evaluation could be performed later on this day. Two other sessions were performed two days later. For concision, the results of those sessions are not reported here.

Discussion

The locomotor system largely relies on automatic processes, which are regulated by adaptive movement control. Elaborated movement control requires cerebral mechanisms that include movement initiation and inhibition, visuospatial integration of environmental information (Drew et al., 1996; Grillner et al., 1997; Milner & Goodale, 1995; Takakusaki, 2013), speed regulation and in certain cases adjustment of the time at which each step occur. The later ability allows humans and certain bird species (Patel, 2006; Patel & Iversen, 2014) to precisely synchronize their movement with rhythmic acoustic events from the environment. In contrast with other mammals, the locomotion in humans seems to *require* supra-mesencephalic neural processes:

hence, decorticated cats are still able to walk and perform goal-oriented rhythmic motor actions that include searching for food and feeding themselves (Bjursten et al., 1976), whereas patients with disorders of consciousness that are characterized by high disturbance in functional connectivity across brain regions (e.g., Laureys & Schiff, 2012) do not walk of feed themselves.

This observation was never unvalidated until recently. Here, we reported two cases of MCS patients that had the ability to walk. Importantly, we demonstrated that the first patient was able to robustly adjust the gait cadence and phase in order to synchronize the steps to the musical beat. This patient quickly evolved from MCS to a state of emergence. Furthermore, we observed a rare pattern of functional connectivity between temporal and motor areas, as assessed by the TMS-EEG evaluation (see supplementary material). We demonstrated that the second patient was able to robustly change the gait cadence when stimulated with music, but was unable to correctly tune the cadence and adjust the phase of the steps in order to properly synchronize the steps to the musical beat. This patient remained in a MCS for years, and suffers from reflex SMA epileptic seizures that are triggered by sharp sounds.

Interestingly, those two cases allowed to study a preserved functions of gait control in a system that is globally non-functional and therefore freed from many interferences. In the other hand, we observed slightly different levels of gait adaptation to the acoustic environment in patients with slightly different preservations of functional neural structures. Our results suggest that precise phase alignment and successful frequency tuning requires a higher level of functionality within supramesencephalic neural centers. In contrast, the second patient that showed less preserved supramesencephalic functionality, critically symptomatic with reflex SMA epilepsy triggered by sharp acoustic stimulations and whose clinical evolution was marked by permanent MCS, was only able to modulate the gait cadence in response to music, without any success in frequency and phase alignment.

The current model of cognitive gait control in humans defines two distinct locomotor pathway (Hamacher et al., 2015; la Fougère et al., 2010). The direct locomotor pathway is thought to be involved in continuous, steady-state locomotion (e.g. locomotion on a flat ground), whereas the indirect locomotor pathway would be responsible for modulation of locomotion and goal-

directed actions (e.g. visuomotor control). The presented results are coherent with this model of gait control, in which the gait cadence rely on the direct locomotor pathway and involves relatively simple mechanisms (e.g., modulation the tonus of mesencephalic nuclei by the cerebellar locomotor region). In contrast, fine synchronization of each step to periodic acoustic events requires another locomotor pathway able to coordinate the activity of different cortical regions of the brain (e.g., Kotz et al., 2013).

Therefore, we suggest that the ability of the first patient to temporally coordinate her gait to the beat of music is significative of a certain level of functional connectivity, which in turn is significant of a certain level of consciousness.

Supplementary material

Patient 1

Clinical evaluation

Behavioural Measurements (CRS-R)

The patient was evaluated by the Coma Science Group from the 03/01/2018 to the 10/01/2018, by mean of the Coma Recovery Scale-Revised – CRS-R (Giacino, Kalmar, & Whyte, 2004; Schnakers et al., 2008).

Spontaneous Behaviours :

The presence of upper limb movements, visual pursuit of people in the room, and contextual emotional behaviours (laugh in funny situations) are reported.

Awakening :

The patient opens the eyes spontaneously and durably in 6/6 evaluations.

Auditory Functions :

The patient can localize a sound in 3/6 evaluations, with a startle response in 2/6 evaluations.

Visual Functions :

The patient presents visual pursuit in 5/6 evaluations, visual fixation in 3/6 evaluations and blinking menace reflex in 3/6 evaluations.

Motor Functions :

An automatic motor response is observed in 5/6 evaluations, with retreat flexor response to pain in 4/6 evaluations.

Oromotor Functions :

Spontaneous vocalization and buccal movements are observed in 2/6 evaluations, and buccal reflexes are observed in 2/6 evaluations.

Communication :

No functional nor intentional communication could be established with the patient.

RMN

Structural RMN

No parenchymal lesion appears on T2 FLAIR sequence, nor on the SWI sequence. Normal aspect of the lateral ventricles and sub-arachnoïd spaces. The brainstem is without particularity. The encephalon is eutrophic.

Voxometry

Voxel based morphometry, compared to a healthy participant control group reveals cortical atrophy at the level of the mean occipital gyrus (red and yellow spots) (Guldenmund et al., 2016).
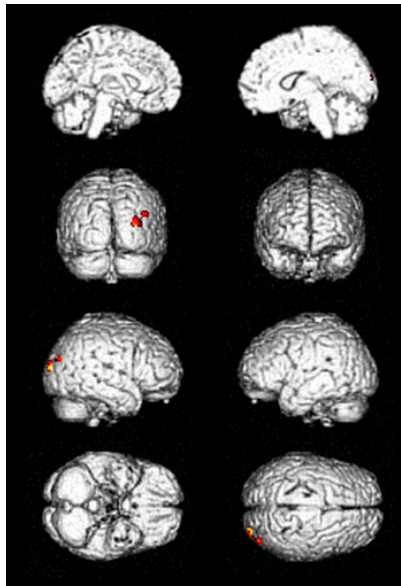
Diffusion Tension Imagery (DTI)

A diffuse loss of long distance neural fibers is observed, with particular focus on peripheral frontal and parietal fibers (Gómez, 2012)
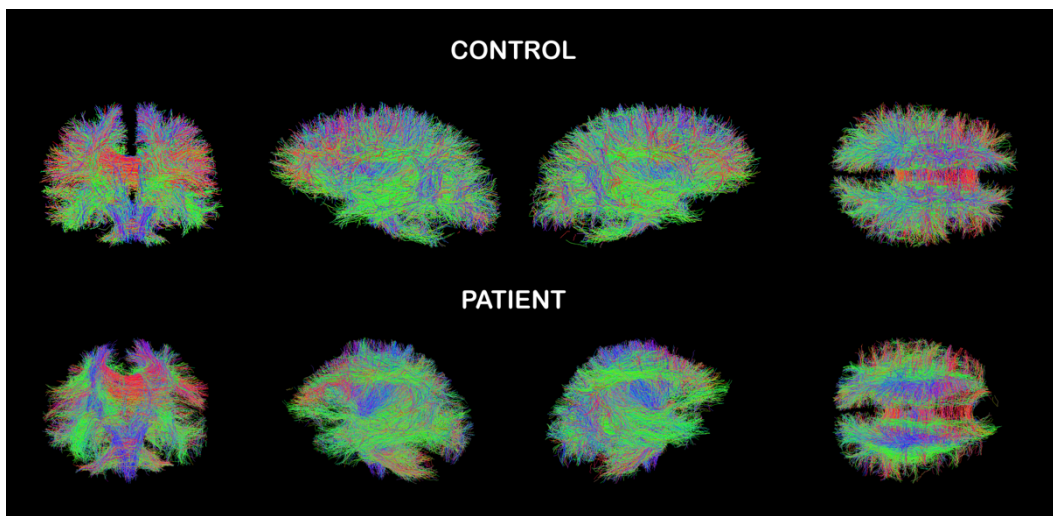
flurorodeoxyglucose Positron Emission Tomography: study of the energetic metabolism after injection of 18F-fluorodeoxyglucose (FDG), under 300 mg Propofol sedation

A global decrease of cortical metabolism of 38% as compared to 34 healthy controls is observed. This observation is made using Statistical Parametric Mapping, SPM12 (Bruno et al., 2012).

Healthy Controls   Patient
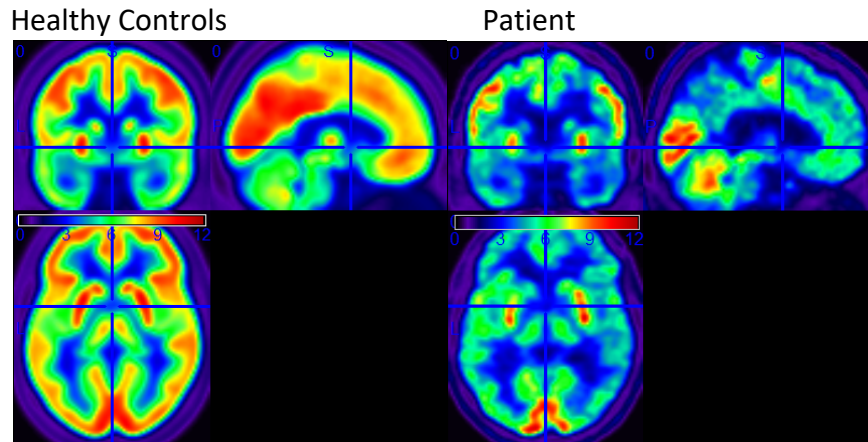
Hypometabolic regions (in blue) include parietal and frontal areas, bilaterally. Preserved regions (in red) include the cerebellum, the thalami, the occipital and primary motor areas, bilaterally.
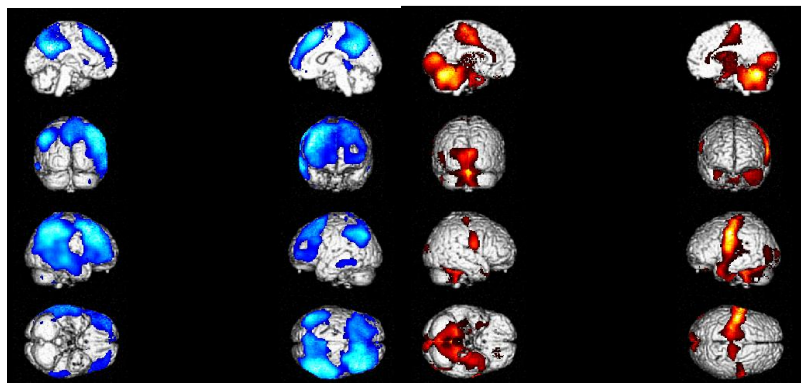
Analysis of energetic consumption of cerebral areas, using the *skin scaled* method shows a decrease of consumption of 62% (59% on the left, 64% on the right) (Thibaut et al., 2012).
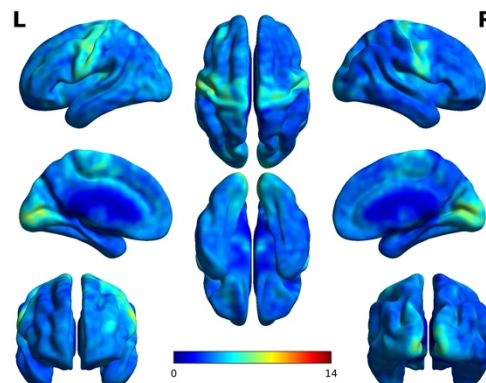
Electroencephalography (Dr E. Rikir)

The EEG signal is hypovolted, marked with numerous artefacts due to the absence of patient collaboration. No focalization, lateralization of paroxysmal activity is observed. The "local-global" auditory paradigm shows a non-significant local MMN effect at 120-140 ms, followed by a significant positivity around 260 ms. A possible global effect between 500 and 600 ms, lateralized to the right, is observed.
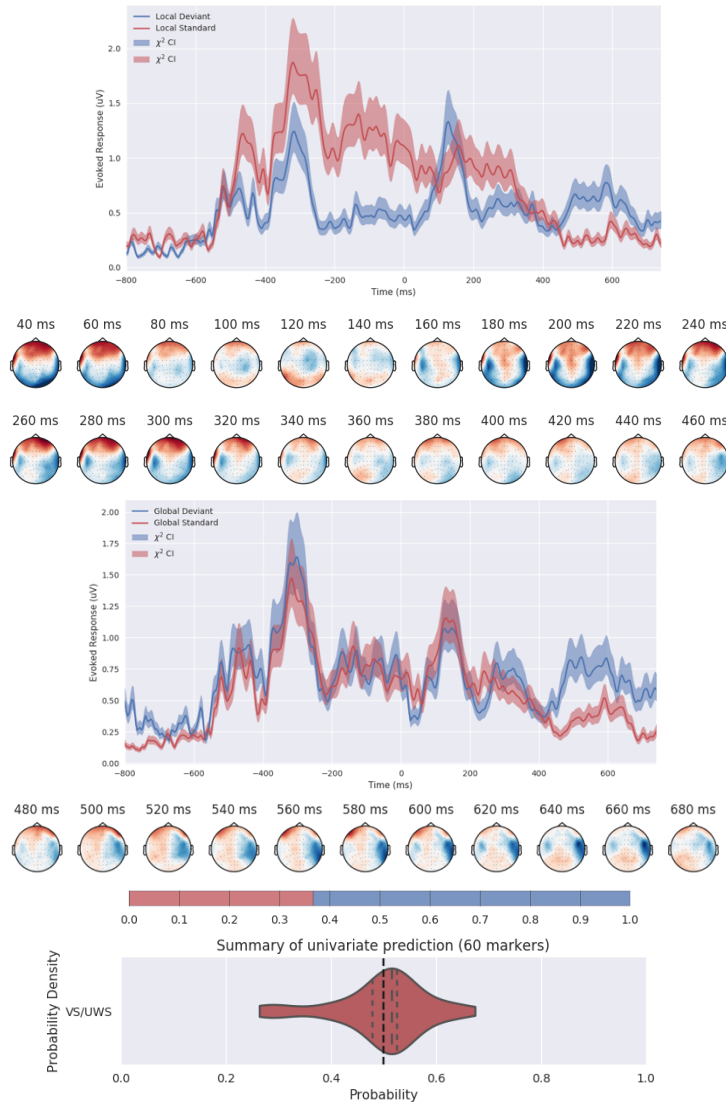
Transcranial magnetic stimulation (TMS) was applied over the motor (1 session), parietal (2 sessions) and pre-motor (1 session) cortices, while recording the electric activity of the brain using EEG.
During the stimulation of the motor cortex, a complex response with elevated PCI was observed (PCI = 0.522 ; H=0.634). No significant response was observed during the other stimulations.
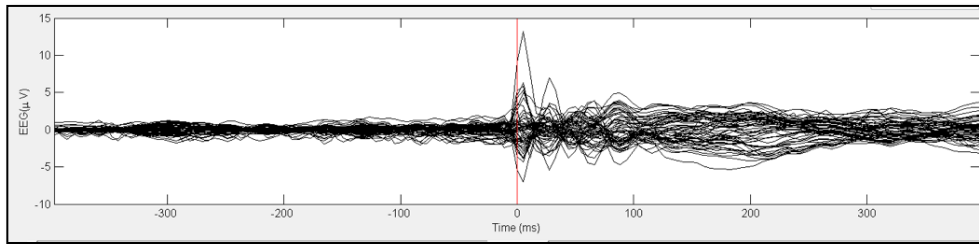
Conclusion
The behavioral evaluation is in favor of a MCS- state, characterized by visual pursuit, visual fixation and automatic motor responses. The neuroimaging results confirm the diagnosis.

Patient 2

Clinical evaluation

Behavioural Measurements (CRS-R)

The patient was evaluated by the Coma Science Group from the 06/06/2017 to the 14/06/107, by mean of the Coma Recovery Scale-Revised – CRS-R (Giacino et al., 2004; Schnakers et al., 2008).

Spontaneous Behaviours :

The presence of upper limb movements, visual pursuit of people in the room, and contextual emotional behaviours (expression of pleasure when listening to music) are reported.

Awakening :

The patient opens the eyes spontaneously and durably in 4/6 evaluations.

Auditory Functions :

The patient can localize a sound in 1/6 evaluations, with a startle response in 2/6 evaluations.

Visual Functions :

The patient presents visual pursuit in 5/6 evaluations, visual fixation in 2/6 evaluations and blinking menace reflex in 4/6 evaluations.

Motor Functions :

An automatic motor response is observed in /6 evaluations, with retreat flexor response to pain in 4/6 evaluations.
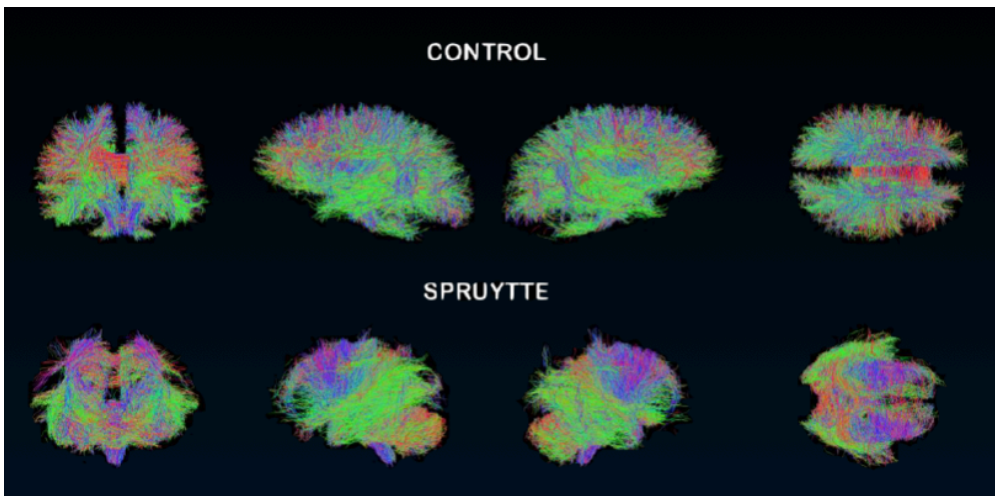
Oromotor Functions :

Spontaneous vocalization and buccal movements are observed in 1/6 evaluations, and buccal reflexes are observed in 6/6 evaluations.
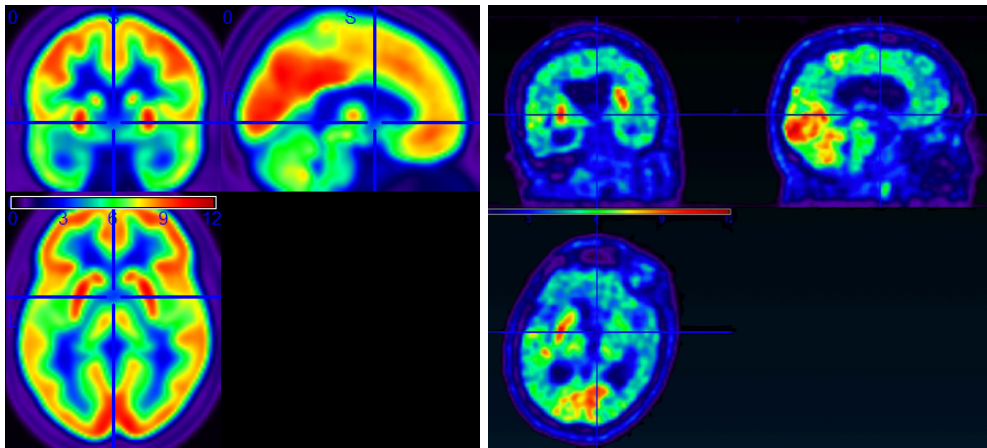
Communication :

No functional nor intentional communication could be established with the patient.

RMN

Diffusion Tension Imagery (DTI)

flurorodeoxyglucose Positron Emission Tomography

Chapter 6 – Discussion

Before finishing this passage in the science of movement, I would like to take the reader in a last journey. It happened a few tens million years ago. You were some sort of prehistoric animal, facing the ocean. You could hear the waves crushing on the shore and this slow, powerful sound was relaxing. You were also feeling the salty sea breeze, and could hear the quivering leaves in the trees behind you. Suddenly, a soft but distinct sound aroused your attention. Then a second, and a third. It was approaching. It got faster: it was coming to you. You started running, fast. If you could make it to the forest, you could probably climb into a tree and save your life…

With time, the locomotor system and its cognitive control have evolved. With arboreal locomotion it became important to precisely control the position and the timing of each grasp (Preuschoft, 2002). Then, the forelimb further evolved and fine object manipulation became possible with even more complex cognitive control (Grillner et al., 1997). In addition, the development of articulated language supported temporally precise communication between auditory regions and motor planning regions of the cortex (Patel & Iversen, 2014). Altogether, these processes of *rhythmic movement generation*, *rhythmic acoustic pattern decoding* and *rhythmic sensorimotor synchronization* form an intricate system of automatic and cognitive controls of movement. This system allows humans to produce extremely skilled movements in synchrony with each other and with the environment, as it is the case, for example, in dance and music playing.

The precise control of rhythmic movements in dance or music playing is enforced by multiple neurophysiological mechanisms which have been the focus of growing scientific interest in the last decades. Of these, the entrainment of neural oscillations to regular sensory inputs forms a core mechanism leading to the anticipation of forthcoming events. Neural oscillations are self-sustaining and dynamically adapting variations of neural ensembles excitability. When a neural oscillator is periodically stimulated by a sensory input, its oscillation can become synchronized to the periodic stimulation and the forthcoming high-excitability phase of the neural oscillation is likely to correspond to a forthcoming periodic external event, which is therefore *anticipated* (see,

e.g., Haegens & Zion Golumbic, 2017; Thut et al., 2011 for review). When the rhythmic pattern of the sensory input varies in a fashion that respects the anticipation, it is considered as *predictable*. Such rhythmic patterns are preferentially operated by the basal ganglia and this timing process is called *beat-based* timing (Teki, Grube, Kumar, et al., 2011). Importantly, the basal ganglia connect broadly distributed regions of the brain, including sensory- and motor- cortices (Chudler, Sugiyama, & Dong, 1995; Fujiyama, 2009; Gybels, Meulders, Callens, & Colle, 1967; Jarbo & Verstynen, 2015; Kotz et al., 2013; Nagy et al., 2006; Postuma & Dagher, 2006), and the entrainment of neural oscillations within this broad neural network allows to anticipatively adjust the timing of a motor action with the forthcoming sensory event (Fujioka et al., 2012).

A second mechanism is necessary to maintain an accurate synchronization of rhythmic movements to rhythmic sensory inputs, and consist in error detection and correction. The precise *absolute duration* timing system emerging from an olivocerebellar network (Hary & Moore, 1985; Llinás & Yarom, 1981; Teki, Grube, Kumar, et al., 2011; Wing, 2002) can compare the timing of an anticipated event with the timing of the actual forthcoming event (Teki, Grube, & Griffiths, 2011). If an error is detected, it is possible to adapt or ignore it (Merker et al., 2009). An event-by-event adaptation leads to *tracking* synchrony (i.e., reproduction of the variations of the rhythmic pattern of sensory inputs) and ignoring the perturbations leads to *central tendency* synchrony (i.e., production of a rhythmic movement at the estimated average tempo of the rhythmic sensory input).

In order to better understand the different mechanisms of precise rhythmic motor control, I first had to grasp some key phenomena of natural rhythms. Undeniably, natural rhythms are not "simple" mechanistic oscillatory system, with constant parameters such as frequency, phase and amplitude. Actually, all natural rhythms tend to follow a 1/f spectral distribution (Arendt, 1998; Goodwin, 1997; Lloyd & Rossi, 1993; Rankin et al., 2009; Rietveld, 1993; Torre, Varlet, & Marmelat, 2013). Hence, low-frequency oscillations have stronger magnitudes than high-frequency oscillations. This could be illustrated by the power of the waves crushing on the sea shore compared with the light quivering leaves of the scene described in the introduction of this conclusion. Together with this spectral distribution comes sequential dependencies and auto-correlations: the large fluctuations of tempo are slow and progressive (and convey information

about forthcoming events) while the fast and ever-changing fluctuations of tempo are small in magnitude (and do not convey the relevant information about forthcoming events). Spontaneous rhythmic movements follow the same patterns of tempo fluctuations (Torre & Delignières, 2008), and acoustic rhythms fluctuating according to this pattern are easily anticipated and therefore predictable (Rankin et al., 2014). In contrast, when the structure of a rhythm is perturbed, the spectral distribution changes: the low-frequency fluctuations (i.e., information) decrease in magnitude and the high-frequency fluctuations (i.e., noise) gain in magnitude. Anticipation becomes more difficult and such a rhythm is therefore unpredictable (Rankin et al., 2014).

Considering this, I developed novel tools to directly compare, in behavioral and in electroencephalographic patient studies, the entrainment to acoustic rhythms with predictable vs. unpredictable fluctuations of tempo. To my knowledge, few studies (and virtually no neurophysiological study) directly compared those two conditions. A widespread paradigm consisted in comparing the neural processing of acoustic rhythms with no tempo fluctuations to the neural processing of acoustic rhythms with random tempo fluctuations (e.g., Fujioka et al., 2012; Lehmann, Jimena Arias, Schönwiesner, Arias, & Schönwiesner, 2016; Schwartze, Stockert, & Kotz, 2015; Teki, Grube, Kumar, et al., 2011). I suggest that this approach could unintentionally underestimate error correction mechanisms in beat-based timing processes (see Teki, Grube, & Griffiths, 2011 for informative discussions; see section 3.3.3.3.3. for illustration on Fujioka et al., 2012). The research techniques that I developed were introduced in Chapter 3.

First, I developed an experimental paradigm, an experimental set-up and a matlab toolbox that allows exploring the rhythmic synchronization of the gait to various acoustic rhythms. These tools evaluate the ability of patients to adapt their gait cadence to the tempo of the acoustic rhythm. Importantly, they evaluate the probability of each measure *at the individual level*, which means that it is possible to state with confidence whether an individual adapted its gait cadence to the acoustic rhythm without the need of a control group or repeated measures. Furthermore, the analyses of sensorimotor synchronization that I developed in the matlab toolbox do not require that participants produce one motor event (e.g., a tap or a step) for each acoustic event. Therefore, it is for example possible to evaluate whether a participant follows the fluctuations of

tempo (e.g., if he speeds up when the tempo is faster, and slows down when the tempo is slower) even though his steps are not aligned to the acoustic events at all.

Second, I developed an EEG time-warping approach to study non-strictly periodic EEG signals. I demonstrated how this method could be used to "tag" the neural activity related to the production of natural rhythmic movements. Importantly, this method concentrates, in the EEG spectrum, the neural activity that is phase-locked to the non-strictly periodic events of interest (e.g., a rhythmic movement, or an acoustic rhythm with fluctuations of tempo) independently of the actual period. In contrast, another method called "EEG false-sequencing" concentrates, in the EEG spectrum, the neural activity that is time-locked to each non-strictly periodic event of interest. Therefore, it is possible to get a direct insight on the dynamics of the non-strictly periodic neural process by comparing its magnitude, in the EEG spectrum, after concentration using both the EEG time-warping and false sequencing methods. If the neural activity adapts to each period of the non-strictly periodic rhythm—a dynamic that is expected to occur in neural oscillations, the EEG time-warping yields a measure of greater magnitude. In contrast, if the neural activity is independent of the duration between the consecutive events of the non-strictly periodic rhythm—a dynamic that is expected to occur in transient process of repeated events, the EEG false-sequencing yields a measure of greater magnitude.

Once I had adequate tools to quantitively measure the behavioral and the electrophysiological processes of rhythmic sensorimotor synchronization, I investigated the neural entrainment in healthy participants, and gathered these experimental findings in Chapter 4.

First, I measured the EEG responses elicited by acoustic rhythms with predictable and unpredictable fluctuations of tempo. Both predictable and unpredictable acoustic rhythms can yield expectations regarding the forthcoming acoustic events. For the predictable rhythms, the expectations are locally adapted regarding the local tempo tendency. For the unpredictable rhythms, the expectations tend to correspond to a central tendency. In both predictable and unpredictable tempo, the expectations can be respected or violated by the forthcoming acoustic events. The transient responses evoked by the acoustic events that violate the expectations show a component which maximal amplitude occurs approximately 145 ms after the event onset. This

component is a negative or a positive deflection in the EEG signal, regarding whether the acoustic event occurs before or after the expectation, respectively. Importantly, when participants passively listened to the acoustic beat, the amplitude of this component varied linearly with the discordance between the expectation (as modeled by a phase-shifted Butterworth low-pass filter) and the actual event timing, and no difference could be observed between the predictable and the unpredictable condition. In contrast, when participants tapped to the acoustic rhythm and therefore received real-time feedback about their tapping accuracy, the amplitude of the response component varied linearly with the discordance between the expectation (as modeled by a phase-shifter Butterworth low-pass filter) and the actual event timing but its amplitude was more negative for the predictable condition, as compared to the unpredictable condition. This difference could be attributed to the fact that participant could use the information of their tapping accuracy to *adjust* their tapping in the predictable condition (e.g., stop decelerating the tapping tempo as soon as the acoustic rhythm starts to accelerate), whereas they should rather ignore the information of their tapping accuracy in the unpredictable condition. In addition, I showed that the dynamics of the neural oscillations entrained to the non-strictly periodic acoustic rhythms were better adapting to the fluctuations of tempo when participants tapped in synchrony to the acoustic rhythm, as compared to when they passively listened to it.

Second, I investigated how body movements shape the neural representation of a complex acoustic rhythm. The complex acoustic rhythm consisted in the superimposition of three isochronous beats: a first one with a 1.2 s interbeat interval, a second with a 0.6 s interbeat interval, and a third with a 0.4 s interbeat interval. The resulting pattern can give rise to a pulse at any of the three frequencies, but for psychophysical reasons (e.g., an acoustic event that is preceded and followed by similar acoustic events is less salient than a sound that is preceded or followed by a silence), the pulse corresponding to the 0.4 s interbeat interval is easier to feel. After moving to the 0.4 s interbeat interval beat, the neural representation of this complex acoustic rhythm showed a selective entrainment to the frequencies related to the movements that had been performed, as compared to when participants listened to the acoustic rhythm before having performed the movements. In contrast, after moving to the 0.6 s interbeat interval

beat, the neural representation of the complex acoustic rhythm remained similar to before having moved to it.

Finally, I could conduct two studies in which I explored the cognitive control of gait in patients, using the research techniques that I previously developed and tested in healthy participants. With these studies, I aspired to contribute in building an accurate knowledge of the automatic and the cognitive control of locomotion, and to improve the possibilities of proposing a precise medicine that take into account the complex and intricated physiopathology of gait disorder at the individual level.

In a first study, I showed that patients who had a better shaping of their neural representation of a complex acoustic rhythm after performing bodily movement aiming at disambiguation the acoustic rhythm were also the patient that would show an improvement in their synchronization of gait to a musical beat. Importantly, these results suggest that the patients that would most benefit from a training program consisting of walking with music are the patient with present but under exploited cognitive, beat-based timing resources. In contrast, the cognitive burden of music rhythm processing could rather hinder patients with lower beat-based timing abilities.

In a second study, I reported the cases of two young women who evolved from a hypoglycemic coma to a minimally conscious state. Curiously, they were able to walk, which is a unique observation. One patient who showed relatively little structural brain alteration was able to synchronize her gait to various acoustic rhythms. Importantly, she could not only adapt the cadence of her gait to match the tempo of the acoustic rhythms: she could also walk in phase with the beat of the music and she could follow the fluctuations of tempo when they were predictable. In contrast, the other patient who had a partial epilepsy located in the supplementary motor area could only change the cadence of her gait and eventually follow the fluctuations of tempo when they were predictable, without successfully match the tempo of the acoustic rhythms. Importantly, the first patient quickly emerged from minimally conscious state, while the second patient remained in minimally conscious state for several years. Importantly, these results suggest that both patients were able to integrate information from their environment, despite the profound disorder of consciousness. Furthermore, these results suggest that the control of

gait that allows an individual to precisely synchronize each step to the beat of music differ from the control of gait that allows an individual to regulate gait cadence.

To finish this journey in the science of movement, I would like to suggest a last hypothesis. Even though I couldn't test it specifically, I have often observed that participants that did not synchronize properly their steps to the music tended to speed up their gait rather than slowing it down or keeping it unchanged. Interestingly, the manifest pleasure that participants had in walking with music was not dependent on the success of their synchronization. I suggest that the primitive system that underlie the ability to adapt body movements to music is anchored in a survival mechanism aiming at detecting specific acoustic patterns suggestive of the danger of an approaching predator and triggering a "fight of fly" response. This response is intrinsically emotional and is systematically biased towards an increase in gait cadence. In contrast, the system that allows precise synchronization of movements to acoustic rhythms is dependent on a developed system requiring complex cognitive control, is critically influenced by training, and varies considerably across individuals.

Références bibliographiques

Adrian, E., & Matthews, B. (1934). The Berger rhythm: potential changes from the occipital lobes in man. *Brain*, *57*(4), 355–385. https://doi.org/10.1093/brain/awp324

Alexander, G. E., & Crutcher, M. D. (1990). Functional architecture of basal ganglia circuits: neural substrates of parallel processing. *Trends in Neurosciences*, *13*(7), 266–271. Retrieved from http://www.ncbi.nlm.nih.gov/pubmed/1695401

Allman, M. J., & Meck, W. H. (2012). Pathophysiological distortions in time perception and timed performance. *Brain*, *135*(Pt 3), 656–677. https://doi.org/10.1093/brain/awr210

Aravamuthan, B. R., Muthusamy, K. A., Stein, J. F., Aziz, T. Z., & Johansen-Berg, H. (2007). Topography of cortical and subcortical connections of the human pedunculopontine and subthalamic nuclei. *NeuroImage*, *37*(3), 694–705. https://doi.org/10.1016/j.neuroimage.2007.05.050

Arendt, J. (1998). Biological rhythms: the science of chronobiology. *Journal of the Royal College of Physicians of London*, *32*(1), 27–35. Retrieved from http://www.ncbi.nlm.nih.gov/pubmed/9507438

Armstrong, D. (1988). The supraspinal control of mammalian locomotion. *The Journal of Physiology*, *405*, 1–37. Retrieved from http://www.ncbi.nlm.nih.gov/pubmed/3076600

Armstrong, D., & Drew, T. (1984). Locomotor-related neuronal discharges in cat motor cortex compared with peripheral receptive fields and evoked movements. *The Journal of Physiology*, *346*, 497–517. https://doi.org/10.1113/jphysiol.1984.sp015037

Arnal, L. H., Doelling, K. B., & Poeppel, D. (2015). Delta–Beta Coupled Oscillations Underlie Temporal Prediction Accuracy. *Cerebral Cortex*, *25*(9), 3077–3085. https://doi.org/10.1093/cercor/bhu103

Arnal, L. H., & Giraud, A.-L. (2012). Cortical oscillations and sensory predictions. *Trends in Cognitive Sciences*, *16*, 390–398. https://doi.org/10.1016/j.tics.2012.05.003

Aschersleben, G. (2002). Temporal Control of Movements in Sensorimotor Synchronization. *Brain and Cognition*, *48*(1), 66–79. https://doi.org/10.1006/brcg.2001.1304

Aschersleben, G., & Prinz, W. (1995). Synchronizing actions with events- the role of sensory information. *Perception & Psychophysics*, *57*(3), 305–317.

Bach, M., & Meigen, T. (1999). Do's and don'ts in Fourier analysis of steady-state potentials. *Documenta Ophthalmologica*, *99*(1), 69–82. https://doi.org/10.1023/A:1002648202420

Bell, A. J., & Sejnowski, T. J. (1995). An information-maximization approach to blind separation and blind deconvolution. *Neural Computation*, *7*(6), 1129–1159. Retrieved from http://www.ncbi.nlm.nih.gov/pubmed/7584893

Benoit, C.-E., Dalla Bella, S., Farrugia, N., Obrig, H., Mainka, S., & Kotz, S. A. (2014). Musically Cued Gait-Training Improves Both Perceptual and Motor Timing in Parkinson's Disease. *Frontiers in Human Neuroscience*, *8*(July), 494. https://doi.org/10.3389/fnhum.2014.00494

Berens, P. (2009). **CircStat** : A *MATLAB* Toolbox for Circular Statistics. *Journal of Statistical Software*. https://doi.org/10.18637/jss.v031.i10

Berger, H. (1929). Über das elektrenkephalogramm des menschen (On the human electroencephalogram). *Archiv f. Psychiatrie u. Nervenkrankheiten.*, *87*, 527–570.

Besle, J., Bertrand, O., & Giard, M. H. (2009). Electrophysiological (EEG, sEEG, MEG) evidence for multiple audiovisual interactions in the human auditory cortex. *Hearing Research*, *258*(1–2), 143–151. https://doi.org/10.1016/j.heares.2009.06.016

Bishop, G. H. (1932). Cyclic changes in excitability of the optic pathway of the rabbit. *American Journal of Physiology--Legacy Content*, *103*(1), 213–224.

Bjursten, L. M., Norrsell, K., & Norrsell, U. (1976). Behavioural repertory of cats without cerebral cortex from infancy. *Experimental Brain Research*, *25*(2), 115–130. https://doi.org/10.1007/BF00234897

Bogner, J. A., Corrigan, J. D., Stange, M., & Rabold, D. (1999). Reliability of the Agitated Behavior Scale. *The Journal of Head Trauma Rehabilitation*, *14*(1), 91–96. Retrieved from http://www.ncbi.nlm.nih.gov/pubmed/9949251

Brochard, R., Abecasis, D., Potter, D., Ragot, R., & Drake, C. (2003). The "ticktock" of our internal clock: direct brain evidence of subjective accents in isochronous sequences. *Psychol Sci*, *14*(4), 362–366. Retrieved from http://pss.sagepub.com/content/14/4/362.full.pdf

Bruno, M.-A., Majerus, S., Boly, M., Vanhaudenhuyse, A., Schnakers, C., Gosseries, O., … Laureys, S. (2012). Functional neuroanatomy underlying the clinical subcategorization of minimally conscious state patients. *Journal of Neurology*, *259*(6), 1087–1098. https://doi.org/10.1007/s00415-011-6303-7

Buiatti, M., Peña, M., & Dehaene-Lambertz, G. (2009). Investigating the neural correlates of continuous speech computation with frequency-tagged neuroelectric responses. *NeuroImage*, *44*(2), 509–519. https://doi.org/10.1016/j.neuroimage.2008.09.015

Buzsáki, G., Anastassiou, C. A., & Koch, C. (2012). The origin of extracellular fields and currents--EEG, ECoG, LFP and spikes. *Nature Reviews. Neuroscience*, *13*(6), 407–420. https://doi.org/10.1038/nrn3241

Buzsáki, G., & Draguhn, A. (2004). Neuronal oscillations in cortical networks. *Science (New York, N.Y.)*, *304*(5679), 1926–1929. https://doi.org/10.1126/science.1099745

Buzsáki, G., & Llinás, R. R. (2017). Space and time in the brain. *Science*, *358*(6362), 482–485. https://doi.org/10.1126/science.aan8869

Capilla, A., Pazo-Alvarez, P., Darriba, A., Campo, P., & Gross, J. (2011). Steady-State Visual Evoked Potentials Can Be Explained by Temporal Superposition of Transient Event-Related Responses. *PLoS ONE*, *6*(1), e14543. https://doi.org/10.1371/journal.pone.0014543

Casarotto, S., Bianchi, A. M., Cerutti, S., & Chiarenza, G. A. (2005). Dynamic time warping in the analysis of event-related potentials. *IEEE Engineering in Medicine and Biology Magazine : The Quarterly Magazine of the Engineering in Medicine & Biology Society*, *24*(1), 68–77. Retrieved from http://www.ncbi.nlm.nih.gov/pubmed/15709539

Chapin, H., Jantzen, K., Scott Kelso, J. A., Steinberg, F., & Large, E. W. (2010). Dynamic Emotional and Neural Responses to Music Depend on Performance Expression and Listener Experience. *PLoS ONE*, *5*(12), e13812. https://doi.org/10.1371/journal.pone.0013812

Chatfield, C. (1989). Non-linear and non-stationary time series analysis: M.B. Priestley, (Academic Press, London, 1988), £25.00, pp. 237. *International Journal of Forecasting*, *5*(3), 428–429. https://doi.org/https://doi.org/10.1016/0169-2070(89)90048-4

Chatfield, C. (2003). *The analysis of time series: an introduction* (6th ed.). Chapman & Hall/CRC. Retrieved from https://books.google.be/books?hl=fr&lr=&id=qKzyAbdaDFAC&oi=fnd&pg=PP1&dq=time+series+analysis+correlations&ots=syx06aYDMj&sig=sjO1PxMWtpcQUOlSW97PCADDEbs#v=onepage&q=time series analysis correlations&f=false

Chemin, B., Huang, G., Mulders, D., & Mouraux, A. (2018). EEG time-warping to study non-strictly-periodic EEG signals related to the production of rhythmic movements. *Journal of Neuroscience Methods*, *308*, 106–115. https://doi.org/10.1016/j.jneumeth.2018.07.016

Chemin, B., Mouraux, A., & Nozaradan, S. (2014). Body Movement Selectively Shapes the Neural Representation of Musical Rhythms. *Psychological Science*, (October). https://doi.org/10.1177/0956797614551161

Chen, Y., Ding, M., & Kelso, J. A. S. (1997). Long Memory Processes ($1 / f \alpha$ Type) in Human Coordination. *Physical Review Letters*, *79*(22), 4501–4504. https://doi.org/10.1103/PhysRevLett.79.4501

Chudler, E. H., Sugiyama, K., & Dong, W. K. (1995). Multisensory convergence and integration in the neostriatum and globus pallidus of the rat. *Brain Research*, *674*(1), 33–45. https://doi.org/10.1016/0006-8993(94)01427-J

Cohen, M. X., & Gulbinaite, R. (2017). Rhythmic entrainment source separation: Optimizing analyses of neural responses to rhythmic sensory stimulation. *NeuroImage*, *147*, 43–56. https://doi.org/10.1016/j.neuroimage.2016.11.036

Collura, T. (1996). Human steady-state visual and auditory evoked potential components during a selective discrimination task. *Journal of Neurotherapy*, *1*(3), 1–9. https://doi.org/10.1300/J184v01n03_01

Costa-Faidella, J., Baldeweg, T., Grimm, S., & Escera, C. (2011). Interactions between "what" and "when" in the auditory system: temporal predictability enhances repetition suppression. *The Journal of Neuroscience*, *31*(50), 18590–18597. https://doi.org/10.1523/JNEUROSCI.2599-11.2011

Coull, J. T. (2009). Neural substrates of mounting temporal expectation. *PLoS Biology*, *7*(8). https://doi.org/10.1371/journal.pbio.1000166

Craig, J. C. (1973). A constant error in the perception of brief temporal intervals. *Perception & Psychophysics*, *13*(1), 99–104. https://doi.org/10.3758/BF03207241

Cravo, A. M., Rohenkohl, G., Wyart, V., & Nobre, A. (2013). Temporal expectation enhances contrast sensitivity by phase entrainment of low-frequency oscillations in visual cortex. *The Journal of Neuroscience*, *33*(9), 4002–4010. https://doi.org/10.1523/JNEUROSCI.4675-12.2013

Dalla Bella, S., Benoit, C.-E., Farrugia, N., Schwartze, M., & Kotz, S. A. (2015). Effects of musically cued gait training in Parkinson's disease: Beyond a motor benefit. *Annals of the New York Academy of Sciences*. https://doi.org/10.1111/nyas.12651

Dalla Bella, S., & Sowiński, J. (2015). Uncovering Beat Deafness: Detecting Rhythm Disorders with Synchronized Finger Tapping and Perceptual Timing Tasks. *Journal of Visualized Experiments*, (March), 1–11. https://doi.org/10.3791/51761

de Lange, F. P., Rahnev, D. A., Donner, T. H., & Lau, H. (2013). Prestimulus Oscillatory Activity over Motor Cortex Reflects Perceptual Expectations. *Journal of Neuroscience*, *33*(4), 1400–1410. https://doi.org/10.1523/JNEUROSCI.1094-12.2013

del Olmo, M., Arias, P., Furio, M., Pozo, M., & Cudeiro, J. (2006). Evaluation of the effect of training using auditory stimulation on rhythmic movement in Parkinsonian patients - a combine motor and [18F]-FDG PET study. *Parkinsonism Related Disorders*, *12*, 155–164.

Delorme, A., & Makeig, S. (2004). EEGLAB: an open source toolbox for analysis of single-trial EEG dynamics including independent component analysis. *Journal of Neuroscience Methods*, *134*(1), 9–21. https://doi.org/10.1016/J.JNEUMETH.2003.10.009

Ding, L., Ni, Y., Sweeney, J., & He, B. (2011). Sparse Cortical Current Density Imaging in Motor Potentials Induced by Finger Movement. *Journal of Neural Engeneering*, *8*(3). https://doi.org/10.1007/s10439-011-0452-9.Engineering

Dinov, M., Lorenz, R., Scott, G., Sharp, D. J., Fagerholm, E. D., & Leech, R. (2016). Novel Modeling of Task vs. Rest Brain State Predictability Using a Dynamic Time Warping Spectrum: Comparisons and Contrasts with Other Standard Measures of Brain Dynamics. *Frontiers in Computational Neuroscience*, *10*, 46. https://doi.org/10.3389/fncom.2016.00046

Dominici, N., Ivanenko, Y. P., Cappellini, G., D'Avella, A., Mond??, V., Cicchese, M., … Lacquaniti, F. (2011). Locomotor primitives in newborn babies and their development. *Science*, *334*(6058), 997–999. https://doi.org/10.1126/science.1210617

Drake, C., Jones, M., & Baruch, C. (2000). The development of rhythmic attending in auditory sequences: attunement, referent period, focal attending. *Cognition*, *77*(3), 251–288. Retrieved from www.elsevier.com/locate/cognit

Drew, T., Jiang, W., Kably, B., & Lavoie, S. (1996). Role of the motor cortex in the control of visually triggered gait modifications. *Canadian Journal of Physiology and Pharmacology*, *74*(4), 426–442. Retrieved from http://www.ncbi.nlm.nih.gov/pubmed/8828889

Ellis, T., de Goede, C. J., Feldman, R. G., Wolters, E. C., Kwakkel, G., & Wagenaar, R. C. (2005). Efficacy of a physical therapy program in patients with Parkinson's disease: A randomized controlled trial. *Archives of Physical Medicine and Rehabilitation*, *86*(4), 626–632. https://doi.org/10.1016/j.apmr.2004.08.008

Field, A. (2013). *Discovering Statistics with IBM SPSS*. (Sage, Ed.). Newbury Park, CA.

Fisher, N. I. (1993). *Statistical Analysis of Circular Data*. Cambridge: Cambridge University Press. https://doi.org/10.1017/CBO9780511564345

Fortune, E., Morrow, M. M. B., & Kaufman, K. R. (2014). Assessment of gait kinetics using triaxial accelerometers. *Journal of Applied Biomechanics*, *30*(5), 668–674. https://doi.org/10.1123/JAB.2014-0037

Fraisse, P. (1984). Perception and estimation of time. *Annual Review of Psychology*, *35*, 1–36. https://doi.org/10.1146/annurev.ps.35.020184.000245

Freeman, W. J., Holmes, M., & Bruke, B. (2003). Spatial spectra of scalp EEG and EMG from awake humans. *Clinical Neurophysiology*, *114*(6). https://doi.org/10.1111/ina.12046

Fries, P., Reynolds, J. H., Rorie, A. E., & Desimone, R. (2001). Modulation of oscillatory neuronal synchronization by selective visual attention. *Science (New York, N.Y.)*, *291*(5508), 1560–1563. https://doi.org/10.1126/science.291.5508.1560

Frigo, M., & Johnson, S. (1998). FFTW: an adaptive software architecture for the FFT. In *Proceedings of the 1998 IEEE International Conference on Acoustics, Speech and Signal Processing.* (Vol. 3, pp. 1381–1384).

Fujii, S., Hirashima, M., Kudo, K., Ohtsuki, T., Nakamura, Y., & Oda, S. (2011). Synchronization Error of Drum Kit Playing with a Metronome at Different Tempi by Professional Drummers. *Music Perception: An Interdisciplinary Journal*, *28*(5), 491–503. https://doi.org/10.1525/mp.2011.28.5.491

Fujii, S., Watanabe, H., Oohashi, H., Hirashima, M., Nozaki, D., & Taga, G. (2014a). Precursors of dancing and singing to music in three- To four-months-old infants. *PLoS ONE*, *9*(5), 97680. https://doi.org/10.1371/journal.pone.0097680

Fujii, S., Watanabe, H., Oohashi, H., Hirashima, M., Nozaki, D., & Taga, G. (2014b). Precursors of dancing and singing to music in three- To four-months-old infants. *PLoS ONE*, *9*(5), 1–12. https://doi.org/10.1371/journal.pone.0097680

Fujioka, T., Trainor, L. J., Large, E. W., & Ross, B. (2012). Internalized timing of isochronous sounds is represented in neuromagnetic β oscillations. *The Journal of Neuroscience*, *32*(5), 1791–1802. https://doi.org/10.1523/JNEUROSCI.4107-11.2012

Fujiyama, F. (2009). [Anatomical connections of the basal ganglia]. *Brain and Nerve = Shinkei Kenkyū No Shinpo*, *61*(4), 341–349. Retrieved from http://www.ncbi.nlm.nih.gov/pubmed/19378803

Galambos, R., Makeig, S., & Talmachoff, P. J. (1981). A 40-Hz auditory potential recorded from the human scalp. *Proceedings of the National Academy of Sciences of the United States of America*, *78*(4), 2643–2647. https://doi.org/10.1073/pnas.78.4.2643

Garcia-Rill, E., Hyde, J., Kezunivic, N., Urbano, F. J., & Petersen, E. (2015). The physiology of the pedunculopontine nucleus-Implications for deep brain stimulation. *Journal of Neural Transmission*, *112*(2), 225–235. https://doi.org/10.1007/s00702-014-1243-x.

Georgopoulos, A. P. (1995). Current issues in directional motor control. *Trends in Neurosciences*, *18*(11), 506–510. https://doi.org/10.1016/0166-2236(95)92775-L

Georgopoulos, A. P., & Grillner, S. (1989). Visuomotor Coordination in Reaching and Locomotion. *Science*, *245*(4923), 1209–1210. https://doi.org/10.1177/0022146510383838

Gerloff, C., Toro, C., Uenishi, N., Cohen, L., Leocani, L., & Hallett, M. (1997). Steady-state movement-related cortical potentials: a new approach to assessing cortical activity associated with fast repetitive finger movements. *Electroencephalogr Clin Neurophysiol*, *102*(2), 106–113. Retrieved from http://www.ncbi.nlm.nih.gov/pubmed/9060861

Gerloff, C., Uenishi, N., Nagamine, T., Kunieda, T., Hallett, M., & Shibasaki, H. (1998). Cortical activation during fast repetitive finger movements in humans: steady-state movement-related magnetic fields and their cortical generators. *Electroencephalogr Clin Neurophysiol*, *109*, 444–453.

Getting, P. (1989). Emerging Principles Governing the Operation of Neural Networks. *Annual Review of Neuroscience*, *12*, 185–204.

Giacino, J. T., Kalmar, K., & Whyte, J. (2004). The JFK Coma Recovery Scale-Revised: Measurement characteristics and diagnostic utility. *Archives of Physical Medicine and Rehabilitation*, *85*(December), 2020–2029. https://doi.org/10.1016/j.apmr.2004.02.033

Glass, L. (2001). Synchronization and rhythmic processes in physiology. *Nature*, *410*(6825), 277–284. https://doi.org/10.1038/35065745

Goetz, C. G., Tilley, B. C., Shaftman, S. R., Stebbins, G. T., Fahn, S., Martinez-Martin, P., … Zweig, R. M. (2008). Movement Disorder Society-Sponsored Revision of the Unified Parkinson's Disease Rating Scale (MDS-UPDRS): Scale presentation and clinimetric testing results. *Movement Disorders*, *23*(15), 2129–2170. https://doi.org/10.1002/mds.22340

Gómez. (2012). DTI based structural damage characterization for disorders of consciousness. In *19e International Conference on Image Processing*.

Goodwin, B. C. (1997). Temporal organization and disorganization in organisms. *Chronobiology International*, *14*(5), 531–536. Retrieved from http://www.ncbi.nlm.nih.gov/pubmed/9298288

Graham Brown, T. (1911). The Intrinsic Factors in the Act of Progression in the Mammal. *Proceedings of the Royal Society of London.*, *84*(572), 308–319. https://doi.org/10.1098/rspb.1911.0077

Grahn, J. A. (2012). Neural mechanisms of rhythm perception: current findings and future perspectives. *Top Cogn Sci*, *4*(4), 585–606. https://doi.org/10.1111/j.1756-8765.2012.01213.x

Grahn, J. A., & Brett, M. (2009). Impairment of beat-based rhythm discrimination in Parkinson's disease. *Cortex*, *45*(1), 54–61. https://doi.org/10.1016/j.cortex.2008.01.005

Grahn, J. A., Parkinson, J. A., & Owen, A. M. (2008). The cognitive functions of the caudate nucleus. *Progress in Neurobiology*, *86*(3), 141–155. https://doi.org/10.1016/j.pneurobio.2008.09.004

Grahn, J. A., & Rowe, J. B. (2009). Feeling the beat: premotor and striatal interactions in musicians and nonmusicians during beat perception. *The Journal of Neuroscience : The Official Journal of the Society for Neuroscience*, *29*(23), 7540–7548. https://doi.org/10.1523/JNEUROSCI.2018-08.2009

Grahn, J. A., & Rowe, J. B. (2013). Finding and feeling the musical beat: Striatal dissociations between detection and prediction of regularity. *Cerebral Cortex*, *23*(4), 913–921. https://doi.org/10.1093/cercor/bhs083

Grey Walter, W. (1950). RHYTHM AND REASON. *Electroencephalography and Clinical Neurophysiology*, *2*(1–4), 203. https://doi.org/10.1038/183220c0

Grey Walter, W., Cooper, R., Aldridge, V., McCallum, W., & Winter, A. (1964). Contingent negative variation: an electric sign of sensorimotor association and expectancy in the human brain. *Nature*, *203*, 1195–1268.

Grillner, S. (1975). Locomotion in vertebrates: central mechanisms and reflex interaction. *Physiological Reviews*, *55*(2), 247–304.

Grillner, S. (1985). Neurobiological Bases of Rhythmic Motor Acts in Vertebrates. *Science*, *228*(4696), 143–149.

Grillner, S., Georgopoulos, A. P., & Jordan, L. M. (1997). Selection and initiation of motor behavior. In P. Stein, S. Grillner, A. Selverston, & D. Stuart (Eds.), *Neurons, Networks and Motor Behavior* (MIT press, pp. 3–19). Cambrdge, MA. Retrieved from papers3://publication/uuid/D61F4D45-A92F-4427-B81C-F9870CAF5F00

Groppe, D. M., Urbach, T. P., & Kutas, M. (2011). Mass univariate analysis of event-related brain potentials/fields I: a critical tutorial review. *Psychophysiology*, *48*(12), 1711–1725. https://doi.org/10.1111/j.1469-8986.2011.01273.x

Grube, M., Cooper, F. E., Chinnery, P. F., & Griffiths, T. D. (2010). Dissociation of duration-based and beat-based auditory timing in cerebellar degeneration. *Proceedings of the National Academy of Sciences of the United States of America*, *107*(25), 11597–11601. https://doi.org/10.1073/pnas.0910473107

Grube, M., Lee, K.-H., Griffiths, T. D., Barker, A. T., & Woodruff, P. W. (2010). Transcranial magnetic theta-burst stimulation of the human cerebellum distinguishes absolute, duration-based from relative, beat-based perception of subsecond time intervals. *Frontiers in Psychology*, *1*, 171. https://doi.org/10.3389/fpsyg.2010.00171

Guldenmund, P., Soddu, A., Baquero, K., Vanhaudenhuyse, A., Bruno, M.-A., Gosseries, O., … Gómez, F. (2016). Structural brain injury in patients with disorders of consciousness: A voxel-based morphometry study. *Brain Injury*, *30*(3), 343–352. https://doi.org/10.3109/02699052.2015.1118765

Gwin, J. T., Gramann, K., Makeig, S., & Ferris, D. P. (2010). Removal of Movement Artifact From High-Density EEG Recorded During Walking and Running. *Journal of Neurophysiology*, *103*(6), 3526–3534. https://doi.org/10.1152/jn.00105.2010

Gybels, J., Meulders, M., Callens, M., & Colle, J. (1967). [Sensorimotor integration in the caudate nucleus]. *Nederlands Tijdschrift Voor Geneeskunde*, *111*(16), 757–759. Retrieved from http://www.ncbi.nlm.nih.gov/pubmed/6044060

Haegens, S., & Zion Golumbic, E. (2017). Rhythmic facilitation of sensory processing: A critical review. *Neuroscience and Biobehavioral Reviews*, *86*(December 2017), 150–165. https://doi.org/10.1016/j.neubiorev.2017.12.002

Halsband, U., Ito, N., Tanji, J., & Freund, H. J. (1993). The role of premotor cortex and the supplementary motor area in the temporal control of movement in man. *Brain : A Journal of Neurology*, *116 (Pt 1)*, 243–266. Retrieved from http://www.ncbi.nlm.nih.gov/pubmed/8453461

Hamacher, D., Herold, F., Wiegel, P., Hamacher, D., & Schega, L. (2015). Brain activity during walking: A systematic review. *Neuroscience and Biobehavioral Reviews*, *57*, 310–327. https://doi.org/10.1016/j.neubiorev.2015.08.002

Hari, R., Hamalainen, M., & Joutsiniemi, S. (1989). Neuromagnetic steady-state response to auditory stimuli. *J Acoust SOC Am*, *86*, 1033–1039.

Hartley, D. (1749). *Observations on Man, his Frame, his Duty and his Expectations*. (S. Richardson, Ed.). London.

Hary, D., & Moore, G. (1985). Temporal tracking and synchronization strategies. *Human Neurobiology*, *4*, 73–77.

Hary, D., & Moore, G. (1987). On performance and stability of human metronome-synchronization strategies. *British Journal of Mathematical & Psychological Psychology*, *40*, 109–124.

Hausdorff, J. M. (2009). Gait dynamics in Parkinson's disease: common and distinct behavior among stride length, gait variability, and fractal-like scaling. *Chaos (Woodbury, N.Y.)*, *19*(2), 026113. https://doi.org/10.1063/1.3147408

Hausdorff, J. M., Lowenthal, J., Herman, T., Gruendlinger, L., Peretz, C., & Giladi, N. (2007). Rhythmic auditory stimulation modulates gait variability in Parkinson's disease. *European Journal of Neuroscience*, *26*(8), 2369–2375. https://doi.org/10.1111/j.1460-9568.2007.05810.x

Hausdorff, J. M., Purdon, P., Peng, C., Ladin, Z., Wei, J., & Goldberger, A. (1996). Fractal dynamics of human gait: stability of long-range correlations in stride interval fluctuations. *Journal of Applied Physiology*, *80*(5), 1448–1457. https://doi.org/10.1152/jappl.1996.80.5.1448

Haykin, S., & Van Veen, B. (1999). *Signals and Systems*. (B. Zobrist, Ed.) (John Wiley). New York.

Henry, M. J., Herrmann, B., & Grahn, J. A. (2017). What can we learn about beat perception by comparing brain signals and stimulus envelopes? *PLoS ONE*, *12*(2). https://doi.org/10.1371/journal.pone.0172454

Hove, M. J., Fairhurst, M. T., Kotz, S. A., & Keller, P. E. (2013). Synchronizing with auditory and visual rhythms: an fMRI assessment of modality differences and modality appropriateness. *NeuroImage*, *67*, 313–321. https://doi.org/10.1016/j.neuroimage.2012.11.032

Hove, M. J., & Keller, P. E. (2015). Impaired movement timing in neurological disorders: Rehabilitation and treatment strategies. *Annals of the New York Academy of Sciences*, *1337*, 111–117. https://doi.org/10.1111/nyas.12615

Howell, D. (2002). *Statistical Methods for Psychology* (5th Editio). Pacific Grove CA: Duxbury.

Huang, H. C., & Jansen, B. H. (1985). EEG waveform analysis by means of dynamic time-warping. *International Journal of Bio-Medical Computing*, *17*(2), 135–144. Retrieved from http://www.ncbi.nlm.nih.gov/pubmed/4055119

Huang, Y., Gu, L., Yang, J., & Wu, X. (2017). Bouncing Ball with a Uniformly Varying Velocity in a Metronome Synchronization Task. *Journal of Visualized Experiments*, (127). https://doi.org/10.3791/56205

Iansek, R., Danoudis, M., & Bradfield, N. (2013). Gait and cognition in Parkinson's disease: implications for rehabilitation. *Reviews in the Neurosciences*, *24*(3), 293–300. https://doi.org/10.1515/revneuro-2013-0006

Insel, T. R., & Cuthbert, B. N. (2015). Brain disorders? Precisely. *Science*, *348*(6234), 499–500. https://doi.org/10.1126/science.aab2358

Ivry, R. B., & Keele, S. W. (1989). Timing functions of the cerebellum. *Journal of Cognitive Neuroscience*, *1*(2), 136–152. https://doi.org/10.1162/jocn.1989.1.2.136

Jahanshahi, M., Jones, C. R., Dirnberger, G., & Frith, C. D. (2006). The substantia nigra pars compacta and temporal processing. *J Neurosci*, *26*(47), 12266–12273. https://doi.org/10.1523/jneurosci.2540-06.2006

Jahn, K., Deutschländer, A., Stephan, T., Strupp, M., Wiesmann, M., & Brandt, T. (2004). Brain activation patterns during imagined stance and locomotion in functional magnetic resonance imaging. *NeuroImage*, *22*(4), 1722–1731. https://doi.org/10.1016/J.NEUROIMAGE.2004.05.017

Janata, P., Tomic, S. T., & Haberman, J. M. (2012). Sensorimotor coupling in music and the psychology of the groove. *Journal of Experimental Psychology. General*, *141*(1), 54–75. https://doi.org/10.1037/a0024208

Jäncke, L., Loose, R., Lutz, K., Specht, K., & Shah, N. (2000). Cortical activationd during paced finger-tapping applying visual and auditory pacing stimuli. *Cognitive Brain Research*, *10*, 51–66.

Jaques-Dalcroze, E. (1920). *Le rythme, la musique et l'éducation [Rhythm, music and education].* (Fœtisch). Lausanne, Switzerland.

Jarbo, K., & Verstynen, T. D. (2015). Converging structural and functional connectivity of orbitofrontal, dorsolateral prefrontal, and posterior parietal cortex in the human striatum. *Journal of Neuroscience*, (4).

Jeon, H. -a., Anwander, a., & Friederici, a. D. (2014). Functional Network Mirrored in the Prefrontal Cortex, Caudate Nucleus, and Thalamus: High-Resolution Functional Imaging and Structural Connectivity. *Journal of Neuroscience*, *34*(28), 9202–9212. https://doi.org/10.1523/JNEUROSCI.0228-14.2014

Jones, M. (1976). Time, our lost dimension: toward a new theory of perception, attention, and memory. *Psychol Rev*, *83*(5), 323–355.

Jones, M., & Boltz, M. (1989). Dynamic Attending and Responses to Time. *Psychological Review*, *96*(3).

Jung, T. P., Makeig, S., Westerfield, M., Townsend, J., Courchesne, E., & Sejnowski, T. J. (2000). Removal of eye activity artifacts from visual event-related potentials in normal and clinical subjects. *Clinical Neurophysiology*, *111*(10), 1745–1758. https://doi.org/10.1016/S1388-2457(00)00386-2

Karas, P. J., Mikell, C. B., Christian, E., Liker, M. A., & Sheth, S. A. (2013). Deep brain stimulation: a mechanistic and clinical update. *Neurosurgical Focus*, *35*(5), E1. https://doi.org/10.3171/2013.9.FOCUS13383

Kayser, C., Montemurro, M. A., Logothesis, N., & Panzeri, S. (2009). Spike-phase coding boosts and stabilizes information carried by spatial and temporal spike patterns. *Neuron*, *61*, 597–608.

Keitel, C., Thut, G., & Gross, J. (2017). Visual cortex responses reflect temporal structure of continuous quasi-rhythmic sensory stimulation. https://doi.org/10.1016/j.neuroimage.2016.11.043

Keller, P. E. (2008). Joint Action in Music Performance. *Enacting Intersubjectivity: A Cognitive and Social Perspective on the Study of Interactions*, 205–221. Retrieved from http://www.neurovr.org/emerging/book8/14_Keller.pdf

Keller, P. E., Schultz, B. G., van der Steen, M. C., & Mills, P. F. (2015). Individual Differences in Temporal Anticipation and Adaptation During Sensorimotor Synchronization. *Timing & Time Perception*, *3*(1–2), 13–31. https://doi.org/10.1163/22134468-03002040

Kline, J. E., Huang, H. J., Snyder, K. L., & Ferris, D. P. (2015). Isolating gait-related movement artifacts in electroencephalography during human walking. *Journal of Neural Engeneering*, *12*(4), 87–92. https://doi.org/10.1088/1741-2560/12/4/046022

Kornhuber, H., & Deecke, L. (1965). Himpotentialaenderungen bei Willkuerbewegungen und passiven Bewegungen des Menschen: Bereit-schaft-sotentiale und reafferente Potentiale. *Pfluegers Arch. Gesamte Physiol. Menschen Tiere*, *81*, 284–298.

Kotz, S. A., Anwander, A., Axer, H., & Knösche, T. R. (2013). Beyond cytoarchitectonics: the internal and external connectivity structure of the caudate nucleus. *PloS One*, *8*(7), e70141. https://doi.org/10.1371/journal.pone.0070141

Kotz, S. A., & Schwartze, M. (2011). Differential Input of the Supplementary Motor Area to a Dedicated Temporal Processing Network: Functional and Clinical Implications. *Frontiers in Integrative Neuroscience*, *5*(December), 2007–2010. https://doi.org/10.3389/fnint.2011.00086

Kotz, S. A., Schwartze, M., & Schmidt-Kassow, M. (2009). Non-motor basal ganglia functions: A review and proposal for a model of sensory predictability in auditory language perception. *Cortex*, *45*, 982–990.

Krause, V., Pollok, B., & Schnitzler, A. (2010). Perception in action: The impact of sensory information on sensorimotor synchronization in musicians and non-musicians. *Acta Psychologica*, *133*(1), 28–37. https://doi.org/10.1016/j.actpsy.2009.08.003

Kringelbach, M. L. (2011). Balancing the brain : resting state networks and deep brain stimulation, *5*(May), 1–5. https://doi.org/10.3389/fnint.2011.00008

la Fougère, C., Zwergal, A., Rominger, A., Förster, S., Fesl, G., Dieterich, M., … Jahn, K. (2010). Real versus imagined locomotion: A [18F]-FDG PET-fMRI comparison. *NeuroImage*, *50*(4), 1589–1598. https://doi.org/10.1016/j.neuroimage.2009.12.060

Lakatos, P., Chen, C. M., O-Connell, M. N., Mills, A., & Schroeder, C. E. (2007). Neuronal Oscillations and Multisensory Ineractions in Primary Auditory Cortex. *Neuron*, *53*(2), 279–292. https://doi.org/10.1016/j.neuron.2006.12.011.

Lakatos, P., Karmos, G., Mehta, A. D., Ulbert, I., & Schroeder, C. E. (2008). Entrainment of neuronal oscillations as a mechanism of attentional selection. *Science (New York, N.Y.)*, *320*(5872), 110–113. https://doi.org/10.1126/science.1154735

Lakatos, P., Musacchia, G., O'Connel, M. N., Falchier, A. Y., Javitt, D. C., & Schroeder, C. E. (2013). The spectrotemporal filter mechanism of auditory selective attention. *Neuron*, *77*(4), 750–761. https://doi.org/10.1016/j.neuron.2012.11.034

Large, E. W. (2000). On synchronizing movements to music. *Human Movement Science*, *19*(4), 527–566.

Large, E. W. (2008). Resonating to Musical Rhythm: Theory and Experiment. In Grondin S (Ed.), *Psychology of Time* (Emerald Gr, pp. 189–231). https://doi.org/10.1016/b978-0-08046-977-5.00006-5

Large, E. W., Herrera, J. A., & Velasco, M. J. (2015). Neural Networks for Beat Perception in Musical Rhythm. *Frontiers in Systems Neuroscience*, *9*, 159. https://doi.org/10.3389/fnsys.2015.00159

Large, E. W., & Jones, M. (1999). The Dynamics of attending; how people track time-varying events. *Psychological Review*, *106*(1).

Launay, J., Dean, R., & Bailes, F. (2011). Using changing anisochrony in a sensorimotor synchronization paradigm to investigate error correction and long-term memory. In *13rd International Rhythm Perception and Production Workshop*. Leipzig, Germany.

Laureys, S., & Schiff, N. D. (2012). Coma and consciousness: paradigms (re)framed by neuroimaging. *NeuroImage*, *61*(2), 478–491. https://doi.org/10.1016/j.neuroimage.2011.12.041

Lehmann, A., Jimena Arias, D., Schönwiesner, M., Arias, D. J., & Schönwiesner, M. (2016). Tracing the Neural Basis of Auditory Entrainment. *Neuroscience*, *337*, 306–314. https://doi.org/10.1016/j.neuroscience.2016.09.011

Leman, M. (2007). *Embodied music cognition and mediation technology*. Cambridge, Massachusetts: MIT Press.

Lewis, P. a., & Miall, R. C. (2003). Distinct systems for automatic and cognitively controlled time measurement: Evidence from neuroimaging. *Current Opinion in Neurobiology*, *13*(2), 250–255. https://doi.org/10.1016/S0959-4388(03)00036-9

Liddell, E., & Phillips, C. (1944). Pyramidal section in the cat. *Brain*, *67*(1), 1–9. https://doi.org/doi.org/10.1093/brain/67.1.1

Lim, I., van Wegen, E., de Goede, C., Deutekom, M., Nieuwboer, A., & Willems, A. (2005). Effects of external rhythmical cueing on gait in patients with Parkinson's disease: a systematic review. *Clinical Rehabilitation*, *19*(7), 695–713.

Llinás, R. R. (1988). The intrinsic electrophysiological properties of mammalian neurons: Insights into central nervous system function. *Science*, *242*(4886), 1654–1664. https://doi.org/10.1126/science.3059497

Llinás, R. R. (2014). The olivo-cerebellar system: a key to understanding the functional significance of intrinsic oscillatory brain properties. *Frontiers in Neural Circuits*, *7*(January), 1–13. https://doi.org/10.3389/fncir.2013.00096

Llinás, R. R., & Yarom, Y. (1981). Electrophysiology of mammalian inferior olivary neurones in vitro. Different types of voltage-dependent ionic conductances. *The Journal of Physiology*, *315*, 549–567. https://doi.org/VL - 315

Lloyd, D., & Rossi, E. L. (1993). Biological rhythms as organization and information. *Biological Reviews of the Cambridge Philosophical Society*, *68*(4), 563–577. Retrieved from http://www.ncbi.nlm.nih.gov/pubmed/8130327

London, J. (2004). *Hearing in time: Psychological aspects of musical meter*. London, England: Oxford University Press.

London, J. (2012). Musical Meter, Social Cognition, and Musical Expression: An Inquiry in Cognitive Aesthetics. *Studies in Honor of Eugene Narmour*, 1–19.

Macefield, V. G. (2009). Long Loop Reflexes. In M. D. Binder, N. Hirokawa, & U. Windhorst (Eds.), *Encyclopedia of Neuroscience* (pp. 2180–2183). Berlin, Heidelberg: Springer Berlin Heidelberg. https://doi.org/10.1007/978-3-540-29678-2_2822

Madison, G., & Merker, B. H. (2002). On the limits of anisochrony in pulse attribution. *Psychol Res*, *66*(3), 201–207. https://doi.org/10.1007/s00426-001-0085-y

Makeig, S. (2002). Response: event-related brain dynamics -- unifying brain electrophysiology. *Trends in Neurosciences*, *25*(8), 390. Retrieved from http://www.ncbi.nlm.nih.gov/pubmed/12127749

Marder, E., & Bucher, D. (2001). Central pattern generators and the control of rythmic movements. *Current Biology*, *11*, R986–R996. https://doi.org/10.1016/S0960-9822(01)00581-4

Maris, E., & Oostenveld, R. (2007). Nonparametric statistical testing of EEG- and MEG-data. *Journal of Neuroscience Methods*, *164*(1), 177–190. https://doi.org/10.1016/j.jneumeth.2007.03.024

Marras, C. (2015). Subtypes of Parkinson's disease: state of the field and future directions. *Current Opinion in Neurology*, *28*(4), 383–386.

Matell, M. S., & Meck, W. H. (2004). Cortico-striatal circuits and interval timing: coincidence detection of oscillatory processes. *Brain Res Cogn Brain Res*, *21*(2), 139–170. https://doi.org/10.1016/j.cogbrainres.2004.06.012

McNeill, W. (1995). *Keeping together in time: Psychological aspects of musical meter*. Oxford, UK: Oxford University Press.

Merchant, H., Harrington, D. L., & Meck, W. H. (2013). Neural basis of the perception and estimation of time. *Annu Rev Neurosci*, *36*, 313–336. https://doi.org/10.1146/annurev-neuro-062012-170349

Merchant, H., & Honing, H. (2013). Are non-human primates capable of rhythmic entrainment? Evidence for the gradual audiomotor evolution hypothesis. *Frontiers in Neuroscience*, *7*, 274. https://doi.org/10.3389/fnins.2013.00274

Merchant, H., Luciana, M., Hooper, C., Majestic, S., & Tuite, P. (2008). Interval timing and Parkinson's disease: heterogeneity in temporal performance. *Experimental Brain Research*, *184*(2), 233–248. https://doi.org/10.1007/s00221-007-1097-7

Merker, B. H., Madison, G. S., & Eckerdal, P. (2009). On the role and origin of isochrony in human rhythmic entrainment. *Cortex*, *45*(1), 4–17. https://doi.org/10.1016/j.cortex.2008.06.011

Michon, J. (1967). *Timing in temporal tracking.* (van Gorcum). Assen, The Netherlands.

Middleton, F. A., & Strick, P. L. (2000). Basal ganglia and cerebellar loops: Motor and cognitive circuits. *Brain Research Reviews*, *31*(2–3), 236–250. https://doi.org/10.1016/S0165-0173(99)00040-5

Milner, A. D. (A. D., & Goodale, M. A. (1995). *The visual brain in action*. Oxford University Press.

Minassian, K., Hofstoetter, U. S., Dzeladini, F., Guertin, P. A., & Ijspeert, A. (2017). The Human Central Pattern Generator for Locomotion: Does It Exist and Contribute to Walking? *The Neuroscientist*, *23*(6), 649–663. https://doi.org/10.1177/1073858417699790

Morillon, B., & Schroeder, C. E. (2015). Neuronal oscillations as a mechanistic substrate of auditory temporal prediction. *Annals of the New York Academy of Sciences*, *1337*(1), 26–31. https://doi.org/10.1111/nyas.12629

Morton, S. M., & Bastian, A. J. (2006). Cerebellar Contributions to Locomotor Adaptations during Splitbelt Treadmill Walking. *Journal of Neuroscience*, *26*(36), 9107–9116. https://doi.org/10.1523/JNEUROSCI.2622-06.2006

Mouraux, A., & Iannetti, G. D. (2008). Across-trial averaging of event-related EEG responses and beyond. *Magnetic Resonance Imaging*, *26*(7), 1041–1054. https://doi.org/10.1016/j.mri.2008.01.011

Mouraux, A., Iannetti, G. D., Colon, E., Nozaradan, S., Legrain, V., & Plaghki, L. (2011). Nociceptive steady-state evoked potentials elicited by rapid periodic thermal stimulation of cutaneous nociceptors. *J Neurosci*, *31*(16), 6079–6087. https://doi.org/10.1523/JNEUROSCI.3977-10.2011

Näätänen, R., Paavilainen, P., Rinne, T., & Alho, K. (2007). The mismatch negativity (MMN) in basic research of central auditory processing: A review. *Clinical Neurophysiology*, *118*(12), 2544–2590. https://doi.org/10.1016/j.clinph.2007.04.026

Nagy, A., Eördegh, G., Paróczy, Z., Márkus, Z., & Benedek, G. (2006). Multisensory integration in the basal ganglia. *European Journal of Neuroscience*, *24*(3), 917–924. https://doi.org/10.1111/j.1460-9568.2006.04942.x

Nilsson, J., & Thorstensson, A. (1987). Adaptability in frequency and amplitude of leg movements during human locomotion at different speeds. *Acta Physiologica*, *129*(1), 107–114. https://doi.org/10.1111/j.1748-1716.1987.tb08045.x

Nobre, A., Correa, A., & Coull, J. (2007). The hazards of time. *Current Opinion in Neurobiology*, *17*(4), 465–470. https://doi.org/10.1016/J.CONB.2007.07.006

Nobre, A., & Van Ede, F. (2017). Anticipated moments: temporal structure in attention. *Nature Reviews Neuroscience*, *19*, 34–48.

Noga, B. R., Sanchez, F. J., Villamil, L. M., O'Toole, C., Kasicki, S., Olszewski, M., … Jordan, L. M. (2017). LFP Oscillations in the Mesencephalic Locomotor Region during Voluntary Locomotion. *Frontiers in Neural Circuits*, *11*(May), 1–17. https://doi.org/10.3389/fncir.2017.00034

Nombela, C., Hughes, L. E., Owen, A. M., & Grahn, J. A. (2013). Into the groove: Can rhythm influence Parkinson's disease? *Neuroscience and Biobehavioral Reviews*, *37*(10), 2564–2570. https://doi.org/10.1016/j.neubiorev.2013.08.003

Nozaradan, S. (2014). Exploring how musical rhythm entrains brain activity with electroencephalogram frequency-tagging. *Philosophical Transactions of the Royal Society of London. Series B, Biological Sciences*, *369*(1658), 1–10. https://doi.org/10.1098/rstb.2013.0393

Nozaradan, S., Keller, P. E., Rossion, B., & Mouraux, A. (2017). EEG Frequency-Tagging and Input–Output Comparison in Rhythm Perception. *Brain Topography*, *31*(2), 1–8. https://doi.org/10.1007/s10548-017-0605-8

Nozaradan, S., Mouraux, A., Jonas, J., Colnat-Coulbois, S., Rossion, B., & Maillard, L. (2016). Intracerebral evidence of rhythm transform in the human auditory cortex. *Brain Structure and Function*. https://doi.org/10.1007/s00429-016-1348-0

Nozaradan, S., Peretz, I., & Keller, P. E. (2016). Individual Differences in Rhythmic Cortical Entrainment Correlate with Predictive Behavior in Sensorimotor Synchronization. *Scientific Reports*, *6*(20612), 20612. https://doi.org/10.1038/srep20612

Nozaradan, S., Peretz, I., Missal, M., & Mouraux, A. (2011). Tagging the neuronal entrainment to beat and meter. *J Neurosci*, *31*(28), 10234–10240. https://doi.org/10.1523/JNEUROSCI.0411-11.2011

Nozaradan, S., Peretz, I., & Mouraux, A. (2012a). Selective neuronal entrainment to the beat and meter embedded in a musical rhythm. *The Journal of Neuroscience*, *32*(49), 17572–17581. https://doi.org/10.1523/JNEUROSCI.3203-12.2012

Nozaradan, S., Peretz, I., & Mouraux, A. (2012b). Steady-state evoked potentials as an index of multisensory temporal binding. *NeuroImage*, *60*(1), 21–28. https://doi.org/10.1016/j.neuroimage.2011.11.065

Nozaradan, S., Schönwiesner, M., Caron-Desrochers, L., & Lehmann, A. (2016). Enhanced brainstem and cortical encoding of sound during synchronized movement. *NeuroImage*, *142*, 231–240. https://doi.org/10.1016/j.neuroimage.2016.07.015

Nozaradan, S., Schönwiesner, M., Keller, P. E., Lenc, T., & Lehmann, A. (2018). Neural bases of rhythmic entrainment in humans: critical transformation between cortical and lower-level representations of auditory rhythm. *European Journal of Neuroscience*, *47*(January), 321–332. https://doi.org/10.1111/ejn.13826

Nozaradan, S., Schwartze, M., Obermeier, C., & Kotz, S. A. (2017). Specific Contributions of Basal Ganglia and Cerebellum To The Neural Tracking of Rhythm. *Cortex*, *95*(August), 156–168. https://doi.org/10.1016/j.cortex.2017.08.015

Nozaradan, S., Zerouali, Y., Peretz, I., & Mouraux, A. (2013). Capturing with EEG the Neural Entrainment and Coupling Underlying Sensorimotor Synchronization to the Beat. *Cereb Cortex*, *25*(3), 736–747. https://doi.org/10.1093/cercor/bht261

O'Boyle, D. J., Freeman, J. S., & Cody, F. W. (1996). The accuracy and precision of timing of self-paced, repetitive movements in subjects with Parkinson's disease. *Brain : A Journal of Neurology*, *119 (Pt 1)*, 51–70. Retrieved from http://www.ncbi.nlm.nih.gov/pubmed/8624694

Obeso, J. A., Rodriguez-Oroz, M. C., Stamelou, M., Bhatia, K. P., & Burn, D. J. (2014). The expanding universe of disorders of the basal ganglia. *The Lancet*, *384*(9942), 523–531. https://doi.org/10.1016/S0140-6736(13)62418-6

Oppenheim, A. V. (1999). *Discrete-Time Signal Processing*. Pearson Education. Retrieved from https://books.google.be/books?id=geTn5W47KEsC

Palmer, C. (1997). Music performance. *Annual Review of Psychology*, *48*(1), 115–138. https://doi.org/10.1146/annurev.psych.48.1.115

Parker, K. L., Lamichhane, D., Caetano, M. S., & Narayanan, N. S. (2013). Executive dysfunction in Parkinson's disease and timing deficits. *Front Integr Neurosci*, *7*, 75. https://doi.org/10.3389/fnint.2013.00075

Pastor, M. A., Artieda, J., Jahanshahi, M., & Obeso, J. A. (1992). Time estimation and reproduction is abnormal in Parkinson's disease. *Brain*, *115 Pt 1*, 211–225.

Patel, A. D. (2006). Musical rhythm, linguistic rhythm, and human evolution. *Music Perception*, *24*(1), 99–103. https://doi.org/Doi 10.1525/Mp.2006.24.1.99

Patel, A. D. (2014). The Evolutionary Biology of Musical Rhythm: Was Darwin Wrong? *PLoS Biology*, *12*(3), 1–6. https://doi.org/10.1371/journal.pbio.1001821

Patel, A. D., & Iversen, J. R. (2014). The evolutionary neuroscience of musical beat perception: the Action Simulation for Auditory Prediction (ASAP) hypothesis. *Frontiers in Systems Neuroscience*, *8*(May), 1–14. https://doi.org/10.3389/fnsys.2014.00057

Pecenka, N., & Keller, P. E. (2011). The role of temporal prediction abilities in interpersonal sensorimotor synchronization. *Experimental Brain Research*. https://doi.org/10.1007/s00221-011-2616-0

Penhune, V. B., Zatorre, R. J., & Evans, A. C. (1998). *Cerebellar Contributions to Motor Timing: A PET Study of Auditory and Visual Rhythm Reproduction*. Retrieved from https://www.researchgate.net/profile/Alan_Evans/publication/13454516_Cerebellar_Contributions_to_Motor_Timing_A_PET_Study_of_Auditory_and_Visual_Rhythm_Reproduction/links/00b7d524b64e748640000000/Cerebellar-Contributions-to-Motor-Timing-A-PET-Study-of-Auditory-and-Visual-Rhythm-Reproduction.pdf

Peretz, I. (1990). Processing of local and global musical information by unilateral brain-damaged patients. *Brain : A Journal of Neurology*, *113 (Pt 4*, 1185–1205. Retrieved from http://www.ncbi.nlm.nih.gov/pubmed/2397389

Perez, O., Kass, R. E., & Merchant, H. (2013). Trial time warping to discriminate stimulus-related from movement-related neural activity. *Journal of Neuroscience Methods*, *212*(2), 203–210. https://doi.org/10.1016/j.jneumeth.2012.10.019

Pfeuty, M., Ragot, R., & Pouthas, V. (2003). Processes involved in tempo perception: A CNV analysis. *Psychophysiology*, *40*(1), 69–76. https://doi.org/10.1111/1469-8986.00008

Phillips-Silver, J., Aktipis, C. A., & Bryant, A. G. (2010). The Ecology of Entrainment: Foundations of Coordinated Rhythmic Movement. *Music Perception*.

Phillips-Silver, J., & Trainor, L. J. (2005). Feeling the Beat - Movement Influences Infant Rhythm Perception. *Science*, *308*.

Phillips-Silver, J., & Trainor, L. J. (2007). Hearing what the body feels: auditory encoding of rhythmic movement. *Cognition*, *105*(3), 533–546. https://doi.org/10.1016/j.cognition.2006.11.006

Phillips-Silver, J., & Trainor, L. J. (2008). Vestibular influence on auditory metrical interpretation. *Brain Cogn*, *67*(1), 94–102. https://doi.org/10.1016/j.bandc.2007.11.007

Picton, T., John, M., Dimitrijevic, A., & Purcell, D. (2003). Human auditory steady-state responses. *International Journal of Audiology*, *42*, 177–219.

Pikovsky, A., Rosenblum, M., & Kurths, J. (2003). *Synchronization: A Universal Concept in Nonlinear Sciences*. New York: Cambridge University Press.

Plourde, G., Stapells, D. R., & Picton, T. W. (1991). The human auditory steady-state evoked potentials. *Acta Oto-Laryngologica*, (S491), 153–160. https://doi.org/10.3109/00016489109136793

Postuma, R. B., & Dagher, A. (2006). Basal ganglia functional connectivity based on a meta-analysis of 126 positron emission tomography and functional magnetic resonance imaging publications. *Cerebral Cortex*, *16*(10), 1508–1521. https://doi.org/10.1093/cercor/bhj088

Povel, D.-J., & Essens, P. J. (1985). Perception of Temporal Patterns. *Music Perception: An Interdisciplinary Journal*, *2*(4), 411–440. https://doi.org/10.2307/40285311

Preuschoft, H. (2002). What does "arboreal locomotion" mean exactly and what are the relationships between "climbing", environment and morphology? *Zeitschrift Für Morphologie Und Anthropologie*. E. Schweizerbart'sche Verlagsbuchhandlung. https://doi.org/10.2307/25757603

Prichard, D., & James, T. (1994). Generating surrogate data for time series. *Phys Rev Lett*, *73*(7), 951–954.

Quek, G., & Rossion, B. (2016). Predictability does not generate or modulate category-selective processes in fast periodic visual stimulation streams. *Journal of Vision*, *16*(12), 723. https://doi.org/10.1167/16.12.723

Quek, & Rossion, B. (2017). Category-selective human brain processes elicited in fast periodic visual stimulation streams are immune to temporal predictability. *Neuropsychologia*, *104*(July), 182–200. https://doi.org/10.1016/j.neuropsychologia.2017.08.010

Radenoviü, D., Vuksanoviû, V., Radenoviû, ýedomir, Beleslin, B., Vesna, V., ýedomir, R., & Bogdan, B. (1998). Oscillatory phenomena, processes and mechanisms: physical and biological analogy, *34*(1), 247–258. Retrieved from http://imsi.rs/ippa_web/21simpozijum/issues/34(1)/IPPA1998341_247_258.pdf

Rajendran, V. G., Harper, N. S., Willmore, B. D., Hartmann, W. M., & Schnupp, J. W. (2013). Temporal predictability as a grouping cue in the perception of auditory streams. *J Acoust Soc Am*, *134*(1), El98-104. https://doi.org/10.1121/1.4811161

Rankin, S. K., Fink, P. W., & Large, E. W. (2014). Fractal structure enables temporal prediction in music. *The Journal of the Acoustical Society of America*, *136*(4), EL256-62. https://doi.org/10.1121/1.4890198

Rankin, S. K., Large, E. W., & Fink, P. W. (2009). Fractal Tempo Fluctuation and Pulse Prediction. *Music Perception*, *26*(5), 401–413. https://doi.org/10.1525/mp.2009.26.5.401

Rao, S., Harrington, D., Haaland, K., Bobholz, J., Cox, R., & Binder, J. (1997). Distributed neural systems underlying the timing of movements. *The Journal of Neuroscience : The Official Journal of the Society for Neuroscience*, *17*(14), 5528–5535. Retrieved from http://www.ncbi.nlm.nih.gov/pubmed/9204934

Rao, S., Mayer, A. R., & Harrington, D. L. (2001). The evolution of brain activation during temporal processing. *Nature Neuroscience*, *4*(3), 317–323. https://doi.org/10.1038/85191

Rauschecker, J. P. (2012). Ventral and dorsal streams in the evolution of speech and language. *Frontiers in Evolutionary Neuroscience*, *4*, 7. https://doi.org/10.3389/fnevo.2012.00007

Regan, D. (1966). Some characteristics of average steady-state and transient responses evoked by modulated light. *Electroencephalography and Clinical Neurophysiology*, *20*(3), 238–248. https://doi.org/10.1016/0013-4694(66)90088-5

Repp, B. H. (2000). Compensation for subliminal timing perturbations in perceptual-motor synchronization. *Psychological Research*, *63*, 106–128.

Repp, B. H. (2001a). Phase correction, phase resetting, and phase shifts after subliminal timing perturbations in sensorimotor synchronization. *Journal of Experimental Psychology. Human Perception and Performance*, *28*, 410–430.

Repp, B. H. (2001b). Processes underlying adaptation to tempo changes in sensorimotor synchronization. *Human Movement Science*, *20*, 277–321.

Repp, B. H. (2002a). Phase correction following a perturbation in sensorimotor synchronization depends on sensory information. *Journal of Motor Behavior*, *34*(3), 291–298. https://doi.org/10.1080/00222890209601947

Repp, B. H. (2002b). Phase correction in sensorimotor synchronization: Nonlinearities in voluntary and involuntary responses to perturbations. *Human Movement Science*, *21*, 1–37.

Repp, B. H. (2002c). The embodiment of musical structure: effects of musical context on sensorimotor synchronization with complex timing patterns.

Repp, B. H. (2005). Sensorimotor synchronization: a review of the tapping literature. *Psychonomic Bulletin & Review*, *12*(6), 969–992. https://doi.org/10.3758/BF03206433

Repp, B. H., & Keller, P. E. (2004). Adaptation to tempo changes in sensorimotor synchronization: Effects of intention, attention, and awareness. *Quarterly Journal of Experimental Psychology*, *57*(A), 499–521.

Repp, B. H., & Keller, P. E. (2008). Sensorimotor synchronization with adaptively timed sequences. *Human Movement Science*, *27*(3), 423–456. https://doi.org/10.1016/j.humov.2008.02.016

Repp, B. H., Keller, P. E., & Jacoby, N. (2012). Quantifying phase correction in sensorimotor synchronization: Empirical comparison of three paradigms. *Acta Psychologica*, *139*(2), 281–290. https://doi.org/10.1016/j.actpsy.2011.11.002

Repp, B. H., & Moseley, G. (2012). Anticipatory phase correction in sensorimotor synchronization. *Human Movement Science*, *31*, 1118–1136. https://doi.org/10.1016/j.humov.2011.11.001

Repp, B. H., & Su, Y.-H. (2013). Sensorimotor synchronization: a review of recent research (2006-2012). *Psychonomic Bulletin & Review*, *20*(3), 403–452. https://doi.org/10.3758/s13423-012-0371-2

Retter, T. L., & Rossion, B. (2016). Uncovering the neural magnitude and spatio-temporal dynamics of natural image categorization in a fast visual stream. *Neuropsychologia*, *91*, 9–28. https://doi.org/10.1016/j.neuropsychologia.2016.07.028

Rietveld, W. J. (1993). Chronobiology: neural pacemakers of biological rhythms. *Annali Dell'Istituto Superiore Di Sanità*, *29*(4), 501–510. Retrieved from http://www.ncbi.nlm.nih.gov/pubmed/7985916

Rilling, J. K., Glasser, M. F., Preuss, T. M., Ma, X., Zhao, T., Hu, X., & Behrens, T. E. J. (2008). The evolution of the arcuate fasciculus revealed with comparative DTI. *Nature Neuroscience*, *11*(4), 426–428. https://doi.org/10.1038/nn2072

Rossion, B. (2014). Understanding individual face discrimination by means of fast periodic visual stimulation. *Experimental Brain Research*, *232*(6), 1599–1621. https://doi.org/10.1007/s00221-014-3934-9

Rossion, B., Torfs, K., Jacques, C., & Liu-Shuang, J. (2015). Fast periodic presentation of natural images reveals a robust face-selective electrophysiological response in the human brain. *Journal of Vision*, *15*(1), 15.1.18. https://doi.org/10.1167/15.1.18

Santens, P., Boon, P., Van Roost, D., & Caemaert, J. (2003). The pathophysiology of motor symptoms in Parkinson's disease. *Acta Neurologica Belgica*, *103*, 129–134.

Schachner, A., Brady, T. F., Pepperberg, I. M., & Hauser, M. D. (2009). Spontaneous Motor Entrainment to Music in Multiple Vocal Mimicking Species. *Current Biology*, *19*(10), 831–836. https://doi.org/10.1016/j.cub.2009.03.061

Schnakers, C., Majerus, S., Giacino, J., Vanhaudenhuyse, A., Bruno, M.-A., Boly, M., … Laureys, S. (2008). A French validation study of the Coma Recovery Scale-Revised (CRS-R). *Brain Injury*, *22*(10), 786–792. https://doi.org/10.1080/02699050802403557

Schroeder, C. E., & Foxe, J. (2005). Multisensory contributions to low-level, 'unisensory' processing. *Current Opinion in Neurobiology*, *15*(4), 454–458. https://doi.org/10.1016/J.CONB.2005.06.008

Schroeder, C. E., & Lakatos, P. (2009). Low-frequency neuronal oscillations as instruments of sensory selection. *Trends in Neurosciences*, *32*(1), 9–18. https://doi.org/10.1016/j.tins.2008.09.012

Schroeder, C. E., Lakatos, P., Kajikawa, Y., Partan, S., & Puce, A. (2008). Neuronal oscillations and visual amplification of speech. *Trends in Cognitive Sciences*, *12*, 106–113.

Schroeder, C. E., Wilson, D. A., Radman, T., Scharfman, H., & Lakatos, P. (2010). Dynamics of Active Sensing and perceptual selection. *Curr Opin Neurobiol*, *20*(2), 172–176. https://doi.org/10.1016/j.conb.2010.02.010

Schwartze, M., Stockert, A., & Kotz, S. A. (2015). Striatal contributions to sensory timing: Voxel-based lesion mapping of electrophysiological markers. *Cortex*, *71*, 332–340. https://doi.org/10.1016/j.cortex.2015.07.016

Seel, R. T., Sherer, M., Whyte, J., Katz, D. I., Giacino, J. T., Rosenbaum, A. M., … Zasler, N. (2010). Assessment Scales for Disorders of Consciousness: Evidence-Based Recommendations for Clinical Practice and Research. *Archives of Physical Medicine and Rehabilitation*, *91*(12), 1795–1813. https://doi.org/10.1016/j.apmr.2010.07.218

Semjen, A., Schulze, H. H., & Vorberg, D. (2000). Timing precision in continuation and synchronization tapping. *Psychological Research*, *63*(2), 137–147. https://doi.org/10.1007/PL00008172

Shik, M., & Orlovsky, G. (1976). Neurophysiology of locomotor automatism. *Physiological Reviews*, *56*(3), 465. https://doi.org/10.1152/physrev.1976.56.3.465

Shik, M., Severin, F., & Orlovskii, G. (1966). [Control of walking and running by means of electric stimulation of the midbrain]. *Biofizika*, *11*(4), 659.

Spaak, E., de Lange, F. P., & Jensen, O. (2014). Local entrainment of α oscillations by visual stimuli causes cyclic modulation of perception. *The Journal of Neuroscience : The Official Journal of the Society for Neuroscience*, *34*(10), 3536–3544. https://doi.org/10.1523/JNEUROSCI.4385-13.2014

Spaulding, S. J., Barber, B., Colby, M., Cormack, B., Mick, T., & Jenkins, M. E. (2013). Cueing and Gait Improvement Among People With Parkinson's Disease: A Meta-Analysis. *Archives of Physical Medicine and Rehabilitation*, *94*(3), 562–570. https://doi.org/10.1016/j.apmr.2012.10.026

Sporns, O., Tononi, G., & Edelman, G. M. (2000). Connectivity and complexity the relationship between neuroanatomy and brain dynamics. *Neural Netw.*

Stefani, A., Lozano, A. M., Peppe, A., Stanzione, P., Galati, S., Tropepi, D., … Mazzone, P. (2007). Bilateral deep brain stimulation of the pedunculopontine and subthalamic nuclei in severe Parkinson's disease. *Brain*, *130*(6), 1596–1607. https://doi.org/10.1093/brain/awl346

Stefanics, G., Hangya, B., Hernadi, I., Winkler, I., Lakatos, P., & Ulbert, I. (2010). Phase Entrainment of Human Delta Oscillations Can Mediate the Effects of Expectation on Reaction Speed. *Journal of Neuroscience*, *41*, 13578–13585. https://doi.org/10.1523/JNEUROSCI.0703-10.2010

Stephen, D. G., Stepp, N., Dixon, J. A., & Turvey, M. T. (2008). Strong anticipation: Sensitivity to long-range correlations in synchronization behavior. *Physica A: Statistical Mechanics and Its Applications*, *387*(21), 5271–5278. https://doi.org/10.1016/j.physa.2008.05.015

Steriade, M. (2001). Impact of network activities on neuronal properties in corticothalamic systems. *Journal of Neurophysiology*, *86*(1), 1–39. https://doi.org/10.1017/S1472928801000139

Steriade, M. (2006). Grouping of brain rhythms in corticothalamic systems. *Neuroscience*, *137*(4), 1087–1106. https://doi.org/10.1016/j.neuroscience.2005.10.029

Steriade, M., Gloor, P., Llinás, R. R., Lopes da Silva, F. H., & Mesulam, M. M. (1990). Basic mechanisms of cerebral rhythmic activities. *Electroencephalography and Clinical Neurophysiology*, *76*(6), 481–508. https://doi.org/10.1016/0013-4694(90)90001-Z

Steriade, M., & Llinás, R. R. (1988). The Functional States of the Thalamus and the Associated Neuronal Interplay. *Physiological Reviews*, *68*(3), 649–742. https://doi.org/10.1136/bmj.2.4211.407-b

Stevens, L. (1886). On time-sense. *Mind*, *11*, 393–404.

Sugano, Y., Keetels, M., & Vroomen, J. (2017). Audio-motor but not visuo-motor temporal recalibration speeds up sensory processing. *PLoS ONE*, *12*(12). https://doi.org/10.1371/journal.pone.0189242

Takakusaki, K. (2013). Neurophysiology of gait: From the spinal cord to the frontal lobe. *Movement Disorders*, *28*(11), 1483–1491. https://doi.org/10.1002/mds.25669

Tal, I., Large, E. W., Rabinovitch, E., Wei, Y., Schroeder, C. E., Poeppel, D., & Zion Golumbic, E. (2017). Neural Entrainment to the Beat: The "Missing-Pulse" Phenomenon. *The Journal of Neuroscience*, *37*(26), 6331–6341. https://doi.org/10.1523/JNEUROSCI.2500-16.2017

Teki, S., Grube, M., & Griffiths, T. D. (2011). A unified model of time perception accounts for duration-based and beat-based timing mechanisms. *Frontiers in Integrative Neuroscience*, *5*, 90. https://doi.org/10.3389/fnint.2011.00090

Teki, S., Grube, M., Kumar, S., & Griffiths, T. (2011). Distinct neural substrates of duration-based and beat-based auditory timing. *J Neurosci*, *31*(10), 3805–3812. https://doi.org/10.1523/JNEUROSCI.5561-10.2011

Thaut, M., McIntosh, G. C., Rice, R. R., Miller, R. A., Rathbun, J., & Brault, J. M. (1996). Rhythmic auditory stimulation in gait training for Parkinson's disease patients. *Movement Disorders*, *11*(2), 193–200. https://doi.org/10.1002/mds.870110213

Thaut, M., Tian, B., & Azimi-Sadjadi, M. R. (1998). Rhythmic finger tapping to cosine-wave modulated metronome sequences: Evidence of subliminal entrainment. *Human Movement Science*, *17*(6), 839–863. https://doi.org/10.1016/S0167-9457(98)00031-1

Thevathasan, W., Debu, B., Aziz, T., Bloem, B. R., Blahak, C., Butson, C., … Moro, E. (2018). Pedunculopontine nucleus deep brain stimulation in Parkinson's disease: A clinical review. *Movement Disorders*, *33*(1), 10–20. https://doi.org/10.1002/mds.27098

Thibaut, A., Bruno, M., Chatelle, C., Gosseries, O., Vanhaudenhuyse, A., Demertzi, A., … Laureys, S. (2012). Metabolic activity in external and internal awareness networks in severely brain-damaged patients. *Journal of Rehabilitation Medicine*, *44*(6), 487–494. https://doi.org/10.2340/16501977-0940

Thut, G., Miniussi, C., & Gross, J. (2012). The functional importance of rhythmic activity in the brain. *Current Biology*, *22*(16), R658–R663. https://doi.org/10.1016/j.cub.2012.06.061

Thut, G., Schyns, P. G., & Gross, J. (2011). Entrainment of Perceptually Relevant Brain Oscillations by Non-Invasive Rhythmic Stimulation of the Human Brain. *Frontiers in Psychology*, *2*, 170. https://doi.org/10.3389/fpsyg.2011.00170

Todd, N. P. M., Lee, C. S., & O'Boyle, D. J. (2002). A sensorimotor theory of temporal tracking and beat induction. *Psychological Research*, *66*(1), 26–39. Retrieved from http://www.ncbi.nlm.nih.gov/pubmed/11963275

Torre, K., & Delignières, D. (2008). Unraveling the finding of 1/f β noise in self-paced and synchronized tapping: a unifying mechanistic model. *Biological Cybernetics*, *99*(2), 159–170. https://doi.org/10.1007/s00422-008-0247-8

Torre, K., Varlet, M., & Marmelat, V. (2013). Brain and Cognition Predicting the biological variability of environmental rhythms : Weak or strong anticipation for sensorimotor synchronization ? *Brain and Cognition*, *83*(3), 342–350. https://doi.org/10.1016/j.bandc.2013.10.002

Tranchant, P., & Vuvan, D. T. (2015). Current conceptual challenges in the study of rhythm processing deficits. *Frontiers in Neuroscience*, *9*, 197. https://doi.org/10.3389/fnins.2015.00197

Tranchant, P., Vuvan, D. T., & Peretz, I. (2016). Keeping the Beat: A Large Sample Study of Bouncing and Clapping to Music. *PloS One*, *11*(7), e0160178. https://doi.org/10.1371/journal.pone.0160178

Treisman, M. (1963). Temporal discrimination and the indifference interval. Implications for a model of the "internal clock". *Psychological Monographs*, *77*(13), 1–31. https://doi.org/10.1037/h0093864

van den Broeke, E. N., Lambert, J., Huang, G., & Mouraux, A. (2016). Central Sensitization of Mechanical Nociceptive Pathways Is Associated with a Long-Lasting Increase of Pinprick-Evoked Brain Potentials. *Frontiers in Human Neuroscience*, *10*, 531. https://doi.org/10.3389/fnhum.2016.00531

van der Steen, M. C., Jacoby, N., Fairhurst, M. T., & Keller, P. E. (2015). Sensorimotor synchronization with tempo-changing auditory sequences: Modeling temporal adaptation and anticipation. *Brain Research*. https://doi.org/10.1016/j.brainres.2015.01.053

van der Steen, M. C., & Keller, P. E. (2013). The ADaptation and Anticipation Model (ADAM) of sensorimotor synchronization. *Frontiers in Human Neuroscience*, *7*, 253. https://doi.org/10.3389/fnhum.2013.00253

Van Ede, F., Quinn, A. J., Woolrich, M. W., & Nobre, A. (2018). Neural Oscillations: Sustained Rhythms or Transient Burst- Events? *Trends in Neurosciences*, *14*(7), 415–417. https://doi.org/10.1016/j.tins.2018.04.004

van Noorden, L., & Moelants, D. (1999). Resonance in the Perception of Musical Pulse. *Ournal,of New Music Research*, *28*(1), 43–66.

Velasco, M. J., & Large, E. W. (2011). Pulse Detection in Syncopated Rhythms Using Neural Oscillators. *12th International Society for Music Information Retrieval Conference (ISMIR 2011)*, (Ismir), 185–190.

Von Wilzenben, H. (1942). *Methods in the treatment of post encephalic Parkinson's* (Grune and). New York.

Wang, X. J. (2010). Neurophysiological and computational principles of cortical rhythms in cognition. *Physiol Rev*, *90*(3), 1195–1268. https://doi.org/10.1152/physrev.00035.2008

Warlop, T. (2017). *The temporal organization of stride duration variability for assessing gait stability. Clinical application to Parkinson's disease*. Université Catholique de Louvain.

Warlop, T., Chemin, B., Cambier, C., Nozaradan, S., Detrembleur, C., Crevecoeur, F., … Lejeune, T. (2015). Does metronome really help timing gait in Parkinson's disease? *Annals of Physical and Rehabilitation Medicine*, *58*(e73). https://doi.org/10.1016/j.rehab.2015.07.180

Wing, A. (1980). The long and short of timing in response sequences. In G. S. and J. Requin (Ed.), *Tutorials in Motor Behavior* (pp. 469–486). North Holland.

Wing, A. (2002). Voluntary Timing and Brain Function: An Information Processing Approach. *Brain and Cognition*, *48*(1), 7–30. https://doi.org/10.1006/BRCG.2001.1301

Wing, A., Daffertshofer, A., & Pressing, J. (2004). Multiple time scales in serial production of force: A tutorial on power spectral analysis of motor variability. *Human Movement Science*, *23*(5), 569–590. https://doi.org/10.1016/j.humov.2004.10.002

Wing, A., & Kristofferson, A. (1973a). Response delays and the timing of discrete motor responses. *Perception & Psychophysics*, *14*(1), 5–12. https://doi.org/10.3758/BF03198607

Wing, A., & Kristofferson, A. (1973b). The timing of interresponse intervals. *Perception & Psychophysics*, *13*(1963), 455–460. https://doi.org/10.3758/BF03205802

Womelsdorf, T., Schoffelen, J.-M., Oostenveld, R., Singer, W., Desimone, R., Engel, A. K., & Fries, P. (2007). Modulation of Neuronal Interactions Through Neuronal Synchronization. *Science*, *316*(5831), 1609–1612. https://doi.org/10.1126/science.1139597

Wu, T., Hallett, M., & Chan, P. (2015). Motor automaticity in Parkinson's disease. *Neurobiology of Disease*, *82*, 226–234. https://doi.org/10.1016/j.nbd.2015.06.014

Yu, H., Russell, D. M., & Stenard, D. (2003). Task-effector asymmetries in a rhythmic continuation task. *Journal of Experimental Psychology: Human Perception and Performance*, *29*(3), 616–630. https://doi.org/10.1037/0096-1523.29.3.616

Zendel, B. R., Ross, B., & Fujioka, T. (2011). The Effects of Stimulus Rate and Tapping Rate on Tapping Performance. *Music Perception: An Interdisciplinary Journal*, *29*(1), 65–78. https://doi.org/10.1525/mp.2011.29.1.65

Zhang, L., Peng, W., Zhang, Z., & Hu, L. (2013). Distinct features of auditory steady-state responses as compared to transient event-related potentials. *PLoS ONE*, *8*(7), e69164. https://doi.org/10.1371/journal.pone.0069164

Zhou, H., Melloni, L., Poeppel, D., & Ding, N. (2016). Interpretations of Frequency Domain Analyses of Neural Entrainment: Periodicity, Fundamental Frequency, and Harmonics. *Frontiers in Human Neuroscience*, *10*, 274. https://doi.org/10.3389/fnhum.2016.00274

Zoefel, B., ten Oever, S., & Sack, A. T. (2018). The Involvement of Endogenous Neural Oscillations in the Processing of Rhythmic Input: More Than a Regular Repetition of Evoked Neural Responses. *Frontiers in Neuroscience*, *12*(March), 1–13. https://doi.org/10.3389/fnins.2018.00095